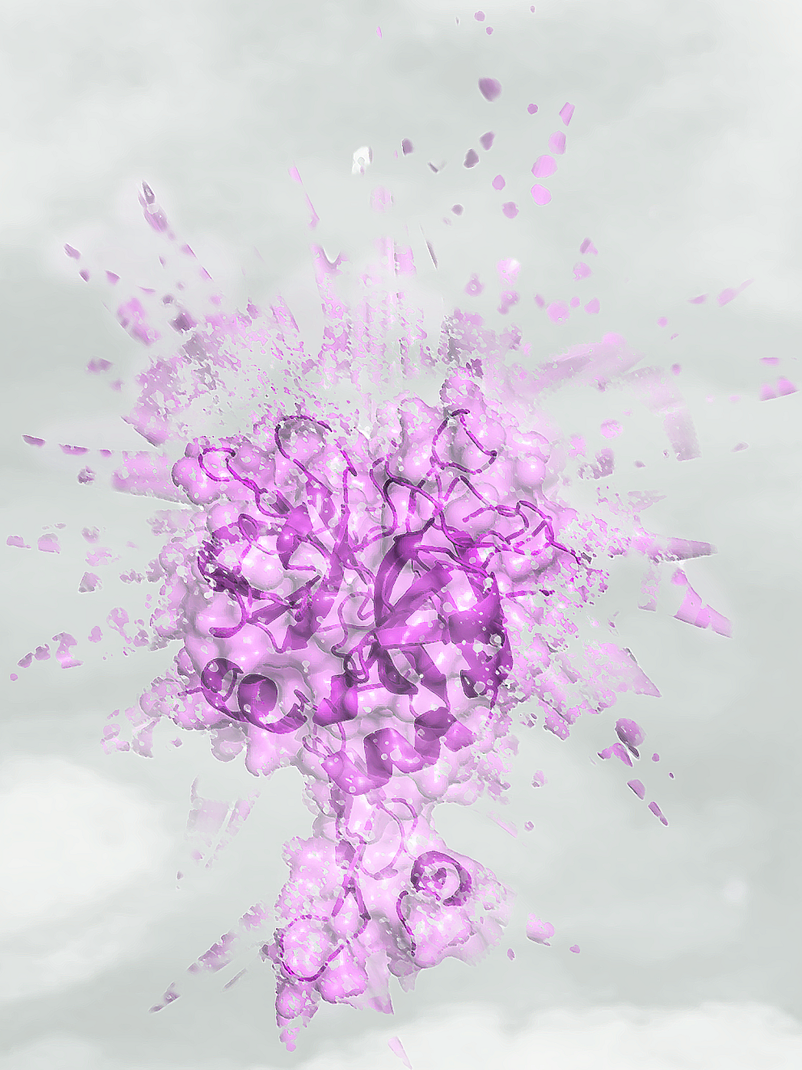

Nadia Freato *Viribus unitis* - the molecular synergism between coagulation factors VIII and IX 2021

# *Viribus unitis* - the molecular synergism between coagulation factors VIII and IX

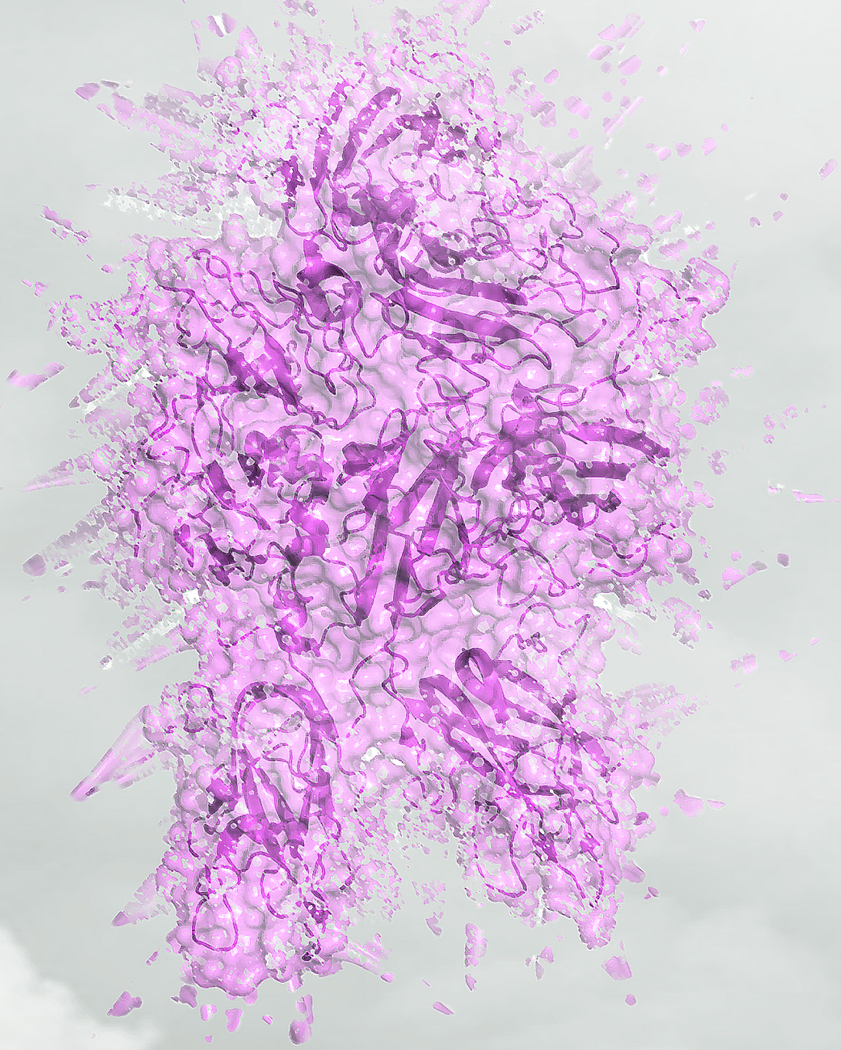

**Nadia Freato**

***Viribus unitis* - the molecular synergism between coagulation factors VIII and IX**

by **Nadia Freato**

To be defended on **Wednesday February 24th 2021 at 2:30 pm**

The public defence will be broadcasted on livestream.

**Paranymphs:**

Małgorzata Przeradzka
m.a.przeradzka@gmail.com

Ellie Karampini
elliekarampini@rcsi.ie

# *Viribus unitis* - the molecular synergism between coagulation factors VIII and IX

Nadia Freato

The research described in this thesis was performed at the Department of Molecular and Cellular Hemostasis of Sanquin Research, Amsterdam, The Netherlands

Cover design and layout of the book by Nadia Freato. The front illustration is based on the FVIII crystal structure by Ngo et al. (Protein Data Bank code: 3cdz) while the back illustration shows the FIXa crystal structure published by Hopfner et al. (Protein Data Bank code: 1rfn).


ISBN: 978-94-6419-106-6
Printed by Gilderprint B.V., Enschede, The Netherlands

Financial support for printing was kindly provided by Sanquin Research.

# *Viribus unitis* - the molecular synergism between coagulation factors VIII and IX

Met vereende krachten - de moleculaire synergie tussen de stollingfactoren VIII en IX

(met een samenvatting in het Nederlands)

## Proefschrift

ter verkrijging van de graad van doctor aan de Universiteit Utrecht
op gezag van de rector magnificus, prof.dr. H.R.B.M. Kummeling,
ingevolge het besluit van het college voor promoties
in het openbaar te verdedigen op

woensdag 24 februari 2021 des middags te 2.30 uur

door

**Nadia Freato**

geboren op 6 juli 1989 te Cittadella, Italië

Promotoren: Prof. dr. K. Mertens
Prof. dr. A.B. Meijer

Copromotor: Dr. M. van den Biggelaar

Financial support by the Dutch Heart Foundation for the publication of this thesis is gratefully aknowledged.

## TABLE OF CONTENTS

# Chapter 1

## General introduction

## SCOPE OF THIS THESIS

The process of haemostasis involves an intricate and balanced series of events aiming to prevent blood loss. Upon vessel damage, as the first step in wound healing, haemostasis (bleeding arrest) is achieved by three means: vasoconstriction, platelet plug formation and clot formation. Haemostasis not only contributes to the repair of vascular injury, but is also involved in maintaining blood flow, and moving the clot once the injury been repaired (fibrinolysis). Thus, blood coagulation holds an important role in haemostasis and consists of a fine balance between the action of pro-thrombotic and anti-coagulant factors. When the equilibrium between the two is disturbed, life-threatening conditions may arise[1].

During the past few decades, fundamental steps towards the understanding of molecular and dynamic mechanisms sustaining the coagulation cascade have been taken. Blood coagulation consists of a cascade of enzymatic reactions in which enzymes in collaboration with their cofactors or inhibitors preserve and maintain the blood stream[2,3]. Coagulation complexes are often highly homologous in terms of structure/function relationship. Nevertheless, protein-protein interactions within the coagulation system are highly specific. This is due to fine-tuned regulatory and allosteric mechanisms that assure functional uniqueness to each coagulation protein[4]. To date, many of these regulatory mechanisms and molecular interactions have remained to be resolved. Although the study of functional variants associated with bleeding disorders is greatly assisting the understanding of the mechanism of action of coagulation enzymes and cofactors, the release of the first 3D crystal structures have supplied the field with an extraordinary amount of information[5–7]. However, despite the fact that many isolated haemostatic proteins could finally be visualized, for most protein complexes structural information is still lacking. In addition, the rigidity of crystal structures complicates the linkage between structural properties and biological function.

In the present thesis some of these issues have been addressed using Hydrogen-Deuterium eXchange (HDX), covalent labelling by tandem-mass-tags (TMTs) coupled to mass spectrometry and protein engineering (mutagenesis and functional characterization). In **Chapter 2** we explored the structural differences between Factor V (FV) and Factor VIII (FVIII). These two cofactors serve different roles in the coagulation although they are highly homologous. Inspection of crystal structure, mutagenesis and functional assays were used to discovery unique structural elements involved in FVIII cofactor function. The structural changes that occur upon FVIII activation and the subsequent binding to its enzyme partner activated Factor IX (FIXa) were further explored by HDX in **Chapter 3**. Mass spectrometry analysis combined with mutagenesis studies led to identification of a previously unidentified region on activated FVIII (FVIIIa) that is important for its cofactor role in the stimulation of FIXa.

Since the interaction of FVIIIa with FIXa is fundamental for propagation of coagulation and given the poor intrinsic activity of FIXa by itself, we studied which allosteric changes are necessary for FIXa to reach proper catalysis in **Chapter 4**. HDX was further employed for the analysis of FIXa complexed with FVIIIa and bound to a pseudo-substrate. This study led to the identification of a FVIIIa binding site on FIXa and simultaneously allowed the discrimination of the allosteric changes that need to occur in FIXa to reach proper catalysis. While these findings suggest that FIXa requires both substrate and cofactor to develop full catalytic potential, it is not clear whether free FIXa is more enzyme- or zymogen-like. In **Chapter 5**, we used TMT labelling and HDX to address this question by comparing the FIX zymogen, FIXa and inhibitor-bound FIXa. We found that FIXa is predominantly zymogen-like, but does display a few enzyme-like properties that are inherent to its proteolytic processing.

## THE BLOOD COAGULATION CASCADE

The phenomenon of “thrombus” (clot) formation has intrigued philosophers and physicians since antiquity, so much so that a first written attempt was organized in the Hippocratic Collection (5$^{th}$ century B.C.) gathering multiple theories, from the elemental theory to the humoralism (humoral theory) postulated by Hippocrates (ca 460-370 B.C.)[8]. The humoral theory is based on the definition of four body fluids (blood, mucus, yellow and black bile) and built up the ground towards the definition of human physiology. The word “thrombus” was used for a plethora of medical conditions, from the clot that could be found inside the vessels, to the stones expelled with urine. In *De Natura Hominis,* Hippocrates first describes “the solid blood” to indicate a clot. Plato (ca 424/423-348/347 B.C.), founder of the Academy in Athens, believed that fibres were formed as soon as the blood cooled[8]. These fibres were actually fibrin, the ultimate product of the coagulation cascade. Aristotle (384-322 B.C.) in accordance to the elemental theory thought that these fibres were made of earth and if removed from the blood, the blood could no longer coagulate[8]. With the advent of the microscope, Marcello Malpighi in 1686 was the first to confirm Aristotle’s theory and separate the several elements of blood into cells, fibres and serum. A modern description of blood coagulation dates back to the 1960’s with the theories of a “waterfall” or “cascade” attributed to Davie, Ratnoff and Macfarlane[2,9]. Their pioneering papers in Nature and Science laid the basis for a modern view of blood coagulation. Today we know that the coagulation cascade, which leads to the formation of what Plato described as *fibres*, mainly consists of a sequential activation

of precursors (zymogens) into active serine proteases that in collaboration with their cofactors, catalyse the conversion of the precursor downstream in the cascade.

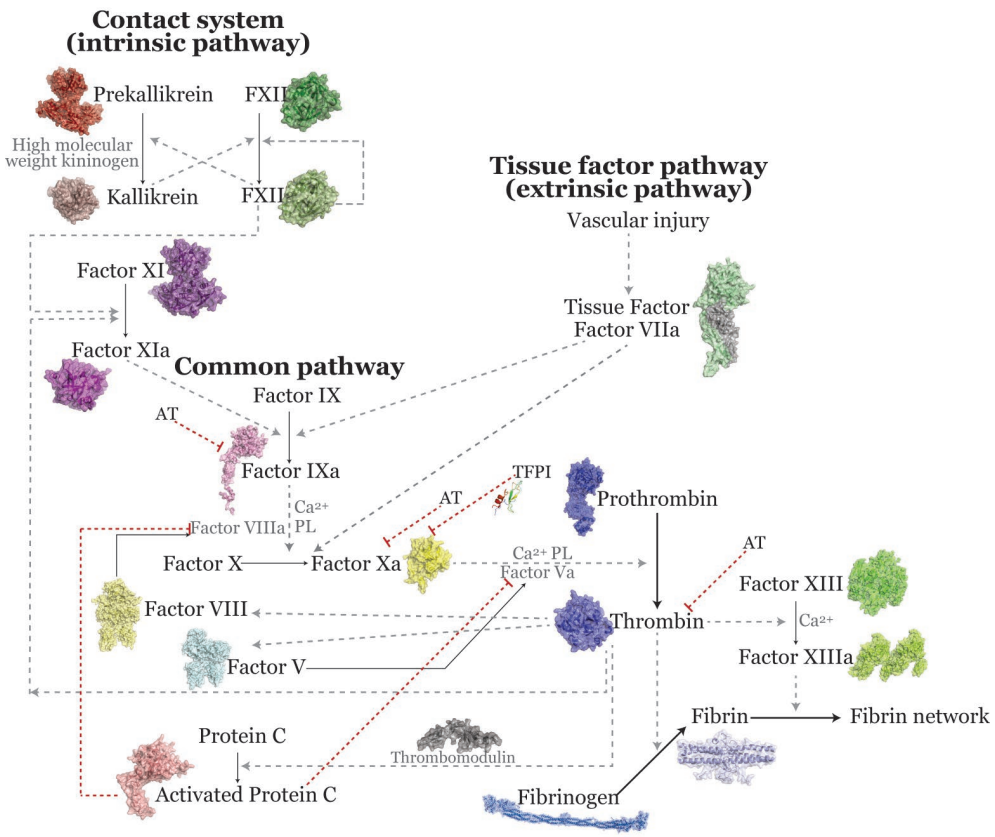


**Figure 1**
Schematic representation of the blood coagulation cascade. A crystal structure for every available enzyme or cofactor is depicted. PDB codes used: prekallikrein 6i44[60], kallikrein 5f8t[61], FXII 4xde[62], FXIIa 6b74[63], FXI 5eok[64], FXIa 5e2o[65], FIXa protease domain and EGF-2 2wpm[66], FIXa EGF-1 domain 1edm[67], FIXa Gla domain 1mgx[22], FVIIa and TF 1dan[7], FXa 5voe[68], FVIII 3cdz[6], FVai 1sdd[69], TFPI 1irh[70], prothrombin 5edm[71], thrombomodulin and thrombin 1dx5[72], APC 3f6u[73], FXIII 1fie[74], FXIIIa 5mho[75], fibrinogen 3ghg[76], fibrin 2a45[77]. The black arrows indicate the conversion of a zymogen or precursor into its activated form. The proteolytic enzyme mediating this conversion is indicated by grey dashed arrows. Red dashed lines indicate inhibition processes.

The clotting cascade is initiated by two mechanisms: the intrinsic and the extrinsic pathways that subsequently converge in a common pathway (Figure 1). The intrinsic pathway is activated by the exposure of negatively charged surfaces upon vessel damage. Here, the zymogen Factor XII (FXII), upon surface binding, changes its





conformation promoting a minor catalytic activity that triggers its self-cleavage and its activation by kallikrein (PKa). A positive feedback loop is then initiated in which activated FXII (FXIIa) cleaves prekallikrein (PK) complexed with high molecular weight kininogen (HK) into PKa. The serine protease FXIIa also converts Factor XI (FXI) into activated FXI (FXIa)[10]. The extrinsic pathway is triggered by substances exposed by the damaged tissue including the transmembrane protein tissue factor (TF). Traces of the protease activated Factor VII (FVIIa) are present in the blood stream[11], although in insufficient amount to initiate coagulation. Only the formation of the FVIIa-TF complex assures a proper catalytic activity of FVIIa.

Extrinsic and intrinsic pathway converge in the common pathway of the blood coagulation cascade, FVIIa in complex with TF activates the zymogen Factor IX (FIX) into the active enzyme activated FIX (FIXa). Moreover, FVIIa efficiently converts Factor X into activated FX (FXa)[12–14]. The traces of generated FXa convert small amounts of the key enzyme prothrombin into thrombin. The thrombin generated thereby is essential as an amplifier of the coagulation process activating the platelets and activating Factor V (FV), Factor VIII (FVIII) and FXI[15–18]. Concurrently, FXIa, generated by thrombin or FXIIa in the extrinsic pathway, converts more FIX into FIXa[19]. The generated FIXa assembles with the cofactor activated FVIII (FVIIIa) on activated platelets and with the substrate FX the complex takes the name of FXa-generating complex. Subsequently, FXa assembles with its cofactor activated FV (FVa) and efficiently converts more prothrombin into thrombin. Finally, thrombin promotes the fibrin clot formation converting fibrinogen into fibrin and Factor XIII (FXIIIa) into activated FXIII (FXIIIa). The latter assures the formation of the insoluble fibrin clot by cross-linking the fibrin polymers.

The coagulation cascade is also tightly regulated by inhibitors. The protein Tissue Factor Pathway Inhibitor (TFPI) for instance blocks the FVIIa-TF complex thereby inhibiting the intrinsic pathway. In addition, antithrombin (AT) as a potent inhibitor of the activity of serine proteases efficiently inhibits thrombin, FIXa and FXa. When bound to the cofactor thrombomodulin, thrombin converts Protein C into Activated Protein C (APC). APC complexed with the cofactor Protein S cleaves and inactivates FVa and FVIIIa, thereby terminating the clotting cascade.

## THE FACTOR X-ACTIVATING COMPLEX

The present thesis focusses on the first step of the common pathway of the coagulation cascade, the activation of FX by the FIXa-FVIIIa complex in which the serine protease FIXa assembles with its cofactor FVIIIa on a negatively charged surface in presence of calcium ions.

## Factor IX and Factor IXa

Human FIX is secreted by hepatocytes as zymogen of the serine protease FIXa. Prior to secretion FIX undergoes intracellular processing which includes the removal of the propeptide which is required for the proper Vitamin-K dependent γ-carboxylation of the protein[20]. FIX is then secreted as a single-chain 415 amino acids (56 kDa) molecule in the blood stream. As a Vitamin K-dependent protein, FIX shares the domain organization and functional homology with other serine proteases of the coagulation cascade like FVII, FX and Protein C. The structure of FIX consists of an N-terminal γ-carboxylated Gla domain, followed by two epidermal growth factor (EGF)-like domains, an activation peptide and a protease domain where, once activated, the catalytic activity resides[21] (Figure 2).

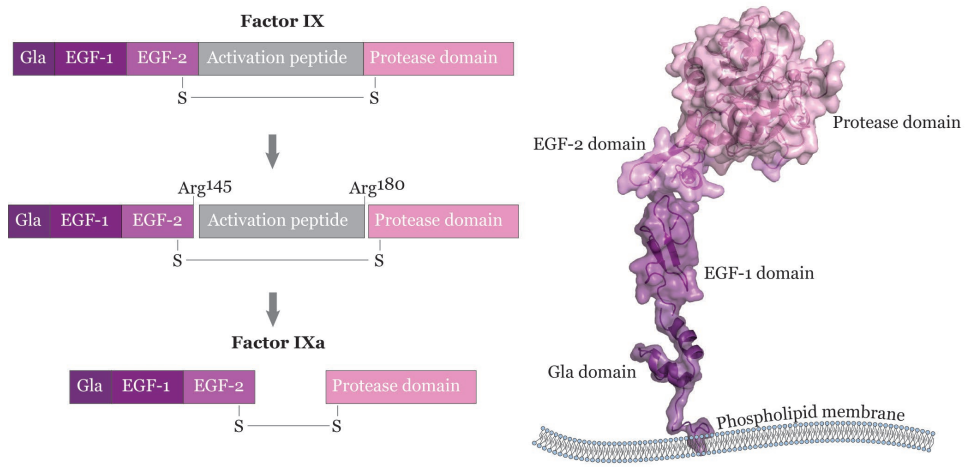


**Figure 2**
A schematic representation of FIX and FIXa domain organization is shown. The structure of FIXa is displayed on the right side of the Figure (PDB codes: FIXa protease domain and EGF-2 2wpm[66], FIXa EGF-1 domain 1edm[67], FIXa Gla domain 1mgx[22]).

The Gla domain is fundamental for the interaction with the negatively charged phospholipids necessary to promote the formation of the FIXa-FVIIIa complex. The membrane interaction occurs via γ-carboxyglutamic acid (Gla) residues. By virtue of the negative charges added by the Gla residues, the Gla domain coordinates high and low affinity divalent cations, in particular calcium ions[22–24]. The first EGF-like domain (EGF-1) also contains a high affinity binding site for calcium ions and two glycosylation sites[5]. It has been shown that the proper contact between the EGF-1





domain and the second EGF-like domain (EGF-2) is important for the enzymatic function[25]. The EGF-2 domain is connected to the activation peptide, a heavily glycosylated region that is removed upon activation. Finally, the protease domain, at the C-terminus of the protein is highly homologous to the one of other serine proteases and to the parental chymotrypsin. Among other similarities, the catalytic triad is the most conserved feature in the FIX protease domain consisting of the residues His221{$57_{CT}$}, Asp269{$102_{CT}$} and Ser365{$195_{CT}$}. Historically, a dual numbering is assigned to the FIX residues of the protease domain: the FIX numbering, and the chymotrypsinogen numbering, derived from the sequence alignment of FIX to the ancestor of the serine protease family, chymotrypsin. Therefore, in this thesis the chymotrypsinogen numbering is also reported with the acronym CT in subscript.

The conversion of FIX into FIXa undergoes the classical trypsinogen-trypsin transition[26] and is mediated proteolytically by FXIa or the FVIIa-TF complex in presence of calcium. Two cleavages occur in the FIX molecule between Arg145 and Ala146 and between Arg180 and Val181{$16_{CT}$}. The resulting molecule is an active enzyme consisting of two separate chains, a light chain of 18 kDa consisting of the Gla domain and the two EGFs domains and a heavy chain of 28 kDa composed by the protease domain[27]. The two chains are held together by a single disulphide bridge between Cys132 and Cys289{$122_{CT}$}. Similarly to other coagulation proteases like FVIIa, but unlike thrombin, the activation of FIX does not confer full catalytic potential and reveals to be more complex. In particular it requires additional steps that to date are not fully understood, including the binding to the cofactor FVIIIa[28,29].

## Factor VIII and Factor VIIIa

FVIII is synthetized in endothelial cells, mainly of the liver, as a large single chain glycoprotein of 2341 amino acids. Upon removal of the signal peptide (19 amino acids), FVIII is secreted as a heterodimer[30]. The FVIII molecule is organized into three homologous A domains, a B domain and two homologous C domains. Short acidic segments border the A domains (Figure 3). The overall structure can be ordered as A1-a1-A2-a2-B-a3-A3-C1-C2[30,31]. Post-translational modifications include specific sulphated tyrosine residues within the acidic regions and N-linked glycosylation. Processing of FVIII prior to secretion (cleavage by furin) results in a light chain composed by a3-A3-C1-C2 domains (80 kDa) and a heavy chain with A1-a1-A2-a2-B domains whose molecular weight ranges between 90 and 220 kDa due to limited proteolysis in the B domain[31,32]. The heavy and the light chain are held together by electrostatic and metal ion-dependent interactions[31,33]. The 3-D crystal structures of FVIII revealed useful insights for the understanding of the spatial organization of the domains. In particular FVIII can be visualized as a propeller-shaped molecule in which the A domains are stacked together on top of the two parallel C domains. FVIII

is highly homologous to FV which participates as a cofactor of FXa in the conversion of prothrombin into thrombin.

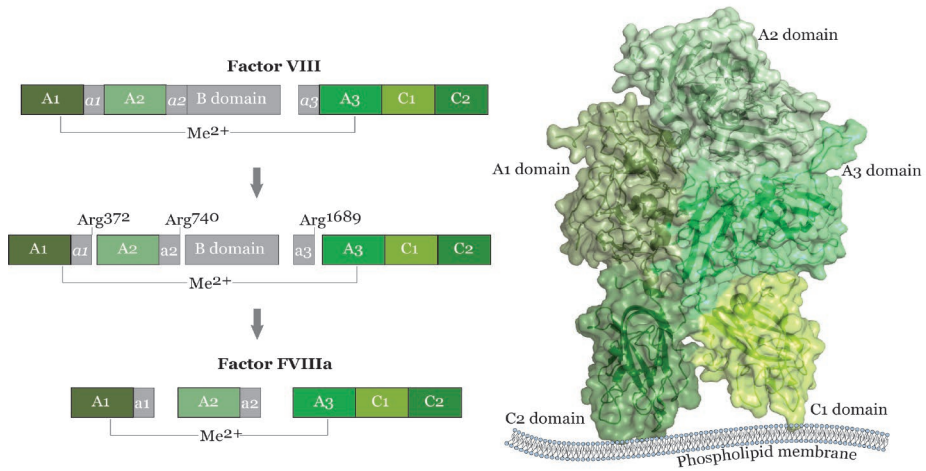


**Figure 3.**
A schematic representation of FVIII and FVIIIa domain organization is shown. The structure of FVIII is displayed on the right side of the Figure (PDB code: 3cdz[6]).

In plasma, the FVIII heterodimer circulates in a tight complex with the chaperone protein Von Willebrand Factor (VWF). VWF protects FVIII from degradation and plasma clearance[34]. VWF interaction sites have been identified in FVIII in the acidic region (a3) at the N-terminal side of the A3 domain and in the C1-C2 domains[35,36]. Upon initiation of the coagulation cascade, FVIII is converted by thrombin into the heterotrimer FVIIIa. Thrombin, or FXa, cleave in the heavy chain at positions Arg372 and Arg740 and in the light chain at Arg1689[30]. The proteolytic cleavages lead to the release of the B domain and the a3 domain and dissociation of the FVIII-VWF complex. Moreover, as a consequence of the activation process, the A2 domain is no longer covalently attached to the heavy chain. FVIIIa binds with high affinity to procoagulant membranes that expose phosphatidylserine (PS) through its C domains[37–40]. Therefore, FVIIIa provides a platform for the interaction with FIXa resulting in the fully active FX-activating complex. The dissociation of this complex occurs through spontaneous dissociation of the loosely attached A2 domain. Through dissociation of the A2 domain FVIIIa consequently loses its cofactor function[41,42]. Alternatively, FVIIIa is inactivated by APC, FIXa, FXa and plasmin[43–46]

## Haemophilia

The importance of the FXa-generating complex is critical since the functional





absence of FVIIIa or FIXa leads to the life-threatening bleeding disorders Haemophilia A or B, respectively. Both Haemophilia types are X-linked disorders with an incidence of 1 in 5,000 males for Haemophilia A and 1 in 30,000 males for Haemophilia B. Haemophilia has a long history in the European royal family. The most well-known story is the one of the carrier Queen Victoria of England who ruled from 1837-1901 and transmitted the disease to her daughters Alice and Beatrice, who became carriers and to her son Leopold, who suffered from Haemophilia. From Alice and Beatrice, the disease spread to the Russian, Prussians and Spanish royals.

Haemophilia can be distinguished in three forms: mild, moderate and severe based on the amount of functional coagulation factors present in plasma[47]. These disorders have been associated with a large number of mutations in FVIII and FIX genes ranging from the replacement of single amino acid residues, internal deletions and the introduction of a stop codon that leads to a truncation and thereby complete absence of the mature protein (splice variants). Mutations can occur at the protein core of FVIII and FIX causing a misfolding of the 3-D structure and thereby hinder secretion. Alternatively, mutations can occur within interactive surface loops thereby disrupting important interactive sites with protein partners or lipids. In Haemophilia B mutations of FIX are found at sites that are important for the protein regulation (allosteric regulation)[47–49]. However, the structural impact of most of these mutations has remained poorly understood.

## FIXa and FVIIIa interaction in the FX-activating complex

The study of mutants that are associated with Haemophilia greatly assisted the discovery of the interactive sites between FVIIIa and FIXa, provided deep functional knowledge and led to several therapeutic options for those affected. However, the mechanisms of FVIIIa-mediated catalytic rate enhancement of FIXa remain enigmatic to date. Multiple interactions are required for the enzyme-cofactor assembly. FIXa binds through the N-terminal section of the Gla domain (residues 3-11) to phospholipids that contain negative charges[24]. Compared with FIXa, FVIIIa shows higher affinity for phospholipid membranes, suggesting that FVIIIa brings FIXa to the procoagulant surface. It has been well established that a specificity for the negatively-charged phosphatidylserine (PS) exists[39,50]. The lipid binding occurs via the C domains in FVIIIa. In particular it was shown that the interaction is mediated through hydrophobic loops (spikes) that decorate the bottom of the C domains[38,40]. The primary lipid binding interactor is the C2 domain, but the C1 domain was described to mediate a high affinity interaction as well[36,40,51,52].

Extensive studies have been performed in the past on the interactive sites between FVIIIa and FIXa. Four potential FIXa binding regions have been located on FVIIIa (Figure 4). Region Ser558-Gln565 of the FVIIIa A2 domain in particular, has

previously been suggested to directly interact with FIXa. In fact, peptides belonging to the 556-559 region were found to inhibit both FX activation and the activity of FIXa protease domain in studies with isolated protein subunits[53,54]. Through FX activation studies, another putative binding region was found at the C-terminus of the A2 domain (Arg698-Asp712). Through homology studies and the functional evaluation of Haemophilia B mutants, it was proposed that the A2 domain binds the residues 301-303 and the α-helix region 333-339 on the protease domain of FIXa[55,56]. It was furthermore proposed that the light chain of FVIIIa directly interacts with the light chain of FIXa. In particular, region 1811-1818 on the A3 domain of FVIIIa was shown to include a binding site for FIXa[38]. Moreover, mutation of a glutamic acid residue at position 78 in the FIXa light chain was shown to impair complex formation affecting the FXa-generation[25]. It has been suggested that the interaction between the light chains of both enzyme and cofactor is the driving force behind the complex formation, which is then further stabilized by the interaction between the A2 domain of FVIIIa and the protease domain of FIXa[54,55,57]. Despite all this knowledge, however, molecular details assisting the activation of FXa in the FIXa-FVIIIa complex remain elusive. The interaction sites described in this paragraph, being inferred from functional studies, still lack structural confirmation. In other words, the structural dynamics sustaining FIXa catalysis and the mechanisms of activity amplification by the cofactor FVIII require further investigation.

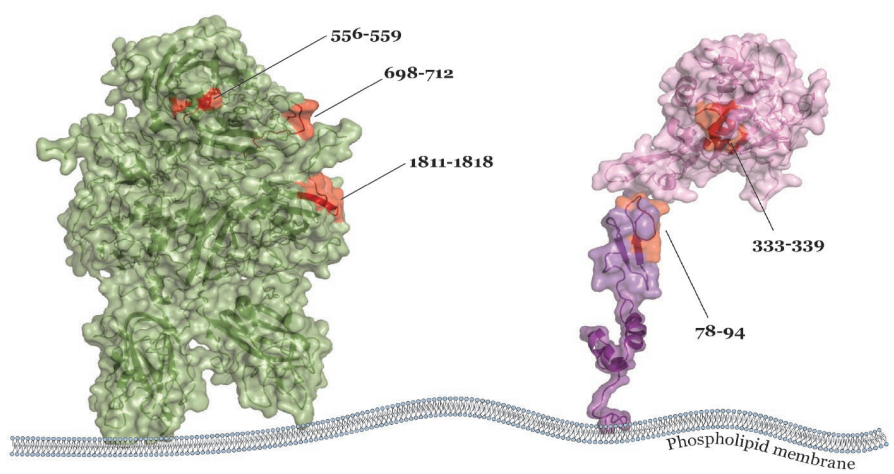


**Figure 4.**
Known interaction sites in FVIII (PDB code: 3cdz[6]), left panel, and FIXa (PDB codes: FIXa protease domain and EGF-2 2wpm[66], FIXa EGF-1 domain 1edm[67], FIXa Gla domain 1mgx[22]), right panel as inferred from functional studies.





### Structural studies of the FIXa-FVIII complex

The first crystal structure of FIXa was for the porcine protein and was released by Brandstetter and colleagues in 1995[5]. Subsequently, two structures for human FVIII were resolved in 2008[6,58]. The necessity of a membrane surface and the presence of structural elements incompatible with the generation of crystals hinder the visualization of the FIXa-FVIIIa complex. This is further complicated by the inherent instability of FVIII after activation. Moreover, all the available FIXa crystals could be obtained only in presence of inhibitors that block or "freeze" the FIXa structure, which obviously impedes the appreciation of the dynamics sustaining complex formation and catalysis.

## MASS SPECTROMETRY TO IDENTIFY AND UNRAVEL CONFORMATIONAL CHANGES AND BINDING SITES

Mass spectrometry in combination with footprinting approaches and covalent labelling techniques has been employed to identify interaction sites between protein partners and changes in conformation induced by ligand binding. Examples include the use of isobaric mass tags targeting specific amino acid residues, crosslinking reagents and Hydrogen-Deuterium eXchange. The basic concept relies on the fact that protein regions located at the surface are easily modified compared to regions that are less exposed to the surface. Among these less exposed regions, protein areas that are actively involved in an interaction with a protein partner have also a decreased labelling efficiency. An advantage of these footprinting methods is that the labelling reactions can be performed in an aqueous environment and therefore the dynamics of a protein or protein complex can be maintained. In this thesis we employ Hydrogen-Deuterium eXchange coupled to Mass Spectrometry (HDX-MS) in order to unravel binding sites between in the FIXa-FVIIIa complex and the allosteric regulation at the basis of complex function.

### Hydrogen-Deuterium eXchange Mass Spectrometry

HDX-MS relies on the principle that a protein in an aqueous environment naturally exchanges its hydrogens with the surrounding water. This can be exploited by incubating a protein in deuterated water ($D_2O$). Hydrogens exchange with deuterium and the deuterium incorporation can be measured by mass spectrometry. Importantly, the exchange rates are influenced by the type of bond. Hydrogen of C-H bonds display insignificantly slow exchange to be measured while hydrogens of the side chains exchange too fast. Only hydrogen of the amide backbone can be effectively monitored[59].

Various structural elements display different exchange rates. For instance,

α-helices and β-sheets which contain many hydrogen bonds show a relatively low exchange, while the HDX rate is higher for less structured regions like surface loops. Protein binding partners can also influence exchange rates. In fact, protein interfaces engaged in interactions with a ligand have a less effective exchange while regions liberated from the binding will exchange faster. Temperature and pH are very important factors that can be used to modulate HDX. Low temperature and pH are used to quench the exchange. A challenge in HDX protocols is hydrogen/deuterium back-exchange prior mass spectrometer analysis. A fast-proteolytic digestion and a low pH and temperature are generally used to overcome this phenomenon.

## ISSUES ADDRESSED IN THIS THESIS

In **Chapter 2** a structural approach is taken to compare the highly homologous FV and FVIII structures in order to find unique elements assisting FVIII cofactor function. Given the great potential of HDX in analysing the dynamics of protein structures, we employ this technique to address the structural changes that occur upon activation and protein-protein interaction in FVIII (**Chapter 3**) and in FIXa (**Chapter 4**). In **Chapter 5** we dive deeper in the understanding of FIXa functioning and enzymatic structural elements, employing also primary amine labelling coupled to mass spectrometry.





## REFERENCES


1. Versteeg HH, Heemskerk JWM, Levi M, Reitsma PH. New Fundamentals in Hemostasis. *Physiol Rev*. 2013;93(1):327-358.

2. Davie EW, Ratnoff OD. Waterfall sequence for intrinsic blood clotting. *Science*. 1964;145(3638):1310-1312.

3. Nemerson Y, Furie B, Jackson CM. Zymogens and cofactors of blood coagulation. *Crit Rev Biochem Mol Biol*. 1980;9(1):45–85.

4. Goettig P, Brandstetter H, Magdolen V. Surface loops of trypsin-like serine proteases as determinants of function. *Biochimie*. 2019;166:52-76.

5. Brandstetter H, Bauer M, Huber R, Lollar P, Bode W. X-ray structure of clotting factor IXa: active site and module structure related to Xase activity and hemophilia B. *Proc Natl Acad Sci U A*. 1995;92(21):9796–9800.

6. Ngo JC, Huang M, Roth DA, Furie BC, Furie B. Crystal structure of human factor VIII: implications for the formation of the factor IXa-factor VIIIa complex. *Structure*. 2008;16(4):597–606.

7. Banner DW, D'Arcy A, Chene C, et al. The crystal structure of the complex of blood coagulation factor VIIa with soluble tissue factor. *Nature*. 1996;380(6569):41–46.

8. Tsoucalas G, Karamanou M, Papaioannou TG, Sgantzos M. Theories About Blood Coagulation in the Writings of Ancient Greek Medico-philosophers. *Curr Pharm Des*. 2017;23(9):1275-1278.

9. Macfarlane RG. An enzyme cascade in the blood clotting mechanism, and its function as a biochemical amplifier. *Nature*. 1964;202:498-499.

10. de Maat S, Tersteeg C, Herczenik E, Maas C. Tracking down contact activation - from coagulation in vitro to inflammation in vivo. *Int J Lab Hematol*. 2014;36(3):374-381.

11. Morrissey JH, Macik BG, Neuenschwander PF, Comp PC. Quantitation of activated factor VII levels in plasma using a tissue factor mutant selectively deficient in promoting factor VII activation. *Blood*. 1993;81(3):734-744.

12. Morrison SA, Jesty J. Tissue factor-dependent activation of tritium-labeled factor IX and factor X in human plasma. *Blood*. 1984;63(6):1338-1347.

13. Jesty J, Silverberg SA. Kinetics of the tissue factor-dependent activation of coagulation Factors IX and X in a bovine plasma system. *J Biol Chem*. 1979;254(24):12337-12345.

14. Krishnaswamy S, Field KA, Edgington TS, Morrissey JH, Mann KG. Role of the membrane surface in the activation of human coagulation factor X. *J Biol Chem*. 1992;267(36):26110–26120.

15. Osterud B, Rapaport SI. Activation of factor IX by the reaction product of tissue factor and factor VII: additional pathway for initiating blood coagulation. *Proc Natl Acad Sci U S A*. 1977;74(12):5260-5264.

16. Brummel KE, Paradis SG, Butenas S, Mann KG. Thrombin functions during tissue factor-induced blood coagulation. *Blood*. 2002;100(1):148-152.

17. Butenas S, van 't Veer C, Mann KG. Evaluation of the initiation phase of blood coagulation using ultrasensitive assays for serine proteases. *J Biol Chem*. 1997;272(34):21527-21533.

18. Pieters J, Lindhout T, Hemker HC. In situ-generated thrombin is the only enzyme that effectively activates factor VIII and factor V in thromboplastin-activated plasma. *Blood*. 1989;74(3):1021-1024.

19. Walsh PN. Roles of platelets and factor XI in the initiation of blood coagulation by thrombin. *Thromb Haemost*. 2001;86(1):75-82.

20. Wojcik EG, Van Den Berg M, Poort SR, Bertina RM. Modification of the N-terminus of human factor IX by defective propeptide cleavage or acetylation results in a destabilized calcium-induced conformation: effects on phospholipid binding and activation by factor XIa. *Biochem J*. 1997;323 ( Pt 3):629–636.

21. Furie B, Furie BC. The molecular basis of blood coagulation. *Cell*. 1988;53(4):505-518.

22. Freedman SJ, Blostein MD, Baleja JD, Jacobs M, Furie BC, Furie B. Identification of the phospholipid binding site in the vitamin K-dependent blood coagulation protein factor IX. *J Biol Chem*. 1996;271(27):16227–16236.

23. Freedman SJ, Furie BC, Furie B, Baleja JD. Structure of the metal-free γ-carboxyglutamic acid-rich membrane binding region of factor IX by two-dimensional NMR spectroscopy. *J Biol Chem*. 1995;270(14):7980-7987.

24. Jacobs M, Freedman SJ, Furie BC, Furie B. Membrane binding properties of the factor IX gamma-carboxyglutamic acid-rich domain prepared by chemical synthesis. *J Biol Chem*. 1994;269(41):25494–25501.

25. Christophe OD, Lenting PJ, Kolkman JA, Brownlee GG, Mertens K. Blood coagulation factor IX residues Glu78 and Arg94 provide a link between both epidermal growth factor-like domains that is crucial in the interaction with factor VIII light chain. *J Biol Chem*. 1998;273(1):222–227.

26. Bode W. The transition of bovine trypsinogen to a trypsin-like state upon strong ligand binding. II. The binding of the pancreatic trypsin inhibitor and of isoleucine-valine and of sequentially related peptides to trypsinogen and to p-guanidinobenzoate-trypsinoge. *J Mol Biol*. 1979;127(4):357–374.

27. Bajaj SP, Rapaport SI, Russell WA. Redetermination of the rate-limiting step in the activation of factor IX by factor XIa and by factor VIIa/tissue factor. Explanation for different electrophoretic radioactivity profiles obtained on activation of 3H- and 125I-labeled factor IX. *Biochemistry*. 1983;22(17):4047–4053.

28. Byrne R, Link RP, Castellino FJ. A kinetic evaluation of activated bovine blood coagulation factor IX toward synthetic substrates. *J Biol Chem*. 1980;255(11):5336-5341.

29. Zogg T, Brandstetter H. Activation mechanisms of coagulation factor IX. *Biol Chem*. 2009;390(5-6):391–400.

30. Fay PJ. Factor VIII structure and function. *Int J Hematol*. 2006;83(2):103–108.

31. Vehar GA, Keyt B, Eaton D, et al. Structure of human factor VIII. *Nature*. 1984;312(5992):337-342.

32. Andersson LO, Forsman N, Huang K, et al. Isolation and characterization of human factor VIII: molecular forms in commercial factor VIII concentrate, cryoprecipitate, and plasma. *Proc Natl Acad Sci U S A*. 1986;83(9):2979-2983.

33. Lenting PJ, van Mourik JA, Mertens K. The life cycle of coagulation factor VIII in view of its structure and function. *Blood*. 1998;92(11):3983-3996.

34. Pipe SW, Montgomery RR, Pratt KP, Lenting PJ, Lillicrap D. Life in the shadow of a dominant partner: the FVIII-VWF association and its clinical implications for hemophilia A. *Blood*. 2016;128(16):2007-2016.

35. Leyte A, van Schijndel HB, Niehrs C, et al. Sulfation of Tyr1680 of human blood coagulation factor VIII is essential for the interaction of factor VIII with von Willebrand factor. *J Biol Chem*. 1991;266(2):740-746.

36. Gilbert GE, Kaufman RJ, Arena AA, Miao H, Pipe SW. Four hydrophobic amino acids of the factor VIII C2 domain are constituents of both the membrane-binding and von Willebrand factor-binding motifs. *J Biol Chem*. 2002;277(8):6374-6381.

37. Ahmad SS, Walsh PN. Role of the C2 domain of factor VIIIa in the assembly of factor-X activating complex on the platelet membrane. *Biochemistry*. 2005;44(42):13858–13865.

38. Bloem E, van den Biggelaar M, Wroblewska A, et al. Factor VIII C1 domain spikes 2092-2093 and 2158-2159 comprise regions that modulate cofactor function and cellular uptake. *J Biol Chem*. 2013;288(41):29670–29679.

39. Gilbert GE, Drinkwater D. Specific membrane binding of factor VIII is mediated by O-phospho-L-serine, a moiety of phosphatidylserine. *Biochemistry*. 1993;32(37):9577–9585.

40. Gilbert GE, Novakovic VA, Kaufman RJ, Miao H, Pipe SW. Conservative mutations in the C2 domains of factor VIII and factor V alter phospholipid binding and cofactor activity. *Blood*. 2012;120(9):1923–1932.





41. Lollar P, Parker ET. Structural basis for the decreased procoagulant activity of human factor VIII compared to the porcine homolog. *J Biol Chem*. 1991;266(19):12481-12486.

42. Fay PJ, Haidaris PJ, Smudzin TM. Human factor VIIIa subunit structure. Reconstruction of factor VIIIa from the isolated A1/A3-C1-C2 dimer and A2 subunit. *J Biol Chem*. 1991;266(14):8957–8962.

43. Eaton D, Rodriguez H, Vehar GA. Proteolytic processing of human factor VIII. Correlation of specific cleavages by thrombin, factor Xa, and activated protein C with activation and inactivation of factor VIII coagulant activity. *Biochemistry*. 1986;25(2):505-512.

44. Lamphear BJ, Fay PJ. Proteolytic interactions of factor IXa with human factor VIII and factor VIIIa. *Blood*. 1992;80(12):3120–3126.

45. O'Brien DP, Johnson D, Byfield P, Tuddenham EG. Inactivation of factor VIII by factor IXa. *Biochemistry*. 1992;31(10):2805-2812.

46. Nogami K, Shima M, Matsumoto T, Nishiya K, Tanaka I, Yoshioka A. Mechanisms of plasmin-catalyzed inactivation of factor VIII: a crucial role for proteolytic cleavage at Arg336 responsible for plasmin-catalyzed factor VIII inactivation. *J Biol Chem*. 2007;282(8):5287-5295.

47. Mannucci PM, Tuddenham EG. The hemophilias--from royal genes to gene therapy. *N Engl J Med*. 2001;344(23):1773-1779.

48. Franchini M, Mannucci P. Past, present and future of hemophilia: a narrative review. *Orphanet J Rare Dis*. 2012;7(1):24.

49. Furie B, Furie BC. Molecular basis of hemophilia. *Semin Hematol*. 1990;27(3):270–285.

50. Gilbert GE, Novakovic VA, Shi J, Rasmussen J, Pipe SW. Platelet binding sites for factor VIII in relation to fibrin and phosphatidylserine. *Blood*. 2015;126(10):1237–1244.

51. Lu J, Pipe SW, Miao H, Jacquemin M, Gilbert GE. A membrane-interactive surface on the factor VIII C1 domain cooperates with the C2 domain for cofactor function. *Blood*. 2011;117(11):3181–3189.

52. Meems H, Meijer AB, Cullinan DB, Mertens K, Gilbert GE. Factor VIII C1 domain residues Lys 2092 and Phe 2093 contribute to membrane binding and cofactor activity. *Blood*. 2009;114(18):3938–3946.

53. Fay PJ, Beattie T, Huggins CF, Regan LM. Factor VIIIa A2 subunit residues 558-565 represent a factor IXa interactive site. *J Biol Chem*. 1994;269(32):20522–20527.

54. Fay PJ, Koshibu K. The A2 subunit of factor VIIIa modulates the active site of factor IXa. *J Biol Chem*. 1998;273(30):19049–19054.

55. Kolkman JA, Lenting PJ, Mertens K. Regions 301-303 and 333-339 in the catalytic domain of blood coagulation factor IX are factor VIII-interactive sites involved in stimulation of enzyme activity. *Biochem J*. 1999;339:217–221.

56. Bajaj SP, Schmidt AE, Mathur A, et al. Factor IXa:Factor VIIIa interaction. Helix 330-338 of factor IXa interacts with residues 558-565 and spatially adjacent regions of the A2 subunit of factor VIIIa. *J Biol Chem*. 2001;276(19):16302–16309.

57. Mertens K, Celie PH, Kolkman JA, Lenting PJ. Factor VIII-factor IX interactions: molecular sites involved in enzyme-cofactor complex assembly. *Thromb Haemost*. 1999;82(2):209–217.

58. Shen BW, Spiegel PC, Chang CH, et al. The tertiary structure and domain organization of coagulation factor VIII. *Blood*. 2008;111(3):1240–1247.

59. Mayne L. Hydrogen Exchange Mass Spectrometry. *Methods Enzym*. 2016;566:335–356.

60. Li C, Voos KM, Pathak M, et al. Plasma kallikrein structure reveals apple domain disc rotated conformation compared to factor XI. *J Thromb Haemost JTH*. 2019;17(5):759-770. doi:10.1111/jth.14418

61. Xu M, Jiang L, Xu P, Luo Z, Andreasen P, Huang M. The crystal structure of human Plasma Kallikrein in complex with its peptide inhibitor pkalin-2. doi:10.2210/pdb5f8t/pdb

62. Pathak M, Manna R, Li C, et al. Crystal

structures of the recombinant β-factor XIIa protease with bound Thr-Arg and Pro-Arg substrate mimetics. *Acta Crystallogr Sect Struct Biol*. 2019;75(Pt 6):578-591.

63. Dementiev A, Silva A, Yee C, et al. Structures of human plasma β-factor XIIa cocrystallized with potent inhibitors. *Blood Adv*. 2018;2(5):549-558.

64. Wong SS, Østergaard S, Hall G, et al. A novel DFP tripeptide motif interacts with the coagulation factor XI apple 2 domain. *Blood*. 2016;127(23):2915-2923.

65. Smith LM, Orwat MJ, Hu Z, et al. Novel phenylalanine derived diamides as Factor XIa inhibitors. *Bioorg Med Chem Lett*. 2016;26(2):472-478.

66. Zogg T, Brandstetter H. Structural basis of the cofactor- and substrate-assisted activation of human coagulation factor IXa. *Structure*. 2009;17(12):1669–1678.

67. Rao Z, Handford P, Mayhew M, Knott V, Brownlee GG, Stuart D. The structure of a $Ca^{2+}$-binding epidermal growth factor-like domain: its role in protein-protein interactions. *Cell*. 1995;82(1):131-141.

68. Gunaratne R, Kumar S, Frederiksen JW, et al. Combination of aptamer and drug for reversible anticoagulation in cardiopulmonary bypass. *Nat Biotechnol*. 2018;36(7):606-613.

69. Adams TE, Hockin MF, Mann KG, Everse SJ. The crystal structure of activated protein C-inactivated bovine factor Va: Implications for cofactor function. *Proc Natl Acad Sci U S A*. 2004;101(24):8918-8923.

70. Mine S, Yamazaki T, Miyata T, Hara S, Kato H. Structural mechanism for heparin-binding of the third Kunitz domain of human tissue factor pathway inhibitor. *Biochemistry*. 2002;41(1):78-85.

71. Pozzi N, Chen Z, Di Cera E. How the Linker Connecting the Two Kringles Influences Activation and Conformational Plasticity of Prothrombin. *J Biol Chem*. 2016;291(12):6071-6082.

72. Fuentes-Prior P, Iwanaga Y, Huber R, et al. Structural basis for the anticoagulant activity of the thrombin-thrombomodulin complex. *Nature*. 2000;404(6777):518-525.

73. Schmidt AE, Padmanabhan K, Underwood MC, Bode W, Mather T, Bajaj SP. Thermodynamic linkage between the S1 site, the $Na^{+}$ site, and the $Ca^{2+}$ site in the protease domain of human activated protein C (APC). Sodium ion in the APC crystal structure is coordinated to four carbonyl groups from two separate loops. *J Biol Chem*. 2002;277(32):28987–28995.

74. Yee VC, Pedersen LC, Bishop PD, Stenkamp RE, Teller DC. Structural evidence that the activation peptide is not released upon thrombin cleavage of factor XIII. *Thromb Res*. 1995;78(5):389-397.

75. Stieler M, Heine A, Klebe G. FXIIIa in complex with the inhibitor ZED2369. doi:10.2210/pdb5mho/pdb

76. Kollman JM, Pandi L, Sawaya MR, Riley M, Doolittle RF. Crystal structure of human fibrinogen. *Biochemistry*. 2009;48(18):3877-3886.

77. Pechik I, Yakovlev S, Mosesson MW, Gilliland GL, Medved L. Structural basis for sequential cleavage of fibrinopeptides upon fibrin assembly. *Biochemistry*. 2006;45(11):3588-3597.

# Chapter 2

## Unique surface-exposed hydrophobic residues in the C1 domain of factor VIII contribute to cofactor function and Von Willebrand Factor binding

*Małgorzata A. Przeradzka[1], ***Nadia Freato**[1], Mariëtte Boon-Spijker[1], Josse van Galen[1], Carmen van der Zwaan[1], Koen Mertens[1,2], Maartje van den Biggelaar[1], Alexander B. Meijer[1,3]

*Both authors contributed equally to this study

From the Department of [1]Molecular and Cellular Hemostasis, Sanquin Research, 1066 CX Amsterdam, The Netherlands, [2]Department of Pharmaceutics and [3]Department of Biomolecular Mass Spectrometry and Proteomics, Utrecht Institute for Pharmaceutical Sciences (UIPS), Utrecht University, 3584 CG Utrecht, The Netherlands

**J Thromb Haemost. 2020 Feb;18(2):364-372.**

## ESSENTIALS

- Factor VIII C1 domain comprises unresolved factor IXa and Von Willebrand Factor binding sites
- A factor VIII/factor V C1 chimera has decreased affinity for factor IXa and Von Willebrand Factor
- In contrast to factor V, factor VIII C1 domain has unique surface-exposed hydrophobic residues
- The exposed hydrophobic residues contribute to factor IXa and Von Willebrand Factor binding






## ABSTRACT

### Background

The identity of the amino acid regions of factor VIII (FVIII) that contribute to factor IXa (FIXa) and Von Willebrand Factor (VWF) binding has not been fully resolved. Previously, we observed that replacing the FVIII C1 domain for the one of factor V (FV) markedly reduces VWF binding and cofactor function. Compared to the FV C1 domain, this implies that the FVIII C1 domain comprises unique surface-exposed elements involved in VWF and FIXa interaction.

### Objective

The aim of this study is to identify residues in the FVIII C1 domain that contribute to VWF and FIXa binding.

### Methods

Structures and primary sequences of FVIII and FV were compared to identify surface-exposed residues unique to the FVIII C1 domain. The identified residues were replaced into alanine residues to identify their role in FIXa and VWF interaction. This role was assessed employing surface plasmon resonance analysis studies and enzyme kinetic assays.

### Results

Five surface-exposed hydrophobic residues unique to the FVIII C1 domain, i.e.: F2035, F2068, F2127, V2130, I2139 were identified. Functional analysis indicated that residues F2068, V2130 and especially F2127 contribute to VWF and/or FIXa interaction. Substitution into alanine of the also surface-exposed V2125, which is spatially next to F2127, affected only VWF binding.

### Conclusion

The surface-exposed hydrophobic residues in C1 domain contribute to cofactor function and VWF binding. These findings provide novel information on the fundamental role of the C1 domain in FVIII life-cycle.

## INTRODUCTION

Coagulation Factor VIII (FVIII) is a large heterodimeric protein that serves its role in the coagulation cascade as a cofactor for activated Factor IX (FIXa) during the proteolytic conversion of Factor X (FX) into activated FX (FXa). FVIII is essential for proper functioning of the coagulation cascade as its functional absence has been associated with the X-linked bleeding disorder hemophilia A[1].

FVIII is synthesized as a single chain protein of 2332 amino acids, which are organized into three homologous A domains, a B domain and two homologous C domains. Short acidic amino acid regions comprising sulphated tyrosine amino acid residues are at the C-terminal side of A1 and A2 domains and at the N-terminal side of the A3 domain[2,3]. Prior to secretion, FVIII is processed into a heavy chain (domains: A1-A2-B) and a light chain (domains: A3-C1-C2), which remain associated via electrostatic and metal ion-dependent interactions[3]. Because of limited proteolysis of the B domain, the molecular weight of FVIII in plasma ranges between 170 kDa and 300 kDa[2,4–7]. The crystal structures of FVIII show that the A domains are ordered in a triangular shape stacked on top of two C domains aligned in parallel[8–10].

FVIII circulates in plasma in a tight complex with Von Willebrand factor (VWF). In this complex, FVIII is protected from premature ligand binding, proteolytic degradation, and rapid plasma clearance[11,12]. Upon initiation of the coagulation cascade, FVIII is activated by thrombin, which cleaves specific sites next to the acidic regions of FVIII[3]. This leads to the release of the B domain, disconnection of the A1 and A2 domains and dissociation of the FVIII:VWF complex. After activation, FVIII can bind with high affinity to procoagulant phospholipid membranes that expose phosphatidylserine (PS) in the outer leaflet. Activated FVIII (FVIIIa) that is bound to the phospholipid surface provides a platform for effective interaction with FIXa resulting in the activated FX-generating complex.

Because of the high structural similarity between FVIII and factor V (FV), chimeric variants of FVIII and FV have been utilized in a number of studies to gain insight into the structure and function of FVIII and FV[13–16]. Factor V (FV) is the cofactor for FXa in the coagulation cascade and can form together with FXa and procoagulant phospholipid membranes the prothrombinase complex that efficiently converts prothrombin into thrombin[8,17]. Using FVIII/FV chimeric proteins, the phospholipid binding role of the hydrophobic surface loops at the bottom of the C domains has, for instance, been addressed[8,13,18–21]. Another example is that contribution of the C domains to the intracellular trafficking of FVIII to the Weibel-Palade bodies has been studied in endothelial cells using chimeric FVIII/FV variants[15].

Several FIXa and VWF interaction sites have been identified in FVIII. Competition studies with FVIII-derived peptides or isolated subunits indicated that the C2 domain may comprise a binding site for FIXa[22]. Using site directed mutagenesis studies, interaction sites for FIXa have further been identified in the A2 and A3 domain[23,24]. For the interaction with VWF, convincing evidence has been provided that the acidic region at the N-terminal side of the A3 domain is critical[25–27]. It has also been proposed that the C1 and C2 domains contribute to VWF binding as well[18,28,29]. However, a FVIII variant in which the C2 domain was replaced by the C2 domain of FV ($FVIII_{C2FVC2}$) displayed only a small reduction in VWF binding and nearly normal cofactor function[15]. This shows that the main interaction sites for VWF and FIXa are, most likely, outside the C2 domain.

In a previous study, we established that replacing the C1 domain of FVIII with that of FV ($FVIII_{C1FVC1}$) has a major impact on VWF binding and FVIII cofactor function[15]. This suggests that the C1 domain of FV lacks surface-exposed structural elements that can support the interaction with FIXa and VWF. In the present study, we now compare the C1 domains of FVIII and FV to identify the unique surface-exposed elements on the FVIII C1 domain that contribute to cofactor function and VWF binding. Results revealed five surface-exposed hydrophobic residues that were either more polar or more buried in the C1 domain core of FV, i.e.: F2035, F2068, F2127, V2130, I2139. Site directed mutagenesis of FVIII followed by functional studies showed that these residues differentially contribute to FIXa and/or VWF binding. In particular F2127 proved to be important for both the interaction with VWF and FIXa.

## MATERIALS AND METHODS

### Materials

Fine chemicals were from Merck (Darmstadt, Germany), unless otherwise stated. DMEM-F12 medium was from Lonza (Breda, Netherlands), Foetal Calf Serum (FCS) was from Bodinco (Alkmaar, The Netherlands). DMRIE-C reagent and Opti-MEM medium were from Thermo Fisher Scientific (Landsmeer, The Netherlands). Chicken egg L-α-phosphatidylcholine (PC), L-α-phosphatidylethanolamine (PE) and porcine brain L-α-phosphatidylserine (PS) were from Avanti Polar Lipids Inc. (Alabaster, USA). Geneticin G-418 sulphate, precast SDS/PAGE gels and Brilliant Blue Coomassie were from from Invitrogen (Breda, The Netherlands). Tris-HCl was from Invitrogen (Breda, The Netherlands), NaCl was obtained from Fagron (Rotterdam, The Netherlands) and HEPES was from Serva (Heidelberg, Germany). Human Serum Albumin (HSA) was from the Division of Products of Sanquin (Amsterdam, The Netherlands). The FXa substrate S-2765 with the thrombin inhibitor I-2581 was from Chiralix (Nijmegen, Netherlands).

## Alignments of the FVIII and FV models

The crystal structure of the human B-domain deleted FVIII was aligned with the one of the bovine inactivated FVa with Pymol (PyMOL, Molecular Graphics System, v1.3, Schrödinger, LLC). Values of the Accessible Surface Areas (ASA, Å$^2$) were obtained from the "Protein Interfaces, Surfaces and Assemblies Service" (PISA) at the European Bioinformatics Institute (EBI, http://www.ebi.ac.uk/pdbe/prot_int/pistart.html) using the PDB codes 2r7e for the FVIII crystal structure and 1sdd for the FVai crystal structure and then compared with each other. Hydrophobicity of amino acid residues residing on the C1 domain was evaluated according to the hydrophobicity scale[9,30–32]. Alignment of the human FVIII to the bovine and human FV were taken from Liu et al[33].

| Variant | | Primer sequence |
|---|---|---|
| F2035A | sense | 5'-AGCGGCCACATCCGGGACGCCCAGATCACCGCCTCCGGC-3' |
| | anti-sense | 5'-GCCGGAGGCGGTGATCTGGGCGTCCCGGATGTGGCCGCT-3' |
| F2068A | sense | 5'-TGGTCCACCAAAGAGCCCGCCAGCTGGATCAAGGTGGAC-3' |
| | anti-sense | 5'-GTCCACCTTGATCCAGCTGGCGGGCTCTTTGGTGGACCA-3' |
| V2125A | sense | 5'-AGCACCGGCACCCTGATGGCCTTCTTCGGCAACGTGGAC-3' |
| | anti-sense | 5'-GTCCACGTTGCCGAAGAAGGCCATCAGGGTGCCGGTGCT-3' |
| F2127A | sense | 5'-GGCACCCTGATGGTGTTCGCCGGCAACGTGGACAGCAGC-3' |
| | anti-sense | 5'-GCTGCTGTCCACGTTGCCGGCGAACACCATCAGGGTGCC-3' |
| V2130A | sense | 5'-ATGGTGTTCTTCGGCAACGCCGACAGCAGCGGCATCAAG-3' |
| | anti-sense | 5'-CTTGATGCCGCTGCTGTCGGCGTTGCCGAAGAACACCAT-3' |
| I2139A | sense | 5'-AGCGGCATCAAGCACAACGCCTTCAACCCCCCCATCATT-3' |
| | anti-sense | 5'-AATGATGGGGGGGTTGAAGGCGTTGTGCTTGATGCCGCT-3' |

**Table 1.** Primers used in this study to obtain single substitutions of the C1 domain.

## Proteins

B-domain deleted FVIII (GenBank accession number ABV90867.1) was codon optimized and purchased from Thermo Fisher Scientific (USA) in a pcDNA3.1(+) expression vector using NheI and NotI restriction. FVIII B domain-deleted variants with single amino acid substitutions F2035A, F2068A, V2125A, F2127A, V2130A and I2139A were obtained by site-directed mutagenesis. Site-directed mutagenesis was performed using the QuikChange kit (Agilent Technologies, Amstelveen, The Netherlands) using appropriate primers (Table 1). DNA sequences were verified by sequencing analysis of the FVIII encoding parts on the mutated plasmid using BigDye Terminator Sequencing kit (Applied Biosystems, Foster City, USA). Stable transfection of Human Embryonic Kidney 293 cells (HEK293) and protein production was performed as described[34]. Recombinant FVIII mutants and wild-type were purified using VK34 monoclonal antibody[35] as described by Meems et al[36]. SDS-PAGE of the purified FVIII variants is shown in Supplementary Figure 1. Recombinant VWF was prepared as described previously[37]. Human plasma derived FIXa, FX and α-thrombin were purified as indicated[38–40].





## Surface Plasmon Resonance

Binding studies were performed by surface plasmon resonance analysis employing Biacore T-200 biosensor system (GE Healthcare) as described[41]. For assessment of the FVIII-VWF interaction, recombinant VWF was immobilized at the density of 900 RU onto a CM5 sensor chip using the amine coupling method according to the manufacturer's instructions. Varying concentrations of FVIII and mutations thereof were passed over immobilized VWF at a flow rate of 30 µl/min in a buffer containing 20 mM HEPES (pH 7.4), 150 mM NaCl, 5 mM $CaCl_2$ and 0.05% Tween 20 at 25°C. The sensor chip was regenerated after each protein injection using a regeneration buffer containing 20 mM HEPES (pH 7.4), 1 M NaCl, 20 mM EDTA. FVIII binding to VWF was corrected for binding to an empty channel. Responses at equilibrium were plotted as a function of the FVIII concentration to estimate the $K_D$ values.

## Factor X activation studies

FXa generation assays were performed in presence of sonicated lipids as described[21]. Briefly, 25 mM of 15% PS, 20% PE and 65% PC phospholipid vesicles were added to a mix containing 0.3 nM FVIII and 0.2 mM FX. FIXa was mixed in a concentration range from 0 to 16 nM in a buffer containing 50 mM Tris-HCl, 150 mM NaCl 0.2% (w/v) Bovine Serum Albumin (BSA), pH 7.8. Complex formation was allowed as the result of the addition of 1 nM of thrombin and 1.5 mM of $CaCl_2$ at 25°C. The reaction was terminated by addition of 8.8 mM EDTA. Quantity of FXa generated was assessed as described[21].

# RESULTS

## The FVIII C1 domain comprises unique hydrophobic residues that are exposed to the surface.

To identify the surface-exposed structural elements on the C1 domain that are unique to FVIII relative to FV, we compared structures of the C1 domain of human FVIII and FV. Unfortunately, no structure of human FV is available that comprises the complete light chain of human FV. Consequently, detailed informaton about intra and inter domain contacts is lacking. However, there is a crystal strucure of inactivated bovine FV (FVai) in which the C1 domain shares more than 80% primary

sequence identity with the C1 domain of human FV. We therefore compared the surface exposure of the amino acid residues of the human and bovine C1 domain in the crystal structure of human FVIII and bovine FVai (Figure 1A and 1B).

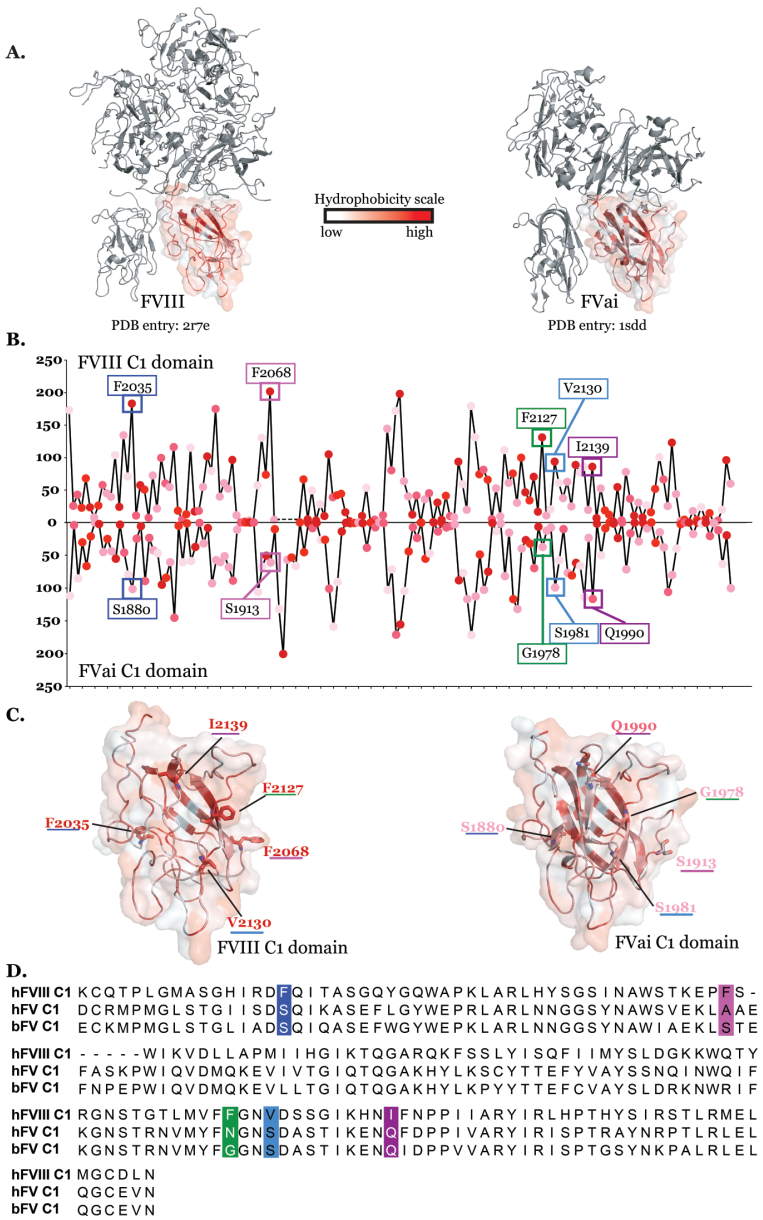


**Figure 1. Comparison between C1 domains of FV and FVIII.**

**A)** On the left is displayed the crystal structure of FVIII [PDB entry: 2r7e] and on the right the structure of inactivated bovine FVa (FVai) [PDB entry: 1sdd][9,32]. The transparent surfaces of the C1 domains are coloured according to the local level of hydrophobicity[31]. **B)** The solvent accessible surface area is plotted as a function of the amino acid position in the C1 domain of FVIII (Top) and FVai (Bottom). The white to red colour code represents the hydrophobicity of the amino acids[31]. **C)** Selected hydrophobic residues from panel B are indicated in the structures of the FVIII C1 domain and FVai C1 domain. **D)** Sequence alignment of human FVIII C1 domain (hFVIII C1), human FV C1 domain (hFV C1) and bovine FV C1 domain (bFV C1). Selected hydrophobic residues from panel B are indicated in the sequence.





Results revealed a unique set of five surface-exposed hydrophobic residues i.e. F2035, F2068, F2127, V2130, I2139 that are either more buried or more polar in FVai than in FVIII (Figure 1C). Sequence alignment of the bovine FV C1 domain with human FV C1 domain showed that the polar nature of these residues is maintained in human FV C1 domain (Figure 1D). The findings together imply that the FVIII C1 domain comprises unique hydrophobic residues that are potentially in contact with the solvent rather than with the interior of the C1 domain core.

## Amino acid residues V2125 and F2127 are crucial for high affinity binding to VWF.

To assess the putative role of the surface-exposed hydrophobic residues for VWF binding, five new recombinant FVIII variants were constructed and purified. In these variants, each one of the identified hydrophobic residues was replaced by an alanine residue i.e. F2035A, F2068A, F2127A, V2130A, I2139A. Surface plasmon resonance (SPR) analysis was employed to evaluate the effect of the substitutions on VWF binding. To this end, increasing concentration of the FVIII variants were passed over VWF that was immobilized on a CM5 sensor chip (Figure 2). Results showed that the interaction between FVIII and VWF could not be accurately described by single site binding model. This may be compatible with the observation that multiple contacts sites have been identified between FVIII and VWF[18,25–29,42]. To still gain insight into the binding efficiency, we plotted the maximum binding response as a function of the employed FVIII concentration. The concentration at which half-maximum is reached is used as a measure for this binding efficiency. Results showed that replacement of F2035, V2130 and I2139 by an alanine residue had little, or no effect at all, on the interaction with VWF. In contrast, the substitution at position 2068 resulted in reduced VWF binding. A marked reduction in VWF binding was observed for the F2127A variant. This was reflected by a ~4-fold increase in FVIII concentration that was required to reach half-maximum binding (Figure 2H and Table 2). Notably, V2125 is in close proximity to F2127 (Cα-Cα distance = 6,9 Å according to the crystal structure by Shen et al[9]) and is also exposed to the solvent. We therefore decided to assess whether a FVIII V2125A variant exhibits reduced VWF binding as well.

SPR analysis showed that replacement of V2125 to alanine indeed markedly reduces the binding to VWF. The FVIII concentration, at which half maximum binding is reached, was more than 6-fold increased compared to that required for FVIII-WT (Figure 2H and Table 2). These data suggest that F2068 and especially F2127 and V2125 contribute to the interaction with VWF.

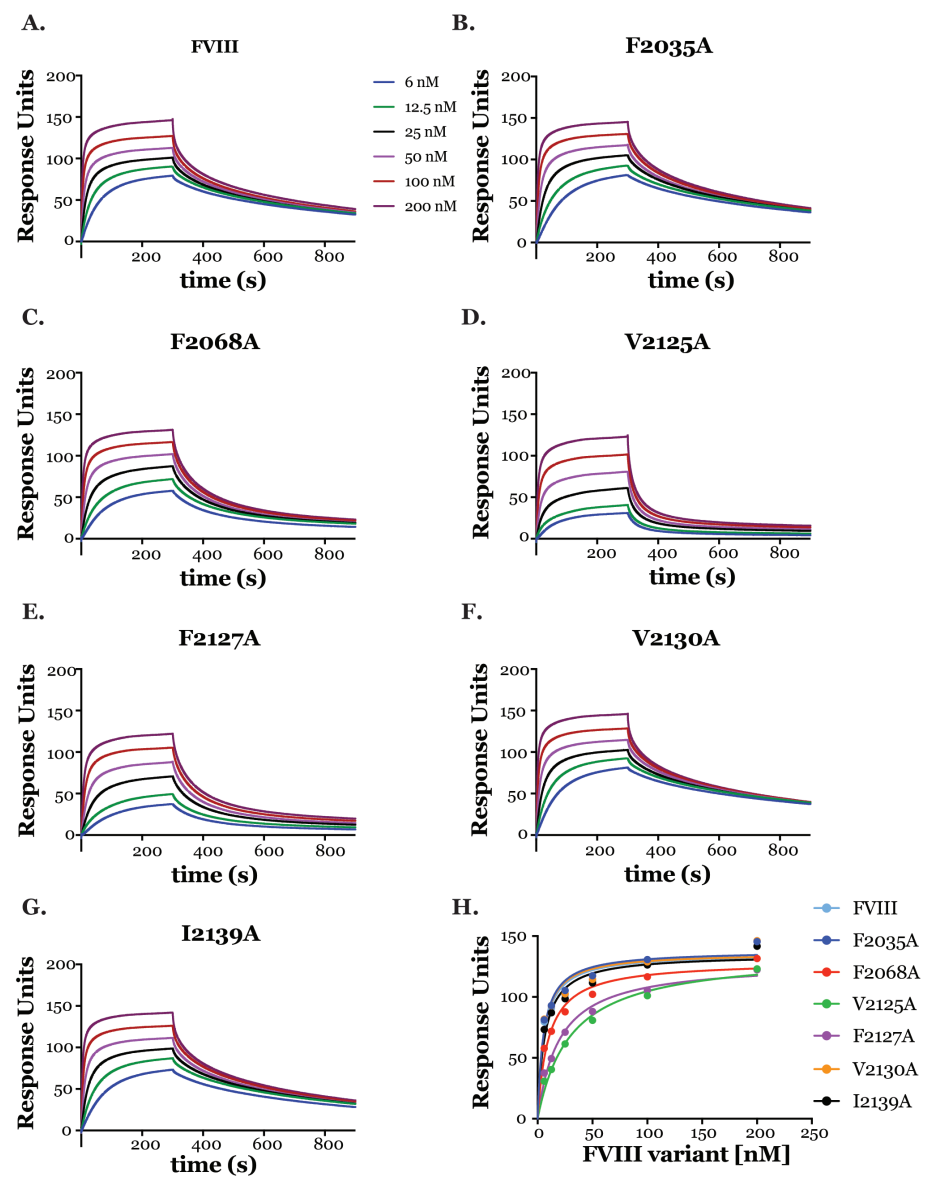


**Figure 2. Binding of FVIII variants to VWF using SPR analysis.** Panels A to G, Various concentrations (6-200 nM) of the indicated FVIII variants were passed over VWF that was immobilized onto a CM5 sensor chip. The binding response is indicated as Response Units (RU) and was assessed in 20 mM HEPES (pH 7.4), 150 mM NaCl, 5 mM CaCl2, 0.05% (v/v) Tween 20 at a flow rate of 30 µl/min at 25°C. Binding to VWF was corrected for the binding to a channel without VWF. **H)** The maximum RU plotted as a function of employed concentration of the FVIII variants.





**Replacement of surface-exposed hydrophobic residues by alanine affects cofactor function.**

The FXa generation efficiency of the FVIII variants was assessed to verify the role of the exposed hydrophobic residues for cofactor function. FXa generation was evaluated at increasing concentrations of FIXa in presence of the thrombin-activated FVIII variants, phospholipids and calcium ions (Figure 3). The concentration of FIXa at which the half-maximum rate (half-Vmax) of FXa generation is reached can be used as an estimation of the apparent FIXa binding affinity of the FVIII variant (Table 2). The results show that V2125A and I2139A substitutions did not affect the efficiency of FX conversion in presence of increasing concentrations of FIXa. F2035A presented only a minor reduction in its ability to stimulate FIXa compared to FVIII-WT, whereas for the F2068A and V2130A variant FXa generation was moderately impaired. The F2068A variant mainly displayed a reduced maximum rate of FXa generation. The variant F2127A showed the strongest defect in cofactor function. For this variant, the FIXa concentration to reach half-Vmax was more than 6-fold higher than required for FVIII-WT. These results suggest that the residues F2068 and V2130 and especially phenylalanine at position 2127 contribute to the interaction with FIXa.

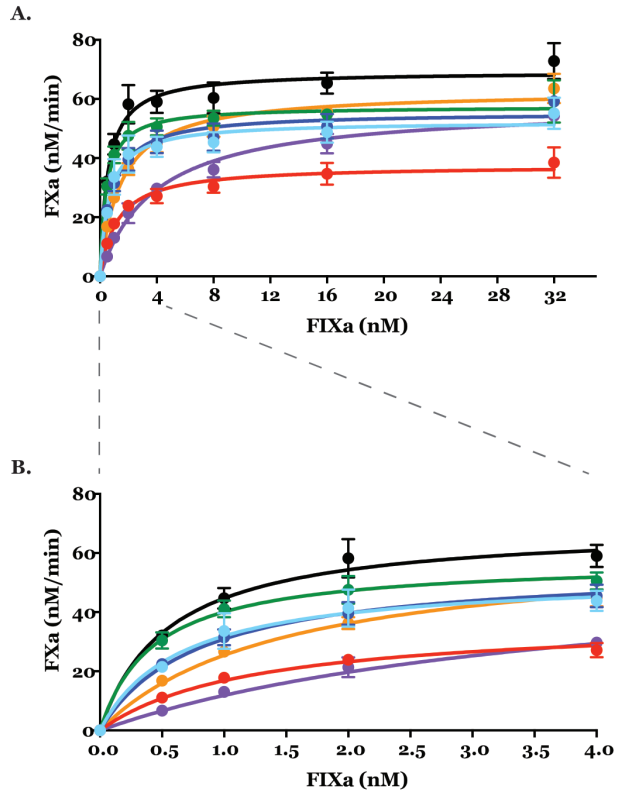


**Figure 3. FXa generation by FIXa in presence of FVIII variants. A, B)** FX was converted into FXa in presence of increasing concentrations of FIXa (0.5-16 nM), phospholipids, $Ca^{2+}$ ions and 0.3 nM of the FVIII variants as described in materials and methods. FVIII wild-type is represented in light blue, F2035A in blue, F2068A in red, V2125A in green, F2127A in purple, V2130A in orange and I2139A in black. Data represent the mean value +/- SD of three independent experiments.

| | Apparent Kd (nM) | |
|---|---|---|
| **FVIII Variant** | **VWF binding** | **FIXa interaction** |
| FVIII | 5.7 ± 1.8 | 0.6 ± 0.1 |
| F2035A | 5.5 ± 1.4 | 0.8 ± 0.1 |
| F2068A | 9.7 ± 1.9 | 1.2 ± 0.2 |
| V2125A | 29.9 ± 4.9 | 0.4 ± 0.1 |
| F2127A | 19.6 ± 2.9 | 3.9 ± 0.4 |
| V2130A | 5.4 ± 1.6 | 1.5 ± 0.1 |
| I2139A | 6.6 ± 1.7 | 0.6 ± 0.1 |

**Table 2.** Apparent equilibrium dissociation constants ($K_D$) of FVIII variants in interaction with FIXa (figure 3) and VWF (figure 2).

## DISCUSSION

There is a strong structure and function relationship between FVIII and FV. This aspect has provided the unique opportunity in this and other studies to gain insight into the ligand-interactive regions of FVIII and FV[13,15–17]. In the present study, we built upon the previous observation that replacement of the C1 domain of FVIII with that of FV ($FVIII_{C1FVC1}$) affects cofactor function[15]. These findings together suggest that the role of the C1 domain of FVIII is more important and complex than previously assumed. Wakabayashi et al. have come to a similar conclusion employing a FVIII variant comprising two FVIII C2 domains ($FVIII_{C2FVIIIC2}$)[43]. Intriguingly, the impaired cofactor function as a function of the FIXa concentration of the $FVIII_{C2FVIIIC2}$ variant was remarkably similar to that of the $FVIII_{C1FVC1}$ variant[15,43]. The partial functional defect of both chimeras may be explained by a putative misalignment of the non-native FVIII A3 - FV C1 and FVIII A3 - FVIII C2 domain interface[43]. Although we do not exclude this possibility, we assessed in this study whether there may be unique structural elements in the FVIII C1 domain that mediate the interaction with FIXa and VWF.

The identification of the five surface-exposed hydrophobic amino acids in the FVIII C1 domain is remarkable in that hydrophobic residues are usually not interacting with the surrounding solvent (Figure 1)[44]. Like in the FV C1 domain, structure and primary sequence comparison between the C1 and C2 domain of FVIII shows that the corresponding residues are also polar in the FVIII C2 domain (Figure 4). This further demonstrates the uniqueness of the surface-exposed hydrophobic residues in the FVIII C1 domain. Our study now reveals that the residues F2068, F2127, V2130 are of functional importance for FVIII biology as these residues contribute to VWF and/or FIXa interaction (Figure 2 and 3). No apparent role for FVIII cofactor





function or VWF binding could be attributed to the other surface-exposed residues. Why the FVIII C1 domain comprises these hydrophobic residues remains therefore a topic for further investigation.

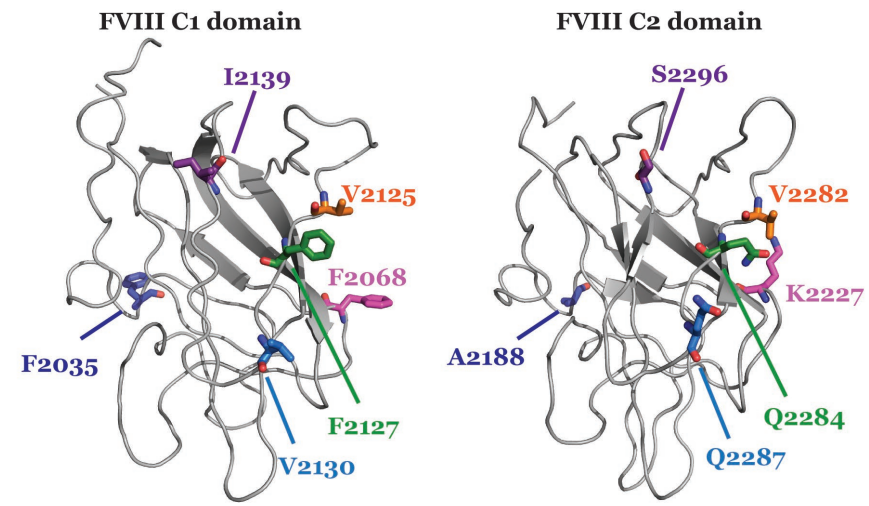


**Figure 4. Comparison of the C1 and C2 domain of FVIII.** On the left is displayed the crystal structure of the FVIII C1 domain [PDB entry: 2r7e[9]] and on the right the FVIII C2 domain. The analysed surface exposed hydrophobic residues of the C1 residues and the corresponding residues in the C2 domain are indicated in the figure.

A previous Hydrogen Deuterium eXchange Mass Spectrometry (HDX-MS) study on FVIII in complex with the FVIII-binding D'D3 fragment of VWF revealed altered hydrogen-deuterium exchange in three FVIII regions in presence of D'D3 i.e. W2062-S2069, T2086-S2095 and S2157-L2166[28]. Based on this observation, the authors concluded that these regions contribute to VWF binding. The VWF binding residue F2068 is indeed part of one of these regions which is compatible with this conclusion (Table 2, Figure 2). Although the authors did find reduced deuterium incorporation in region M2124-Y2148, it was excluded from the analysis because of inconsistent results. Yet, residue F2127, which is part of this region, contributes the most to VWF binding among the identified residues in this study (Table 2, Figure 2). We propose that region M2124-Y2148 comprises a VWF binding region after all. It should be considered, however, that HDX-MS mainly records perturbations in deuterium uptake at the amide backbone level and does not provide any information on the side chains of amino acid residues. A direct interaction between the side chain of F2127 of FVIII and VWF without or minimal alterations of the hydrogen bonding network of the protein backbone may, therefore, remain undetected by

HDX-MS. This may provide an alternative explanation about why HDX-MS did not consistently identify M2124-Y2148 as a region that comprises VWF binding residues. Irrespective of these notions, our study and the HDX-MS study provide complementary information about the role of the C1 domain in VWF binding.

Multiple binding sites have been identified in FVIII for FIXa and VWF in this and other studies[18,25–29]. The relative contribution of each of the identified residues for the overall interaction between FVIII and FIXa/VWF remains to be established. F2127, however, proves to be important for the interaction with both FIXa as well as for VWF binding. This observation is compatible with the protective role of VWF in preventing premature FIXa binding to FVIII. Most likely, VWF not only sterically hinders the interaction between FVIII and FIXa, it may partially share the binding regions on FVIII with FIXa. The proximity of F2127 to the hydrophobic V2125 suggests the involvement of the latter in VWF binding and cofactor function as well. Surprisingly, the variant V2125A displayed a marked reduction in VWF binding, but had no effect in FIXa interaction (Figure 2, Figure 3). As displayed in Figure 4, the counterpart of C1 V2125, in C2 is also a valine residue (V2282) suggesting that hydrophobicity at this level may be a conserved feature among the C domains. Therefore, while F2127 appears to be specific for VWF and FIXa interaction, V2125 could be rather of support in the interaction with VWF. The importance of F2127 for FVIII function is also demonstrated by the notion that substitution of this residue into a serine residue is associated with hemophilia A[45–49]. The results of our study now provide a possible mechanistic explanation for the cause of the bleedings observed in the patients a F2127S variant of FVIII. VWF and/or FIXa binding to this FVIII variant may be affected in the patients.

Taken together, our findings provide novel information about the role of the C1 domain in supporting both VWF and FIXa binding. In this view, these findings also stress the importance of the FVIII C1 domain for enhancing the enzymatic activity of FIXa. We propose that activation of FVIII, followed by FVIII-VWF complex dissociation, liberates the now surface-exposed hydrophobic residues for optimal interaction with FIXa.

## AUTHOR CONTRIBUTION

Contribution: M.A.P., M.B.S., N.F., C.v.d.Z. and J.v.G. performed experiments; M.A.P., N.F., M.v.d.B, K.M. and A.B.M designed the research; M.A.P., M.B.S, N.F., A.B.M. analysed results; M.A.P. and N.F. made the figures, M.A.P., N.F. and A.B.M. wrote the paper.





## CONFLICT OF INTERESTS

The authors declare no conflict of interest.

## FUNDING INFORMATION

This study has been funded by Product and Process Development, Sanquin, The Netherlands (PPOP-13-002).

## REFERENCES


1. Mannucci PM, Tuddenham EG. The hemophilias--from royal genes to gene therapy. N. Engl. J. Med. 2001;344:1773–9.

2. Vehar GA, Keyt B, Eaton D, Rodriguez H, O'Brien DP, Rotblat F, et al. Structure of human factor VIII. Nature 1984;312:337–42.

3. Fay PJ. Factor VIII structure and function. Int J Hematol 2006;83:103–108.

4. Lenting PJ, van Mourik JA, Mertens K. The life cycle of coagulation factor VIII in view of its structure and function. Blood 1998;92:3983–96.

5. Andersson LO, Forsman N, Huang K, Larsen K, Lundin A, Pavlu B, et al. Isolation and characterization of human factor VIII: molecular forms in commercial factor VIII concentrate, cryoprecipitate, and plasma. Proc. Natl. Acad. Sci. U. S. A. 1986;83:2979–83.

6. Fass DN, Knutson GJ, Katzmann JA. Monoclonal antibodies to porcine factor VIII coagulant and their use in the isolation of active coagulant protein. Blood 1982;59:594–600.

7. Truett MA, Blacher R, Burke RL, Caput D, Chu C, Dina D, et al. Characterization of the polypeptide composition of human factor VIII:C and the nucleotide sequence and expression of the human kidney cDNA. DNA Mary Ann Liebert Inc 1985;4:333–49.

8. Ngo JCK, Huang M, Roth DA, Furie BC, Furie B. Crystal Structure of Human Factor VIII: Implications for the Formation of the Factor IXa-Factor VIIIa Complex. Structure 2008;16:597–606.

9. Shen BW, Spiegel PC, Chang C, Huh J, Lee J, Kim J, et al. The tertiary structure and domain organization of coagulation factor VIII. Blood 2008;111:1240–7.

10. Svensson LA, Thim L, Olsen OH, Nicolaisen EM. Evaluation of the metal binding sites in a recombinant coagulation factor VIII identifies two sites with unique metal binding properties. Biol. Chem. 2013;394(6):761-765

11. Pipe SW, Montgomery RR, Pratt KP, Lenting PJ, Lillicrap D. Life in the shadow of a dominant partner: the FVIII-VWF association and its clinical implications for hemophilia A. Blood 2016;128:2007–16.

12. Takeyama M, Nogami K, Okuda M, Shima M. von Willebrand factor protects the Ca2+-dependent structure of the factor VIII light chain. Br J Haematol 2009;146:531–537.

13. Gilbert GE, Novakovic VA, Kaufman RJ, Miao H, Pipe SW. Conservative mutations in the C2 domains of factor VIII and factor V alter phospholipid binding and cofactor activity. Blood 2012;120:1923–1932.

14. Bloem E, Meems H, van den Biggelaar M, Mertens K, Meijer AB. A3 domain region 1803-1818 contributes to the stability of activated factor VIII and includes a binding site for activated factor IX. J Biol Chem 2013;288:26105–26111.

15. Ebberink EH, Bouwens EA, Bloem E, Boon-Spijker M, Van den Biggelaar M, Voorberg J, et al. Factor VIII/V C-domain swaps reveal discrete C-domain roles in factor VIII function and intracellular trafficking. Haematologica. 2017;102:686–694

16. Bovenschen N, Boertjes RC, van Stempvoort G, Voorberg J, Lenting PJ, Meijer AB, et al. Low density lipoprotein receptor-related protein and factor IXa share structural requirements for binding to the A3 domain of coagulation factor VIII. J. Biol. Chem. 2003;278:9370–7.

17. Bos MHA, Camire RM. Blood coagulation factors V and VIII: Molecular Mechanisms of Procofactor Activation. J. Coagul. Disord. 2010;2:19–27.

18. Gilbert GE, Kaufman RJ, Arena AA, Miao H, Pipe SW. Four hydrophobic amino acids of the factor VIII C2 domain are constituents of both the membrane-binding and von Willebrand factor-binding motifs. J Biol Chem 2002;277:6374–6381.

19. Lu J, Pipe SW, Miao H, Jacquemin M, Gilbert GE. A membrane-interactive surface on the factor VIII C1 domain cooperates with the C2 domain for cofactor function. Blood 2011;117:3181–3189.

20. Novakovic VA, Cullinan DB, Wakabayashi H, Fay PJ, Baleja JD, Gilbert GE. Membrane-binding properties of the Factor VIII C2 domain. Biochem J 2011;435:187–196.

21. Meems H, Meijer AB, Cullinan DB, Mertens K, Gilbert GE. Factor VIII C1 domain residues Lys 2092 and Phe 2093 contribute to membrane binding and cofactor activity. Blood 2009;114:3938–3946.

22. Soeda T, Nogami K, Nishiya K, Takeyama M, Ogiwara K, Sakata Y, et al. The factor VIIIa C2 domain (residues 2228-2240) interacts with the factor IXa Gla domain in the factor Xase complex. J. Biol. Chem. 2009;284:3379–88.

23. Vincent Jenkins P, Freas J, Schmidt KM, Zhou Q, Fay PJ. Mutations associated with hemophilia A in the 558-565 loop of the factor VIIIa A2 subunit alter the catalytic activity of the factor Xase complex. Blood 2002;100:501–8.

24. Lenting PJ, Donath MJ, van Mourik JA, Mertens K. Identification of a binding site for blood coagulation factor IXa on the light chain of human factor VIII. J Biol Chem 1994;269:7150–7155.

25. Leyte A, van Schijndel HB, Niehrs C, Huttner WB, Verbeet MP, Mertens K, et al. Sulfation of Tyr1680 of human blood coagulation factor VIII is essential for the interaction of factor VIII with von Willebrand factor. J. Biol. Chem. 1991;266:740–6.

26. Saenko EL, Scandella D. The acidic region of the factor VIII light chain and the C2 domain together form the high affinity binding site for von willebrand factor. J. Biol. Chem. 1997;272:18007–14.

27. Lollar P, Hill-Eubanks DC, Parker CG. Association of the factor VIII light chain with von Willebrand factor. J. Biol. Chem. 1988;263:10451–5.

28. Chiu PL, Bou-Assaf GM, Chhabra ES, Chambers MG, Peters RT, Kulman JD, et al. Mapping the interaction between factor VIII and von Willebrand factor by electron microscopy and mass spectrometry. Blood 2015;126:935–938.

29. Jacquemin M, Lavend'homme R, Benhida A, Vanzieleghem B, d'Oiron R, Lavergne JM, et al. A novel cause of mild/moderate hemophilia A: mutations scattered in the factor VIII C1 domain reduce factor VIII binding to von Willebrand factor. Blood 2000;96:958–65.

30. Krissinel E, Henrick K. Inference of macromolecular assemblies from crystalline state. J. Mol. Biol. 2007;372:774–97.

31. Eisenberg D, Schwarz E, Komaromy M, Wall R. Analysis of membrane and surface protein sequences with the hydrophobic moment plot. J. Mol. Biol. 1984;179:125–42.

32. Adams TE, Hockin MF, Mann KG, Everse SJ. The crystal structure of activated protein C-inactivated bovine factor Va: Implications for cofactor function. Proc Natl Acad Sci U A 2004;101:8918–23.

33. Liu ML, Shen BW, Nakaya S, Pratt KP, Fujikawa K, Davie EW, et al. Hemophilic factor VIII C1- and C2-domain missense mutations and their modeling to the 1.5-angstrom human C2-domain crystal structure. Blood 2000;96:979–87.

34. Fribourg C, Meijer AB, Mertens K. The interface between the EGF2 domain and the protease domain in blood coagulation factor IX contributes to factor VIII binding and factor X activation. Biochemistry 2006;45:10777–10785.

35. van den Brink EN, Turenhout EA, Bank CM, Fijnvandraat K, Peters M, Voorberg J. Molecular analysis of human anti-factor VIII antibodies by V gene phage display identifies a new epitope in the acidic region following the A2 domain. Blood 2000;96:540–5.

36. Meems H, Van Den Biggelaar M, Rondaij M, van der Zwaan C, Mertens K, Meijer AB. C1 domain residues Lys 2092 and Phe 2093 are of major importance for the endocytic uptake of coagulation factor VIII. Int. J. Biochem. Cell Biol. 2011;43:1114–21.

37. Van Den Biggelaar M, Bierings R, Storm G, Voorberg J, Mertens K. Requirements for cellular co-trafficking of factor VIII and von Willebrand factor to Weibel-Palade bodies. J. Thromb. Haemost. 2007;5:2235–42.

38. Mertens K, Bertina RM. Activation of human coagulation factor VIII by activated factor X, the common product of the intrinsic and the extrinsic pathway of blood coagulation. Thromb. Haemost. 1982;47:96–

100.

39. Mertens K, Bertina RM. Pathways in the activation of human coagulation factor X. Biochem. J. 1980;185:647–58.

40. Hendrix H, Lindhout T, Mertens K, Engels W, Hemker HC. Activation of human prothrombin by stoichiometric levels of staphylocoagulase. J. Biol. Chem. 1983;258:3637–44.

41. Bloem E, van den Biggelaar M, Wroblewska A, Voorberg J, Faber JH, Kjalke M, et al. Factor VIII C1 domain spikes 2092-2093 and 2158-2159 comprise regions that modulate cofactor function and cellular uptake. J. Biol. Chem. 2013;288:29670–9.

42. van den Biggelaar M, Meijer AB, Voorberg J, Mertens K. Intracellular cotrafficking of factor VIII and von Willebrand factor type 2N variants to storage organelles. Blood 2009;113:3102–9.

43. Wakabayashi H, Fay PJ. Replacing the factor VIII C1 domain with a second C2 domain reduces factor VIII stability and affinity for factor IXa. J. Biol. Chem. 2013;288:31289–97.

44. Dyson HJ, Wright PE, Scheraga HA. The role of hydrophobic interactions in initiation and propagation of protein folding. Proc. Natl. Acad. Sci. U. S. A. 2006;103:13057–61.

45. Trossaërt M, Regnault V, Sigaud M, Boisseau P, Fressinaud E, Lecompte T. Mild hemophilia A with factor VIII assay discrepancy: using thrombin generation assay to assess the bleeding phenotype. J. Thromb. Haemost. JTH 2008;6:486–93.

46. Castaman G, Mancuso ME, Giacomelli SH, Tosetto A, Santagostino E, Mannucci PM, et al. Molecular and phenotypic determinants of the response to desmopressin in adult patients with mild hemophilia A. J. Thromb. Haemost. JTH 2009;7:1824–31.

47. Green PM, Bagnall RD, Waseem NH, Giannelli F. Haemophilia A mutations in the UK: results of screening one-third of the population. Br. J. Haematol. 2008;143:115–28.

48. Martín-Salces M, Venceslá A, Alvárez-Román MT, Rivas I, Fernandez I, Butta N, et al. Clinical and genetic findings in five female patients with haemophilia A: Identification of a novel missense mutation, p.Phe2127Ser. Thromb. Haemost. 2010;104:718–23.

49. Johnsen JM, Fletcher SN, Huston H, Roberge S, Martin BK, Kircher M, et al. Novel approach to genetic analysis and results in 3000 hemophilia patients enrolled in the My Life, Our Future initiative. Blood Adv. 2017;1:824–34.





## SUPPLEMENTARY FIGURES

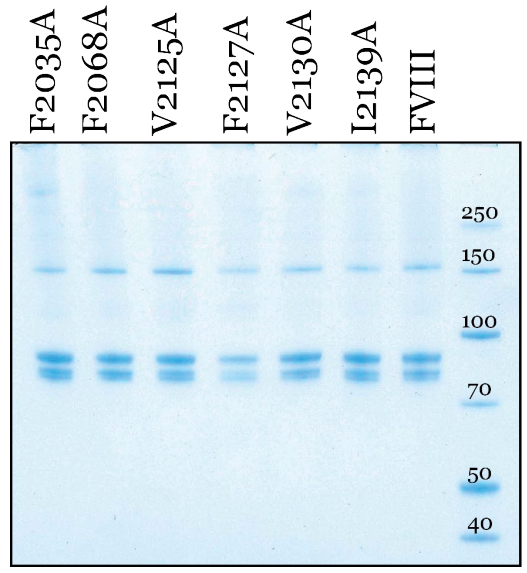


**Supplementary Figure 1.**
SDS-PAGE (4-12% NuPAGE gel) in Coomassie staining of purified FVIII variants (1 mg).

# Chapter 3

## Hydrogen-deuterium exchange mass spectrometry identifies activated factor IX-induced molecular changes in activated factor VIII

*Josse van Galen[1], ***Nadia Freato**[1], Małgorzata A. Przeradzka[1], Eduard HTM Ebberink[1], Mariëtte Boon-Spijker[1], Carmen van der Zwaan[1], Maartje van den Biggelaar[1], Alexander B. Meijer[1,2]

*Both authors contributed equally to this study

From the Department of [1]Molecular and Cellular Hemostasis, Sanquin Research, 1066 CX Amsterdam, The Netherlands, [2]Department of Biomolecular Mass Spectrometry and Proteomics, Utrecht Institute for Pharmaceutical Sciences (UIPS), Utrecht University, 3584 CG Utrecht, The Netherlands

**Thromb Haemost. 2020 Dec 10. doi: 10.1055/s-0040-1721422.**

## ABSTRACT

Hydrogen-Deuterium eXchange Mass Spectrometry (HDX-MS) was employed to gain insight into the changes in factor VIII (FVIII) that occur upon its activation and assembly with activated factor IX (IXa) on phospholipid membranes. HDX-MS analysis of thrombin-activated FVIII (FVIIIa) revealed a marked increase in deuterium incorporation of amino acid residues along the A1-A2 and A2-A3 interface. Rapid dissociation of the A2 domain from FVIIIa can explain this observation. In presence of FIXa, enhanced deuterium incorporation at the interface of FVIIIa was similar to that of FVIII. This is compatible with the previous finding that FIXa contributes to A2 domain retention in FVIIIa. A2 domain region Leu631-Tyr637, which is not part of the interface between the A domains, also showed a marked increase in deuterium incorporation in FVIIIa compared to FVIII. Deuterium uptake of this region was decreased in presence of FIXa beyond that observed in FVIII. This implies that FIXa alters the conformation or directly interacts with this region in FVIIIa. Replacement of Val634 in FVIII by alanine using site-directed mutagenesis almost completely impaired the ability of the activated cofactor to enhance the activity of FIXa. Surface plasmon resonance analysis revealed that the rates of A2 domain dissociation from FVIIIa and FVIIIa-Val634Ala were indistinguishable. HDX-MS analysis showed, however, that FIXa was unable to retain the A2 domain in FVIIIa-Val634Ala. The combined results of this study suggest that the local structure of Leu631-Tyr637 is altered by FIXa and that this region contributes to the cofactor function of FVIII.






## INTRODUCTION

Factor VIII (FVIII) is essential for the proper functioning of the coagulation cascade. Within the cascade, FVIII acts as a cofactor for factor IX (FIX) in the activated factor X (FXa)-generating complex[1]. Functional absence of FVIII is linked to the bleeding disorder hemophilia A stressing the critical role of FVIII for effective bleeding arrest at sites of vessel injury[2]. FVIII consists of A, B and C domains organized as: A1-*a1*-A2-*a2*-B-*a3*-A3-C1-C2[3,4]. *a1*, *a2*, and *a3* represent short acidic amino acid regions comprising sulfated tyrosine residues. During synthesis, FVIII is cleaved between the B domain and the *a3* region. As a consequence, FVIII circulates in blood as a heterodimeric protein comprising a heavy chain (A1-*a1*-A2-*a2*-B) that is non-covalently linked to a light chain (*a3*-A3-C1-C2). In plasma, FVIII forms a tight complex with Von Willebrand Factor (VWF)[1]. In this complex, FVIII is protected from premature binding to its ligands, proteolytic degradation and fast clearance[4].

FVIII requires activation by thrombin to perform its role in the coagulation cascade. It has also been shown that FXa can activate FVIII[5,6]. Proteolytic cleavage of FVIII occurs after Arg372 (between *a1* and A2 domain), Arg740 (between *a2* and the B domain), and Arg1689 (between *a3* and A3 domain). This leads to the release from FVIII of the B domain and the *a3* region as well as dissociation of the FVIII-VWF complex[1,4]. The resulting activated FVIII (FVIIIa) is a heterotrimer that consists of three non-covalently linked units i.e.: A1-*a1*, A2-*a2*, A3-C1-C2. Once activated, FVIIIa can assemble with activated FIX (FIXa) on phosphatidylserine-containing membranes. Within the complex, FVIIIa enhances the catalytic activity of FIXa approximately 200,000 fold[7]. To prevent uncontrolled activation of FX, FVIIIa can be inactivated via proteolytic cleavage by Activated Protein C (APC) or via spontaneous dissociation of the A2 domain from FVIIIa[4,8–10]. It has been shown that the rate of A2 domain dissociation is reduced when FVIIIa is in complex with FIXa[1].

Crystallographic and electron microscopy studies on FVIII have provided insights into the structure of FVIII[11–13]. These structures reveal that the A domains form a propeller-shaped structure on top of two parallelly aligned C domains. Molecular modelling studies combined with previous site-directed mutagenesis studies have shown that the C domains mainly interact with phospholipid membranes whereas the A domains interact with FIXa and FX[14–17]. Despite the progress that has been made, detailed information is still lacking concerning molecular rearrangements in FVIII that take place upon its activation and its subsequent assembly with FIXa on phospholipid membranes.

Hydrogen-deuterium exchange mass spectrometry (HDX-MS) has been successfully employed to identify protein binding sites in protein complexes. In addition, it has provided insight into putative local conformational changes in proteins

upon complex formation or protein activation[18–20]. HDX-MS takes advantage from the fact that hydrogens, including those at the protein backbone, naturally exchange for deuterium atoms when a protein is transferred from $H_2O$ to $D_2O$. Comparing the bound and unbound proteins, the rate of deuterium exchange can be altered at sites where proteins interact or conformational changes occur[18–22]. In the present study, we employed HDX-MS to assess changes in FVIII upon activation and binding to FIXa in presence of procoagulant phospholipid membranes.

## METHODS

### Materials

DMEM/F12 was from Lonza (Breda, the Netherlands), fetal calf serum from Bodinco (Alkmaar, the Netherlands). L-α-phosphatidylethanolamine transphosphatidylated (Egg, Chicken), L-α-phosphatidylserine (Brain, Porcine) and L-α-phosphatidylcholine (Egg, Chicken) were from Avanti Polar Lipids (Alabaster, Alabama, USA). Geneticin, Ultrapure Urea, Molecular Biology grade 5M NaCl solution and Tris-HCl, Precast SDS/PAGE gels, Brilliant Blue Coomassie (CBB) and DMRIE-C reagent were from Invitrogen (Breda, The Netherlands). PageRuler™ Unstained Broad Range Protein Ladder and Tris(2-carboxyethyl)phosphine hydrochloride (TCEP-HCl) were obtained from Thermo Fisher Scientific (Breda, The Netherlands). NaCl was purchased from Fagron (Rotterdam, The Netherlands) and HEPES was from Serva (Heidelberg, Germany). Formic acid, acetonitrile and ultra-pure water for mass spectrometry were from Biosolve (Valkenswaard, the Netherlands). Deuterium Oxide 99.9% and leech-derived hirudin was from Sigma-Aldrich (Saint Louis, MO, USA). BigDye Terminator Sequencing kit was obtained from Applied Biosystem (Foster City, USA). QuikChange site directed mutagenesis kit was purchased from Agilent Technologies (Santa Clara, California, USA). All other chemicals were from Merck (Darmstadt, Germany).

### Proteins

Plasma-derived thrombin and FIXa were obtained as described previously[23,24]. Active site titration combined with Bradford analysis revealed a more than 90% purity of the employed FIXa batch[25,26]. CLB-CAg9, CLB-EL14, CLB-VK34 and CLB-CAg117 antibody are described[27,28]. B-domain deleted FVIII (GenBank accession number ABV90867.1) was codon optimized and purchased from Thermo Fisher Scientific (USA) in pcDNA3.1(+) expression vector using *Nhe*I and *Not*I restriction. FVIII-V634A mutant (Legacy numbering is used throughout this paper) was generated using the QuikChange site directed mutagenesis kit. Mutagenesis was confirmed using BigDye Terminator. B-domain deleted FVIII expressing stable HEK293 cells were generated by transfection of FVIII expression vectors using DMRIE-C reagent, after which cells were cultured in presence of 1 mg/ml G-418. Clones were selected and expressing clones were identified using ELISA (CAg117-CAg9$^{PO}$). Expressed proteins were purified using CLB-VK34 antibody as described[28]. Protein concentrations were determined as described[29]. Although the SDS-PAGE revealed that FVIII-V634A was more than 95% pure (Supplementary Figure S1A) the specific activity was only 140 U/mg. This implies a poor activity of the variant. SDS-PAGE and activation characteristics of FVIII, FVIII-V634A and FIXa are shown in Supplementary Figure S1.

### Liposome preparation

L-α-Phosphatidylethanolamine (PE), L-α-phosphatidylserine (PS) and L-α-phosphatidylcholine (PC) were mixed in 4:3:13 molar ratio, respectively. After evaporation of organic solvents, lipids were resuspended in Tris-Buffered Saline (TBS, pH 7.4) and aliquots were stored at -80°C. Liposomes were prepared by sonication and centrifugation at 16,000 x g for 30 min at 4°C. Phosphate content was determined by phosphate measurement according to Rouser[30]. Liposomes were stored maximum 1 week at 4°C.

### Hydrogen-deuterium exchange mass spectrometry

22.5 µl of FVIII (final concentration 2.4 µM) was preincubated with 6.7 µl lipids (final concentration 0.16 mM) at room temperature for 5 minutes in a buffer containing 460 mM NaCl, 10 mM CaCl2 and 20 mM Imidazole pH 7.3. Subsequently, 10 µl of preincubated FVIII was mixed with 4.9 µl of FIXa (13.8 µM in 50 mM NaCl, 25 mM Tris-HCl, pH 7.5, 50% glycerol) or with buffer alone and incubated 90 seconds at RT. Then, this was mixed with 2.5 µl thrombin (1.35 µM in TBS with 10 mM CaCl2 and 12.5% glycerol) or with buffer alone and was incubated for 60 seconds at RT. The final concentration of FVIII after thrombin addition was 1.4 µM, 92 µM for the lipids, 3.9 µM for FIXa and 0.2 µM for thrombin. Immediately after this incubation the sample was placed in a LEAP PAL system (LEAP Technologies, Morrisville, NC, USA), cooled at 4°C and the sample was further processed for deuterium exchange. Briefly, 3 µl sample was diluted in 27 µl buffer (130 mM NaCl, 20 mM Imidazole pH 7.3, 10 mM CaCl2 in H2O or 98% D2O) for 100 s at 24°C. By this dilution the final concentration of NaCl in the sample was 150 mM. Then 25 µl of the diluted sample was quenched in 25 µl quenching solution (1 g TCEP dissolved in 2 ml 2M Urea, 1M NaOH) for 1 min at 4°C. Further processing of in-line digestion into peptides and liquid chromatography of the sample was carried out in a cooled (4°C) environment under an isocratic flow of 5% acetonitrile, 0.1% formic acid at a flow of 100 µl/min. Samples were digested on a pepsin column (Poroszyme Immobilized Pepsin

Cartridge) and peptides were bound to a trap (Acclaim Guard Column 120 C18, 5 µm, 2.0x10 mm Thermofisher). Peptides were eluted from the trap and resolved over a 30 mm length, 1 mm diameter C18 column, particle size 3 µm (Hypersil Gold C18, Thermo Cat no 25003-031030) using a 12 minutes gradient from 0-64% acetonitrile at 50 µl/min. Peptides in the mobile phase were measured by an LTQ Orbitrap-XL (Thermo). Using an ESI source an electrospray was created at 4.5 kV with 30, 10 and 10 arbitrary units of sheath, auxiliary and sweep gas, respectively. Signal was obtained in positive mode, in the mass range of 300-2000 m/z by resolution of 30000. A reference peptide list was generated by fragmenting FVIII-DB WT using CID fragmentation on an LTQ Orbitrap-XL (Thermo) and by HCD on an Orbitrap-Fusion (Thermo) and analysis using Peaks Studio 7.0 (Bioinformatics Solutions Inc). Deuterium uptake was calculated using HDExaminer (Sierra Analytics) for peptides within 1 minute retention time. Then, the identified peptides were investigated manually for misidentifications or other errors. Peptides of which the deuterium incorporation could not accurately be calculated due to low intensity or high complexity were discarded. The percentage of deuterium uptake was calculated for each peptide relative to the theoretical maximum deuterium incorporation. Differences in uptake of more than 5% compared to the theoretical maximum were modelled in the FVIII structure using PyMol software (Schrodinger, LLC).

### Surface plasmon resonance analysis

Surface plasmon resonance (SPR) using a Biacore T200 (GE Life Sciences) was performed as described[31]. Briefly, human anti-FVIII C2 domain antibody CLB-EL14 IgG4 was coupled to a CM5 chip to a density of 5000 response units (RU) according to manufacturer's suggestions. FVIII (wild-type or V634A) was bound to the anti-FVIII C2 antibody on the chip to 2500 RU in a buffer of 150 mM NaCl, 5 mM $CaCl_2$, 0.05% (v/v) Tween 20, 20 mM HEPES, pH 7.4. 2 nM thrombin was passed over FVIII for 1 minute and dissociation of FVIII-A2 domain was monitored.

### FXa generation assays

FXa generation was performed as described in Meems et al[14]. Briefly, FVIII (0.3 nM) or FVIII-V634A (0.3 nM) were incubated with FX (200 nM) and various concentration of FIXa (0-64 nM) in presence Thrombin (1 nM), 25 µM of phospholipids and 1.5 mM $CaCl_2$ in a buffer containing 150 mM NaCl, 50 mM Tris-HCl plus 0.2% (w/v) fatty acid free bovine serum albumin, pH 7.8 in a final volume of 40 µl at 25°C. The reaction was stopped after 2 minutes by adding 50 µl of 16 mM EDTA in assay buffer. Factor Xa activity was determined in a microtiter plate reader (Spectramax, Molecular Devices) at 25°C using S-2765 chromogenic substrate. The effect of FIXa on the decline of FVIIIa cofactor function over time has been





performed as described[31]. Briefly, 0.3 nM FVIII or FVIII-V634A was activated by 2 nM thrombin in the presence of 25 uM phospholipid vesicles, 1.5 mM $CaCl_2$, 40 mM Tris-HCl (pH 7.8), 150 mM NaCl, and 0.2% (w/v) BSA. At 9 time intervals after activation, FXa generation was allowed for 1 min by addition of 16 nM FIXa and 200 nM FX. In a parallel experiment, the FVIII and FVIII-V634A were activated under the same conditions but then in the presence of 16 nM FIXa. At 9 time intervals after activation, FXa generation was allowed by the addition of 200 nM FX. FXa generation was measured as described before[14].

## RESULTS

### HDX-MS of thrombin-activated FVIII in the presence and absence of FIXa.

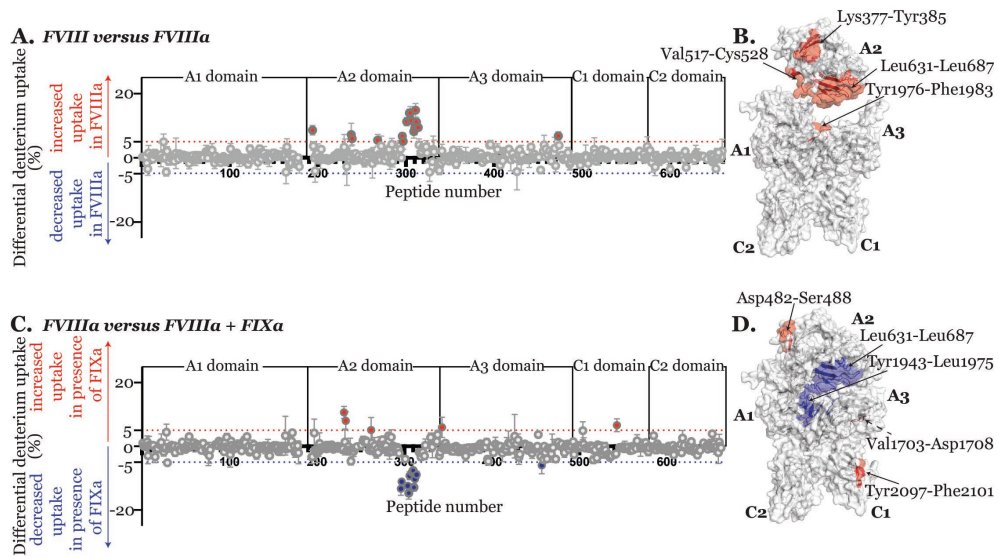


**Figure 1. HDX-MS on FVIII, FVIIIa and FVIIIa in presence of FIXa**

FVIII, FVIIIa or FVIIIa with FIXa were incubated in deuterated buffer for 100s in presence of procoagulant phospholipid membranes. The percentage of deuterium incorporation of a peptide was assessed relative to the theoretical maximum of incorporation in that peptide. The amino acid sequence of the peptides, shown by the ID-number on the x-axis in panels A and C, is provided in Supplementary Table S1. Panel A shows the differential deuterium incorporation between FVIII and FVIIIa. The y-axis displays the percentage of deuterium uptake of the peptides of FVIIIa subtracted with that of FVIII. The peptides revealing a difference of more than 5% or less than -5% are indicated on the structure of FVIII in panel B (PDB: 3cdz[11]). Panel C shows the differential deuterium incorporation of FVIIIa in presence and absence of FIXa. The y-axis displays the percentage of deuterium uptake of a peptides of FVIIIa subtracted with that of FVIIIa in presence of FIXa. Peptides that showed a difference of more than 5% or less than -5% are indicated on the structure of FVIII in panel D (PDB: 3cdz[11]). The average of three independent experiments is shown in panels A and C. Error bars represent the standard deviation.

FVIII was activated by thrombin with and without FIXa to assess the molecular changes in FVIII using HDX-MS. Activation was performed in the presence of procoagulant phospholipids to facilitate the interaction with FIXa[4]. To obtain a global overview of the molecular changes in FVIII, we incubated the protein mixtures for 100 seconds in $D_2O$ after which the proteins were processed for MS analysis. In total, we obtained 663 peptides covering 89% of FVIII (Supplementary Figure S2 and Supplementary Table S1). Compared to FVIII, a marked increase in deuterium incorporation was observed in FVIIIa mainly for A2 domain peptides located at the interface between the A2 and A3 domain. On the A3 domain, one peptide at the interface with the A2 domains also showed a marked increase in deuterium uptake (Figure 1A and 1B). The results suggest a conformational change at the involved FVIII regions, or that these regions become more exposed to the solvent after activation of FVIII. Intriguingly, in presence of FIXa, peptides at the interface between the A domains of FVIIIa showed a decrease in deuterium incorporation compared to FVIIIa in absence of FIXa (Figure 1C and 1D). Notably, two peptides covering region Leu631-Trp637, which is not part of the interface, also showed a prominent decrease in deuterium uptake in presence of FIXa. Several identified peptides displayed an increased deuterium incorporation in A2, A3 and C1 domain i.e. (Asp482-Ser488, Val1703-Asp1708, Tyr2097-Phe2101) (Figure 1C and 1D). The results together imply that multiple regions located at the interface or surface of the A domains display differential deuterium incorporation upon activation of FVIII or upon interaction of FVIIIa with FIXa.

## Time-resolved HDX-MS of FVIII, and FVIIIa in the presence and absence of FIXa

To gain more insight into the altered deuterium uptake of the peptides in FVIIIa in presence or absence of FIXa, HDX was also assessed at different time intervals (see Supplementary Figure S3 for the full set of deuterium uptake plots). To this end, FVIII, FVIIIa, and FVIIIa in presence of FIXa were incubated with phospholipids in $D_2O$ for 10, 30 and 100 seconds. In FVIII, the A2 domain interface peptide Leu668-Phe678, Met680-Leu687 and Tyr656-Thr667 showed a deuterium uptake of 6% of the theoretical maximum uptake at 10 seconds, which increased to 11% at 100 seconds (Figure 2A). Upon activation of FVIII by thrombin, deuterium uptake for these peptides was increased by 11 to 14% for all the time points. Remarkably, in presence of FIXa, the levels of deuterium incorporation for the peptides at the domain interface were almost indistinguishable from that of FVIII prior to thrombin activation (Figure 2A). These findings together may be explained by the rapid dissociation of the A2 domain from FVIIIa which leads to the increased deuterium uptake of peptides at the A2 interface. Within the FVIIIa-FIXa complex, FIXa is





known to reduce the rate of A2 domain dissociation for FVIIIa thereby stabilizing FVIIIa[1]. This phenomenon may explain the reduced deuterium incorporation of the interface peptides when FVIII is activated in presence of FIXa.

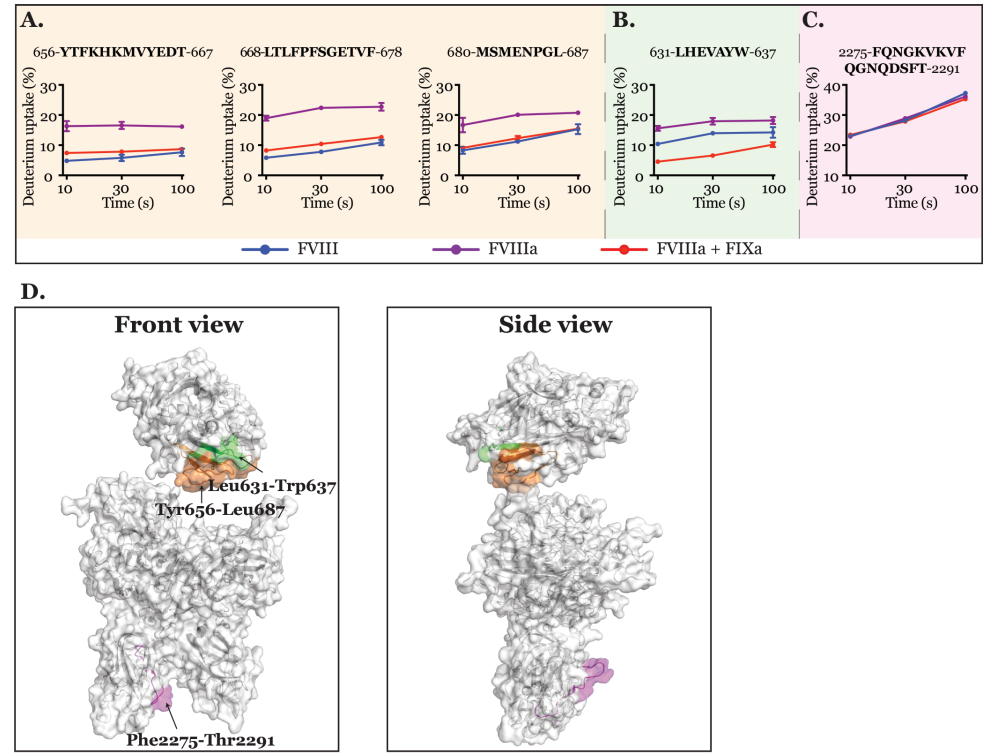


**Figure 2. Time dependent deuterium incorporation of FVIII, FVIIIa and FVIIIa in presence of FIXa**

FVIII, FVIIIa and FVIIIa in presence of FIXa were incubated with deuterium for 10, 30 or 100 seconds and the level of deuterium uptake was assessed by HDX-MS. The percentage of deuterium uptake relative to the maximum theoretical uptake is shown on the y-axis of the panel A-C. Panels A show the deuterium uptake of the interface peptides 656-YTFKHKMVYEDT-667, 668-LTLFPFSGETVF-678 and 680-MSMENPGL-687. Panel B displays deuterium uptake of A2 domain peptide 631-LHEVAYW-637 which is not part of the A domain interface. Panel C shows a representative peptide that displayed no change in deuterium incorporation i.e. C2 domain peptide 2275-FQNGKVKVFQGNQDSFT-2291. The mean of two independent experiments is shown in the panels A-C. Error bars represent the spread between the actual data points. Panel D shows the regions that are covered by the peptides on the crystal structure of FVIII (PDB: 3cdz[11]).

## A2 domain region Leu631-Trp637 contributes to cofactor function

The trend of deuterium incorporation obtained for peptides overlapping region Leu631-Trp637 was distinct from that of the peptides at the A2 – A3 domain interface. In presence of FIXa, deuterium uptake in this region of FVIIIa was reduced

beyond that observed in FVIII prior to thrombin activation (Figure 2B). Intriguingly, substitution of Val634 by an alanine has been associated with mild to moderate hemophilia A[32,33]. A residual FVIII activity of 2-5% has been assessed in patients with mild hemophilia A[32,33]. To gain more insight into the role of Val634 for FVIII function, we constructed and purified a FVIII-V634A variant (Supplemental Figure S1). Results revealed a marked decrease of efficiency of FVIIIa-V634A in enhancing the activity of FIXa compared to FVIIIa (Figure 3). No defect in thrombin activation of the variant could be observed (Supplemental Figure S1B). The findings also show that the FIXa concentration required to reach half–maximum of FXa generation is about 18-fold higher for the FVIIIa-V634A compared to FVIIIa (Figure 3A and 3B). These observations suggest that FVIIIa-V634A may have an altered interaction with FIXa. It cannot be excluded, however, that the Val634Ala mutation leads to an accelerated rate of A2 domain dissociation upon activation of the FVIIIa-V634A variant.

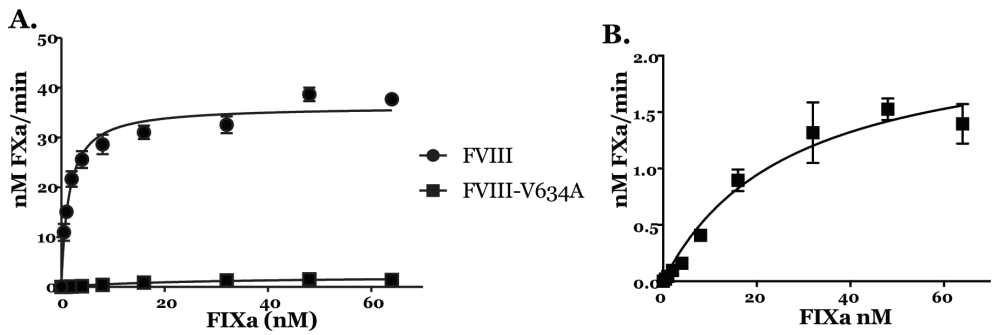


**Figure 3. FXa generation by FIXa in presence of FVIII or FVIII-V634A**

A) Activation of FX was assessed by increasing concentration of FIXa (0 – 64 nM) in the presence of 0.3 nM FVIII or FVIII-V634A, 200 nM FX, 1 nM thrombin, 1.5 mM $CaCl_2$ and 25 µM phospholipids as described in Materials and Methods. FVIII is shown in circles and FVIII-V634A in squares B) In panel B, the y-axis is adjusted and shows FXa generation by FIXa in the presence of FVIII-V634A.

## A2 domain retention studies in FVIII and FVIII-V634A

SPR analysis was performed to assess whether activated FVIII-V634A exhibits an increased rate of A2 domain dissociation compared to activated FVIII. To this end, FVIII and the FVIII-V634A variant were immobilized via an anti-C2 domain antibody to the same density on the surface of an CM5 sensor chip. The FVIII variants were subsequently activated by thrombin. The decrease in Response Units (RU) reflects the dissociation rate of the A2 domain from FVIIIa as described[31,34]. Results revealed no difference in A2 dissociation between FVIIIa and FVIIIa-V634A (Figure 4A). This suggests that an increased instability of FVIIIa-V634A does not explain the impaired





activity of this variant. The result also confirms that the variant exhibits no activation defect.

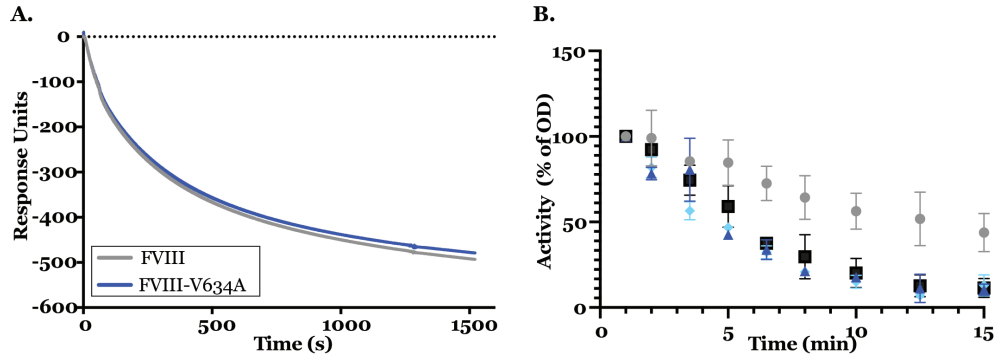


**Figure 4. A2 domain dissociation from activated FVIII and FVIII-V634A**

A) Stability of activated FVIII and FVIII-V634A assessed by SPR analysis. FVIII and FVIII-V634A were immobilized on a CM5 sensor chip to a density of 2500 response units via anti C2 domain antibody EL14. 2 nM thrombin in 150 mM NaCl, 5 mM CaCl2, 0.05% (v/v) Tween 20, 20 mM HEPES, pH 7.4 was passed over the immobilized FVIII for 60 s. The decrease in Response Units, caused by A2 domain dissociation from activated FVIII (grey line) and FVIII-V634A (blue line), was monitored as a function of time. B) Stability of FVIII and FVIII-V634A assessed by enzyme kinetics. 0.3 nM FVIII (black squares) or FVIII-V634A (light blue diamonds) was activated by 2 nM thrombin as described in Materials and methods. At the indicated time points, 16 nM FIXa and 200 nM FX were added to allow FXa generation. 0.3 nM FVIII (grey circles) or FVIII-V634A (dark blue triangles) was activated by 2 nM thrombin in presence of 16 nM FIXa. At the indicated time points, 200 nM FX was added to allow FXa generation.

The stability of FVIIIa and FVIIIa-V634A was also evaluated using an enzyme kinetics assay. To this end, FVIII and FVIIIa-V634A were activated in the presence and absence of FIXa on phospholipid membranes. The ability of FVIIIa and FVIIIa-V634A to enhance the activity of FIXa was followed in time (Figure 4). Both FVIIIa and FVIIIa-V634A showed the same decrease in enhancing the activity of FIXa when the cofactors were activated in the absence of FIXa. Notably, only the FVIIIa showed a delayed decrease in enhancing the FIXa activity when both cofactors were activated in the presence of FIXa. This implies that FIXa is unable to stabilize the activated FVIII-V634A variant.

HDX-MS was employed to establish whether there are major conformational changes between FVIII and FVIII-V634A. Comparison of FVIIIa and FVIIIa-V634A revealed, however, no difference in deuterium uptake between the two proteins (Figure 5A). This implies that there is no major structural change, if any at all, in the FVIIIa-V634A variant compared to FVIIIa. In presence of FIXa, however, deuterium incorporation of thrombin-activated FVIII-V634A was almost indistinguishable from that of FVIIIa and FVIIIa-V634A in absence of FIXa (Figure 1C *versus* Figure 5B). This confirms the result obtained by the enzyme kinetics assay that FIXa is unable to

retain the A2 domain in FVIIIa-V634A. Taken together, the combined findings show that region Leu631-Trp637 contributes to cofactor function. In addition, the FVIII-V634A variant exhibits and altered interaction with FIXa.

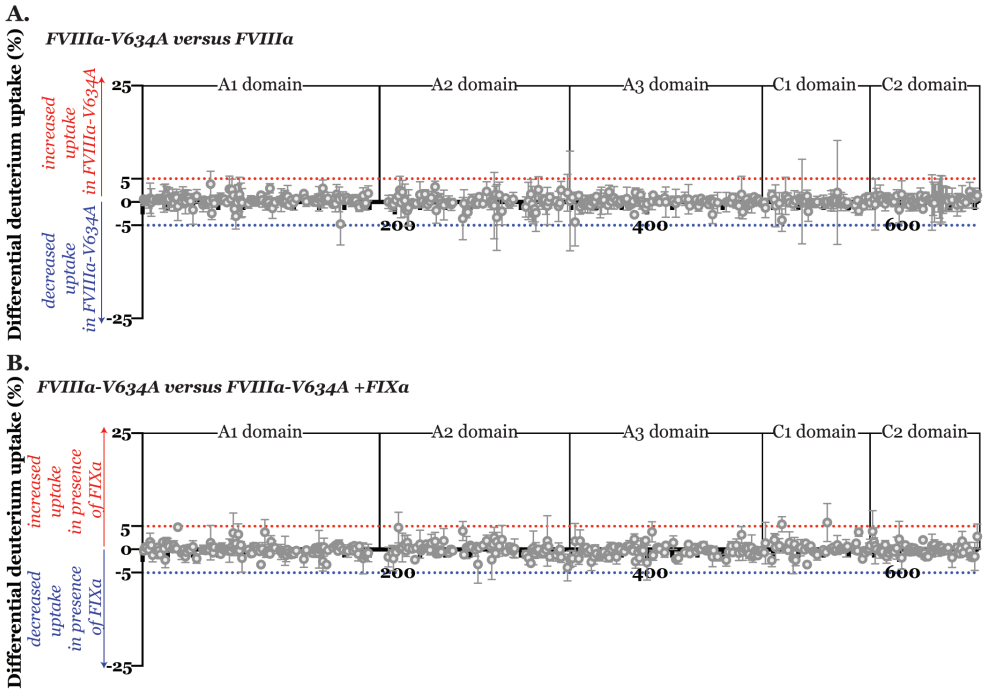


**Figure 5. HDX-MS on FVIII and FVIII-V634A in presence and absence of FIXa**
FVIII and FVIII-V634A in presence and absence of FIXa were incubated for 100s in deuterated buffer. The percentage of deuterium incorporation of a peptide was assessed relative to the theoretical maximum of incorporation in that peptide. The amino acid sequence of the peptides, shown by the ID-number on the x-axis in the panels A and B, is provided in Supplemental Table S1. Panel A shows the differential deuterium incorporation between FVIIIa and FVIIIa-V634A. The y-axis displays the percentage of deuterium uptake of the peptides of FVIIIa subtracted with that of FVIIIa-V634A. Panel B shows the differential deuterium incorporation between FVIIIa-V634A and FVIIIa-V634A in presence of FIXa. The y-axis displays the percentage of deuterium uptake of the peptides of FVIIIa-V634A subtracted with that of FVIII-V634A in presence of FIXa. The average of three independent experiments is shown in panel A and B. Error bars represent the standard deviation.

## DISCUSSION

In this study, we investigated the deuterium perturbations in coagulation FVIII upon thrombin activation and its assembly with FIXa on phospholipid membranes. FVIII activation resulted in a marked increase in deuterium incorporation mainly in A2 domain regions at the interface with the A3 domain (Figure 1A and 1B). This observation is compatible with the self-dampening of cofactor activity which is the





result of the rapid A2 domain dissociation from FVIIIa[35]. The interactive regions are fully exposed to the solvent after dissociation of the A2 domain thereby facilitating deuterium incorporation at these sites. In this view, it remains remarkable, however, that no changes are observed in the A1 domain at the A1–A2 domain interface. Also, for the A3 domain, only a short stretch of amino acids revealed enhanced incorporation (Figure 1A and 1B). This suggests that there is only a limited interaction between amino acid residues at the interface between the A domains. Full contact between the A domains is, however, not to be expected. The affinity of the A2 domain for the A1 and A2 domain should be low to facilitate rapid dissociation from FVIIIa[4]. Although it remains speculation, our data may imply that only A3 domain peptide region Tyr1976-Phe1983 interacts with the A2 in FVIIIa. If so, this would then explain why the HDX of other regions in the A1 and A3 domain remain unchanged. This would also imply that the isolated A2 domain undergoes a major structural change at the interface region after its dissociation. This may also contribute to the poor ability of the isolated A2 domain to enhance the activity of FIXa[1,36].

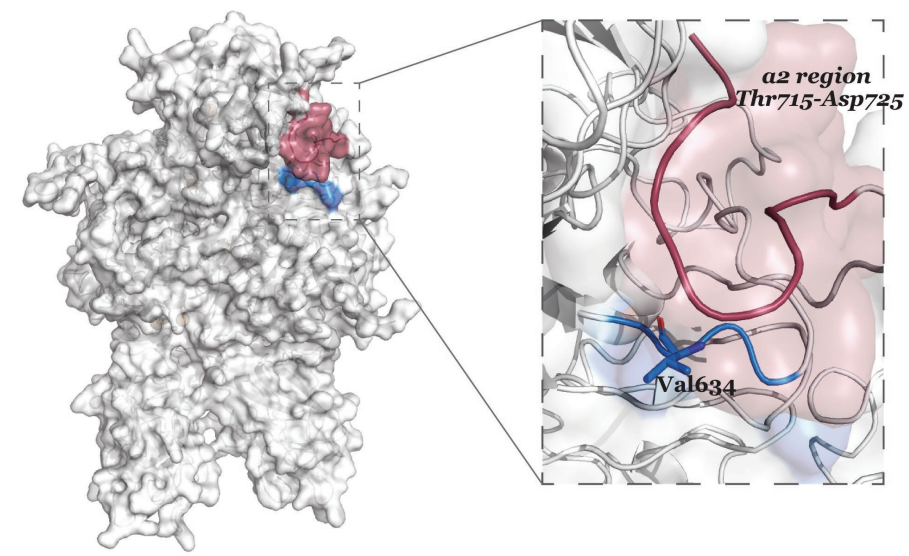


**Figure 6. FVIII *a2* region partially covers A2 region Leu631-Trp637**
Part of the crystal structure of FVIII is shown in a surface representation (PDB code: 2r7e[13]). FVIII region Leu631-Trp637 is colored in blue while the *a2* region Thr715-Asp725 is displayed in red.

Changes were also observed for amino acid regions that are outside the interface between the A domains. The peptides overlapping Leu631-Trp637 showed an increased deuterium uptake upon activations of FVIII (Figure 2B and 2D).

Interestingly, the crystal structure of FVIII published by Shen et al. shows that the acidic *a2* regions partially covers Leu631-Trp637 (Figure 6)[13]. Thrombin cleavage at the arginine residue that flanks the *a2* regions may fully expose the Leu631-Trp637 region to the protein surface thereby explaining the enhanced deuterium uptake. In presence of FIXa, the deuterium uptake of Leu631-Trp637 was decreased beyond that of FVIII prior to its activation (Figure 2B). This suggests that FIXa either changes the local conformation or directly interacts with this region.

The functional importance of region Leu631-Trp637 is demonstrated by the observation that the FVIII-V634A variant is almost unable to enhance the activity of FIXa (Figure 3). This is in line with previous observations that the natural Val634Ala variant of FVIII is linked to hemophilia A[32]. It is, however, surprising that this single substitution has such a major impact on the cofactor function. Although, the HDX of peptides including Val634Ala variant cannot be directly compared with HDX-MS of its wild-type counterpart concerning the Leu631-Trp637 site, almost no difference in HDX was observed between FVIII-V634A and FVIII (Figure 5A). This suggests that the substitution has no major impact on the overall structure of FVIII. While HDX-MS did reveal changes compatible with A2 domain retention in FVIII in presence of FIXa, these changes were absent for the activated Val634Ala variant (Figure 1C *versus* Figure 5B). Results from the enzyme kinetics assay were compatible with this observation. FIXa was able to stabilize the cofactor function of WT-FVIII and not that of FVIII-Val634Ala (Figure 4B). This together implies that there may be an altered interaction between FIXa and the A2 domain of FVIII-V634A.

Several putative FIXa-interactive regions have been identified on FVIII (Supplementary Figure S4A). A limitation of the present study is that no reliable HDX information could be obtained for region 484-507[6,37,38] and 558-565[6,17] because a lack of sequence coverage or inconsistent results. For region 2228-2240[39] and 1811-1818[40], no changes were observed in HDX in presence of FIXa. It should be noted, however, that HDX-MS provides only information about deuterium exchange of the amide hydrogens of the protein backbone. Hydrogens of the side chain residues exchange either too fast or not at all on the measured time scale. If mainly the charged lysine residues of e.g. region 1811-1818 interact directly with FIXa without altering the local conformation of this region, no difference in deuterium incorporation would then be expected.

Irrespective of this limitation, the study did provide novel information about the FVIIIa-FIXa complex assembly. We found a previously undescribed role for region Leu631-Trp637 in enhancing the activity of FIXa. Notably, superposition of the structure of FIXa and FVIII on the homologous prothrombinase complex revealed that Val634 may be indeed located at the A2 domain/protease domain interface close to FIXa 330-helix (Supplementary Figure S4D). Although it remains somewhat





speculative, it does support the conclusion that region Leu631-Trp637 may directly interact with FIXa.

## ACKNOWLEDGEMENTS

We would like to thank Max Hoek for writing a script to organize peptides.

## AUTHOR CONTRIBUTIONS

JG, NF, MB and MP performed experiments; CZ provided technical assistance; JG, NF, MvdB and AM designed the experiments; EE assisted with setting up HDX-MS experiments; JG, NF, MP and MB analyzed results; NF and JG made the figures, JG, NF, MvdB and AM wrote the paper.

## CONFLICT OF INTEREST

The authors declare no competing financial interests

## FUNDING

This study has been funded by Landsteiner Stichting voor Bloedtransfusie Research (LSBR 1417).

## REFERENCES


1. Fay PJ. Activation of factor VIII and mechanisms of cofactor action. *Blood Rev*. 2004;18(1):1–15.

2. Mannucci PM, Tuddenham EG. The hemophilias--from royal genes to gene therapy. *N Engl J Med*. 2001;344(23):1773-1779.

3. Vehar GA, Keyt B, Eaton D, et al. Structure of human factor VIII. *Nature*. 1984;312(5992):337-342.

4. Lenting PJ, van Mourik JA, Mertens K. The life cycle of coagulation factor VIII in view of its structure and function. *Blood*. 1998;92(11):3983-3996.

5. Kamikubo Y, Mendolicchio GL, Zampolli A, et al. Selective factor VIII activation by the tissue factor-factor VIIa-factor Xa complex. *Blood*. 2017;130(14):1661-1670.

6. Fay PJ. Factor VIII structure and function. *Int J Hematol*. 2006;83(2):103–108.

7. van Dieijen G, Tans G, Rosing J, Hemker HC. The role of phospholipid and factor VIIIa in the activation of bovine factor X. *J Biol Chem*. 1981;256(7):3433-3442.

8. Fay PJ. Subunit structure of thrombin-activated human factor VIIIa. *Biochim Biophys Acta*. 1988;952(2):181–190.

9. Lollar P, Parker CG. pH-dependent denaturation of thrombin-activated porcine factor VIII. *J Biol Chem*. 1990;265(3):1688-1692.

10. Lollar P, Parker ET. Structural basis for the decreased procoagulant activity of human factor VIII compared to the porcine homolog. *J Biol Chem*. 1991;266(19):12481-12486.

11. Ngo JC, Huang M, Roth DA, Furie BC, Furie B. Crystal structure of human factor VIII: implications for the formation of the factor IXa-factor VIIIa complex. *Structure*. 2008;16(4):597–606.

12. Stoilova-McPhie S, Villoutreix BO, Mertens K, Kemball-Cook G, Holzenburg A. 3-Dimensional structure of membrane-bound coagulation factor VIII: modeling of the factor VIII heterodimer within a 3-dimensional density map derived by electron crystallography. *Blood*. 2002;99(4):1215–1223.

13. Shen BW, Spiegel PC, Chang CH, et al. The tertiary structure and domain organization of coagulation factor VIII. *Blood*. 2008;111(3):1240–1247.

14. Meems H, Meijer AB, Cullinan DB, Mertens K, Gilbert GE. Factor VIII C1 domain residues Lys 2092 and Phe 2093 contribute to membrane binding and cofactor activity. *Blood*. 2009;114(18):3938–3946.

15. Gilbert GE, Kaufman RJ, Arena AA, Miao H, Pipe SW. Four hydrophobic amino acids of the factor VIII C2 domain are constituents of both the membrane-binding and von Willebrand factor-binding motifs. *J Biol Chem*. 2002;277(8):6374–6381.

16. Bajaj SP, Schmidt AE, Mathur A, et al. Factor IXa:Factor VIIIa interaction. Helix 330-338 of factor IXa interacts with residues 558-565 and spatially adjacent regions of the A2 subunit of factor VIIIa. *J Biol Chem*. 2001;276(19):16302–16309.

17. Fay PJ, Beattie T, Huggins CF, Regan LM. Factor VIIIa A2 subunit residues 558-565 represent a factor IXa interactive site. *J Biol Chem*. 1994;269(32):20522–20527.

18. Pantazatos D, Gessner CR, Woods Jr. VL, Gilbert GE. Changes in the Factor VIII C2 domain upon membrane binding determined by hydrogen-deuterium exchange MS. *Biochem J*. 2014;461(3):443–451.

19. Bloem E, van den Biggelaar M, Wroblewska A, et al. Factor VIII C1 domain spikes 2092-2093 and 2158-2159 comprise regions that modulate cofactor function and cellular uptake. *J Biol Chem*. 2013;288(41):29670–29679.

20. Przeradzka MA, van Galen J, Ebberink EHTM, et al. D' domain region Arg782-Cys799 of von Willebrand factor contributes to factor VIII binding. *Haematologica*. 2020;105(6):1695-1703.

21. van den Biggelaar M, Madsen JJ, Faber JH, et al. Factor VIII Interacts with the Endocytic Receptor Low-density Lipoprotein Receptor-related Protein 1 via an Extended Surface Comprising "Hot-Spot" Lysine Residues. *J Biol Chem*. 2015;290(27):16463-16476.

22. Song H, Olsen OH, Persson E, Rand KD. Sites involved in intra- and interdomain allostery associated with the activation of factor VIIa pinpointed by hydrogen-deuterium exchange and electron transfer dissociation mass spectrometry. *J Biol Chem*. 2014;289(51):35388-35396.

23. Hendrix H, Lindhout T, Mertens K, Engels W, Hemker HC. Activation of human prothrombin by stoichiometric levels of staphylocoagulase. *J Biol Chem*. 1983;258(6):3637-3644.

24. Mertens K, Bertina RM. Activation of human coagulation factor VIII by activated factor X, the common product of the intrinsic and the extrinsic pathway of blood coagulation. *Thromb Haemost*. 1982;47(2):96-100.

25. Bradford MM. A rapid and sensitive method for the quantitation of microgram quantities of protein utilizing the principle of protein-dye binding. *Anal Biochem*. 1976;72:248-254.

26. Lenting PJ, ter Maat H, Clijsters PP, Donath MJ, van Mourik JA, Mertens K. Cleavage at arginine 145 in human blood coagulation factor IX converts the zymogen into a factor VIII binding enzyme. *J Biol Chem*. 1995;270(25):14884-14890.

27. Foster PA, Fulcher CA, Marti T, Titani K, Zimmerman TS. A major factor VIII binding domain resides within the amino-terminal 272 amino acid residues of von Willebrand factor. *J Biol Chem*. 1987;262(18):8443-8446.

28. Meems H, van den Biggelaar M, Rondaij M, van der Zwaan C, Mertens K, Meijer AB. C1 domain residues Lys 2092 and Phe 2093 are of major importance for the endocytic uptake of coagulation factor VIII. *Int J Biochem Cell Biol*. 2011;43(8):1114-1121.

29. van den Biggelaar M, Bierings R, Storm G, Voorberg J, Mertens K. Requirements for cellular co-trafficking of factor VIII and von Willebrand factor to Weibel-Palade bodies. *J Thromb Haemost JTH*. 2007;5(11):2235-2242.

30. Rouser G, Siakotos AN, Fleischer S. Quantitative analysis of phospholipids by thin-layer chromatography and phosphorus analysis of spots. *Lipids*. 1966;1(1):85-86.

31. Bloem E, Meems H, van den Biggelaar M, Mertens K, Meijer AB. A3 domain region 1803-1818 contributes to the stability of activated factor VIII and includes a binding site for activated factor IX. *J Biol Chem*. 2013;288(36):26105–26111.

32. McGinniss MJ, Kazazian HH, Hoyer LW, Bi L, Inaba H, Antonarakis SE. Spectrum of mutations in CRM-positive and CRM-reduced hemophilia A. *Genomics*. 1993;15(2):392-398.

33. Ahmed RPH, Ivaskevicius V, Kannan M, Seifried E, Oldenburg J, Saxena R. Identification of 32 novel mutations in the factor VIII gene in Indian patients with hemophilia A. *Haematologica*. 2005;90(2):283-284.

34. Bloem E, Meems H, van den Biggelaar M, van der Zwaan C, Mertens K, Meijer AB. Mass spectrometry-assisted study reveals that lysine residues 1967 and 1968 have opposite contribution to stability of activated factor VIII. *J Biol Chem*. 2012;287(8):5775–5783.

35. Fay PJ, Jenkins PV. Mutating factor VIII: lessons from structure to function. *Blood Rev*. 2005;19(1):15–27.

36. Mertens K, Celie PH, Kolkman JA, Lenting PJ. Factor VIII-factor IX interactions: molecular sites involved in enzyme-cofactor complex assembly. *Thromb Haemost*. 1999;82(2):209–217.

37. Healey JF, Lubin IM, Nakai H, et al. Residues 484-508 contain a major determinant of the inhibitory epitope in the A2 domain of human factor VIII. *J Biol Chem*. 1995;270(24):14505-14509.

38. Jenkins PV, Dill JL, Zhou Q, Fay PJ. Clustered basic residues within segment 484-510 of the factor VIIIa A2 subunit contribute to the catalytic efficiency for factor Xa generation. *J Thromb Haemost JTH*. 2004;2(3):452-458.

39. Soeda T, Nogami K, Nishiya K, et al. The factor VIIIa C2 domain (residues 2228-2240) interacts with the factor IXa Gla domain in the factor Xase complex. *J Biol Chem*. 2009;284(6):3379-3388.

40. Bovenschen N, Boertjes RC, van Stempvoort G, et al. Low density lipoprotein receptor-related protein and factor IXa share structural requirements for binding to the A3 domain of coagulation factor VIII. *J Biol Chem*. 2003;278(11):9370-9377.





## SUPPLEMENTARY MATERIAL

**A.**

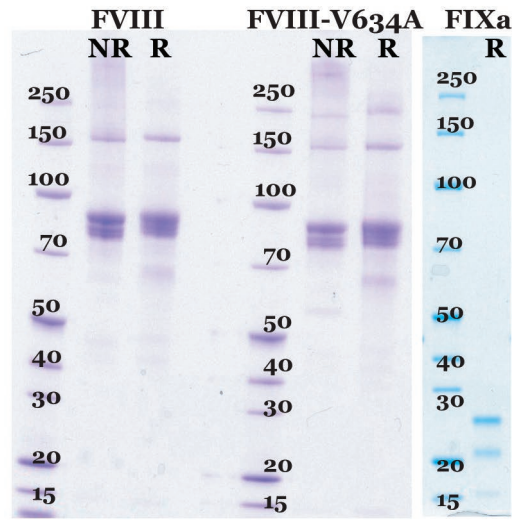


**B.**

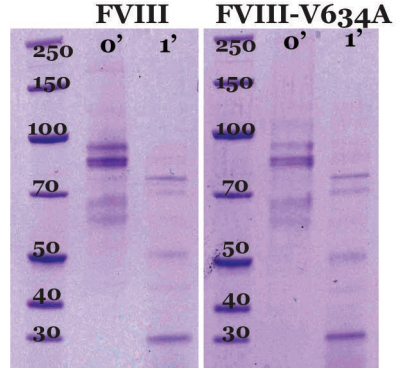


**Supplementary Figure S1. Characterization of protein preparations**

A) SDS-PAGE with Brilliant Blue Coomassie staining of purified recombinant FVIII-WT, FVIII-V634A and FIXa. NR indicates non-reduced and R indicates reduced. The protein marker is indicated next to FVIII, FVIII-V634A and FIXa. B) SDS-PAGE with Brilliant Blue Coomassie staining of Thrombin activated FVIII-WT and FVIII-V634A. To this end, 480 nM of FVIII-WT or FVIII-V634A were activated by 16 nM of thrombin for 1 minute in presence of 10 mM $CaCl_2$ in TBS. Thrombin was blocked with 1:5 molar excess of hirudin.

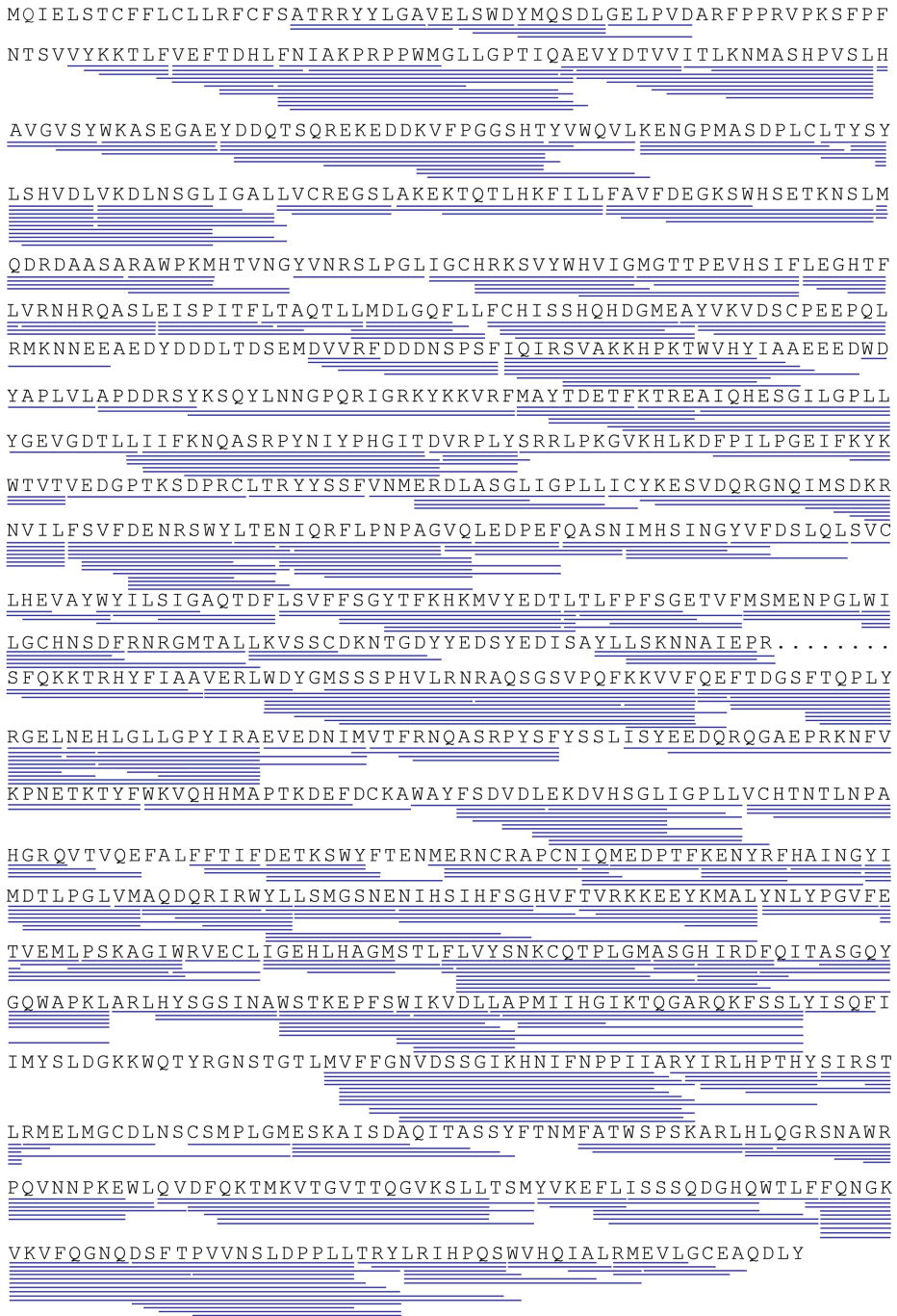


**Supplementary Figure S2. Coverage of FVIII sequence by the peptides identified by HDX-MS analysis**

The primary sequence of FVIII is shown. The blue lines indicate the peptides that were identified by HDX-MS analysis.





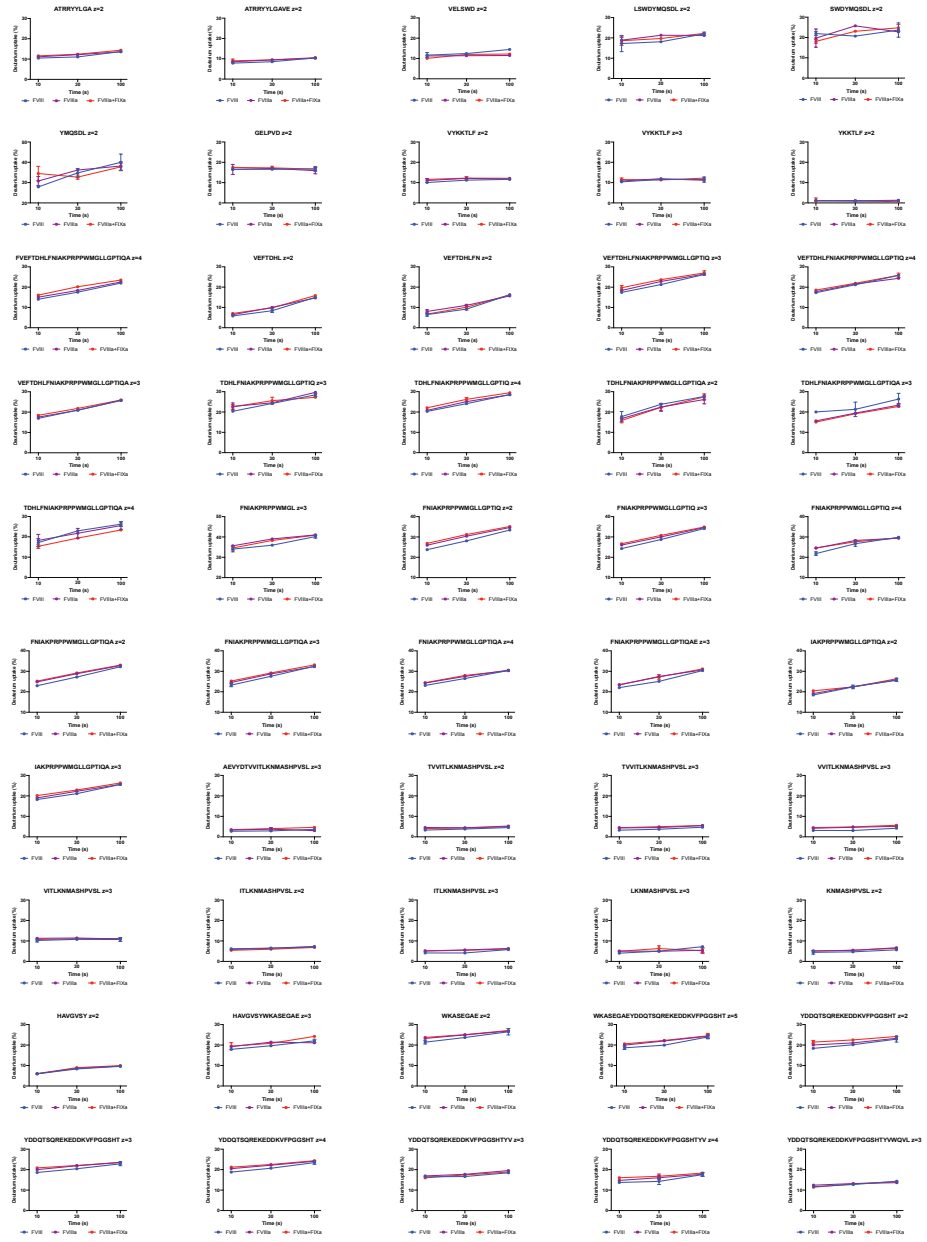

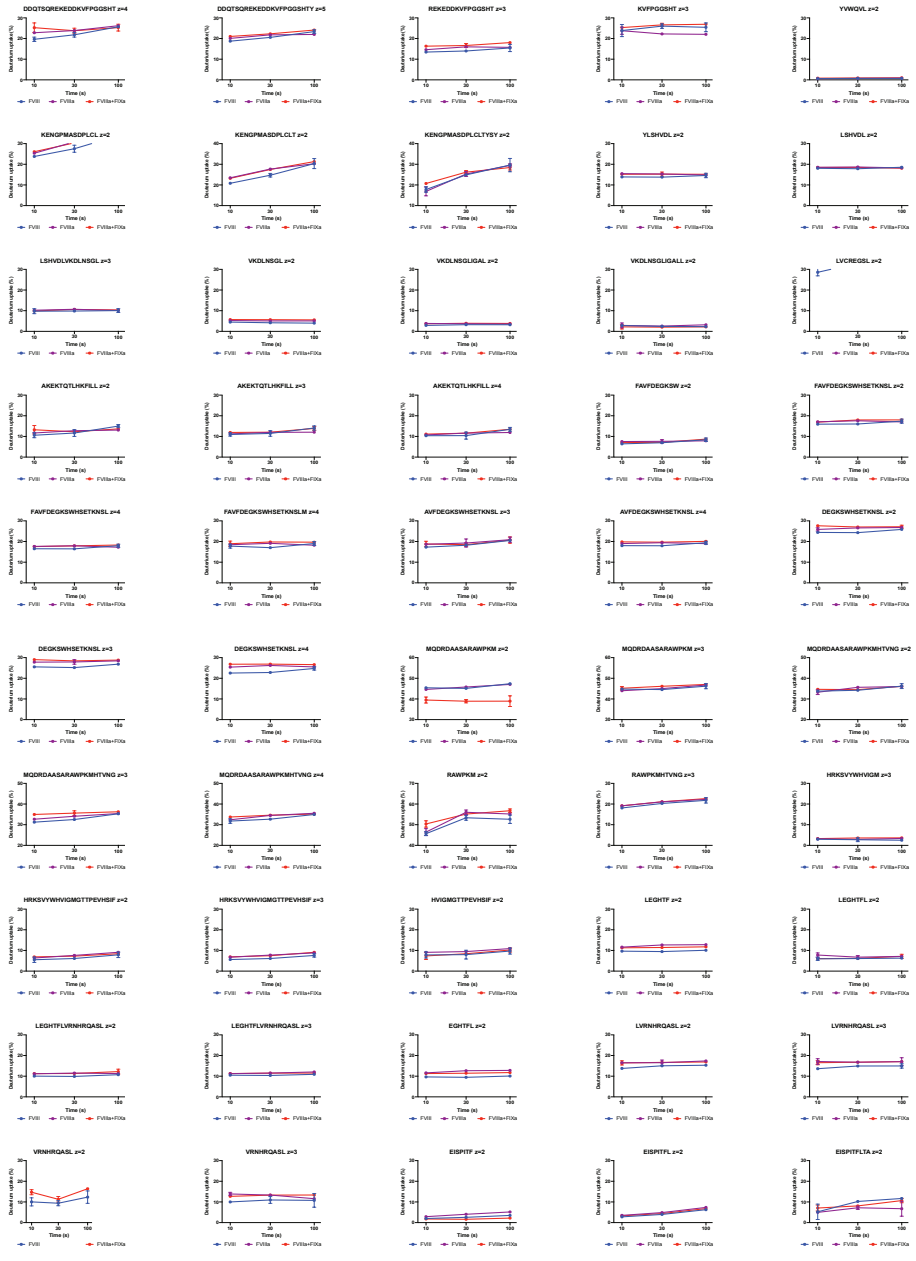
DDQTSQREKEDDKVFPGGSHT z=4
DDQTSQREKEDDKVFPGGSHTY z=5
REKEDDKVFPGGSHT z=3
KVFPGGSHT z=3
YVWQVL z=2
KENGPMASDPLCL z=2
KENGPMASDPLCLT z=2
KENGPMASDPLCLTYSY z=2
YLSHVDL z=2
LSHVDL z=2
LSHVDLVKDLNSGL z=3
VKDLNSGL z=2
VKDLNSGLIGAL z=2
VKDLNSGLIGALL z=2
LVCREGSL z=2
AKEKTQTLHKFILL z=2
AKEKTQTLHKFILL z=3
AKEKTQTLHKFILL z=4
FAVFDEGKSW z=2
FAVFDEGKSWHSETKNSL z=2
FAVFDEGKSWHSETKNSL z=4
FAVFDEGKSWHSETKNSLM z=4
AVFDEGKSWHSETKNSL z=3
AVFDEGKSWHSETKNSL z=4
DEGKSWHSETKNSL z=2
DEGKSWHSETKNSL z=3
DEGKSWHSETKNSL z=4
MQDRDAASARAWPKM z=2
MQDRDAASARAWPKM z=3
MQDRDAASARAWPKMHTVNG z=2
MQDRDAASARAWPKMHTVNG z=3
MQDRDAASARAWPKMHTVNG z=4
RAWPKM z=2
RAWPKMHTVNG z=3
HRKSVYWHVIGMG z=3
HRKSVYWHVIGMGTTPEVHSIF z=2
HRKSVYWHVIGMGTTPEVHSIF z=3
HVIGMGTTPEVHSIF z=2
LEGHTF z=2
LEGHTFL z=2
LEGHTFLVRNHRQASL z=2
LEGHTFLVRNHRQASL z=3
EGHTFL z=2
LVRNHRQASL z=2
LVRNHRQASL z=3
VRNHRQASL z=2
VRNHRQASL z=3
EISPITF z=2
EISPITFL z=2
EISPITFLTA z=2
Deuterium uptake (%)
Time (s)
FVIII
FVIIIa
FVIIIa+FIXa

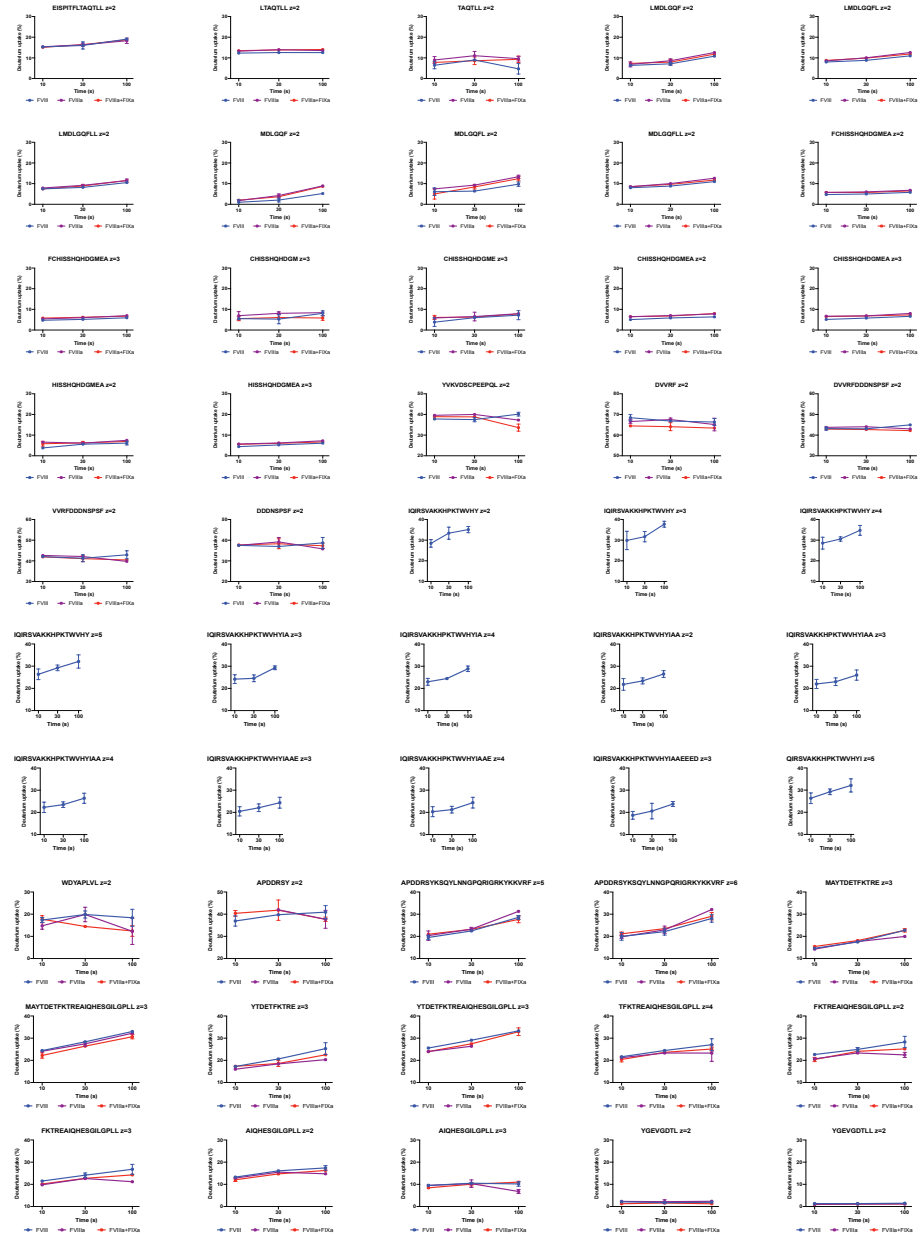
EISPITFLTAQTLL z=2
LTAQTLL z=2
TAQTLL z=2
LMDLGQF z=2
LMDLGQFL z=2
LMDLGQFLL z=2
MDLGQF z=2
MDLGQFL z=2
MDLGQFLL z=2
FCHISSHQHDGMEA z=2
FCHISSHQHDGMEA z=3
CHISSHQHDGM z=3
CHISSHQHDGME z=3
CHISSHQHDGMEA z=2
CHISSHQHDGMEA z=3
HISSHQHDGMEA z=2
HISSHQHDGMEA z=3
YVKVDSCPEEPQL z=2
DVVRF z=2
DVVRFDDDNSPSF z=2
VVRFDDDNSPSF z=2
DDDNSPSF z=2
IQIRSVAKKHPKTWVHY z=2
IQIRSVAKKHPKTWVHY z=3
IQIRSVAKKHPKTWVHY z=4
IQIRSVAKKHPKTWVHY z=5
IQIRSVAKKHPKTWVHYIA z=3
IQIRSVAKKHPKTWVHYIA z=4
IQIRSVAKKHPKTWVHYIAA z=2
IQIRSVAKKHPKTWVHYIAA z=3
IQIRSVAKKHPKTWVHYIAA z=4
IQIRSVAKKHPKTWVHYIAAE z=3
IQIRSVAKKHPKTWVHYIAAE z=4
IQIRSVAKKHPKTWVHYIAAEEED z=3
QIRSVAKKHPKTWVHY1 z=5
WDYAPLVL z=2
APDDRSY z=2
APDDRSYKSQYLNNGPQRIGRKYKKVRF z=5
APDDRSYKSQYLNNGPQRIGRKYKKVRF z=6
MAYTDETFKTRE z=3
MAYTDETFKTREAIQHESGILGPLL z=3
YTDETFKTRE z=3
YTDETFKTREAIQHESGILGPLL z=3
TFKTREAIQHESGILGPLL z=4
FKTREAIQHESGILGPLL z=2
FKTREAIQHESGILGPLL z=3
AIQHESGILGPLL z=2
AIQHESGILGPLL z=3
YGEVGDTL z=2
YGEVGDTLL z=2
Deuterium uptake (%)
Time (s)
FVIII
FVIIIa
FVIIIa+FIXa

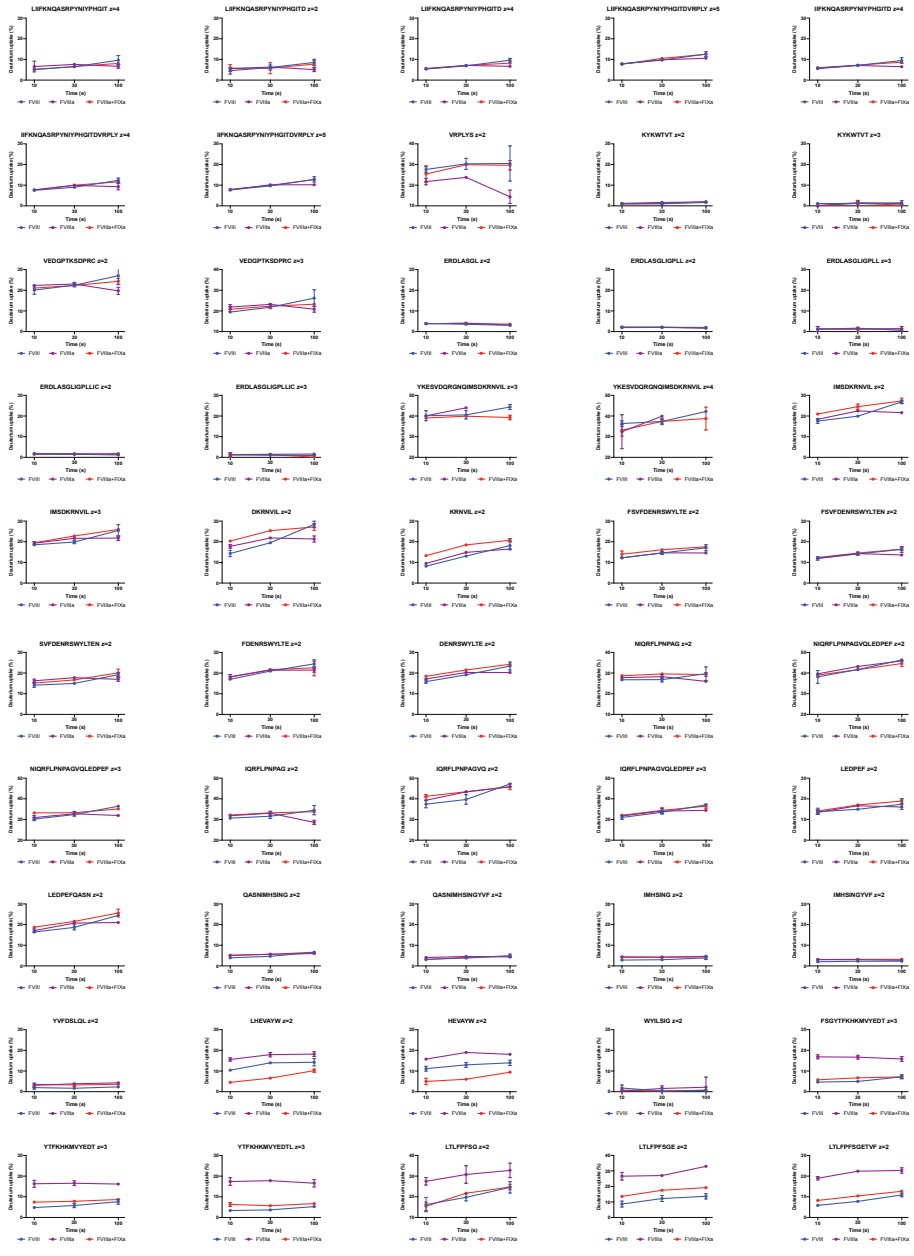
LIIFKNQASRPYNIYPHGIT z=4
LIIFKNQASRPYNIYPHGITD z=2
LIIFKNQASRPYNIYPHGITD z=4
LIIFKNQASRPYNIYPHGITDVRPLY z=5
IIFKNQASRPYNIYPHGITD z=4
IIFKNQASRPYNIYPHGITDVRPLY z=4
IIFKNQASRPYNIYPHGITDVRPLY z=5
VRPLYS z=2
KYKWTVT z=2
KYKWTVT z=3
VEDGPTKSDPRC z=2
VEDGPTKSDPRC z=3
ERDLASGL z=2
ERDLASGLIGPLL z=2
ERDLASGLIGPLL z=3
ERDLASGLIGPLLIC z=2
ERDLASGLIGPLLIC z=3
YKESVDQRGNQIMSDKRNVIL z=3
YKESVDQRGNQIMSDKRNVIL z=4
IMSDKRNVIL z=2
IMSDKRNVIL z=3
DKRNVIL z=2
KRNVIL z=2
FSVFDENRSWYLTE z=2
FSVFDENRSWYLTEN z=2
SVFDENRSWYLTEN z=2
FDENRSWYLTE z=2
DENRSWYLTE z=2
NIQRFLPNPAG z=2
NIQRFLPNPAGVQLEDPEF z=2
NIQRFLPNPAGVQLEDPEF z=3
IQRFLPNPAG z=2
IQRFLPNPAGVQ z=2
IQRFLPNPAGVQLEDPEF z=3
LEDPEF z=2
LEDPEFQASN z=2
QASNIMHSING z=2
QASNIMHSINGYVF z=2
IMHSING z=2
IMHSINGYVF z=2
YVFDSLQL z=2
LHEVAYW z=2
HEVAYW z=2
WYILSIG z=2
FSGYTFKHKMVYEDT z=3
YTFKHKMVYEDT z=3
YTFKHKMVYEDTL z=3
LTLFPFSG z=2
LTLFPFSGE z=2
LTLFPFSGETVF z=2
Deuterium uptake (%)
Time (s)
FVIII
FVIIIa
FVIIIa+FIXa



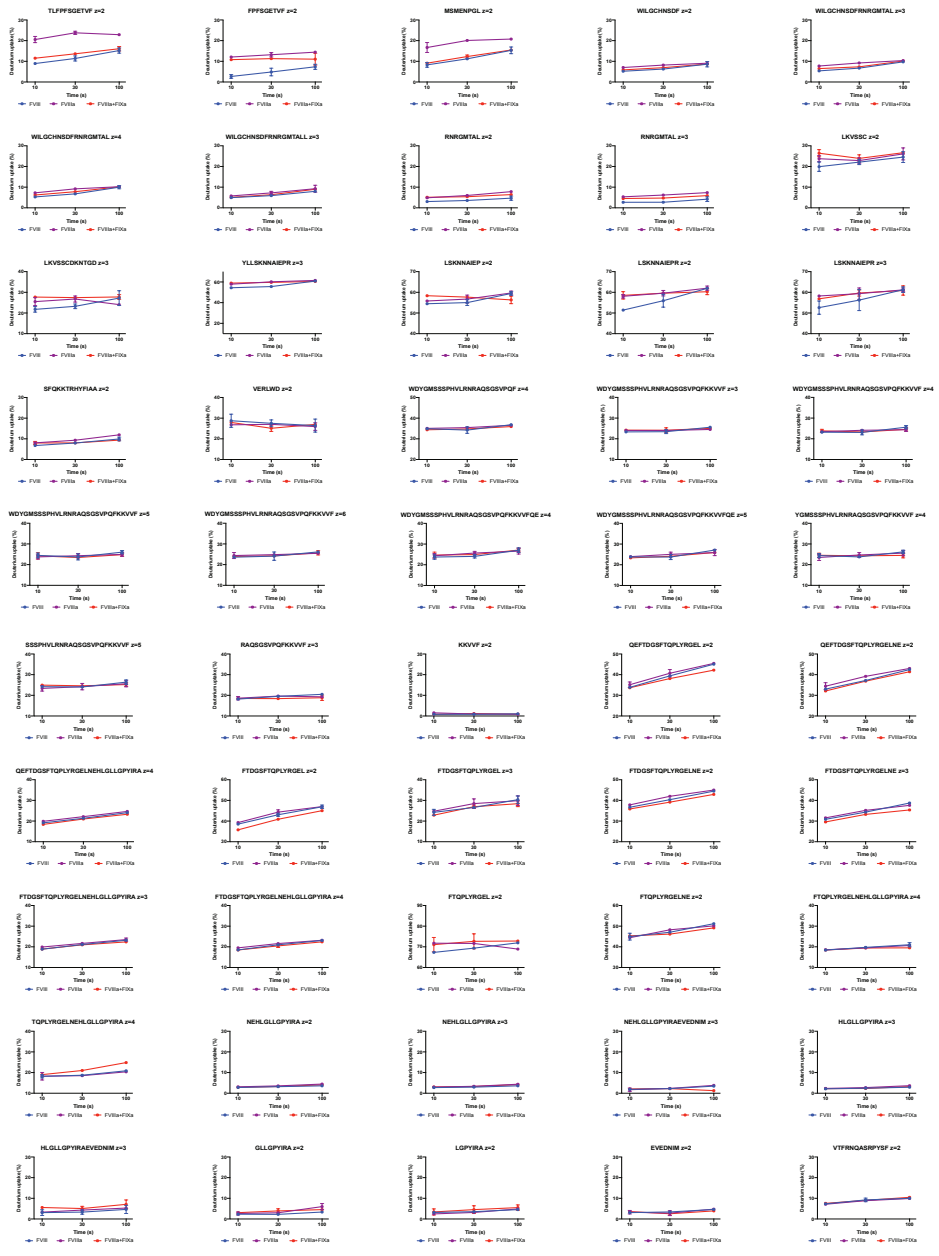
TLFPFSGETVF z=2
FPFSGETVF z=2
MSMENPGL z=2
WILGCHNSDF z=2
WILGCHNSDFRNRGMTAL z=3
WILGCHNSDFRNRGMTAL z=4
WILGCHNSDFRNRGMTALL z=3
RNRGMTAL z=2
RNRGMTAL z=3
LKVSSC z=2
LKVSSCDKNTGD z=3
YLLSKNNAIEPR z=3
LSKNNAIEP z=2
LSKNNAIEPR z=2
LSKNNAIEPR z=3
SFQKKTRHYFIAA z=2
VERLWD z=2
WDYGMSSSPHVLRNRAQSGSVPQF z=4
WDYGMSSSPHVLRNRAQSGSVPQFKKVVF z=3
WDYGMSSSPHVLRNRAQSGSVPQFKKVVF z=4
WDYGMSSSPHVLRNRAQSGSVPQFKKVVF z=5
WDYGMSSSPHVLRNRAQSGSVPQFKKVVF z=6
WDYGMSSSPHVLRNRAQSGSVPQFKKVVFQE z=4
WDYGMSSSPHVLRNRAQSGSVPQFKKVVFQE z=5
YGMSSSPHVLRNRAQSGSVPQFKKVVF z=4
SSSPHVLRNRAQSGSVPQFKKVVF z=5
RAQSGSVPQFKKVVF z=3
KKVVF z=2
QEFTDGSFTQPLYRGEL z=2
QEFTDGSFTQPLYRGELNE z=2
QEFTDGSFTQPLYRGELNHLGLLGPYIRA z=4
FTDGSFTQPLYRGEL z=2
FTDGSFTQPLYRGEL z=3
FTDGSFTQPLYRGELNE z=2
FTDGSFTQPLYRGELNE z=3
FTDGSFTQPLYRGELNEHLGLLGPYIRA z=3
FTDGSFTQPLYRGELNEHLGLLGPYIRA z=4
FTQPLYRGEL z=2
FTQPLYRGELNE z=2
FTQPLYRGELNEHLGLLGPYIRA z=4
TQPLYRGELNEHLGLLGPYIRA z=4
NEHLGLLGPYIRA z=2
NEHLGLLGPYIRA z=3
NEHLGLLGPYIRAEVEDNIM z=3
HLGLLGPYIRA z=3
HLGLLGPYIRAEVEDNIM z=3
GLLGPYIRA z=2
LGPYIRA z=2
EVEDNIM z=2
VTFRNQASRPYSF z=2
Deuterium uptake (%)
Time (s)
FVIII
FVIIIa
FVIIIa+FIXa

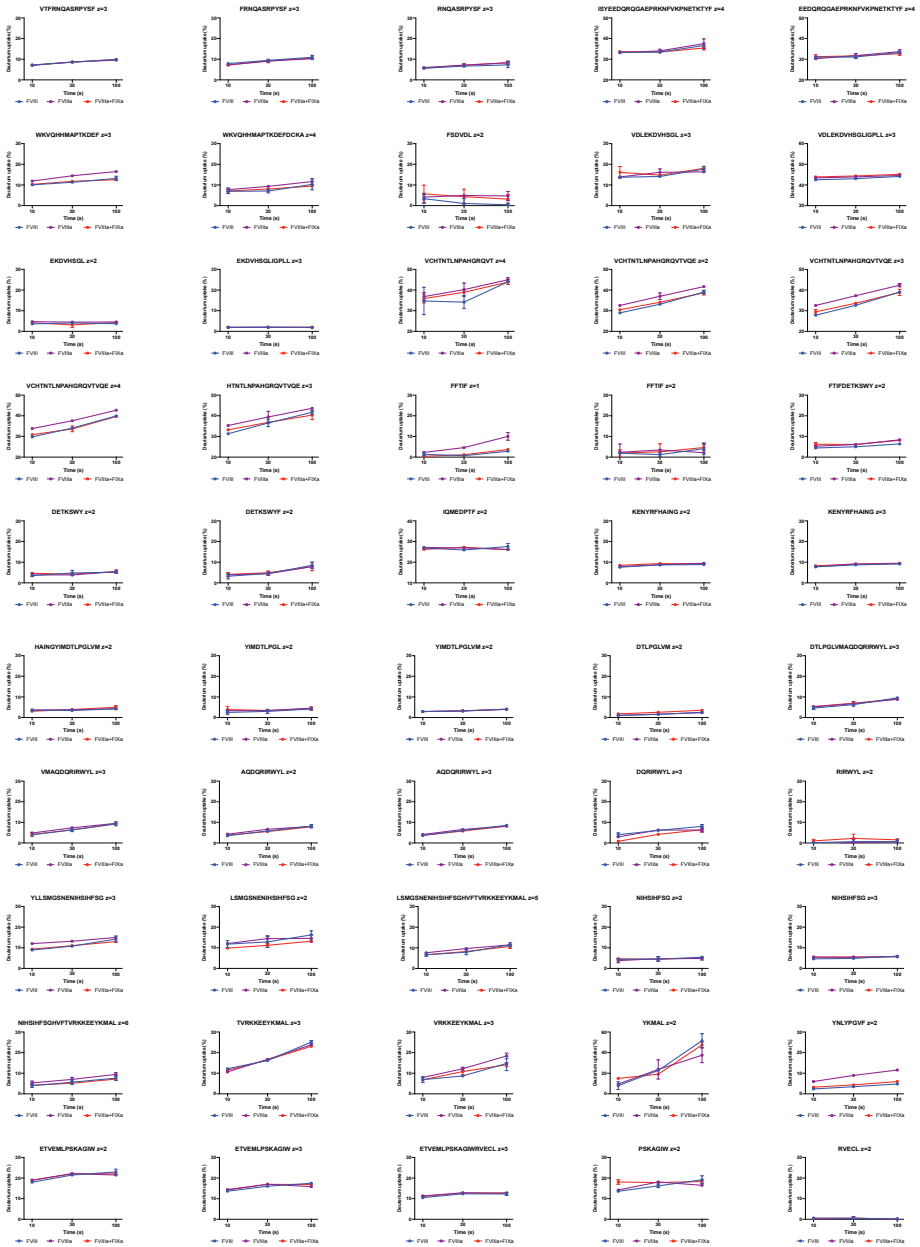
VTFRNQASRPYSF z=3
FRNQASRPYSF z=3
RNQASRPYSF z=3
ISYEEDQRQGAEPRKNFVKPNETKTYF z=4
EEDQRQGAEPRKNFVKPNETKTYF z=4
WKVQHHMAPTKDEF z=3
WKVQHHMAPTKDEFDCKA z=4
FSDVDL z=2
VDLEKDVHSGL z=3
VDLEKDVHSGLIGPLL z=3
EKDVHSGL z=2
EKDVHSGLIGPLL z=3
VCHTNTLNPAHGRQVT z=4
VCHTNTLNPAHGRQVTVQE z=2
VCHTNTLNPAHGRQVTVQE z=3
VCHTNTLNPAHGRQVTVQE z=4
HTNTLNPAHGRQVTVQE z=3
FFTIF z=1
FFTIF z=2
FTIFDETKSWY z=2
DETKSWY z=2
DETKSWYF z=2
IQMEDPTF z=2
KENYRFHAING z=2
KENYRFHAING z=3
HAINGYIMDTLPGLVM z=2
YIMDTLPGL z=2
YIMDTLPGLVM z=2
DTLPGLVM z=2
DTLPGLVMAQDQRRWYL z=3
VMAQDQRIRWYL z=3
AQDQRIRWYL z=2
AQDQRIRWYL z=3
DQRIRWYL z=3
RIRWYL z=2
YLLSMGSNENHSIHFSG z=3
LSMGSNENHSIHFSG z=2
LSMGSNENHSIHFSGHVFTVRKKEEYKMAL z=5
NIHSIHFSG z=2
NIHSIHFSG z=3
NIHSIHFSGHVFTVRKKEEYKMAL z=6
TVRKKEEYKMAL z=3
VRKKEEYKMAL z=3
YKMAL z=2
YNLYPGVF z=2
ETVEMLPSKAGIW z=2
ETVEMLPSKAGIW z=3
ETVEMLPSKAGIWRVECL z=3
PSKAGIW z=2
RVECL z=2
Deuterium update (%)
Time (s)
FVIII
FVIIIa
FVIIIa+FIXa





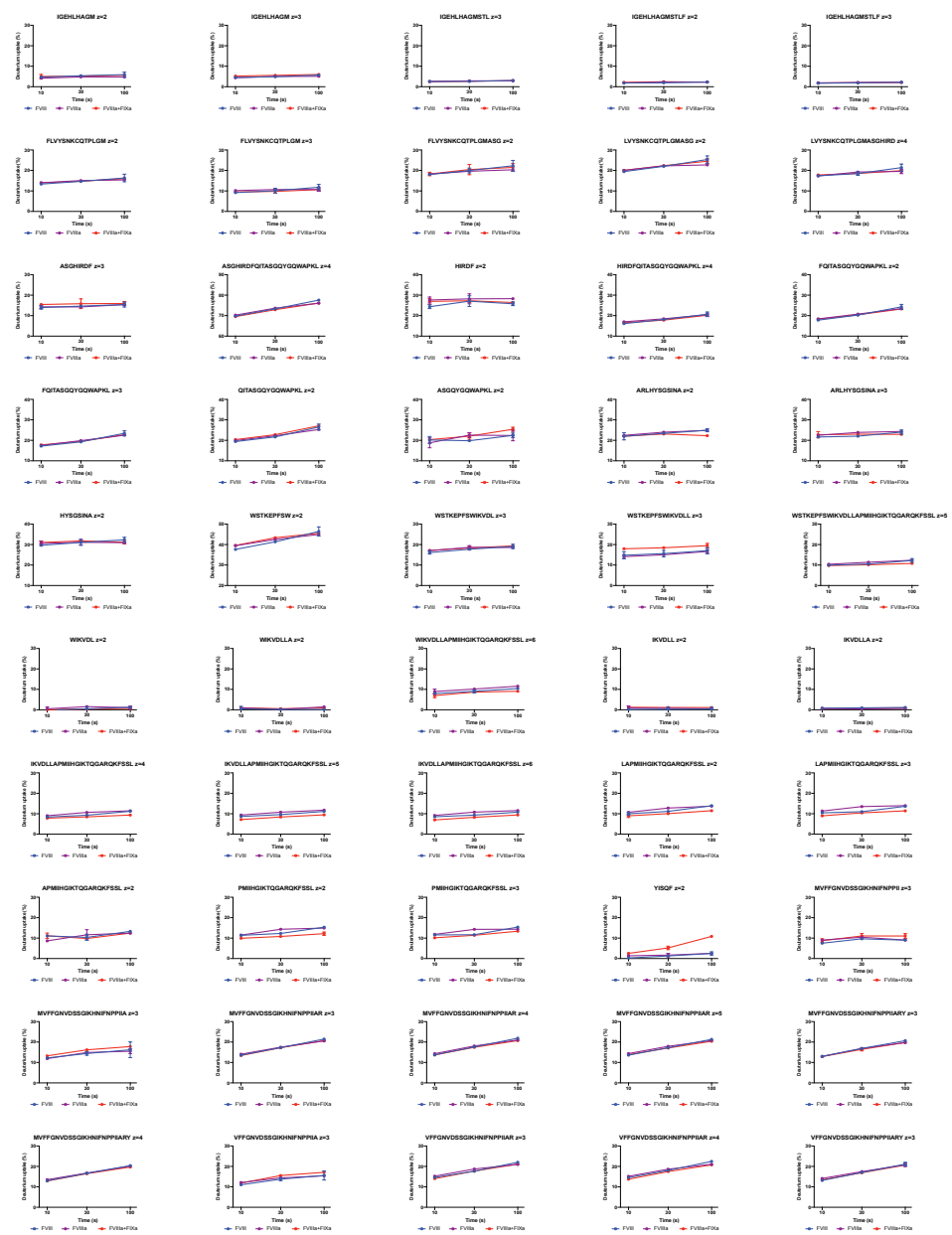
IGEHLHAGM z=2
IGEHLHAGM z=3
IGEHLHAGMSTL z=3
IGEHLHAGMSTLF z=2
IGEHLHAGMSTLF z=3
FLVYSNKCQTPLGM z=2
FLVYSNKCQTPLGM z=3
FLVYSNKCQTPLGMASG z=2
LVYSNKCQTPLGMASG z=2
LVYSNKCQTPLGMASGHIRD z=4
ASGHIRDF z=3
ASGHIRDFQITASGQYGQWAPKL z=4
HIRDF z=2
HIRDFQITASGQYGQWAPKL z=4
FQITASGQYGQWAPKL z=2
FQITASGQYGQWAPKL z=3
QITASGQYGQWAPKL z=2
ASGQYGQWAPKL z=2
ARLHYSGSINA z=2
ARLHYSGSINA z=3
HYSGSINA z=2
WSTKEPFSW z=2
WSTKEPFSWIKVDL z=3
WSTKEPFSWIKVDLL z=3
WSTKEPFSWIKVDLLAPMIIHGIKTQGARQKFSSL z=5
WIKVDL z=2
WIKVDLLA z=2
WIKVDLLAPMIIHGIKTQGARQKFSSL z=6
IKVDLL z=2
IKVDLLA z=2
IKVDLLAPMIIHGIKTQGARQKFSSL z=4
IKVDLLAPMIIHGIKTQGARQKFSSL z=5
IKVDLLAPMIIHGIKTQGARQKFSSL z=6
LAPMIIHGIKTQGARQKFSSL z=2
LAPMIIHGIKTQGARQKFSSL z=3
APMIIHGIKTQGARQKFSSL z=2
PMIIHGIKTQGARQKFSSL z=2
PMIIHGIKTQGARQKFSSL z=3
YISQF z=2
MVFFGNVDSSGIKHNFNPPII z=3
MVFFGNVDSSGIKHNFNPPIIA z=3
MVFFGNVDSSGIKHNIFNPPIIAR z=3
MVFFGNVDSSGIKHNIFNPPIIAR z=4
MVFFGNVDSSGIKHNIFNPPIIAR z=5
MVFFGNVDSSGIKHNIFNPPIIARY z=3
MVFFGNVDSSGIKHNIFNPPIIARY z=4
VFFGNVDSSGIKHNIFNPPIIA z=3
VFFGNVDSSGIKHNIFNPPIIAR z=3
VFFGNVDSSGIKHNIFNPPIIAR z=4
VFFGNVDSSGIKHNIFNPPIIARY z=3
Deuterium update (%)
Time (s)
FVIII
FVIIIa
FVIIIa+FIXa

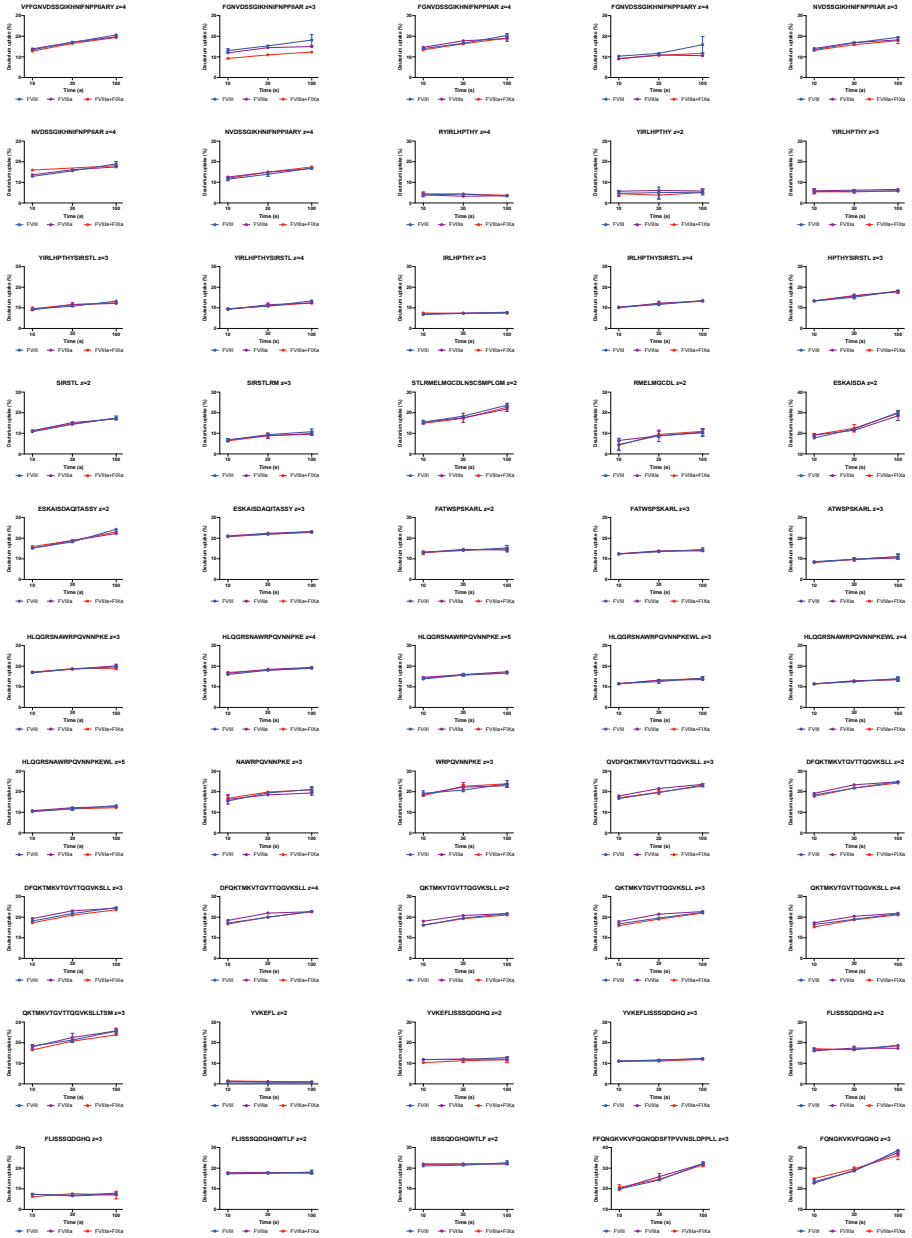


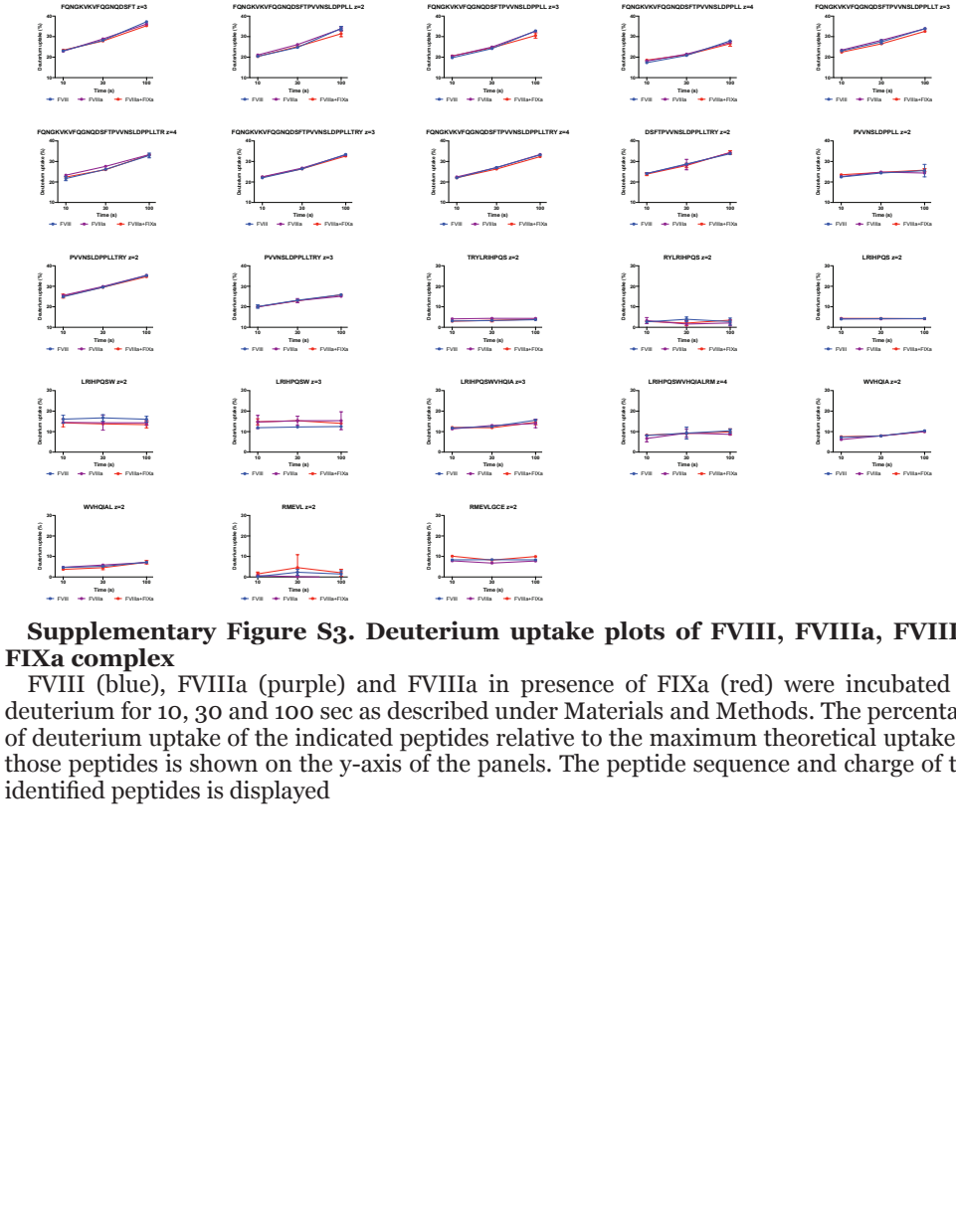


**Supplementary Figure S3. Deuterium uptake plots of FVIII, FVIIIa, FVIIIa-FIXa complex**

FVIII (blue), FVIIIa (purple) and FVIIIa in presence of FIXa (red) were incubated in deuterium for 10, 30 and 100 sec as described under Materials and Methods. The percentage of deuterium uptake of the indicated peptides relative to the maximum theoretical uptake of those peptides is shown on the y-axis of the panels. The peptide sequence and charge of the identified peptides is displayed

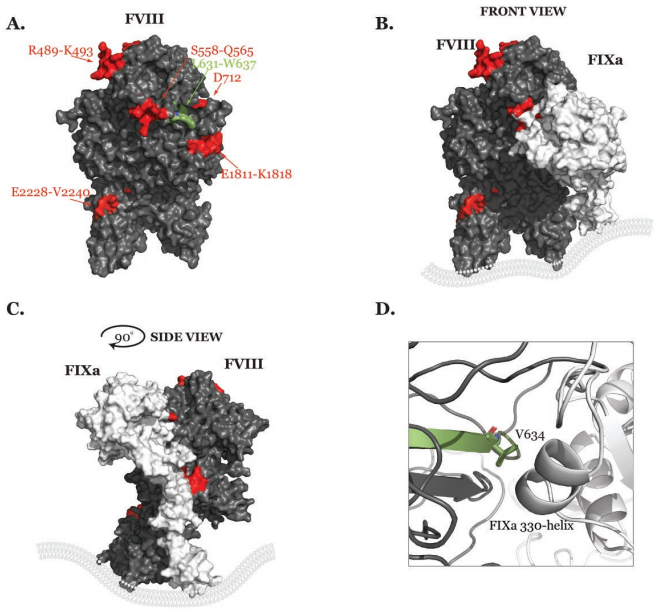


**Supplementary Figure S4. Val634 is located in close proximity to the FIXa 330-helix**

A) Putative FIXa binding sites or regions that may stimulate cofactor function, i.e. residues R489-K493[1–3], S558-Q565[4], D712[5], E1811-K1818[6] and E2228-V2240[7] are indicated in red on the structure of FVIII (PDB: 3cdz[8]). Region L631-W637 is shown in green. B) The structure of FVIII and FIXa were superimposed to the one of the *Pseudonaja textilis* (PDB: 4bxs[9]). Front view of the possible structure of the FIXa-FVIIIa complex is displayed in this panel. (C) Side view of the possible structure of the FIXa-FVIIIa complex. The previously implicated FIXa binding regions R489-K493 and E2228-V2240 do not fit with the model. Of note, the true role of region 484-508 overlapping residues R489-K493 for binding FIXa has been a subject of discussion[10,11]. The same holds true for region 2228-2240. Exchanging the entire C2 domain of FVIII, which includes 2228-2240, with that of FV did not affect enhancement of the FIXa-activity by FVIII[12]. Panel D shows that Val634 is in close proximity to FIXa helix S558-Q565 which has been implicated to contribute to FVIIIa binding.





**Supplementary Table S1**

| PEPTIDE NUMBER | Sequence |
|---|---|
| 1 | ATRRYYLGA |
| 2 | ATRRYYLGAVE |
| 3 | ATRRYYLGAVE |
| 4 | VELSWD |
| 5 | VELSWD |
| 6 | LSWDYMQSDL |
| 7 | SWDYMQSDL |
| 8 | YMQSDL |
| 9 | YMQSDLGELPVD |
| 10 | GELPVD |
| 11 | GELPVD |
| 12 | VYKKTLF |
| 13 | VYKKTLF |
| 14 | YKKTLF |
| 15 | KKTLF |
| 16 | FVEFTDHLFNIAKPRPPWMGLLGPTIQA |
| 17 | VEFTDHL |
| 18 | VEFTDHLFN |
| 19 | VEFTDHLFNIAKPRPPWMGLLGPTIQ |
| 20 | VEFTDHLFNIAKPRPPWMGLLGPTIQ |
| 21 | VEFTDHLFNIAKPRPPWMGLLGPTIQA |
| 22 | FTDHL |
| 23 | TDHLFNIAKPRPPWMGLLGPTIQ |
| 24 | TDHLFNIAKPRPPWMGLLGPTIQ |
| 25 | TDHLFNIAKPRPPWMGLLGPTIQA |
| 26 | TDHLFNIAKPRPPWMGLLGPTIQA |
| 27 | TDHLFNIAKPRPPWMGLLGPTIQA |
| 28 | FNIAKPRPPWM |
| 29 | FNIAKPRPPWMGL |
| 30 | FNIAKPRPPWMGL |
| 31 | FNIAKPRPPWMGL |
| 32 | FNIAKPRPPWMGLLGPTIQ |
| 33 | FNIAKPRPPWMGLLGPTIQ |
| 34 | FNIAKPRPPWMGLLGPTIQ |
| 35 | FNIAKPRPPWMGLLGPTIQA |
| 36 | FNIAKPRPPWMGLLGPTIQA |
| 37 | FNIAKPRPPWMGLLGPTIQA |
| 38 | FNIAKPRPPWMGLLGPTIQAE |
| 39 | NIAKPRPPWMGLLGPTIQA |
| 40 | IAKPRPPWMGLLGPTIQA |
| 41 | IAKPRPPWMGLLGPTIQA |
| 42 | AEVYDTVV |
| 43 | AEVYDTVVITLKNMASHPVSL |
| 44 | EVYDTVV |
| 45 | EVYDTVVITLKNMASHPVSL |
| 46 | EVYDTVVITLKNMASHPVSL |
| 47 | YDTVVITLKNMASHPVSL |
| 48 | TVVITLKNMASHPVSL |
| 49 | TVVITLKNMASHPVSL |
| 50 | VVITLKNMASHPVSL |

| PEPTIDE NUMBER | Sequence |
|---|---|
| 51 | VITLKNMASHPVSL |
| 52 | ITLKNMASHPVSL |
| 53 | ITLKNMASHPVSL |
| 54 | LKNMASHPVSL |
| 55 | LKNMASHPVSL |
| 56 | KNMASHPVSL |
| 57 | HAVGVSY |
| 58 | HAVGVSYWKASEGAE |
| 59 | HAVGVSYWKASEGAE |
| 60 | VSYWKASEGAE |
| 61 | WKASEGAE |
| 62 | WKASEGAEYDDQTSQREKEDDKVFPGGSHT |
| 63 | YDDQTSQREKEDDKVFPGGSHT |
| 64 | YDDQTSQREKEDDKVFPGGSHT |
| 65 | YDDQTSQREKEDDKVFPGGSHT |
| 66 | YDDQTSQREKEDDKVFPGGSHTYV |
| 67 | YDDQTSQREKEDDKVFPGGSHTYV |
| 68 | YDDQTSQREKEDDKVFPGGSHTYVWQVL |
| 69 | DDQTSQREKEDDKVFPGGSHT |
| 70 | DDQTSQREKEDDKVFPGGSHTY |
| 71 | REKEDDKVFPGGSHT |
| 72 | KVFPGGSHT |
| 73 | KVFPGGSHTYVWQVL |
| 74 | VFPGGSHTYVWQVLK |
| 75 | YVWQVL |
| 76 | KENGPMASDPLC |
| 77 | KENGPMASDPLCL |
| 78 | KENGPMASDPLCLT |
| 79 | KENGPMASDPLCLTYSY |
| 80 | LTYSYLSHVDL |
| 81 | LTYSYLSHVDLVKDLNSGLIGAL |
| 82 | YSYLSHVDL |
| 83 | YSYLSHVDLVKDLNSGLIGAL |
| 84 | YLSHVDL |
| 85 | YLSHVDLVKDLNSGL |
| 86 | LSHVDL |
| 87 | LSHVDLVKDLNSGL |
| 88 | LSHVDLVKDLNSGLIGAL |
| 89 | LSHVDLVKDLNSGLIGALL |
| 90 | SHVDLVKDLNSGL |
| 91 | VKDLNSGL |
| 92 | VKDLNSGLIG |
| 93 | VKDLNSGLIGAL |
| 94 | VKDLNSGLIGALL |
| 95 | LVCREGSL |
| 96 | LVCREGSLAKEKTQTLHKFILL |
| 97 | VCREGSL |
| 98 | AKEKTQTLHKFILL |
| 99 | AKEKTQTLHKFILL |
| 100 | AKEKTQTLHKFILL |

| PEPTIDE NUMBER | Sequence |
|---|---|
| 101 | KTQTLHKFILL |
| 102 | FAVFDEGKSW |
| 103 | FAVFDEGKSWHSETKNSL |
| 104 | FAVFDEGKSWHSETKNSL |
| 105 | FAVFDEGKSWHSETKNSL |
| 106 | FAVFDEGKSWHSETKNSLM |
| 107 | FAVFDEGKSWHSETKNSLM |
| 108 | AVFDEGKSWHSETKNSL |
| 109 | AVFDEGKSWHSETKNSL |
| 110 | DEGKSWHSETKNSL |
| 111 | DEGKSWHSETKNSL |
| 112 | DEGKSWHSETKNSL |
| 113 | MQDRDAASA |
| 114 | MQDRDAASARAWPKM |
| 115 | MQDRDAASARAWPKM |
| 116 | MQDRDAASARAWPKMHTVNG |
| 117 | MQDRDAASARAWPKMHTVNG |
| 118 | MQDRDAASARAWPKMHTVNG |
| 119 | QDRDAASARAWPKM |
| 120 | RAWPKM |
| 121 | RAWPKMHTVNG |
| 122 | RAWPKMHTVNG |
| 123 | YVNRSLPGL |
| 124 | IGCHRKSVYWHVIG |
| 125 | IGCHRKSVYWHVIGMGTTPEVHSIF |
| 126 | HRKSVYWHVIG |
| 127 | HRKSVYWHVIGM |
| 128 | HRKSVYWHVIGMGTTPEVHSIF |
| 129 | HRKSVYWHVIGMGTTPEVHSIF |
| 130 | HRKSVYWHVIGMGTTPEVHSIF |
| 131 | HVIGMGTTPEVHSIF |
| 132 | HVIGMGTTPEVHSIF |
| 133 | MGTTPEVHSIF |
| 134 | GTTPEVHSIF |
| 135 | LEGHTF |
| 136 | LEGHTFL |
| 137 | LEGHTFLVRNHRQASL |
| 138 | LEGHTFLVRNHRQASL |
| 139 | EGHTFL |
| 140 | HTFLVRNHRQASL |
| 141 | LVRNHRQASL |
| 142 | LVRNHRQASL |
| 143 | VRNHRQASL |
| 144 | VRNHRQASL |
| 145 | EISPITF |
| 146 | EISPITF |
| 147 | EISPITFL |
| 148 | EISPITFLTA |
| 149 | EISPITFLTAQTLL |
| 150 | ISPITFL |

| PEPTIDE NUMBER | Sequence |
|---|---|
| 151 | LTAQTLL |
| 152 | TAQTLL |
| 153 | TAQTLL |
| 154 | LMDLGQF |
| 155 | LMDLGQFL |
| 156 | LMDLGQFLL |
| 157 | MDLGQF |
| 158 | MDLGQFL |
| 159 | MDLGQFLL |
| 160 | FCHISSHQHDGME |
| 161 | FCHISSHQHDGME |
| 162 | FCHISSHQHDGMEA |
| 163 | FCHISSHQHDGMEA |
| 164 | CHISSHQHDGM |
| 165 | CHISSHQHDGME |
| 166 | CHISSHQHDGMEA |
| 167 | CHISSHQHDGMEA |
| 168 | HISSHQHDGMEA |
| 169 | HISSHQHDGMEA |
| 170 | AYVKVDSCPEEPQL |
| 171 | YVKVDSCPEEPQL |
| 172 | YVKVDSCPEEPQL |
| 173 | YVKVDSCPEEPQLRMKNNEE |
| 174 | VKVDSCPEEPQL |
| 175 | DVVRF |
| 176 | DVVRFDDDNSPSF |
| 177 | VVRFDDDNSPSF |
| 178 | VRFDDDNSPSF |
| 179 | DDDNSPSF |
| 180 | IQIRSVAKKHPKTWVHY |
| 181 | IQIRSVAKKHPKTWVHY |
| 182 | IQIRSVAKKHPKTWVHY |
| 183 | IQIRSVAKKHPKTWVHY |
| 184 | IQIRSVAKKHPKTWVHYIA |
| 185 | IQIRSVAKKHPKTWVHYIA |
| 186 | IQIRSVAKKHPKTWVHYIAA |
| 187 | IQIRSVAKKHPKTWVHYIAA |
| 188 | IQIRSVAKKHPKTWVHYIAA |
| 189 | IQIRSVAKKHPKTWVHYIAAE |
| 190 | IQIRSVAKKHPKTWVHYIAAE |
| 191 | IQIRSVAKKHPKTWVHYIAAEEED |
| 192 | QIRSVAKKHPKTWVHYI |
| 193 | SVAKKHPKTWVHY |
| 194 | SVAKKHPKTWVHY |
| 195 | SVAKKHPKTWVHYIAA |
| 196 | WDYAPLVL |
| 197 | APDDRSY |
| 198 | APDDRSYKSQYLNNGPQRIGRKYKKVRF |
| 199 | APDDRSYKSQYLNNGPQRIGRKYKKVRF |
| 200 | YKSQYLNNGPQRIGRKYKKVRF |

| PEPTIDE NUMBER | Sequence |
|---|---|
| 201 | YKSQYLNNGPQRIGRKYKKVRF |
| 202 | MAYTDETF |
| 203 | MAYTDETFKTRE |
| 204 | MAYTDETFKTRE |
| 205 | MAYTDETFKTREAIQHESGILGPLL |
| 206 | YTDETFKTRE |
| 207 | YTDETFKTREAIQHESGILGPLL |
| 208 | YTDETFKTREAIQHESGILGPLL |
| 209 | TFKTREAIQHESGILGPLL |
| 210 | FKTREAIQHESGILGPLL |
| 211 | FKTREAIQHESGILGPLL |
| 212 | KTREAIQHESGILGPLL |
| 213 | KTREAIQHESGILGPLL |
| 214 | AIQHESGILGPLL |
| 215 | AIQHESGILGPLL |
| 216 | YGEVGDTL |
| 217 | YGEVGDTLL |
| 218 | LIIFKNQASRPYNIYPHGIT |
| 219 | LIIFKNQASRPYNIYPHGIT |
| 220 | LIIFKNQASRPYNIYPHGITD |
| 221 | LIIFKNQASRPYNIYPHGITD |
| 222 | LIIFKNQASRPYNIYPHGITD |
| 223 | LIIFKNQASRPYNIYPHGITDVRPLY |
| 224 | LIIFKNQASRPYNIYPHGITDVRPLY |
| 225 | IIFKNQASRPYNIYPHGIT |
| 226 | IIFKNQASRPYNIYPHGITD |
| 227 | IIFKNQASRPYNIYPHGITD |
| 228 | IIFKNQASRPYNIYPHGITDVRPLY |
| 229 | IIFKNQASRPYNIYPHGITDVRPLY |
| 230 | KNQASRPYNIYPHGITD |
| 231 | DVRPLY |
| 232 | VRPLY |
| 233 | VRPLYS |
| 234 | SRRLPKGVKHLKDFPILPGEIFKYKWTVT |
| 235 | FPILPGEIFKYKWTVT |
| 236 | KYKWTVT |
| 237 | KYKWTVT |
| 238 | VEDGPTKSDPRC |
| 239 | VEDGPTKSDPRC |
| 240 | LTRYYSSF |
| 241 | VNMERDLASGLIGPLL |
| 242 | VNMERDLASGLIGPLL |
| 243 | ERDLASGL |
| 244 | ERDLASGLIGPLL |
| 245 | ERDLASGLIGPLL |
| 246 | ERDLASGLIGPLLIC |
| 247 | ERDLASGLIGPLLIC |
| 248 | ICYKESVDQRGNQIMSDKRNVIL |
| 249 | ICYKESVDQRGNQIMSDKRNVIL |
| 250 | ICYKESVDQRGNQIMSDKRNVIL |

| PEPTIDE NUMBER | Sequence |
|---|---|
| 251 | YKESVDQRGNQIMSDKRNVIL |
| 252 | YKESVDQRGNQIMSDKRNVIL |
| 253 | KESVDQRGNQIMSDKRNVIL |
| 254 | IMSDKRNVIL |
| 255 | IMSDKRNVIL |
| 256 | SDKRNVIL |
| 257 | DKRNVIL |
| 258 | KRNVIL |
| 259 | FSVFDENRSWY |
| 260 | FSVFDENRSWYLTE |
| 261 | FSVFDENRSWYLTEN |
| 262 | FSVFDENRSWYLTENIQRFLPNPAG |
| 263 | FSVFDENRSWYLTENIQRFLPNPAGVQ |
| 264 | SVFDENRSWY |
| 265 | SVFDENRSWYLTE |
| 266 | SVFDENRSWYLTEN |
| 267 | FDENRSWYLTE |
| 268 | DENRSWY |
| 269 | DENRSWYLTE |
| 270 | DENRSWYLTEN |
| 271 | DENRSWYLTENIQRFLPNPAGVQ |
| 272 | LTENIQRFLPNPAGVQ |
| 273 | NIQRFLPNPAG |
| 274 | NIQRFLPNPAGVQ |
| 275 | NIQRFLPNPAGVQ |
| 276 | NIQRFLPNPAGVQLEDPEF |
| 277 | NIQRFLPNPAGVQLEDPEF |
| 278 | IQRFLPNPAG |
| 279 | IQRFLPNPAGVQ |
| 280 | IQRFLPNPAGVQLEDPEF |
| 281 | IQRFLPNPAGVQLEDPEF |
| 282 | RFLPNPAGVQ |
| 283 | VQLEDPEF |
| 284 | VQLEDPEFQASN |
| 285 | LEDPEF |
| 286 | LEDPEFQASN |
| 287 | QASNIMHSING |
| 288 | QASNIMHSINGYVF |
| 289 | QASNIMHSINGYVF |
| 290 | IMHSING |
| 291 | IMHSING |
| 292 | IMHSINGYVF |
| 293 | IMHSINGYVFDSLQL |
| 294 | YVFDSLQL |
| 295 | SVCLHE |
| 296 | LHEVAYW |
| 297 | HEVAYW |
| 298 | WYILSIG |
| 299 | WYILSIGAQTDF |
| 300 | YILSIGAQTDF |

| PEPTIDE NUMBER | Sequence |
|---|---|
| 301 | SIGAQTDF |
| 302 | LSVFFSGYTFKHKMVYEDT |
| 303 | LSVFFSGYTFKHKMVYEDTL |
| 304 | FSGYTFKHKMVYEDT |
| 305 | FSGYTFKHKMVYEDTL |
| 306 | YTFKHKMVYEDT |
| 307 | YTFKHKMVYEDT |
| 308 | YTFKHKMVYEDTL |
| 309 | LTLFPFSG |
| 310 | LTLFPFSGE |
| 311 | LTLFPFSGETVF |
| 312 | TLFPFSGETVF |
| 313 | FPFSGETVF |
| 314 | MSMENPGL |
| 315 | MSMENPGLWILGCHNSD |
| 316 | MSMENPGLWILGCHNSDF |
| 317 | WILGCHNSDF |
| 318 | WILGCHNSDFRNRGMTAL |
| 319 | WILGCHNSDFRNRGMTAL |
| 320 | WILGCHNSDFRNRGMTAL |
| 321 | WILGCHNSDFRNRGMTALL |
| 322 | RNRGMTAL |
| 323 | RNRGMTAL |
| 324 | LKVSSC |
| 325 | LKVSSCDKNTGD |
| 326 | LKVSSCDKNTGDY |
| 327 | YLLSKNNAIEP |
| 328 | YLLSKNNAIEPR |
| 329 | YLLSKNNAIEPRS |
| 330 | LSKNNAIEP |
| 331 | LSKNNAIEPR |
| 332 | LSKNNAIEPR |
| 333 | LSKNNAIEPRS |
| 334 | LSKNNAIEPRSF |
| 335 | SQNPPVLKRHQ |
| 336 | EITRTTL |
| 337 | EITRTTLQSDQE |
| 338 | EITRTTLQSDQEE |
| 339 | MKKEDF |
| 340 | SFQKKTRHYFIA |
| 341 | SFQKKTRHYFIAA |
| 342 | FQKKTRHYFIAA |
| 343 | VERLWD |
| 344 | VERLWDYGMSSSPHVLRNRAQSGSVPQFKKVVF |
| 345 | VERLWDYGMSSSPHVLRNRAQSGSVPQFKKVVF |
| 346 | VERLWDYGMSSSPHVLRNRAQSGSVPQFKKVVFQE |
| 347 | WDYGMSSSPHVLRN |
| 348 | WDYGMSSSPHVLRNRAQSGSVPQF |
| 349 | WDYGMSSSPHVLRNRAQSGSVPQF |
| 350 | WDYGMSSSPHVLRNRAQSGSVPQFKKVVF |

| PEPTIDE NUMBER | Sequence |
|---|---|
| 351 | WDYGMSSSPHVLRNRAQSGSVPQFKKVVF |
| 352 | WDYGMSSSPHVLRNRAQSGSVPQFKKVVF |
| 353 | WDYGMSSSPHVLRNRAQSGSVPQFKKVVF |
| 354 | WDYGMSSSPHVLRNRAQSGSVPQFKKVVFQE |
| 355 | WDYGMSSSPHVLRNRAQSGSVPQFKKVVFQE |
| 356 | YGMSSSPHVLRNRAQSGSVPQFKKVVF |
| 357 | MSSSPHVLRNRAQSGSVPQFKKVVF |
| 358 | SSSPHVLRNRAQSGSVPQFKKVVF |
| 359 | RAQSGSVPQFKKVVF |
| 360 | KKVVF |
| 361 | KKVVFQE |
| 362 | QEFTDGSFTQPLYRGEL |
| 363 | QEFTDGSFTQPLYRGEL |
| 364 | QEFTDGSFTQPLYRGELNE |
| 365 | QEFTDGSFTQPLYRGELNE |
| 366 | QEFTDGSFTQPLYRGELNEHLGLLGPYIRA |
| 367 | FTDGSFTQPLYRGEL |
| 368 | FTDGSFTQPLYRGEL |
| 369 | FTDGSFTQPLYRGELNE |
| 370 | FTDGSFTQPLYRGELNE |
| 371 | FTDGSFTQPLYRGELNEHLGLLGPYIRA |
| 372 | FTDGSFTQPLYRGELNEHLGLLGPYIRA |
| 373 | FTQPLYRGEL |
| 374 | FTQPLYRGELNE |
| 375 | FTQPLYRGELNEHLGLLGPYIRA |
| 376 | FTQPLYRGELNEHLGLLGPYIRA |
| 377 | TQPLYRGELNEHLGLLGPYIRA |
| 378 | NEHLGLLGPYIRA |
| 379 | NEHLGLLGPYIRA |
| 380 | NEHLGLLGPYIRAEVEDNIM |
| 381 | HLGLLGPYIRA |
| 382 | HLGLLGPYIRA |
| 383 | HLGLLGPYIRAEVEDNIM |
| 384 | GLLGPYIRA |
| 385 | LGPYIRA |
| 386 | EVEDNIM |
| 387 | MVTFRNQASRPYSF |
| 388 | VTFRNQASRPYSF |
| 389 | VTFRNQASRPYSF |
| 390 | FRNQASRPYSF |
| 391 | FRNQASRPYSF |
| 392 | RNQASRPYSF |
| 393 | ISYEEDQRQGAEPRKNFVKPNETKTYF |
| 394 | EEDQRQGAEPRKNFVKPNETKTYF |
| 395 | WKVQHHMAPTKDEF |
| 396 | WKVQHHMAPTKDEF |
| 397 | WKVQHHMAPTKDEF |
| 398 | WKVQHHMAPTKDEFDCKA |
| 399 | WAYFSDVDLEKDVHSGLIGPLL |
| 400 | FSDVDL |

| PEPTIDE NUMBER | Sequence |
|---|---|
| 401 | FSDVDLEKDVHSGLIGPL |
| 402 | FSDVDLEKDVHSGLIGPLL |
| 403 | SDVDLEKDVHSGL |
| 404 | VDLEKDVHSGL |
| 405 | VDLEKDVHSGLIGPLL |
| 406 | LEKDVHSGL |
| 407 | LEKDVHSGLIGPLL |
| 408 | EKDVHSGL |
| 409 | EKDVHSGLIGPLL |
| 410 | EKDVHSGLIGPLL |
| 411 | EKDVHSGLIGPLLVC |
| 412 | VCHTNTLNPAHGRQ |
| 413 | VCHTNTLNPAHGRQVT |
| 414 | VCHTNTLNPAHGRQVTVQE |
| 415 | VCHTNTLNPAHGRQVTVQE |
| 416 | VCHTNTLNPAHGRQVTVQE |
| 417 | HTNTLNPAHGRQVTVQE |
| 418 | HTNTLNPAHGRQVTVQE |
| 419 | FFTIF |
| 420 | FFTIF |
| 421 | FTIFDETKSWY |
| 422 | FTIFDETKSWYF |
| 423 | DETKSWY |
| 424 | DETKSWYF |
| 425 | DETKSWYFTENM |
| 426 | MERNCRAPCNIQ |
| 427 | ERNCRAPCN |
| 428 | ERNCRAPCNIQ |
| 429 | ERNCRAPCNIQM |
| 430 | IQMEDPTF |
| 431 | IQMEDPTFKENYRF |
| 432 | IQMEDPTFKENYRF |
| 433 | IQMEDPTFKENYRFHAING |
| 434 | IQMEDPTFKENYRFHAING |
| 435 | MEDPTFKENYRFHAING |
| 436 | MEDPTFKENYRFHAING |
| 437 | KENYRF |
| 438 | KENYRFHAING |
| 439 | KENYRFHAING |
| 440 | KENYRFHAINGYIMDTLPGLVM |
| 441 | HAINGYIMDTLPGLVM |
| 442 | YIMDTLPGL |
| 443 | YIMDTLPGLVM |
| 444 | YIMDTLPGLVMAQDQRIRWYL |
| 445 | DTLPGLVM |
| 446 | DTLPGLVMAQDQRIRWYL |
| 447 | VMAQDQRIRWYL |
| 448 | AQDQRIRW |
| 449 | AQDQRIRW |
| 450 | AQDQRIRWYL |

| PEPTIDE NUMBER | Sequence |
|---|---|
| 451 | AQDQRIRWYL |
| 452 | DQRIRWYL |
| 453 | RIRWYL |
| 454 | YLLSMGSNE |
| 455 | YLLSMGSNENIHSIHF |
| 456 | YLLSMGSNENIHSIHFSG |
| 457 | YLLSMGSNENIHSIHFSGHVFTVRKKEEYKMAL |
| 458 | LSMGSNENIHSIHFSG |
| 459 | LSMGSNENIHSIHFSG |
| 460 | LSMGSNENIHSIHFSGHVF |
| 461 | LSMGSNENIHSIHFSGHVF |
| 462 | LSMGSNENIHSIHFSGHVFTVRKKEEYKMAL |
| 463 | LSMGSNENIHSIHFSGHVFTVRKKEEYKMAL |
| 464 | NIHSIHFSG |
| 465 | NIHSIHFSG |
| 466 | NIHSIHFSGHVFTVRKKEEYKMAL |
| 467 | HVFTVRKKEEYKMAL |
| 468 | HVFTVRKKEEYKMAL |
| 469 | TVRKKEEYKMAL |
| 470 | TVRKKEEYKMAL |
| 471 | VRKKEEYKMAL |
| 472 | YKMAL |
| 473 | YNLYPGVF |
| 474 | YNLYPGVFE |
| 475 | YNLYPGVFET |
| 476 | ETVEML |
| 477 | ETVEMLPSKAGI |
| 478 | ETVEMLPSKAGIW |
| 479 | ETVEMLPSKAGIW |
| 480 | ETVEMLPSKAGIWRVECL |
| 481 | VEMLPSKAGIW |
| 482 | LPSKAGIW |
| 483 | PSKAGIW |
| 484 | WRVECL |
| 485 | RVECL |
| 486 | IGEHLHAGM |
| 487 | IGEHLHAGM |
| 488 | IGEHLHAGMSTL |
| 489 | IGEHLHAGMSTL |
| 490 | IGEHLHAGMSTLF |
| 491 | IGEHLHAGMSTLF |
| 492 | HLHAGM |
| 493 | FLVYSNKCQTPLGM |
| 494 | FLVYSNKCQTPLGM |
| 495 | FLVYSNKCQTPLGMASG |
| 496 | FLVYSNKCQTPLGMASGHIRD |
| 497 | LVYSNKCQTPLG |
| 498 | LVYSNKCQTPLGM |
| 499 | LVYSNKCQTPLGMASG |
| 500 | LVYSNKCQTPLGMASGHIRD |

| PEPTIDE NUMBER | Sequence |
|---|---|
| 501 | LVYSNKCQTPLGMASGHIRD |
| 502 | LVYSNKCQTPLGMASGHIRDF |
| 503 | LVYSNKCQTPLGMASGHIRDFQITASGQYGQWAPKL |
| 504 | ASGHIRDF |
| 505 | ASGHIRDF |
| 506 | ASGHIRDFQITASGQYGQWAPKL |
| 507 | HIRDF |
| 508 | HIRDFQ |
| 509 | HIRDFQITASGQYGQWAPKL |
| 510 | HIRDFQITASGQYGQWAPKL |
| 511 | FQITASGQYGQWAPKL |
| 512 | FQITASGQYGQWAPKL |
| 513 | QITASGQYGQWAPKL |
| 514 | QITASGQYGQWAPKL |
| 515 | ASGQYGQWAPKL |
| 516 | ARLHYSGSINA |
| 517 | ARLHYSGSINA |
| 518 | HYSGSINA |
| 519 | HYSGSINAWSTKEPFSWIKVDLLAPMIIHGIKTQGARQKFSSL |
| 520 | WSTKEPFS |
| 521 | WSTKEPFSW |
| 522 | WSTKEPFSWIKVDL |
| 523 | WSTKEPFSWIKVDLL |
| 524 | WSTKEPFSWIKVDLLA |
| 525 | WSTKEPFSWIKVDLLAPMIIHGIKTQGARQKFSSL |
| 526 | WIKVDL |
| 527 | WIKVDLLA |
| 528 | WIKVDLLAPMIIHGIKTQGARQKFSSL |
| 529 | IKVDLL |
| 530 | IKVDLLA |
| 531 | IKVDLLAPMIIHGIKTQGARQKFSSL |
| 532 | IKVDLLAPMIIHGIKTQGARQKFSSL |
| 533 | IKVDLLAPMIIHGIKTQGARQKFSSL |
| 534 | IKVDLLAPMIIHGIKTQGARQKFSSL |
| 535 | LAPMIIHGIKTQGARQKFSSL |
| 536 | LAPMIIHGIKTQGARQKFSSL |
| 537 | APMIIHGIKTQGARQKFSSL |
| 538 | APMIIHGIKTQGARQKFSSL |
| 539 | APMIIHGIKTQGARQKFSSL |
| 540 | PMIIHG |
| 541 | PMIIHGIKTQGARQKFSSL |
| 542 | PMIIHGIKTQGARQKFSSL |
| 543 | YISQF |
| 544 | MVFFGNVDSSGIKHNIFNPPII |
| 545 | MVFFGNVDSSGIKHNIFNPPIIA |
| 546 | MVFFGNVDSSGIKHNIFNPPIIAR |
| 547 | MVFFGNVDSSGIKHNIFNPPIIAR |
| 548 | MVFFGNVDSSGIKHNIFNPPIIAR |
| 549 | MVFFGNVDSSGIKHNIFNPPIIARY |
| 550 | MVFFGNVDSSGIKHNIFNPPIIARY |

| PEPTIDE NUMBER | Sequence |
|---|---|
| 551 | VFFGNVDSSGIKHNIFNPPII |
| 552 | VFFGNVDSSGIKHNIFNPPIIA |
| 553 | VFFGNVDSSGIKHNIFNPPIIAR |
| 554 | VFFGNVDSSGIKHNIFNPPIIAR |
| 555 | VFFGNVDSSGIKHNIFNPPIIARY |
| 556 | VFFGNVDSSGIKHNIFNPPIIARY |
| 557 | VFFGNVDSSGIKHNIFNPPIIARYIRLHPTHY |
| 558 | FGNVDSSGIKHNIFNPPIIAR |
| 559 | FGNVDSSGIKHNIFNPPIIAR |
| 560 | FGNVDSSGIKHNIFNPPIIARY |
| 561 | FGNVDSSGIKHNIFNPPIIARY |
| 562 | NVDSSGIKHNIFNPPIIAR |
| 563 | NVDSSGIKHNIFNPPIIAR |
| 564 | NVDSSGIKHNIFNPPIIARY |
| 565 | NVDSSGIKHNIFNPPIIARY |
| 566 | RYIRLHPTHY |
| 567 | RYIRLHPTHY |
| 568 | YIRLHPTHY |
| 569 | YIRLHPTHY |
| 570 | YIRLHPTHYSIRSTL |
| 571 | YIRLHPTHYSIRSTL |
| 572 | IRLHPTHY |
| 573 | IRLHPTHYSIRSTL |
| 574 | HPTHYSIRSTL |
| 575 | HPTHYSIRSTL |
| 576 | SIRSTL |
| 577 | SIRSTLRM |
| 578 | STLRMELMGCDLNSCSMPLGM |
| 579 | RMELMGCDL |
| 580 | CSMPLGM |
| 581 | ESKAISDA |
| 582 | ESKAISDAQITA |
| 583 | ESKAISDAQITASS |
| 584 | ESKAISDAQITASSY |
| 585 | ESKAISDAQITASSY |
| 586 | FATWSPSKARL |
| 587 | FATWSPSKARL |
| 588 | FATWSPSKARLHL |
| 589 | ATWSPSKARL |
| 590 | HLQGRSNAWRPQVNNPKE |
| 591 | HLQGRSNAWRPQVNNPKE |
| 592 | HLQGRSNAWRPQVNNPKE |
| 593 | HLQGRSNAWRPQVNNPKE |
| 594 | HLQGRSNAWRPQVNNPKEWL |
| 595 | HLQGRSNAWRPQVNNPKEWL |
| 596 | HLQGRSNAWRPQVNNPKEWL |
| 597 | HLQGRSNAWRPQVNNPKEWLQV |
| 598 | QGRSNAWRPQVNNPKEWL |
| 599 | NAWRPQVNNPKE |
| 600 | WRPQVNNPKE |

| PEPTIDE NUMBER | Sequence |
|---|---|
| 601 | QVDFQKTMKVTGVTTQGVKSLL |
| 602 | QVDFQKTMKVTGVTTQGVKSLL |
| 603 | QVDFQKTMKVTGVTTQGVKSLL |
| 604 | QVDFQKTMKVTGVTTQGVKSLLTSM |
| 605 | DFQKTMKVTGVTTQGVKSLL |
| 606 | DFQKTMKVTGVTTQGVKSLL |
| 607 | DFQKTMKVTGVTTQGVKSLL |
| 608 | DFQKTMKVTGVTTQGVKSLLTSM |
| 609 | DFQKTMKVTGVTTQGVKSLLTSM |
| 610 | FQKTMKVTGVTTQGVKSLL |
| 611 | FQKTMKVTGVTTQGVKSLL |
| 612 | QKTMKVTGVTTQGVKSLL |
| 613 | QKTMKVTGVTTQGVKSLL |
| 614 | QKTMKVTGVTTQGVKSLL |
| 615 | QKTMKVTGVTTQGVKSLLTSM |
| 616 | YVKEFL |
| 617 | YVKEFLISSSQDGHQ |
| 618 | YVKEFLISSSQDGHQ |
| 619 | VKEFL |
| 620 | FLISSSQDGHQ |
| 621 | FLISSSQDGHQ |
| 622 | FLISSSQDGHQWTL |
| 623 | FLISSSQDGHQWTLF |
| 624 | LISSSQDGHQWTLF |
| 625 | ISSSQDGHQWTLF |
| 626 | FFQNGKVKVFQGNQDSFTPVVNSLDPPLL |
| 627 | FFQNGKVKVFQGNQDSFTPVVNSLDPPLLTRY |
| 628 | FQNGKVKVFQGNQ |
| 629 | FQNGKVKVFQGNQ |
| 630 | FQNGKVKVFQGNQDSFT |
| 631 | FQNGKVKVFQGNQDSFT |
| 632 | FQNGKVKVFQGNQDSFTPVVNSLDPPLL |
| 633 | FQNGKVKVFQGNQDSFTPVVNSLDPPLL |
| 634 | FQNGKVKVFQGNQDSFTPVVNSLDPPLL |
| 635 | FQNGKVKVFQGNQDSFTPVVNSLDPPLLT |
| 636 | FQNGKVKVFQGNQDSFTPVVNSLDPPLLTR |
| 637 | FQNGKVKVFQGNQDSFTPVVNSLDPPLLTRY |
| 638 | FQNGKVKVFQGNQDSFTPVVNSLDPPLLTRY |
| 639 | FQNGKVKVFQGNQDSFTPVVNSLDPPLLTRYLRIHPQS |
| 640 | FQNGKVKVFQGNQDSFTPVVNSLDPPLLTRYLRIHPQSW |
| 641 | DSFTPVVNSLDPPLL |
| 642 | DSFTPVVNSLDPPLLTRY |
| 643 | DSFTPVVNSLDPPLLTRY |
| 644 | SFTPVVNSLDPPLL |
| 645 | FTPVVNSLDPPLLTRY |
| 646 | PVVNSLDPPLL |
| 647 | PVVNSLDPPLLTRY |
| 648 | PVVNSLDPPLLTRY |
| 649 | TRYLRIHPQS |
| 650 | RYLRIHPQS |

| PEPTIDE NUMBER | Sequence |
|---|---|
| 651 | LRIHPQS |
| 652 | LRIHPQSW |
| 653 | LRIHPQSW |
| 654 | LRIHPQSWVHQIA |
| 655 | LRIHPQSWVHQIA |
| 656 | LRIHPQSWVHQIALRM |
| 657 | WVHQIA |
| 658 | WVHQIAL |
| 659 | IALRM |
| 660 | RMEVL |
| 661 | RMEVLGC |
| 662 | RMEVLGCE |
| 663 | EVLGCEA |

**Supplementary Table S1. Sequence and peptide ID number of the identified peptides**

Amino acid sequence of the identified peptides. The peptide ID number, used in figures 1 and 5 is indicated in the table

## SUPPLEMENTARY REFERENCES


1. Healey JF, Lubin IM, Nakai H, et al. Residues 484-508 contain a major determinant of the inhibitory epitope in the A2 domain of human factor VIII. *J Biol Chem*. 1995;270(24):14505-14509.

2. Jenkins PV, Dill JL, Zhou Q, Fay PJ. Clustered basic residues within segment 484-510 of the factor VIIIa A2 subunit contribute to the catalytic efficiency for factor Xa generation. *J Thromb Haemost JTH*. 2004;2(3):452-458.

3. Fay PJ. Factor VIII structure and function. *Int J Hematol*. 2006;83(2):103–108.

4. Fay PJ, Beattie T, Huggins CF, Regan LM. Factor VIIIa A2 subunit residues 558-565 represent a factor IXa interactive site. *J Biol Chem*. 1994;269(32):20522-20527.

5. Jenkins PV, Dill JL, Zhou Q, Fay PJ. Contribution of factor VIIIa A2 and A3-C1-C2 subunits to the affinity for factor IXa in factor Xase. *Biochemistry*. 2004;43(17):5094–5101.

6. Bovenschen N, Boertjes RC, van Stempvoort G, et al. Low density lipoprotein receptor-related protein and factor IXa share structural requirements for binding to the A3 domain of coagulation factor VIII. *J Biol Chem*. 2003;278(11):9370-9377.

7. Soeda T, Nogami K, Nishiya K, et al. The factor VIIIa C2 domain (residues 2228-2240) interacts with the factor IXa Gla domain in the factor Xase complex. *J Biol Chem*. 2009;284(6):3379-3388.

8. Ngo JC, Huang M, Roth DA, Furie BC, Furie B. Crystal structure of human factor VIII: implications for the formation of the factor IXa-factor VIIIa complex. *Structure*. 2008;16(4):597–606.

9. Lechtenberg BC, Murray-Rust TA, Johnson DJ, et al. Crystal structure of the prothrombinase complex from the venom of Pseudonaja textilis. *Blood*. 2013;122(16):2777–2783.

10. Bajaj SP, Schmidt AE, Mathur A, et al. Factor IXa:Factor VIIIa interaction. Helix 330-338 of factor IXa interacts with residues 558-565 and spatially adjacent regions of the A2 subunit of factor VIIIa. *J Biol Chem*. 2001;276(19):16302–16309.

11. Lollar P, Parker ET, Curtis JE, et al. Inhibition of human factor VIIIa by anti-A2 subunit antibodies. *J Clin Invest*. 1994;93(6):2497-2504.

12. Ebberink EH, Bouwens EA, Bloem E, et al. Factor VIII/V C-domain swaps reveal discrete C-domain roles in factor VIII function and intracellular trafficking. *Haematologica*. *2017;102:686–694*

# Chapter 4

## Factor VIII-driven changes in activated factor IX explored by hydrogen-deuterium exchange mass spectrometry

**Nadia Freato**[1], Eduard H.T.M. Ebberink[1], Josse van Galen[1], Caroline Fribourg[1], Mariëtte Boon- Spijker[1], Floris P.J. van Alphen[1], Alexander B. Meijer[1,2], Maartje van den Biggelaar[1], Koen Mertens[1,3]

From the Department of [1]Molecular and Cellular Hemostasis, Sanquin Research, 1066 CX Amsterdam, The Netherlands, [2]Department of Biomolecular Mass Spectrometry and Proteomics, and [3]Department of Pharmaceutics and Utrecht Institute for Pharmaceutical Sciences (UIPS), Utrecht University, 3584 CG Utrecht, The Netherlands

**Blood. 2020 Dec;136(23):2703-2714.**

## KEY POINTS

- This study reveals the network of allosteric and factor VIII-driven changes in activated FIX associated with catalytic rate enhancement
- Disruption of this network explains why single mutations in FIX may silence the response to FVIII and thereby cause hemophilia B





## ABSTRACT

The assembly of the enzyme activated Factor IX (FIXa) with its cofactor, activated Factor VIII (FVIIIa) is a crucial event in the coagulation cascade. The absence or dysfunction of either enzyme or cofactor severely compromises hemostasis, and causes hemophilia. FIXa is a notoriously inefficient enzyme, and needs FVIIIa to drive its hemostatic potential, by a mechanism that has remained largely elusive to date. In this study we employed Hydrogen-Deuterium eXchange-Mass Spectrometry (HDX-MS) to investigate how FIXa responds to assembly with FVIIIa in presence of phospholipids. This revealed a complex pattern of changes that partially overlaps with those that occur upon occupation of the substrate-binding site by an active site-directed inhibitor. Among the changes driven by both cofactor and substrate, HDX-MS highlighted several surface loops that have been implicated in allosteric networks in related coagulation enzymes. Inspection of FVIIIa-specific changes indicated that three helices are involved in FIXa-FVIIIa assembly. These are part of a basic interface that is also known as Exosite II. Mutagenesis of basic residues herein, followed by functional studies, indeed identified this interface as an extended FVIIIa-interactive patch. HDX-MS was also applied to recombinant FIXa variants that are associated with severe hemophilia B. This revealed that single amino acid substitutions can silence the extended network of FVIIIa-driven allosteric changes. We conclude that HDX-MS has the potential to visualize the functional impact of disease-associated mutations on enzyme-cofactor complexes in the hemostatic system.

## INTRODUCTION

Upon vessel injury the coagulation cascade is activated which, in concert with platelets and vascular components, ultimately leads to fibrin clot formation and hemostasis. One key constituent of the coagulation cascade is the complex of Factor IX (FIX) and Factor VIII (FVIII). Qualitative or quantitative defects of FVIII or FIX are associated with the bleeding disorders hemophilia A or B, respectively[1]. FIX belongs to the chymotrypsin-like serine proteases[2]. These circulate as inactive precursors (zymogens) that need proteolytic activation to develop enzymatic activity, and usually require a cofactor to reach full catalytic potential[2]. The zymogen FIX is a single chain protein that is converted into activated Factor IX (FIXa) by activated factor VII (FVIIa) or activated factor XI[3]. FIXa comprises a light chain with an N-terminal domain rich in g-carboxyglutamic acid (the Gla domain), two epidermal growth factor (EGF)-like domains (EGF-1 and EGF-2) and a heavy chain that represents the C-terminal Protease Domain[3–5]. Like its homologue FVIIa, FIXa displays low intrinsic catalytic potential in the absence of cofactors[2,6]. Full FIXa activity requires assembly with activated Factor VIII (FVIIIa) in presence of $Ca^{2+}$ ions and phospholipids[7]. FVIIIa is the activated derivative of the pro-cofactor FVIII, a large heterodimeric glycoprotein composed of a heavy chain (domains A1-A2-B) and a light chain (domains: A3-C1-C2)[8]. Proteolytic cleavage at domain junctions yields FVIIIa, a trimer of the segments A1 and A3-C1-C2 and the loosely associated A2 domain, thus making FVIIIa a labile component with transient cofactor activity[8]. When assembled in the FIXa-FVIIIa complex, FVIIIa enhances FIXa activity by more than $10^4$-fold, thus driving the conversion of factor X (FX) into activated FX (FXa) to physiologically relevant levels[6].

During the past decades, the identification of molecular variants of FVIII and FIX in hemophilia A and B patients have guided biochemical studies employing site-directed mutagenesis and functional characterization to obtain deeper understanding of FIXa and FVIIIa structure and function. As for the FIXa-FVIIIa complex, putative interactive sites have been inferred mostly by combining functional studies with modeling and crystallography of its constituents or homologs thereof[3,4,7]. For instance, the EGF-1/EGF-2 interface in the FIXa light chain has proven important for FVIIIa-driven rate-enhancement and interaction with the FVIIIa light chain[9,10]. As for the FIXa Protease Domain, the 330-helix{$162_{CT}$} (CT subscript indicates chymotrypsinogen numbering) seems to interact with the 557-565 loop on the A2 domain of FVIIIa, while residues 301-303{$132\text{-}134_{CT}$} may bind FVIIIa residues 698-712[11–13].

Full understanding of FIXa-FVIIIa complex assembly has not been accomplished so far. A complete crystal structure of FIXa, including the lipid-binding Gla-domain, is still lacking, and most of the available human FIXa crystals are limited to truncated EGF-2/Protease Domain constructs[4,5,14,15]. Co-crystallization of FIXa with FVIIIa has been hampered by the inherent instability of the FVIIIa trimer. Another challenge is the need for phospholipids, which are normally supporting assembly of the FIXa-FVIIIa complex[6,7,16]. As a consequence, structural information is still insufficient to understand the molecular mechanism of FVIIIa-driven rate-enhancement of FIXa.

Hydrogen-deuterium exchange mass spectrometry (HDX-MS) is increasingly employed for the study of protein complexes and dynamics. In the field of blood coagulation it has been successfully used to footprint the interaction between, for instance, thrombomodulin and thrombin[17], and FVIII with von Willebrand Factor[18,19], phospholipid membranes[20], and anti-FVIII antibodies[21,22]. In addition, HDX-MS has been used to unravel allosteric networks within thrombin[23–25] and FVIIa[26].

This study aimed to explore cofactor- and substrate-driven events in FIXa in the presence of phospholipids by HDX-MS. Binding and functional studies in combination with HDX-MS of recombinant dysfunctional FIXa variants were further employed to assess the functional implications thereof. This research provides a comprehensive view on the ensemble of cofactor-mediated structural changes and allosteric cross-talk within the FIX molecule.

## MATERIALS & METHODS

### Materials

The QuikChange kit was from Agilent Technologies (Middelburg, The Netherlands). Glu-Gly-Arg-chloromethylketone (EGRck) was from Bachem (Bubendorf, Switzerland). Factor XIa was from Enzyme Research Laboratories (South Bend, IN, USA). Calcium Chloride 1M solution and Deuterium Oxide 99.9% were from Sigma-Aldrich (Saint Louis, MO, USA). Ultrapure Urea, Molecular Biology grade 5M NaCl solution and Tris-HCl were from Invitrogen (Breda, The Netherlands). Chicken egg L-α-phosphatidylcholine (PC) and porcine brain L-α-phosphatidylserine (PS) were from Avanti Polar Lipids Inc. (Alabaster, AL, USA). NaCl was from Fagron (Rotterdam, The Netherlands) and HEPES was from Serva (Heidelberg, Germany). Human Serum Albumin (HSA) was obtained from the Division of Products of Sanquin (Amsterdam, The Netherlands). Tris(2-carboxyethyl)phosphine hydrochloride (TCEP-HCl) was obtained from Thermo Fisher Scientific (Breda, The Netherlands). HEPES Buffer Solution 1M was from Gibco (Paisley, Scotland, UK). All other chemicals were from Merck (Darmstadt, Germany).

### FIX and FIXa variants

FIX variants with mutations E78K, K293A{$126_{CT}$}, R333A{$165_{CT}$}, R338{$170_{CT}$},

K341{$173_{CT}$}, K400A{$230_{CT}$}, R403A{$233_{CT}$} and FIXaR333A+R403A{$165+233_{CT}$} were obtained by site-directed mutagenesis in a pcDNA3.1(-) vector encoding wild-type FIX[27] with the QuikChange kit using appropriate primers. Mutagenesis was confirmed with the complete sequencing of the FIX encoding parts on the mutated plasmid, using BigDye Terminator Sequencing kit (Applied Biosystem, Foster City, USA). Recombinant FIX and FIX variants were expressed in mammalian cells as described elsewhere[27,28]. Recombinant FIX was immunopurified and converted into FIXa by FXIa-mediated limited proteolysis as previously described[27,29] and stored in 20 mM HEPES (pH 7.4), 150 mM NaCl and 50% (v/v) glycerol at -20°C. FIXaEGR was prepared by incubation of FIXa (4 μM) with EGRck (10 mM) for 45 minutes at 37°C in a buffer containing 20 mM HEPES (pH 7.4), 150 mM NaCl, 10 mM $CaCl_2$. Unbound EGRck was removed by dialysis initially against a buffer containing 25 mM HEPES (pH 7.4), 100 mM NaCl, 10mM EDTA, then against 20 mM HEPES (pH 7.4), 150 mM NaCl and 50% (v/v) glycerol, and stored at -20°C. FIXa concentrations were determined by antithrombin titration in the presence of heparin as described[29]. The concentration of FIXaEGR was determined using the Bradford method[30].

### Other proteins employed in this study

Recombinant B-domain-deleted FVIII was purified with the monoclonal antibody VK34[31] and stored at -20°C in a buffer containing 20 mM HEPES (pH 7.4) 800 mM NaCl, 10 mM $CaCl_2$ and 50% (v/v) glycerol. The A2 domain of FVIII was isolated from thrombin-activated FVIII by ion-exchange chromatography as described[10], with the exception that a Source S column was used instead of a Mono S column. FX and α-thrombin were obtained as previously described[32–34].

### Phospholipid vesicles

PS/PC vesicles were prepared by sonication as described[31]. Vesicles contained 50% PS for kinetic studies, and 15% PS for HDX-MS experiments.

### FIXa catalytic activity

FIXa amidolytic activity was assessed using substrate $CH_3SO_2$-(D)-CHG-Gly-Arg-*p*NA in a buffer containing 33% (v/v) ethylene glycol, 100 mM NaCl, 10 mM $CaCl_2$, 0.2 % (w/v) HSA, 50 mM Tris (pH 7.4) at 37°C as described[27]. FX activation was assessed in the presence of varying concentrations FVIIIa and FX in a buffer containing 100 mM NaCl, 10 mM $CaCl_2$, 0.5 % (w/v) ovalbumin, 50 mM Tris (pH 7.4) at 37°C as described[27]. Data were fitted in the Michaelis-Menten equation to obtain $K_m$ and $k_{cat}$ values.





### Surface plasmon resonance (SPR) analysis

SPR studies were performed using the BIAcore3000TM biosensor system and immobilized FVIII A2 domain. FIXa binding was assessed in a buffer containing 150 mM NaCl, 2 mM $CaCl_2$, 0.005% (v/v) Tween-20, 20 mM Hepes (pH 7.4) at 25°C with a flow of 20 ml/min as described in detail elsewhere[27].

### HDX-MS

FIXa (1.7 mM) was incubated with FVIII (3.3 mM) and phospholipids (0.21 mM) in a buffer containing 20 mM HEPES (pH 7.4), 150 mM NaCl, 5 mM $CaCl_2$ for 90 seconds at room temperature. Thrombin prediluted in the same buffer was added to a final concentration of 0.33 mM to allow FVIII activation for 60 seconds at 24°C. In absence of FVIII, the FVIII fraction was substituted with FVIII storage buffer, but thrombin was still added. Samples were handled without prior lipid removal by a LEAP PAL robot (LEAP technologies, Morrisville, NC, USA). Samples (3 ml) were diluted 10-fold in $D_2O$ buffer (20 mM Imidazole (pH 7.3), 133 mM NaCl, 5 mM $CaCl_2$ in 99.9% $D_2O$), allowing HDX for 10, 20, 30, 45, 60, 100, 150, 500, 1000 seconds at 24°C. Water reference samples were diluted in 20 mM Imidazole (pH 7.3), 133 mM NaCl, 5 mM $CaCl_2$ in $H_2O$. HDX experiments involving FIXa mutants used fewer incubation time points, usually 10, 30 and 100 seconds, in order to avoid interference by FVIIIa instability (half-life approximately 10 min[35]). In all cases, after incubation 25 ml of the deuterated mix was quenched at 4°C by addition 25 ml of 1.4 M TCEP-HCl, 2 M Urea, adjusted to pH 2.5 using NaOH. Proteolytic digestion was performed inline, using a Poroszyme Immobilized Pepsin Cartridge (Thermo Fisher Scientific, Breda, the Netherlands) with an isocratic flow of 5% (v/v) acetonitrile, 0.1% (v/v) formic acid at 4°C. Peptides were trapped on an Acclaim Guard Column 120 C18, 5 μm, 2×10 mm (Thermo Fisher) and washed for 30 sec. The trap was then switched with a 10 cm Hypersil GOLD C18 analytic column (Thermo Fisher) with a gradient from 10 to 80% of buffer B (0.1% (v/v) formic acid in 80% (v/v) acetonitrile). Eluted peptides were sprayed into an LTQ Orbitrap-XL (Thermo Fisher) mass spectrometer operating in the positive ion mode. Collision induced dissociation (CID) was used to fragment the 3 most intense precursor ions with tandem mass spectrometry fragmentation.

### Data analysis of HDX-MS

Sequence and retention times of non-deuterated peptides were analysed using PEAKS (PEAKS 7.0, Bioinformatics Solutions Inc). Deuterated peptides were analysed in HDExaminer 2.2.0 (Sierra Analytics). No back-exchange correction was performed since only the relative levels of deuterium incorporation of individual peptides were compared under various conditions. Obtained HDX data are the

result of three to six independent measurements, the mean value was used and the Standard Deviation is displayed for each time point. In addition, heat maps were constructed to visualize HDX data (see Supplementary Section). The software Pymol (Schrödinger, Cambridge, MA, USA) was used to map the peptides on a 3D model structure. To define the extent of a change we subdivided the obtained peptides into three categories: prominent change, moderate change and no appreciable change (criteria are detailed in the figure legends).

## RESULTS

### HDX of FIXa-FVIIIa complex

To allow the assembly of the FIXa-FVIIIa complex, FIXa was incubated with excess of FVIII in presence of thrombin, calcium ions and phospholipids as indicated in Materials & Methods. Our HDX-MS protocol compromised between the lower limit for protein concentrations for optimal recovery and identification of peptides, and the upper limit for phospholipid concentration and PS content in order to still allow proper peptides separation prior to MS measurements. The experimental conditions allow an appreciable amount of complex formation, although in approximately 5-fold excess of protein over FVIII-binding sites on the lipid membrane[36]. We obtained 75 unique FIXa peptides (Figure 1) spanning from the EGF-2 domain throughout the Protease Domain. The coverage of the light chain and the catalytic domain was 33,1% and 98,7%, respectively (Figure 1). Due to the low intensity of Gla domain and the EGF-1 domain peptides of the light chain, fragments belonging to these regions were not consistently detectable and therefore not suitable for further analysis. This is mainly due to the post-translational modifications in the Gla domain (abundant negative charges due to γ-carboxylation) and the EGF-1 domain (glycosylation). Multiple replicates (3-6) showed that our data were highly reproducible. As for the EGF-2 and Protease Domain of FIXa, our data revealed multiple regions of the FIXa molecule that were affected by FVIIIa, covering a major part of the Protease Domain and EGF-2 (Figure 2). We categorised the extent of change in deuterium uptake as prominent, moderate, or no appreciable change. Eight peptides showed a prominent change (dark red in Figure 1 and 2), localizing in the 99-loop$_{CT}$, 162-helix$_{CT}$ and helix 236-240$_{CT}$. Thirteen peptides showed a moderate change (yellow in Figure 1 and 2). These were located in the EGF-2 domain, at the interface of EGF2/Protease Domain, and helix 126-132$_{CT}$, 148-loop$_{CT}$, 170-loop$_{CT}$, and 186-loop$_{CT}$ elsewhere in the Protease Domain. Finally, 54 peptides displayed no appreciable deuterium uptake difference in presence of FVIIIa (light grey in Figure 1, see also Supplementary Figure 1 for the full set of peptides). All observed FVIIIa-induced changes correspond to reduced deuterium uptake, which may be to either direct binding of FVIIIa, or to secondary





effects because of FVIIIa binding to another region in FIXa.

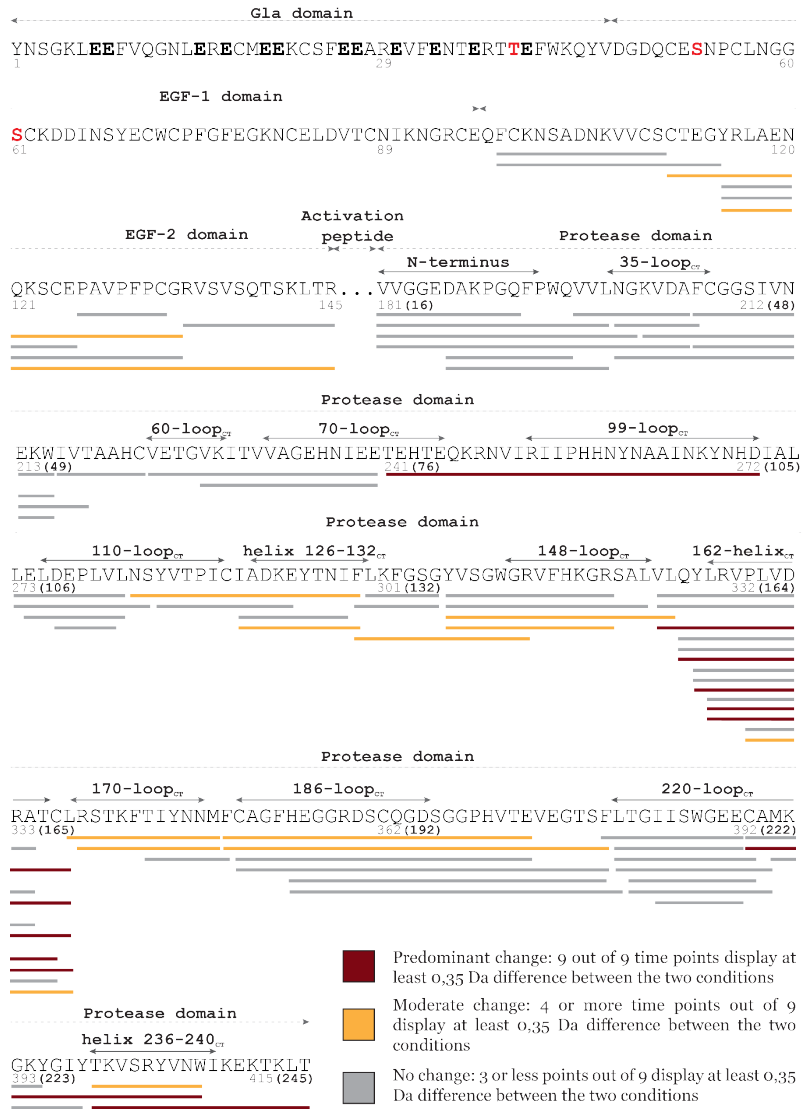


**Figure 1. Coverage of HDX-MS of FIXa-FVIIIa complex.**
HDX-MS experiments involved 9 time points and changes in deuterium uptake were rated as prominent when all 9 time points displayed a reduction in deuterium uptake per peptide of ≥ 0.35 Da for the entire peptide. These were mapped on FIXa sequence in red. Changes were rated moderate when 4–8 time points showed reduction by ≥ 0.35 Da were mapped in yellow. No appreciable change was designated by peptides comprised with less than 3 time points with ≥ 0.35 Da difference in deuterium uptake. FIXa numbering is assigned underneath the sequence with chymotrypsin numbering between brackets. FIXa domains and regions are also indicated. Gla residues are indicated in black bold characters. Glycosylations sites are shown in red.

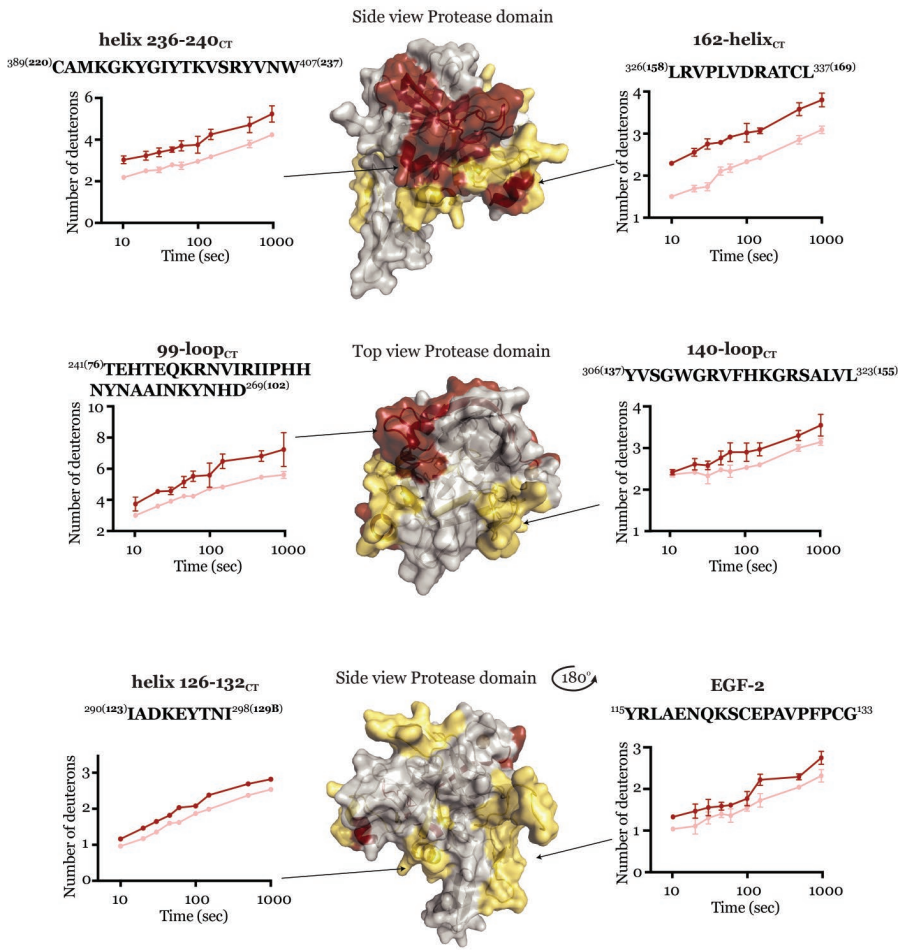


**Figure 2. Deuterium uptake plots of HDX-MS of FIXa-FVIIIa complex**
Changes in deuterium uptake in HDX-MS of FIXa-FVIIIa complex are displayed dark red (predominant change), yellow (moderate change) and grey on the crystal structure of FIXa Protein Data Base (PDB) code 2wpm. Data indicate that major part of the Protease Domain and EGF-2 is affected by FVIIIa. Examples of deuterium uptake plots are also shown. Chymotrypsin numbering is indicated between brackets at the side of the peptide sequence. The red curves indicate FIXa in the absence of FVIIIa. FIXa incubated in presence of FVIIIa is shown in pink. The complete set of peptides is reported in supplemental Figure 1.

Similar experiments were performed in absence of phospholipids. As shown in Supplementary Figure 2, fewer changes were observed. Predominant changes were still observed in the 99-loop$_{CT}$ of the Protease Domain and in peptide F98-S110 of the EGF-2 domain, suggesting that FVIIIa and FIXa do assemble in solution. However, the absence of changes in other FIXa regions demonstrates that most of the changes detected in Figure 1 reflect the lipid-bound fraction of FIXa-FVIIIa complex.





## HDX of active site-inhibited FIXa (FIXaEGR)

Changes in HDX were visualized in Figure 2 using one of the several available crystal structures of the EGF-2/Protease Domain segment, which all are based on active-site-inhibited FIXa 'frozen' in a substrate-bound conformation[14].

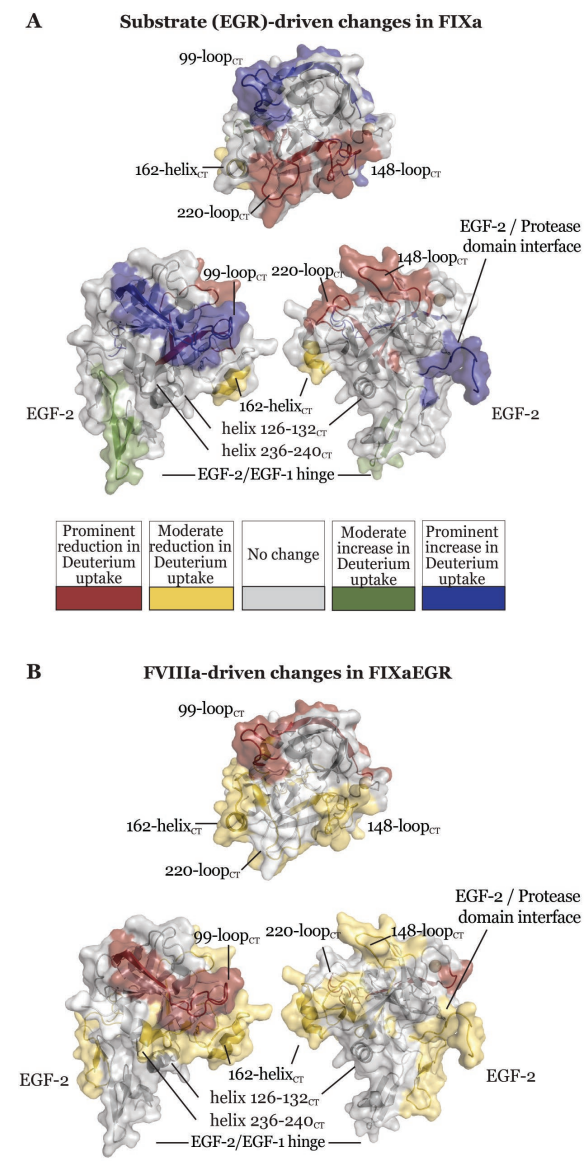


**Figure 3. HDX-MS of FIXa irreversibly bound to the pseudo-substrate Glu-Gly-Arg-chloromethylketone (FIXaEGR).**
A) FIXaEGR was compared to active site free FIXa where changes (mapped on FIXa crystal structure PDB: 2wpm) were detectable for hinge EGF-1/EGF-2, interface EGF-2/Protease Domain, 99-loop$_{CT}$, 148-loop$_{CT}$, 162-helix$_{CT}$ and 220-loop$_{CT}$. B) FIXaEGR was incubated in presence and absence of FVIIIa and differences were highlighted on the FIXa crystal structure. Changes were detectable at EGF-2, interface EGF-2/Protease Domain, 99-loop$_{CT}$, helix 126-132$_{CT}$, 148-loop$_{CT}$, 162-helix$_{CT}$ and helix 236-240$_{CT}$. HDX-MS measurements were based on 3 time points, and mapped following the color coding as indicated. differences were rated as prominent when 3 out of 3 time points showed ≥0.35 Da difference per peptide, moderate with 1 or 2 time points out of 3 and no appreciable change when all time points showed <0.35 Da difference.

Similarly, we employed HDX to explore changes in FIXa occurring upon irreversible inhibition by the pseudo-substrate EGRck (FIXaEGR). Comparison of FIXaEGR with FIXa displayed a variety of changes, comprising both deuterium uptake reduction and increase. An *increase* in deuterium uptake for FIXaEGR was observed in the EGF-1/EGF-2 domain hinge (moderate increase, green in Figure 3A) and in the EGF-2/Protease Domain interface and 99-loop$_{CT}$ (prominent increase, blue in Figure 3A), whereas a *decrease* occurred in the 148-loop$_{CT}$ and 220-loop$_{CT}$ of FIXaEGR (prominent, red in Figure 3A) and 162-helix$_{CT}$ regions (moderate, yellow in Figure 3A). Individual time courses are given in Supplemental Figure 3.

We further examined the effect of assembly of FIXaEGR with FVIIIa and lipids under the conditions of Figure 2. Differences between FIXaEGR in presence and absence of FVIIIa proved to affect peptides very similar to those in non-inhibited FIXa in the presence of FVIIIa (Figure 3B *versus* Figure 2). The effect of assembly of FIXaEGR with FVIIIa is reflected by a prominent reduction of deuterium uptake at the 99-loop$_{CT}$, and moderate reduction at the EGF-2 domain and the EGF-2/Protease Domain interface, and 148-loop$_{CT}$, helix 126-132$_{CT}$, 162-helix$_{CT}$ and 170-loop$_{CT}$, 186-loop$_{CT}$ and helix 236-240$_{CT}$ (see Supplementary Figures 3 and 4A-D).

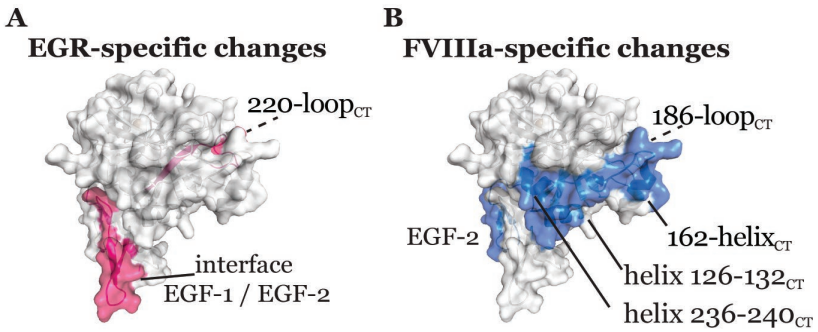


**Figure 4. Cofactor-induced *versus* substrate-induced changes in deuterium uptake.**
A) Among the changes induced by the EGRck alone, the 220-loop$_{CT}$ appears to be the only region involved on the protease domain together with the hinge EGF-1/EGF-2 on the light chain (pink). B) FVIIIa induces changes on EGF-2, helix 126-132$_{CT}$, helix 236-240$_{CT}$ and the C-terminal part of 162-helix$_{CT}$ (blue). Data indicate the cluster of helices helix 126-132$_{CT}$, helix 236-240$_{CT}$ and the C-terminal part of 162-helix$_{CT}$, known as exosite II, as the putative FVIIIa binding site.

Interestingly, the effects of EGR and FVIIIa are non-overlapping in some FIXa regions. For instance, changes at 220-loop$_{CT}$ and EGF-1/EGF-2 hinge peptide F98-G114 are mainly observed upon EGR incorporation (Figure 4A). On the other hand, reduced deuterium incorporation at EGF-2 peptide Y115-G133, helix 126-132$_{CT}$, 162-helix$_{CT}$, the 186-loop$_{CT}$ and helix 236-240$_{CT}$ seem to be predominantly driven by FVIIIa (Figure 4B). Helices 126-132$_{CT}$ and 236-240$_{CT}$ are located close to the 162-helix$_{CT}$, which has been previously implicated in FVIIIa binding[12,13]. These three helices together form the basic surface patch also known as Exosite II, which has been reported to bind heparin, and possibly also FVIIIa[37].





## Functional properties of FIXa variants with substitutions in Exosite II

To verify the involvement of the FIXa helix 126-132$_{CT}$, 162-helix$_{CT}$ and 170-loop$_{CT}$ and helix 236-240$_{CT}$ in FVIIIa-dependent catalysis, we selected the basic residues K293{126$_{CT}$}, R333{165$_{CT}$}, R338{170$_{CT}$}, K341{173$_{CT}$}, K400{230$_{CT}$} and R403{233$_{CT}$} (see Figure 5D) for substitution into alanine. These substitutions did not affect the activity towards the substrate $CH_3SO_2$-(D)-CHG-Gly-Arg-*p*NA (Table 1). The FIXa variants further displayed similar apparent $K_m$ values of FX activation in the presence of $Ca^{2+}$ and phospholipids (Table 1), while $k_{cat}$ values were slightly reduced, in particular for FIXaR333A{165$_{CT}$}. These data imply that these substitutions have limited impact on FIXa catalytic activity in the absence of FVIIIa. Because the 162-helix$_{CT}$ was previously proposed to bind to the A2 domain[12], we assessed the contribution of the single substitutions of Exosite II in FVIIIa A2 domain binding by SPR experiments. Individual association and dissociation curves displayed heterogeneous kinetics, and could serve for qualitative comparison only. Figure 5A shows that all single substitutions reduced the association with the immobilized A2 domain. However, none of the substitutions fully abolished A2 domain binding. The most pronounced A2 domain association defects were observed for FIXaR403A{233$_{CT}$} and, to a lesser extent, for FIXaR333A{165$_{CT}$}, while A2 domain binding was fully abolished by the double substitution FIXaR333A+R403A{165+233$_{CT}$}. These data suggest that multiple residues within Exosite II contribute to an extended FVIIIa binding interface.

FIXa mutants were further characterized to assess their FVIIIa-assisted FX activation. FVIIIa titration experiments showed dose-dependent acceleration of FX activation by wild-type FIXa (wt-FIXa) by several thousand-fold (Figure 5B, Table 1). Four FIXa variants displayed reduced FX activation that seemed compatible with their reduced A2 domain association (Figure 5A). One variant, FIXaR338A{170$_{CT}$} combined slightly reduced A2 domain interaction with increased response to FVIIIa (Figure 5B) and 2-fold *increase* in $k_{cat}$ (Table 1). The most prominent exception, however, was FIXaR333A{165$_{CT}$} which, despite its residual A2 domain association being substantially conserved, lacked any response to FVIIIa (Figure 5B). In FX titration experiments, four of the FIXa mutants displayed typical substrate-dependent rate increase, although $k_{cat}$ was lower than for wt-FIXa (Table 1). However, the two mutants comprising the R333A{165$_{CT}$} substitution displayed abnormal kinetics in that increasing the FX concentration actually reduced activity

(Figure 5C). This substrate inhibition suggests that FIXaR333A{$165_{CT}$} displays a more general defect in assembling the FIXa-FVIIIa-FX complex. These data suggest that residue R333{$165_{CT}$}, while contributing to FVIIIa A2 domain interaction, is particularly crucial for FVIIIa-driven rate enhancement of FIXa.

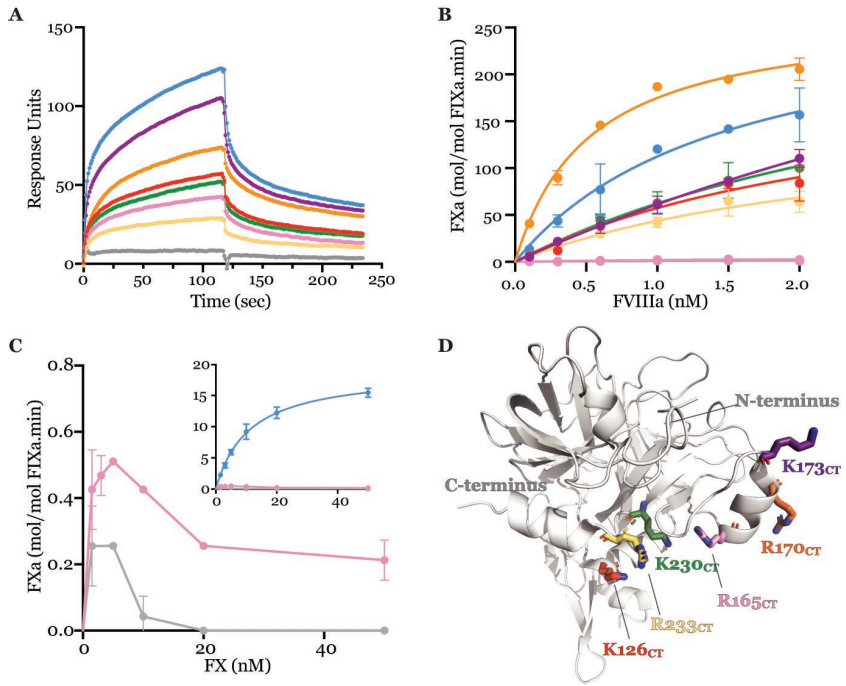


**Figure 5. Functional characterization of FIXa with substitutions in Exosite II.** A) Binding of FIXa variants to the A2 subunit of FVIII was measured by SPR as described in "Materials and Methods". The graph shows association and dissociation curves for wt-FIXa (blue), FIXaK293A{$126_{CT}$} (red), FIXaR333A{$165_{CT}$} (pink), FIXaR338A{$170_{CT}$} (orange), FIXaK341A{$173_{CT}$} (purple) FIXaK400A{$230_{CT}$} (green), FIXaR403A{$233_{CT}$} (yellow) and the double mutant FIXaR333A+R403A{$165+233_{CT}$} (grey) at a concentration of 400 nM. B) FX activation in presence of FVIIIa was performed with various concentrations of FVIII. FVIII was incubated with phospholipids (100 μM), FX (200 nM) and 0.1 nM of wt-FIXa (blue), FIXaK293A{$126_{CT}$} (red), FIXaR333A{$165_{CT}$} (pink), FIXaR338A{$170_{CT}$} (orange), FIXaK341A{$173_{CT}$} (purple) FIXaK400A{$230_{CT}$} (green), FIXaR403A{$233_{CT}$} (yellow) or FIXaR333A+R403A{$165+233_{CT}$} (grey). Data represent the mean of two independent experiments. C) Activation of FX (0-50 nM) by 0.3 nM of FIXaR333A{$165_{CT}$} (pink) or FIXaR333A+R403A{$165+233_{CT}$} (grey). The inset shows the same data with wt-FIXa included. FX activation was assessed in presence of 100 mM phospholipids, and 0.3 nM FVIIIa. Data represent the mean of 2 to 3 independent experiments. D) Basic residues of the a-helix 126-$132_{CT}$, 162-$helix_{CT}$ and a-helix 236-$240_{CT}$ were mutated into alanine residues. Chymotrypsin numbering is indicated (FIXa PDB 2wpm).





**Table 1. Functional properties of FIXa variants with substitutions in exosite II**

| FIXa variant | Amidolytic activity | | FXa generation in absence of FVIIIa | | FXa generation in presence of FVIIIa | |
|---|---|---|---|---|---|---|
| | apparent $K_m$ (mM) | $k_{cat}$ ($s^{-1}$) | apparent $K_m$ (nM) | $10^3$ x $k_{cat}$ ($min^{-1}$) | apparent $K_m$ (nM) | $k_{cat}$ ($min^{-1}$) |
| **FIXa wild-type** | 2.1 ± 0.3 | 13.2 ± 0.5 | 91 ± 6 | 25 ± 1 | 19 ± 6 | 54 ± 4 |
| **FIXaK126A$_{CT}$** | 2.4 ± 0.3 | 10.9 ± 1.7 | 83 ± 19 | 15 ± 1 | 4 ± 1 | 26 ± 1 |
| **FIXaR165A$_{CT}$** | 3.6 ± 0.5 | 11.1 ± 0.8 | 55 ± 9 | 7 ± 1 | N.D. | N.D. |
| **FIXaR170A$_{CT}$** | 1.7 ± 0.2 | 11 ± 0.8 | 68 ± 15 | 17 ± 1 | 20 ± 6 | 100 ± 7 |
| **FIXaK173A$_{CT}$** | 1.9 ± 0.2 | 9.3 ± 0.6 | 82 ± 12 | 11 ± 1 | 9 ± 5 | 39 ± 2 |
| **FIXaK230A$_{CT}$** | 3.9 ± 0.7 | 13.3 ± 2.8 | 53 ± 13 | 14 ± 1 | 9 ± 2 | 30 ± 2 |
| **FIXaR233A$_{CT}$** | 2.8 ± 0.3 | 11.4 ± 1.3 | 90 ± 24 | 14 ± 1 | 3 ± 1 | 17 ± 1 |
| **FIXaR165A+R233A$_{CT}$** | 9.6 ± 3.3 | 14.2 ± 0.8 | 61 ± 14 | 5 ± 1 | N.D. | N.D. |

**Table 1.** Catalytic efficiency of FIXa variants of the Exosite II was evaluated towards varying concentrations of the peptide substrate $CH_3SO_2$-(D)-CHG-Gly-Arg-*p*NA (indicated as amidolytic activity) and of the natural substrate FX in presence of phospholipids and $Ca^{2+}$ ions in the absence and presence of FVIIIa. Experimental conditions are given in "Materials and methods" and in the legend to Figure 5. Data were fitted in the Michaelis-Menten equation to obtain $K_m$ and $k_{cat}$ values. Kinetic parameters represent the mean ± S.D. of 2-3 independent experiments. ND, not determined due to substrate inhibition, see Figure 5C.

## HDX of FVIIIa assembly with FIXaR333A{$165_{CT}$}

We first addressed the possibility that FIXaR333A{$165_{CT}$} mutant displays general defects at the backbone level. In comparison to wt-FIXa, FIXaR333A{$165_{CT}$} displayed a prominent reduction in deuterium incorporation in peptides at the interface between the EGF-1/EGF-2 domains and the EGF-2/Protease Domain (red in Figure 6A). Moderate reduction occurred in surface loops, in particular at 70-$loop_{CT}$, 99-$loop_{CT}$, 148-$loop_{CT}$, 170-$loop_{CT}$ and 186-$loop_{CT}$ (yellow in Figure 6A). We further compared FIXaR333A{$165_{CT}$} in presence and absence of FVIIIa. Interestingly, only few FVIIIa-driven changes occurred (Figure 6B and 6C). A minor reduction of deuterium uptake was observed for the 99-$loop_{CT}$ only, while FVIIIa-induced changes at helix 126-$132_{CT}$, 162-$helix_{CT}$, 170-$loop_{CT}$, 186-$loop_{CT}$ and helix 236-$240_{CT}$ that occur in wt-FIXa (Figure 2) were no longer apparent (see Figure 6C and Supplementary Figures 4E-F).

## HDX of FVIIIa assembly with FIXaE78K

In addition to FIXaR333A{$165_{CT}$}, other FIXa variants have been described with reduced response to FVIIIa[9,10]. Interestingly, these comprise substitutions that are located beyond the FIXa Protease Domain, at the hinge between the EGF-1 and EGF-2 domains in the light chain[9]. One of these, FIXaE78K, was included in this study. In comparison with wt-FIXa, FIXaE78K displayed a moderate increase in deuterium

uptake at the bottom of the EGF-2 domain (green in Figure 7A). The variant further displayed a moderate deuterium incorporation increase at the 186-loop$_{CT}$ level. No other differences were observed for the FIXaE78K variant. When comparing the variant in absence and presence of FVIIIa (see Figure 7C and Supplementary Figures 4G-H.) FIXaE78K displayed a FVIIIa-driven reduction of deuterium uptake in helix 236-240$_{CT}$ and the 99-loop$_{CT}$ (Figure 7B), although less pronounced than in wt-FIXa. In contrast, the typical FVIIIa-driven changes at helix 126-132$_{CT}$, 162-helix$_{CT}$ and 170-loop$_{CT}$ were lacking.

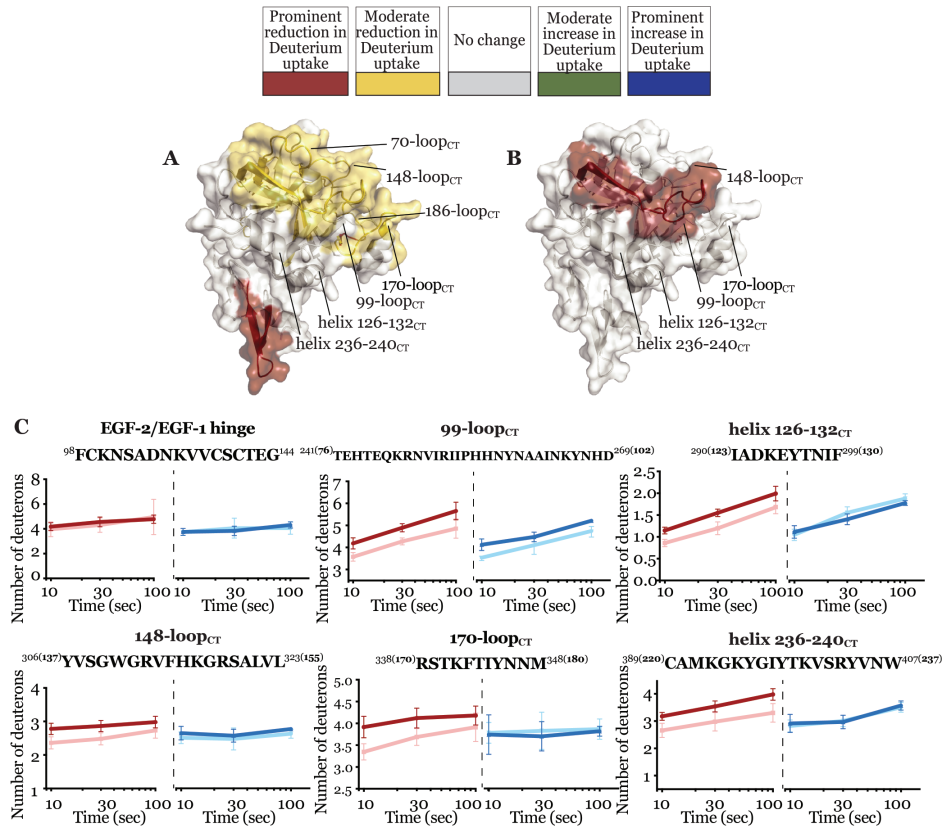


**Figure 6. HDX-MS of the heavy chain variant FIXaR333A{165$_{CT}$}**
FIXaR333A{165$_{CT}$} ability to interact with FVIIIa in the FIXa-FVIIIa complex was investigated with HDX-MS. A-B) FIXa Protease Domain and EGF-2 (PDB: 2wpm). The deuterium uptake changes are colour coded according to their intensity as described in Figure 3. A) Deuterium uptake differences in FIXaR333A{165$_{CT}$} compared to wt-FIXa. B) Deuterium uptake differences in FIXaR333A{165$_{CT}$} compared to FIXaR333A{165$_{CT}$} in presence of FVIIIa. C) Example plots comparing deuterium uptake differences between wt-FIXa in absence (red) or presence (pink) of FVIIIa to FIXaR333A{165$_{CT}$} in absence (dark blue) or presence (light blue) of FVIIIa.





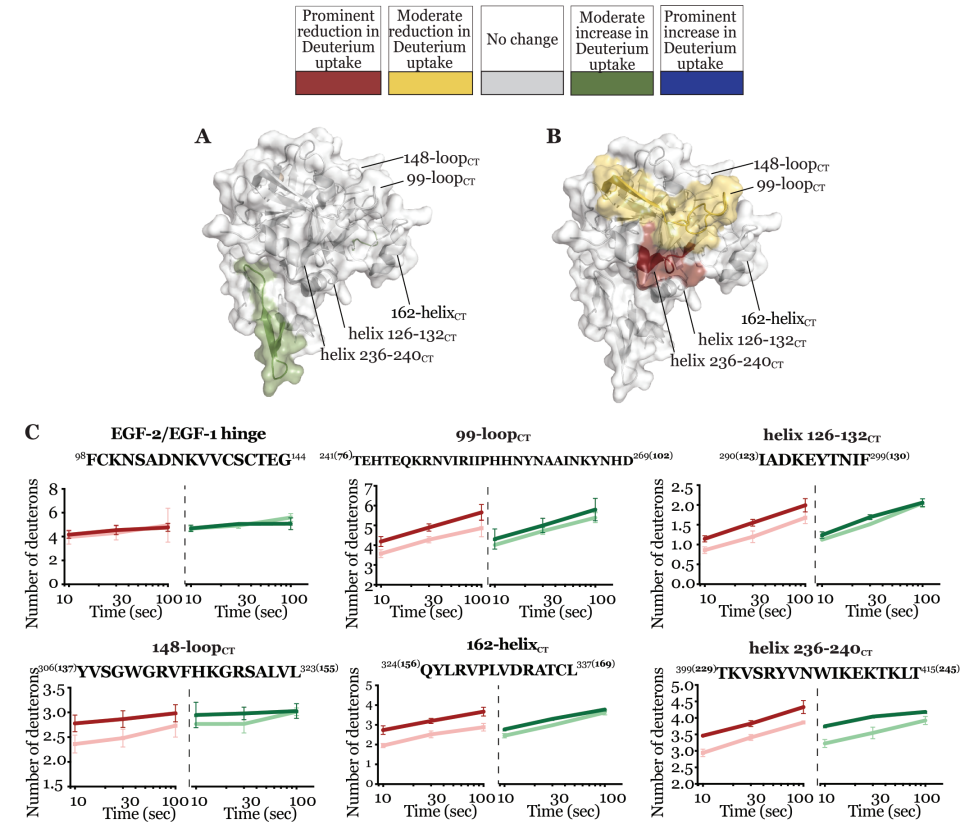


**Figure 7. HDX-MS of the light chain variant FIXaE78K.**
The ability of FIXaE78K to interact with FVIIIa in the FIXa-FVIIIa complex was investigated with HDX-MS. A-B) Protease Domain and EGF-2 are shown (PDB: 2wpm). The deuterium uptake changes are colour coded according to their intensity as described in Figure 3. A) Deuterium uptake differences in FIXaE78K compared to wt-FIXa. B) Deuterium uptake differences in FIXaE78K compared to FIXaE78K in presence of FVIIIa. C) Example plots comparing deuterium uptake differences between wt-FIXa in absence (red) or presence (pink) of FVIIIa to FIXaE78K in absence (dark green) or presence (light green) of FVIIIa.

## DISCUSSION

Blood coagulation involves a cascade wherein activated coagulation proteases act in concert with their specific cofactor. Apart from the FIXa-FVIIIa complex, these include the FVIIa-Tissue Factor (TF) complex and the prothrombinase complex[2]. Understanding the assembly of these enzyme-cofactor complexes and the mechanism of enhancement of enzyme function has remained a challenge for decades. In comparison with the FVIIa-TF complex, the FIXa-FVIIIa complex has remained poorly documented. The crystal structure of FVIIa complexed with a truncated TF has been resolved, which has greatly assisted the interpretation of later studies[38].

The FVIIa-TF complex has also been studied by HDX-MS, and this has revealed an extensive allosteric network in FVIIa[26]. For FIXa and FVIIIa, crystallography and modeling have established structures of the isolated constituents, but experimental data on the complex are limited so far[4,5,14,15,39,40].

In this study, we employed HDX-MS to assess the implications of FVIIIa assembly with FIXa on lipid membranes. Of the numerous changes observed, some appeared predominantly FVIIIa-specific. These include helix 126-132$_{CT}$, 162-helix$_{CT}$ and helix 236-240$_{CT}$ in the basic Exosite II, and probably reflect the footprint of the FVIIIa A2 domain on the catalytic domain (Figures 4 and 5). Other changes were driven by both FVIIIa and EGRck, and are considered to be allosteric. These comprise EGF-2 region Y115-G133, 99-loop$_{CT}$, 148-loop$_{CT}$, N-terminal part of the 162-helix$_{CT}$, and 186-loop$_{CT}$ (Figure 3). This pattern is analogous to that in FVIIa in many respects. For instance, both FIXa and FVIIa display changes in the EGF-2 domain and 148-loop$_{CT}$ upon cofactor binding. Similarly, the allosteric effects of active site occupancy extend into the light chain in both FIXa and FVIIa. This inter-domain cross-talk became apparent by increased deuterium exchange in FIXa (Figure 3A), while a decrease has been reported for FVIIa[26]. Increased flexibility in the EGF-2 domain was also observed in the variant FIXaE78K (Figure 7). This seems not surprising, because this mutation disrupts the contact with R94 at the EGF-1/EGF-2 hinge[4,9]. Remarkably, the compromised light chain in FIXaE78K also disrupts the binding on Exosite II (Figure 7). It seems possible that wrenching the hinge between EGF-1 and EGF-2 causes silencing of the cross-talk between light chain and heavy chain. Alternatively, it may impair the FVIIIa-binding conformation to an extent that also impedes the subsequent docking of the A2 domain to Exosite II. Because we did not recover peptides of the Gla-EGF1 segment, it remains difficult to distinguish between these possibilities.

A common activation-induced change concerns the 99-loop$_{CT}$, which is prominent in FIXa, and has also been found in FVIIa and thrombin[17,26]. In FIXa this loop is believed to obstruct the access to the FIXa active site and needs to be "unlocked" for effective catalysis[5,41,42]. Interestingly, in active-site inhibited FIXa deuterium uptake was *increased*, while the presence of FVIIIa *reduced* deuterium uptake (Figures 2 and 3B). This suggests that EGR binding brings this loop is in an open, but flexible conformation, and that FVIIIa subsequently stabilizes this opened conformation, thus allowing free entrance of the substrate FX to the active site. As such, the cofactor-driven stabilization of this loop seems more dynamic in FIXa-FVIIIa than in FVIIa-TF complex[26]. This might be because to the 99-loop$_{CT}$ in FIXa is longer than in its related coagulation enzymes[41,43].

Our approach further revealed analogy with FVIIa in terms of binding interfaces on the Protease Domain. However, in comparison with the FVIIa-TF crystal structure[38], the binding region in FIXa is more extended, since also helix 236-240$_{CT}$ seems involved in the interaction with FVIIIa (Figures 4B and 5). Possibly, this is due to different cofactor dimensions, as TF is much smaller than FVIII[38]. Nevertheless, the patterns of allosteric changes detected in HDX-MS in FVIIa and FIXa display striking similarity. In contrast to TF, activated Factor V (FVa) in the prothrombinase complex does display homology with FVIII. Although the structure of the FVa-FXa complex has not been resolved, a crystal structure is available of a homologous enzyme-cofactor complex that occurs in snake *Pseudonaja textilis*[44]. This displays a binding interface at Exosite II that also includes helix 236-240$_{CT}$ of the FX homolog. This helix seems to be involved with an acidic surface in its FVa counterpart that is also present in FVIIIa. Interestingly, most of the residues at Exosite II region that we selected for site-directed mutagenesis are reported Hemophilia B variants with defective activity[45]. This phenotype is compatible with reduced FVIIIa A2 domain binding and FX activation (Figure 5).

One key modulator of FIXa activity proved to be residue R333{165$_{CT}$}. Strikingly, FIXaR333A{165$_{CT}$} not only revealed reduced FVIIIa binding (Figure 5A), but in contrast to other Exosite II variants the mutant also displayed prominent substrate inhibition (Figure 5C). This suggests unproductive FX binding to the compromised FIXa-FVIIIa complex, and implies a dual role of 162-helix$_{CT}$ in assembly with both cofactor and substrate. It is noteworthy that the R338A{170$_{CT}$} substitution, which is located in the same helix, is associated with gain-of-function in the presence of FVIIIa (Figure 5B, Table 1). This confirms an earlier study[46], and agrees with the notion that the substitutions R338L (FIX Padua) and R338Q (FIX Shanghai) display supranormal activity[47,48]. Apparently, mutations on this helix may have opposite effects. Possibly, mutations of 162-helix$_{CT}$ alter the FVIIIa-driven allosteric signalling to the active site influencing substrate turnover. In this regard it is interesting that variant R333A{165$_{CT}$} misses the typical FVIIIa-driven change in the 186-loop$_{CT}$ (Figure 6). Presumably, disulphide bridge C168$_{CT}$-C182$_{CT}$ accounts for the communication line between the 162-helix$_{CT}$ and the active site[15]. In support of this view, overlapping peptides spanning the 162-helix$_{CT}$ identified the segment TCL167-169$_{CT}$ as mediating the prominent FVIIIa-dependent response (Figure 1). Similarly, the changes in the 186-loop$_{CT}$ largely depend on the residues FC181-182$_{CT}$ (Supplementary Figure 1).

One surprising observation was that HDX-MS revealed a tangible consequence of the R333{165$_{CT}$} mutation (Figure 6A). In comparison with wt-FIXa, the R333A{165$_{CT}$} variant displayed a general reduction of deuterium exchange in multiple surface loops, suggesting the protease domain to be more rigid. It seems conceivable that, although this variant is not defective in amidolytic activity (Table 1) its overall rigidity contributes to the assembly defect with the natural substrate FX

in presence of FVIIIa. In this regard, it would be interesting to address the effect of FX on FIXa-FVIIIa assembly by HDX-MS. However, it proved challenging to achieve proper FIX peptide separation in presence of membranes and an excess of FVIII-derived peptides, and increasing complexity by including FX seems not feasible at this stage. Our extensive sampling handling procedure prior to MS analysis has the inherent limitation that back-exchange significantly reduces the apparent extent of deuterium incorporation. Consequently, as in other studies employing a similar protocol[17,24,26,49], we report changes on the peptide level, while HDX-MS should have the potential of near-residue resolution. This, however, will require more rigorous strategies to reduce back-exchange[50]. Another issue is the lack of recovery of peptides from Gla-EGF-1 region. The post-translational modifications therein require complementary MS protocols to analyse membrane and FVIIIa binding to this part of the FIXa light chain. Despite these limitations, our current study demonstrates that HDX-MS allows the assessment of structural consequences of single amino acid substitutions. As such, it may also prove useful for addressing the structural impact of disease-associated mutations in other hemostatic proteins.

## AUTHORSHIP

NF, ABM, MvdB and KM designed the study; NF, CF and MBS performed the experimental work; FPJvA, JvG and EHTME developed the HDX-MS protocol; NF, JvG, EHTME, CF, ABM, MvdB and KM analysed and interpreted data; NF made the figures; NF, ABM, MvdB and KM wrote the manuscript.

## DECLARATIONS OF INTERESTS

The authors declare no conflict of interest.

## ACKNOWLEDGEMENT

This study has been funded by the Utrecht Institute for Pharmaceutical Sciences (UIPS) and by the Landsteiner Stichting voor Bloedtransfusie Research (LSBR 1417).





## REFERENCES

1. Mannucci PM, Tuddenham EG. The hemophilias--from royal genes to gene therapy. *N Engl J Med*. 2001;344(23):1773-1779.

2. Nemerson Y, Furie B, Jackson CM. Zymogens and cofactors of blood coagulation. *Crit Rev Biochem Mol Biol*. 1980;9(1):45–85.

3. Schmidt AE, Bajaj SP. Structure-function relationships in factor IX and factor IXa. *Trends Cardiovasc Med*. 2003;13(1):39–45.

4. Brandstetter H, Bauer M, Huber R, Lollar P, Bode W. X-ray structure of clotting factor IXa: active site and module structure related to Xase activity and hemophilia B. *Proc Natl Acad Sci U A*. 1995;92(21):9796–9800.

5. Hopfner KP, Lang A, Karcher A, et al. Coagulation factor IXa: the relaxed conformation of Tyr99 blocks substrate binding. *Structure*. 1999;7(8):989–996.

6. van Dieijen G, Tans G, Rosing J, Hemker HC. The role of phospholipid and factor VIIIa in the activation of bovine factor X. *J Biol Chem*. 1981;256(7):3433–3442.

7. Mertens K, Celie PH, Kolkman JA, Lenting PJ. Factor VIII-factor IX interactions: molecular sites involved in enzyme-cofactor complex assembly. *Thromb Haemost*. 1999;82(2):209–217.

8. Fay PJ. Factor VIII structure and function. *Int J Hematol*. 2006;83(2):103–108.

9. Christophe OD, Lenting PJ, Kolkman JA, Brownlee GG, Mertens K. Blood coagulation factor IX residues Glu78 and Arg94 provide a link between both epidermal growth factor-like domains that is crucial in the interaction with factor VIII light chain. *J Biol Chem*. 1998;273(1):222–227.

10. Celie PH, Van Stempvoort G, Fribourg C, Schurgers LJ, Lenting PJ, Mertens K. The connecting segment between both epidermal growth factor-like domains in blood coagulation factor IX contributes to stimulation by factor VIIIa and its isolated A2 domain. *J Biol Chem*. 2002;277(23):20214–20220.

11. Mathur A, Bajaj SP. Protease and EGF1 domains of factor IXa play distinct roles in binding to factor VIIIa. Importance of helix 330 (helix 162 in chymotrypsin) of protease domain of factor IXa in its interaction with factor VIIIa. *J Biol Chem*. 1999;274(26):18477–18486.

12. Bajaj SP, Schmidt AE, Mathur A, et al. Factor IXa:Factor VIIIa interaction. Helix 330-338 of factor IXa interacts with residues 558-565 and spatially adjacent regions of the A2 subunit of factor VIIIa. *J Biol Chem*. 2001;276(19):16302–16309.

13. Kolkman JA, Lenting PJ, Mertens K. Regions 301-303 and 333-339 in the catalytic domain of blood coagulation factor IX are factor VIII-interactive sites involved in stimulation of enzyme activity. *Biochem J*. 1999;339:217–221.

14. Zogg T, Brandstetter H. Structural basis of the cofactor- and substrate-assisted activation of human coagulation factor IXa. *Structure*. 2009;17(12):1669–1678.

15. Kristensen LH, Olsen OH, Blouse GE, Brandstetter H. Releasing the brakes in coagulation Factor IXa by co-operative maturation of the substrate-binding site. *Biochem J*. 2016;473(15):2395-2411.

16. Gilbert GE, Arena AA. Activation of the factor VIIIa-factor IXa enzyme complex of blood coagulation by membranes containing phosphatidyl-L-serine. *J Biol Chem*. 1996;271(19):11120–11125.

17. Handley LD, Treuheit NA, Venkatesh VJ, Komives EA. Thrombomodulin Binding Selects the Catalytically Active Form of Thrombin. *Biochemistry*. 2015;54(43):6650–6658.

18. Chiu PL, Bou-Assaf GM, Chhabra ES, et al. Mapping the interaction between factor VIII and von Willebrand factor by electron microscopy and mass spectrometry. *Blood*. 2015;126(8):935–938.

19. Przeradzka MA, van Galen J, Ebberink EHTM, et al. D' domain region Arg782-Cys799 of von Willebrand factor contributes to factor VIII binding. *Haematologica*. 2020;105(6):1695-1703.

20. Pantazatos D, Gessner CR, Woods Jr.

VL, Gilbert GE. Changes in the Factor VIII C2 domain upon membrane binding determined by hydrogen-deuterium exchange MS. *Biochem J*. 2014;461(3):443–451.

21. Bloem E, van den Biggelaar M, Wroblewska A, et al. Factor VIII C1 domain spikes 2092-2093 and 2158-2159 comprise regions that modulate cofactor function and cellular uptake. *J Biol Chem*. 2013;288(41):29670–29679.

22. Batsuli G, Deng W, Healey JF, et al. High-affinity, noninhibitory pathogenic C1 domain antibodies are present in patients with hemophilia A and inhibitors. *Blood*. 2016;128(16):2055-2067.

23. Malovichko MV, Sabo TM, Maurer MC. Ligand binding to anion-binding exosites regulates conformational properties of thrombin. *J Biol Chem*. 2013;288(12):8667–8678.

24. Peacock RB, Davis JR, Markwick PRL, Komives EA. Dynamic Consequences of Mutation of Tryptophan 215 in Thrombin. *Biochemistry*. 2018;57(18):2694-2703.

25. Markwick PRL, Peacock RB, Komives EA. Accurate Prediction of Amide Exchange in the Fast Limit Reveals Thrombin Allostery. *Biophys J*. 2019;116(1):49-56.

26. Rand KD, Jørgensen TJD, Olsen OH, et al. Allosteric Activation of Coagulation Factor VIIa Visualized by Hydrogen Exchange. *J Biol Chem*. 2006;281(32):23018-23024.

27. Fribourg C, Meijer AB, Mertens K. The interface between the EGF2 domain and the protease domain in blood coagulation factor IX contributes to factor VIII binding and factor X activation. *Biochemistry*. 2006;45(35):10777–10785.

28. Kolkman JA, Christophe OD, Lenting PJ, Mertens K. Surface loop 199-204 in blood coagulation factor IX is a cofactor-dependent site involved in macromolecular substrate interaction. *J Biol Chem*. 1999;274(41):29087–29093.

29. Lenting PJ, ter Maat H, Clijsters PP, Donath MJ, van Mourik JA, Mertens K. Cleavage at arginine 145 in human blood coagulation factor IX converts the zymogen into a factor VIII binding enzyme. *J Biol Chem*. 1995;270(25):14884-14890.

30. Bradford MM. A rapid and sensitive method for the quantitation of microgram quantities of protein utilizing the principle of protein-dye binding. *Anal Biochem*. 1976;72:248-254.

31. Meems H, van den Biggelaar M, Rondaij M, van der Zwaan C, Mertens K, Meijer AB. C1 domain residues Lys 2092 and Phe 2093 are of major importance for the endocytic uptake of coagulation factor VIII. *Int J Biochem Cell Biol*. 2011;43(8):1114-1121.

32. Mertens K, Bertina RM. Activation of human coagulation factor VIII by activated factor X, the common product of the intrinsic and the extrinsic pathway of blood coagulation. *Thromb Haemost*. 1982;47(2):96-100.

33. Mertens K, Bertina RM. Pathways in the activation of human coagulation factor X. *Biochem J*. 1980;185(3):647-658.

34. Hendrix H, Lindhout T, Mertens K, Engels W, Hemker HC. Activation of human prothrombin by stoichiometric levels of staphylocoagulase. *J Biol Chem*. 1983;258(6):3637-3644.

35. Bloem E, Meems H, van den Biggelaar M, van der Zwaan C, Mertens K, Meijer AB. Mass spectrometry-assisted study reveals that lysine residues 1967 and 1968 have opposite contribution to stability of activated factor VIII. *J Biol Chem*. 2012;287(8):5775–5783.

36. Gilbert GE, Furie BC, Furie B. Binding of human factor VIII to phospholipid vesicles. *J Biol Chem*. 1990;265(2):815–822.

37. Misenheimer TM, Buyue Y, Sheehan JP. The heparin-binding exosite is critical to allosteric activation of factor IXa in the intrinsic tenase complex: the role of arginine 165 and factor X. *Biochemistry*. 2007;46(26):7886–7895.

38. Banner DW, D'Arcy A, Chene C, et al. The crystal structure of the complex of blood coagulation factor VIIa with soluble tissue factor. *Nature*. 1996;380(6569):41–46.

39. Ngo JC, Huang M, Roth DA, Furie BC, Furie B. Crystal structure of human factor VIII: implications for the formation of the factor IXa-factor VIIIa complex. *Structure*. 2008;16(4):597–606.

40. Venkateswarlu D. Structural insights into the interaction of blood coagulation cofactor VIIIa with factor IXa: a computational protein-protein docking and molecular dynamics refinement study. *Biochem Biophys Res Commun*. 2014;452(3):408–414.

41. Hopfner KP, Brandstetter H, Karcher A, et al. Converting blood coagulation factor IXa into factor Xa: dramatic increase in amidolytic activity identifies important active site determinants. *EMBO J*. 1997;16(22):6626–6635.

42. Sichler K, Kopetzki E, Huber R, Bode W, Hopfner KP, Brandstetter H. Physiological fIXa activation involves a cooperative conformational rearrangement of the 99-loop. *J Biol Chem*. 2003;278(6):4121–4126.

43. Kolkman JA, Mertens K. Insertion loop 256-268 in coagulation factor IX restricts enzymatic activity in the absence but not in the presence of factor VIII. *Biochemistry*. 2000;39(25):7398–7405.

44. Lechtenberg BC, Murray-Rust TA, Johnson DJ, et al. Crystal structure of the prothrombinase complex from the venom of Pseudonaja textilis. *Blood*. 2013;122(16):2777–2783.

45. Rallapalli PM, Kemball-Cook G, Tuddenham EG, Gomez K, Perkins SJ. An interactive mutation database for human coagulation factor IX provides novel insights into the phenotypes and genetics of hemophilia B. *J Thromb Haemost*. 2013;11(7):1329–1340.

46. Chang J, Jin J, Lollar P, et al. Changing residue 338 in human factor IX from arginine to alanine causes an increase in catalytic activity. *J Biol Chem*. 1998;273(20):12089–12094.

47. Simioni P, Tormene D, Tognin G, et al. X-Linked Thrombophilia with a Mutant Factor IX (Factor IX Padua). *N Engl J Med*. 2009;361(17):1671-1675.

48. Wu W, Xiao L, Wu X, et al. Factor IX alteration p.Arg338Gln (FIX Shanghai) potentiates FIX clotting activity and causes thrombosis [published online ahead of print 20 February 2020]. *Haematologica*. doi:10.3324/haematol.2019.216713

49. Andersen MD, Faber JH. Structural characterization of both the non-proteolytic and proteolytic activation pathways of coagulation Factor XIII studied by hydrogen–deuterium exchange mass spectrometry. *Int J Mass Spectrom*. 2011;302(1-3):139-148.

50. Walters BT, Ricciuti A, Mayne L, Englander SW. Minimizing back exchange in the hydrogen exchange-mass spectrometry experiment. *J Am Soc Mass Spectrom*. 2012;23(12):2132-2139.

# SUPPLEMENTAL MATERIAL

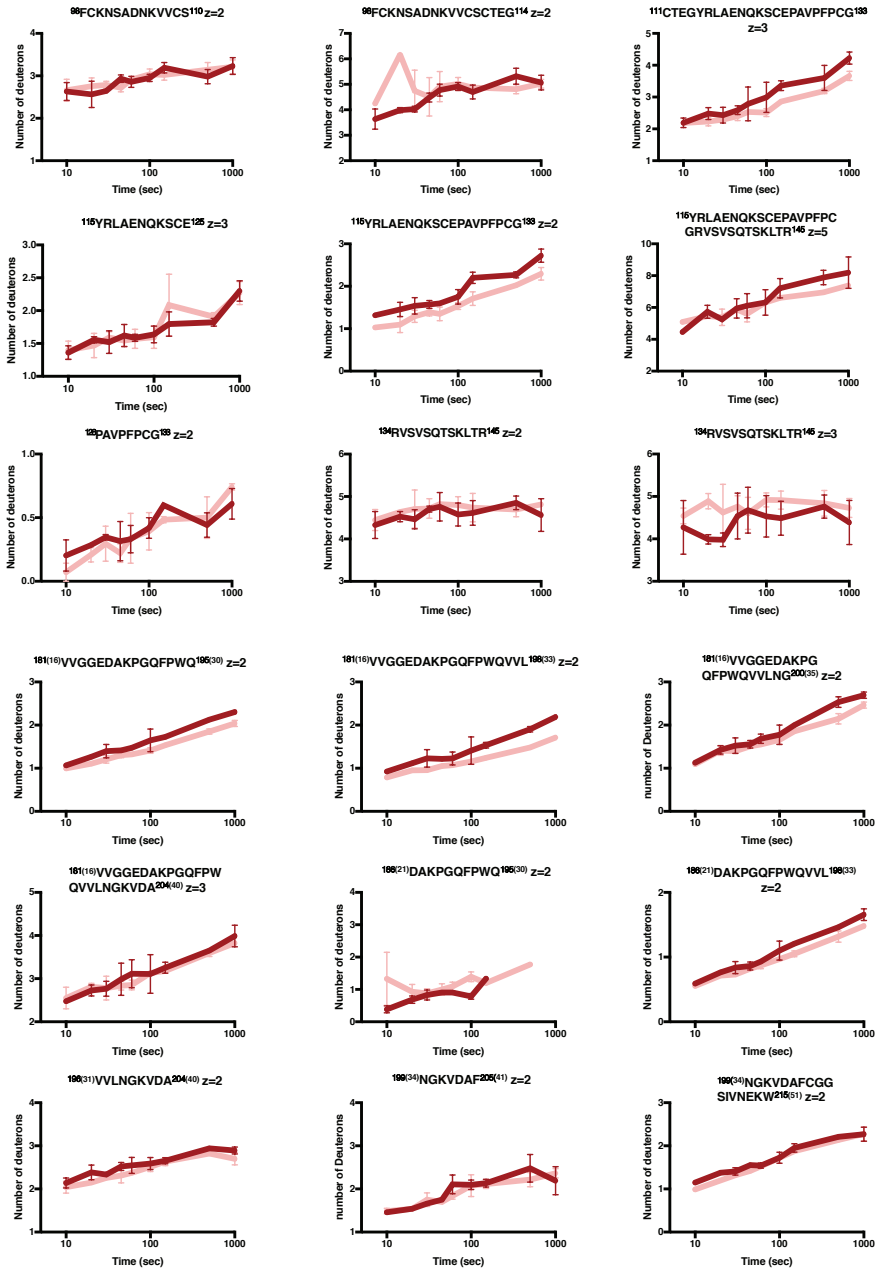


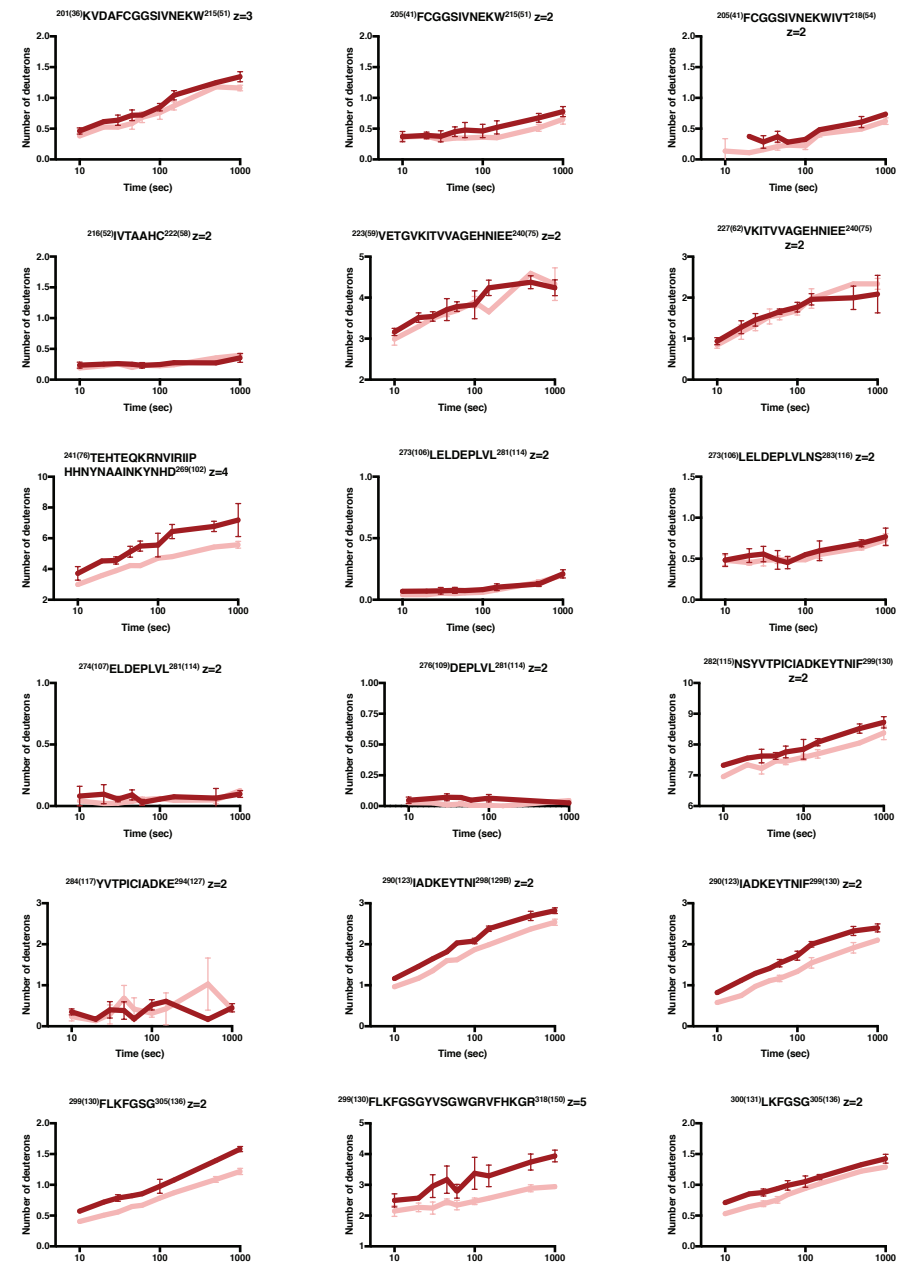

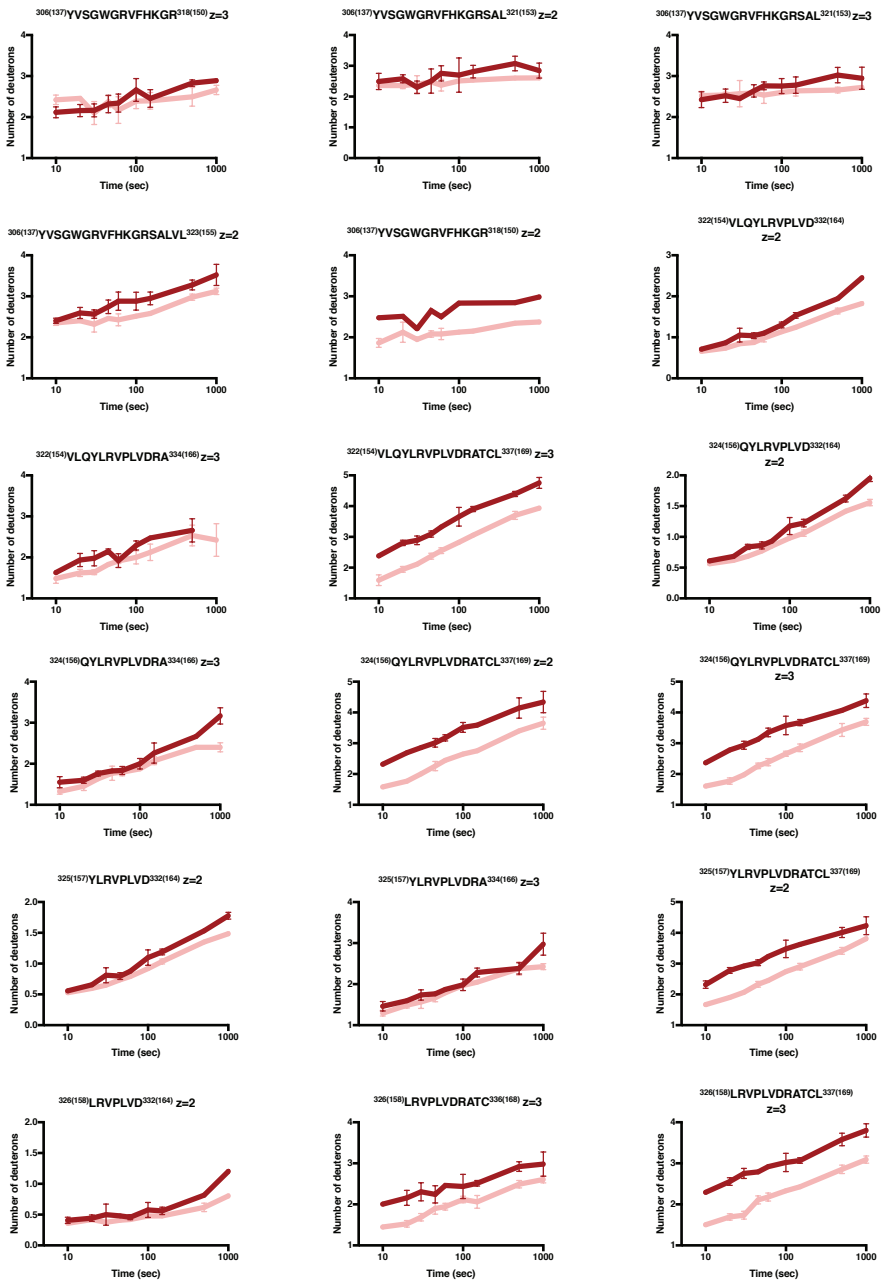
306(137)YVSGWGRVFHKGR318(150) z=3
306(137)YVSGWGRVFHKGRSAL321(153) z=2
306(137)YVSGWGRVFHKGRSAL321(153) z=3
306(137)YVSGWGRVFHKGRSALVL323(155) z=2
306(137)YVSGWGRVFHKGR318(150) z=2
322(154)VLQYLRVPLVD332(164) z=2
322(154)VLQYLRVPLVDRA334(166) z=3
322(154)VLQYLRVPLVDRATCL337(169) z=3
324(156)QYLRVPLVD332(164) z=2
324(156)QYLRVPLVDRA334(166) z=3
324(156)QYLRVPLVDRATCL337(169) z=2
324(156)QYLRVPLVDRATCL337(169) z=3
325(157)YLRVPLVD332(164) z=2
325(157)YLRVPLVDRA334(166) z=3
325(157)YLRVPLVDRATCL337(169) z=2
326(158)LRVPLVD332(164) z=2
326(158)LRVPLVDRATC336(168) z=3
326(158)LRVPLVDRATCL337(169) z=3
Number of deuterons
Time (sec)

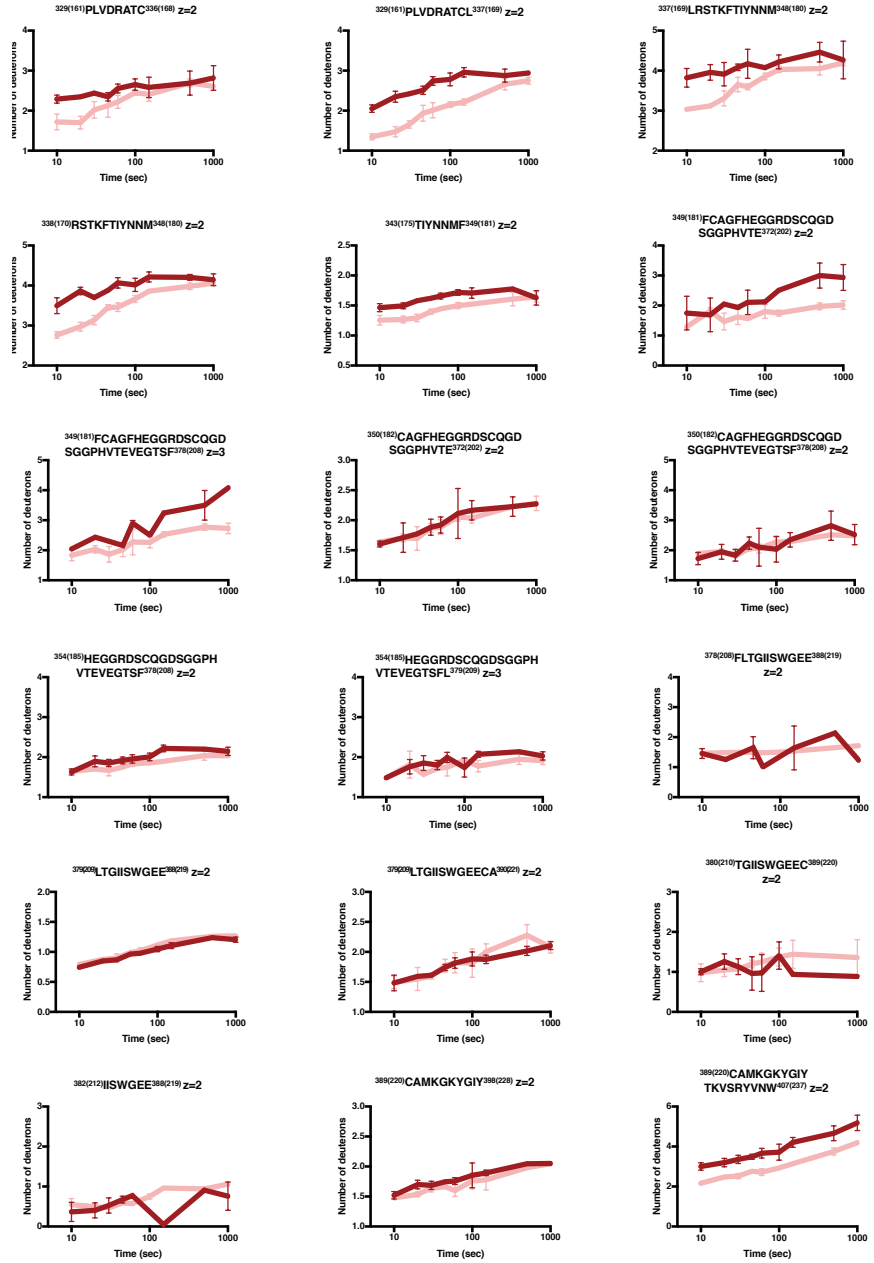
329(161)PLVDRATC336(168) z=2
329(161)PLVDRATCL337(169) z=2
337(169)LRSTKFTIYNNM348(180) z=2
338(170)RSTKFTIYNNM348(180) z=2
343(175)TIYNNMF349(181) z=2
349(181)FCAGFHEGGRDSCQGD SGGPHVTE372(202) z=2
349(181)FCAGFHEGGRDSCQGD SGGPHVTEVEGTSF378(208) z=3
350(182)CAGFHEGGRDSCQGD SGGPHVTE372(202) z=2
350(182)CAGFHEGGRDSCQGD SGGPHVTEVEGTSF378(208) z=2
354(185)HEGGRDSCQGDSGGPH VTEVEGTSF378(208) z=2
354(185)HEGGRDSCQGDSGGPH VTEVEGTSFL379(209) z=3
378(208)FLTGIISWGEE388(219) z=2
379(209)LTGIISWGEE388(219) z=2
379(209)LTGIISWGEECA390(221) z=2
380(210)TGIISWGEEC389(220) z=2
382(212)IISWGEE388(219) z=2
389(220)CAMKGKYGIY398(228) z=2
389(220)CAMKGKYGIY TKVSRYVNW407(237) z=2
Number of deuterons
Time (sec)

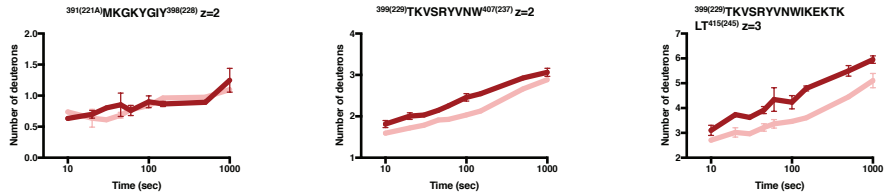


**Supplemental Figure 1. Deuterium uptake plots of FIXa-FVIIIa complex.**
Deuterium uptake plots of FIXa-FVIIIa complex. FIXa (red) was incubated in deuterium for several time points as described under Materials and Methods and compared to FIXa in presence of FVIIIa (pink). Number of deuterons incorporated are reported as a function of time for the individual FIXa peptides, charge state (z) of the peptides is also shown.

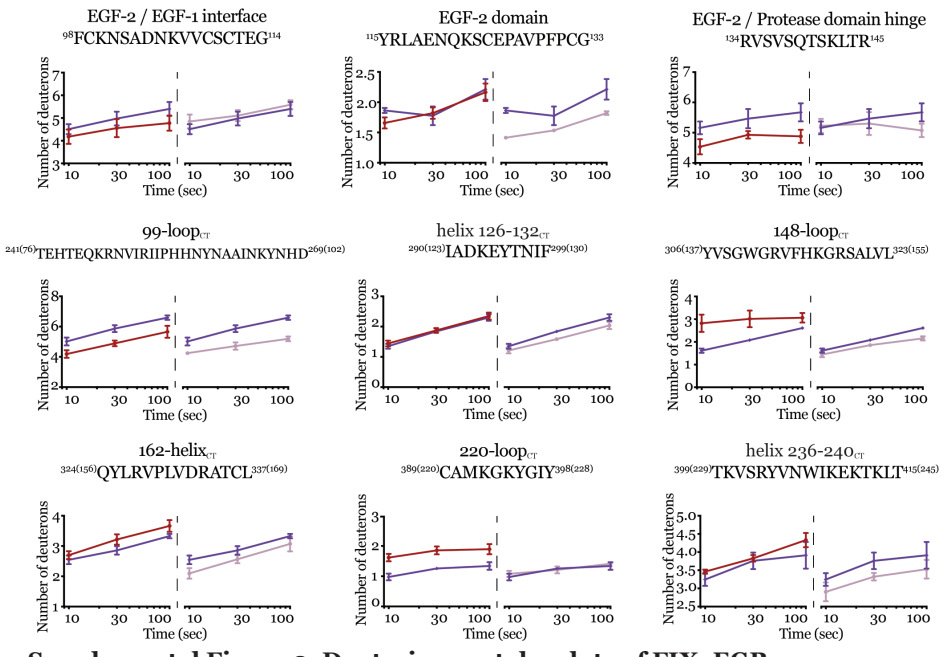


**Supplemental Figure 3. Deuterium uptake plots of FIXaEGR.**
Deuterium uptake plots of FIXaEGR (purple) in comparison to FIXa (red) are displayed on the left parts of the graphs. On the right part of the graph FIXaEGR (purple) is shown in comparison to FIXaEGR in presence of FVIIIa (light purple).





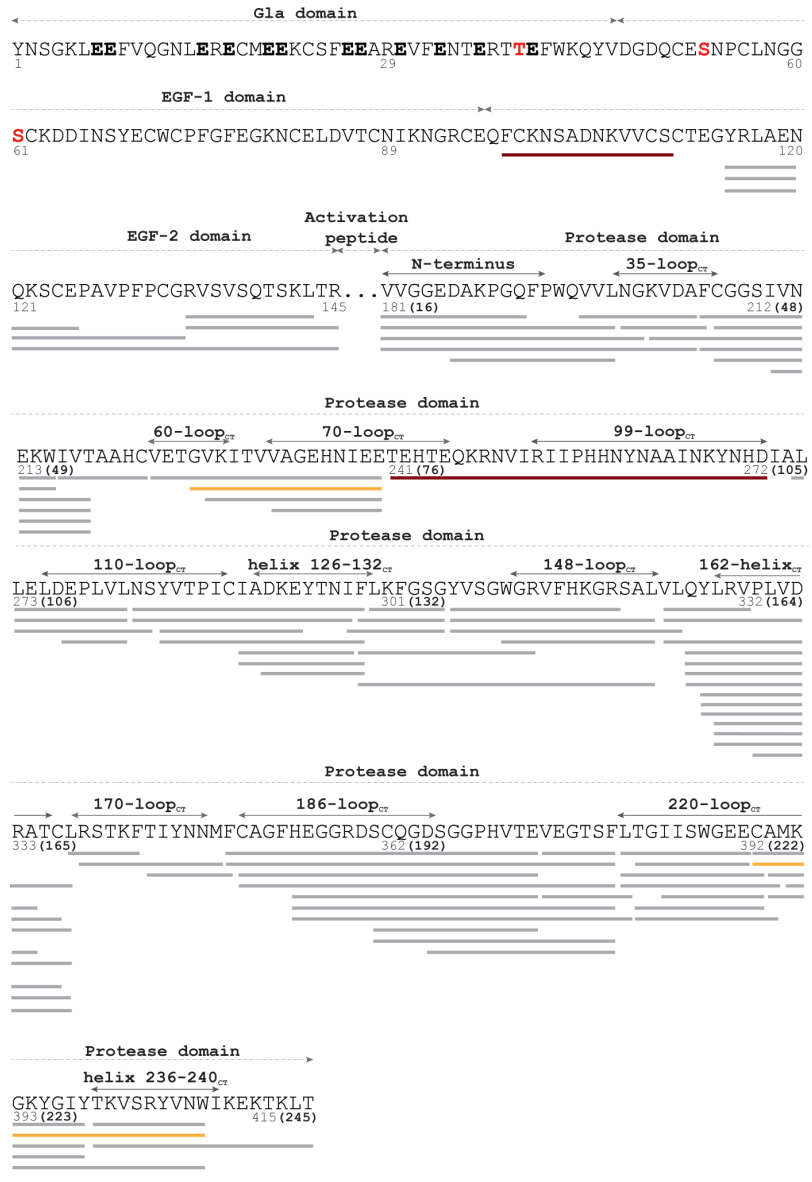


**Supplemental Figure 2.**
**HDX-MS of FIXa-FVIIIa complex in the absence of phospholipids.**
Coverage of HDX-MS of FIXa-FVIIIa complex in absence of phospholipid membranes. All the detected peptides are displayed in dark red (predominant change), yellow (moderate change) and grey (no appreciable change). FIXa numbering is assigned underneath the sequence with chymotrypsin numbering between brackets. FIXa domains and regions are also indicated. Gla residues are indicated in black bold characters, while glycosylation sites are shown in red.

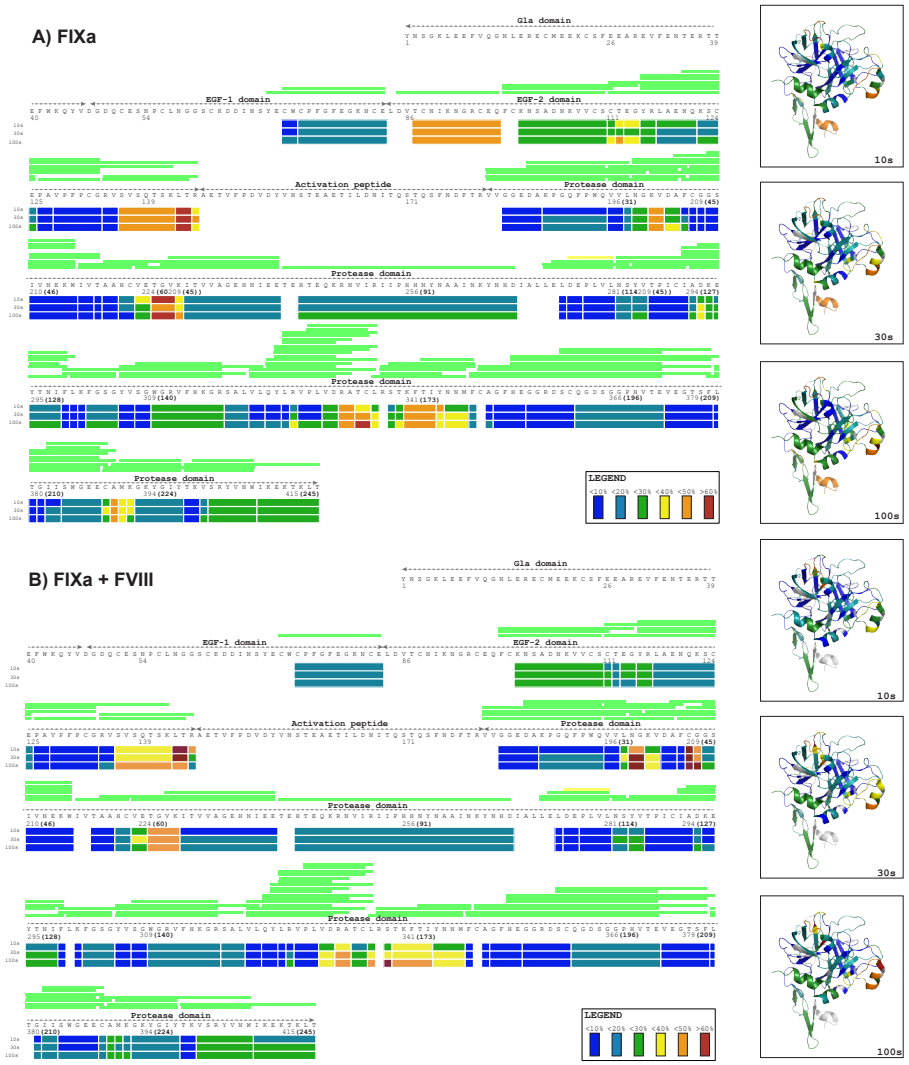
A) FIXa
B) FIXa + FVIII
Gla domain
EGF-1 domain
EGF-2 domain
Activation peptide
Protease domain
LEGEND
<10% <20% <30% <40% <50% >60%
10s
30s
100s

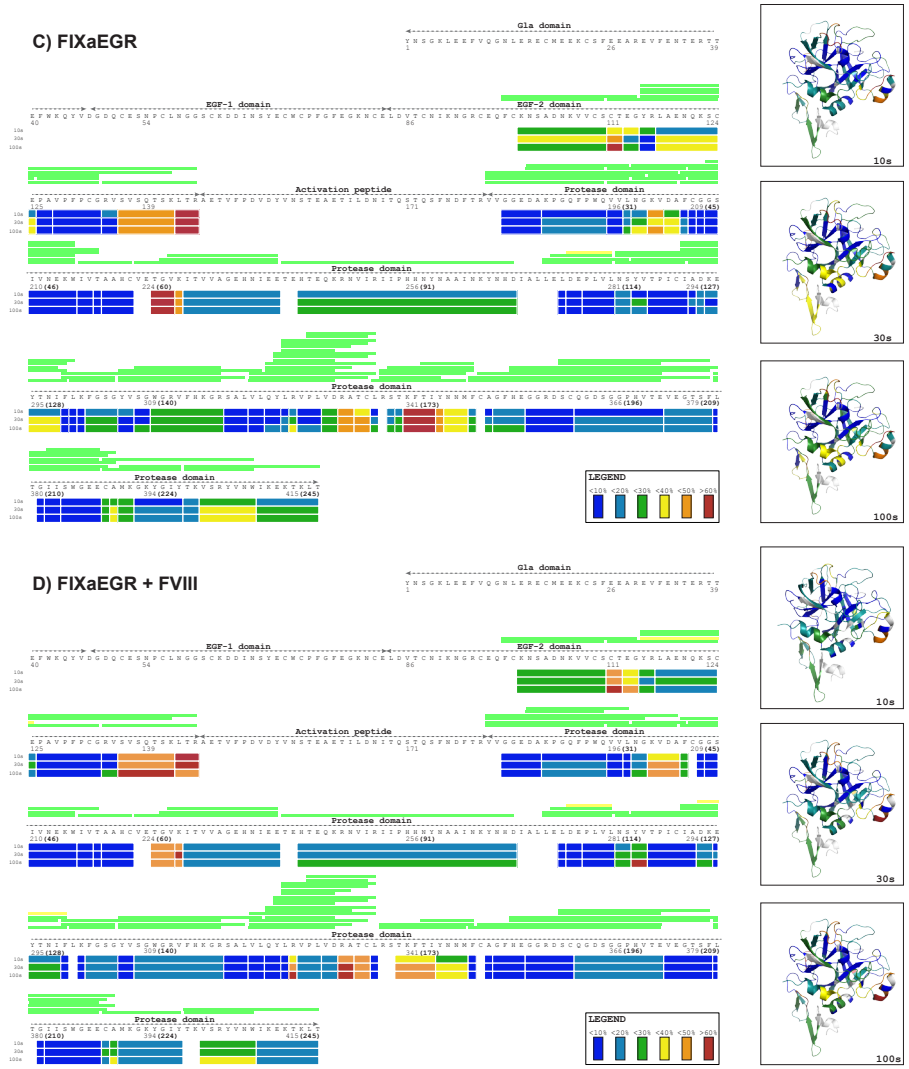
C) FIXaEGR
D) FIXaEGR + FVIII
Gla domain
EGF-1 domain
EGF-2 domain
Activation peptide
Protease domain
LEGEND
<10% <20% <30% <40% <50% >60%
10s
30s
100s

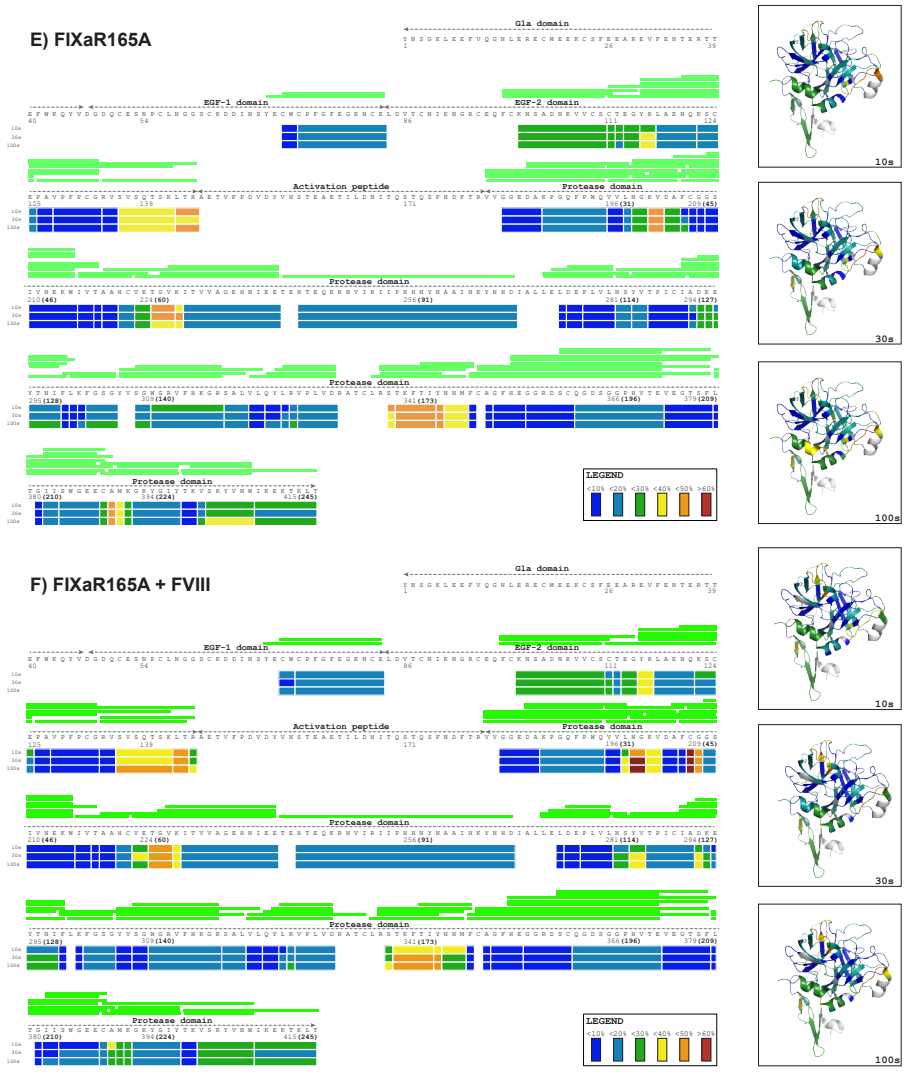


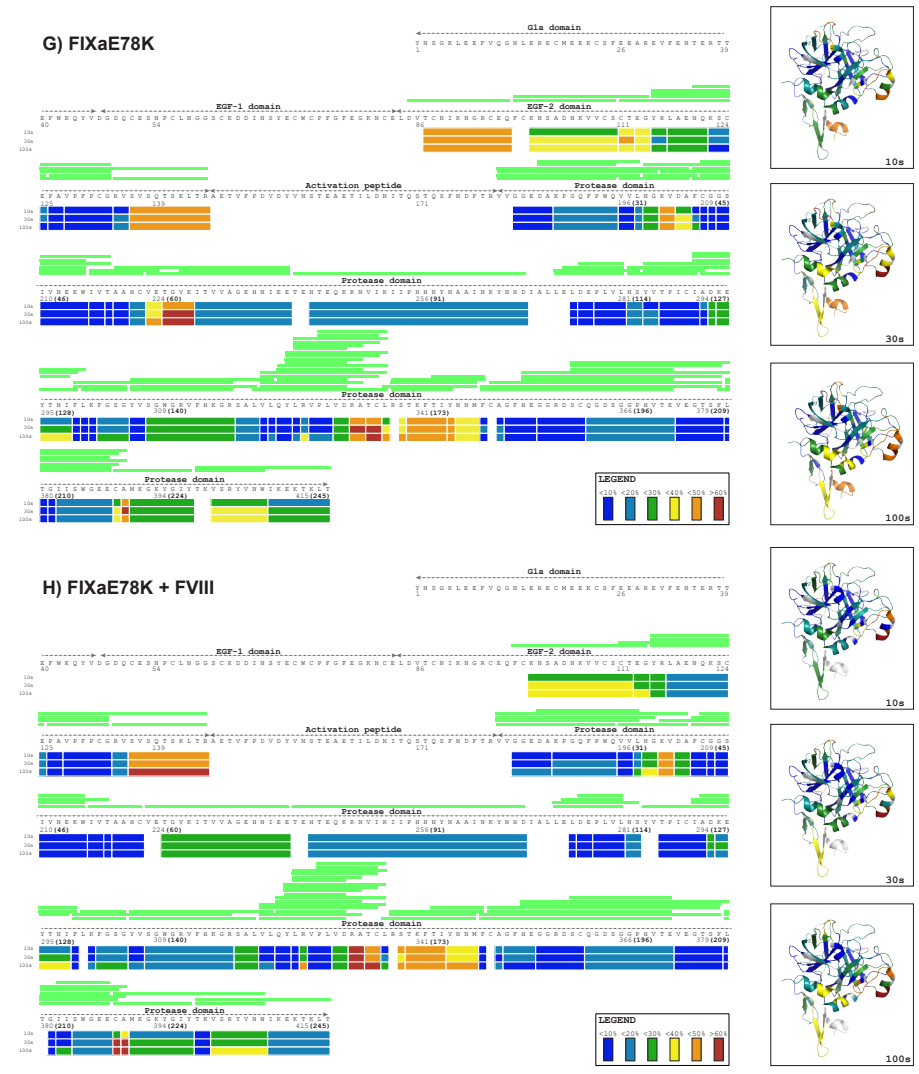


**Supplemental Figure 4.** Heat maps of Hydrogen-Deuterium eXchange studies. HDX heat maps for deuterium uptake and peptide coverage of A) FIXa, lipids and thrombin, B) FIXa in presence of FVIIIa, lipids and thrombin, C) FIXa-EGR, lipids and thrombin, D) FIXaEGR in presence of FVIIIa, lipids and thrombin, E) FIXaR333A{$165_{CT}$}, lipids and thrombin, F) FIXaR333A{$165_{CT}$} in presence of FVIIIa, lipids and thrombin, G) FIXaE78K, lipids and thrombin, H) FIXaE78K in presence of FVIII, lipids and thrombin. The deuteration level percentages are calculated with the software HDExaminer 2.2.0 (Sierra Analytics). Deuteration levels are indicated for each HDX incubation period (10, 30, 100 seconds) and mapped onto a FIXa structure (PDB: 2wpm) in the same orientation as in Figures 4, 6 and 7.

# Chapter 5

## Probing activation-driven changes in coagulation factor IX by mass spectrometry

**Nadia Freato**[1], Floris P.J. van Alphen[1] , , Mariëtte Boon- Spijker[1], Maartje van den Biggelaar[1], Alexander B. Meijer[1,2], Koen Mertens[1,3], Eduard H.T.M. Ebberink[1]

From the Department of [1]Molecular and Cellular Hemostasis, Sanquin Research, 1066 CX Amsterdam, The Netherlands, [2]Department of Biomolecular Mass Spectrometry and Proteomics, and [3]Department of Pharmaceutics and Utrecht Institute for Pharmaceutical Sciences (UIPS), Utrecht University, 3584 CG Utrecht, The Netherlands

**J Thromb Haemost, minor revision requested**

## ESSENTIALS

- Activated Factor IX (FIXa) is a poor enzyme that needs factor VIII-driven stabilization for efficient catalysis
- Mass spectrometry reveals that the protease domain of FIXa is predominantly zymogen-like
- The active conformation involves interplay between the 220-loop, N-terminus, and substrate-binding
- The full catalytic potential of FIXa requires both cofactor- and substrate-driven structural changes






## ABSTRACT

### Background

Activated factor IX (FIXa) is an inefficient enzyme that needs activated factor VIII (FVIII) for full activity. Recently, we identified a network of FVIII-driven changes in FIXa employing Hydrogen-Deuterium eXchange mass spectrometry (HDX-MS). Some changes also occurred in active-site inhibited FIXa, but others were not cofactor-driven, in particular those within the 220-loop (in chymotrypsin numbering).

### Objective

The aim of this work is to better understand the zymogen-to-enzyme transition in FIX, with specific focus on substrate-driven changes at the catalytic site.

### Methods

Footprinting mass spectrometry by HDX and Tandem-Mass Tags (TMT) labelling were used to explore changes occurring upon the conversion from FIX into FIXa. Mutagenesis and kinetic studies served to assess the role of the 220-loop.

### Results

HDX-MS displayed remarkably few differences between FIX and FIXa. In comparison with FIX, FIXa did exhibit decreased deuterium uptake at the N-terminus region. This was more prominent when the FIXa active site was occupied by an irreversible inhibitor. TMT-labelling showed that the N-terminus is largely protected from labelling, and that inhibitor binding increases protection to a minor extent. Occupation of the active site also reduced deuterium uptake within the 220-loop backbone. Mutagenesis within the 220-loop revealed that a putative H-bond network contributes to FIXa activity. TMT-labeling of the N-terminus suggested that these 220-loop variants are more zymogen-like than wild-type FIXa.

### Conclusion

In the absence of cofactor and substrate, FIXa is predominantly zymogen-like. Stabilization in its enzyme-like form involves, apart from FVIII-binding, also interplay between the 220-loop, N-terminus and the substrate binding site.

## INTRODUCTION

Factor IX (FIX) is an essential constituent of the coagulation cascade, which is characterized by the sequential conversion of inactive zymogens into active serine proteases[1,2]. Apart from FIX, other zymogens in the cascade include factor VII (FVII), factor X (FX) and prothrombin. These are the precursors of their active counterparts FIXa, FVIIa, FXa, and thrombin, respectively. As members of the chymotrypsin superfamily of serine proteases, they require limited proteolysis for activation. Proteolysis at the N-terminal region of the catalytic domain exposes a novel N-terminus, which refolds into the protease domain and thereby stabilizes the catalytic site[3–5]. The FIX zymogen circulates as a single-chain molecule. It comprises a g-carboxyglutamic acid-rich domain (Gla domain) at the N-terminus, followed by two epidermal growth factor (EGF)-like domains (EGF1 and EGF2), a glycosylated activation peptide, and the protease domain at the C-terminus[6–8]. FIX is converted into FIXa by FVIIa or activated factor XI (FXIa)[6]. Activation involves the release of the glycosylated activation peptide by two subsequent steps, at Arg145 and Arg180. This results a two-chain molecule, a light chain of amino acids 1-145 (the Gla-EGF1-EGF2 section) and a heavy chain of residues 181-415. The latter represents the serine protease domain, with Val181{$16_{CT}$} as the N-terminus (subscript CT denotes chymotrypsin numbering).

Like other serine proteases, the catalytic domain of FIX displays a dual antiparallel β-barrel architecture, in which the interface between the β-barrel domains encloses the catalytic center and the substrate recognition pockets[3,5]. Apart from these common structural elements, the β-barrels carry eight surface loops that are variable between individual serine proteases. These loops provide insertions that protrude from the protein core, and support unique, protease-specific interactions, or more general allosteric events[9]. The latter includes the 70-$loop_{CT}$, which provides a $Ca^{2+}$-binding site that plays an allosteric role in FVIIa, FIXa and FXa[10–12]. Similarly, the 220-$loop_{CT}$, together with the 180-$loop_{CT}$, comprises a $Na^{+}$-binding site that contributes to the catalytic activity of thrombin, FXa and, to a lesser extent, of FIXa[13–15]. More specific allosteric changes in these proteases are driven by assembly with their natural cofactors, such as in the tissue factor (TF)-FVIIa complex, and in the complex of FIXa with activated factor VIII (FVIIIa)[16,17].

It has been well established that FIXa displays low intrinsic activity, and needs assembly with its cofactor FVIIIa on phospholipid membranes to develop its full enzymatic potential[18,19]. Obviously, the generation of the novel N-terminus, and the putative insertion thereof into the catalytic site, is insufficient to fully activate FIX. While in chymotrypsin limited proteolysis alone seems sufficient to drive the protease domain into the fully active state, the coagulation proteases display a more complex zymogen to protease transition[20–22]. Structural information and rapid kinetics have established that thrombin, despite being fully activated in terms of proteolytic processing, can adopt both protease-like and zymogen-like forms, which are in dynamic equilibrium. This includes the distinction between “fast” and “slow” thrombin, or in more general terms, between zymogen-like enzymes and enzyme-like zymogens[23]. As for the zymogen/enzyme pair FVII/FVIIa, hydrogen/deuterium exchange mass spectrometry (HDX-MS) studies have demonstrated that FVII and FVIIa share the same solution structure, while the transition of FVIIa into a protease-like conformation is driven either by assembly with its cofactor TF, or by the incorporation of an irreversible inhibitor into the active site[17]. This raises the question as to whether FIXa, despite being proteolytically activated, could be predominantly zymogen-like, thus explaining its low enzymatic activity.

We recently explored FVIII-driven changes in FIXa by HDX-MS, and observed a variety of allosteric changes, suggesting an overall rigidification of the FIXa catalytic domain upon FVIIIa binding[16]. Cofactor-induced changes proved to overlap partially with those due to the occupation of the substrate-binding site by an active site-directed inhibitor. Moreover, occupation of the S1 pocket, but not cofactor binding, induced changes in the 220-$loop_{CT}$, reflecting a specific linkage between this loop and maturation of the active site[15,16]. While this implies that FIXa requires both active site occupation and cofactor binding to develop its full catalytic potential, it remains unclear to what extent free FIXa is enzyme- or zymogen-like. In the present paper, we address this question by comparing the FIX zymogen, FIXa and inhibitor-bound FIXa, with particular reference to the interplay between the 220-$loop_{CT}$ and the N-terminus Val181{$16_{CT}$} of the protease domain. Employing HDX-MS combined with Tandem-Mass Tags (TMT) studies, site-directed mutagenesis and functional analysis, we observed that FIXa is predominantly zymogen-like, but does display a few enzyme-like properties that are inherent to its proteolytic activation.

## MATERIALS AND METHODS

### Materials

Chromogenic substrate $CH_3SO_2$-(D)-CHG-Gly-Arg-*p*Na (Pefachrome FIXa) was obtained from Pentapharm (Aesch, Switzerland) and S-2765 containing the thrombin inhibitor I-2581 was from Chromogenix (Milano, Italy). H-Glu-Gly-Arg-chloromethylketone (EGRck) was from Bachem (Bubendorf, Switzerland). Calcium Chloride 1M solution and Deuterium Oxide 99.9% were from Sigma-Aldrich (Saint Louis, MO, USA). Ultrapure Urea, Molecular Biology grade 5M NaCl solution and Tris-HCl were from Invitrogen (Breda, The Netherlands). Chicken egg L-α-phosphatidylcholine (PC) and porcine brain L-α-phosphatidylserine (PS) were

from Avanti Polar Lipids Inc. (Alabaster, AL, USA). *N*-2 hydroxyethylpiperazine-N'-ethanesufonic acid (HEPES) was from Serva (Heidelberg, Germany). Tris(2-carboxyethyl)phosphine hydrochloride (TCEP-HCl), the TMTduplex Isobaric Tagging kit, Zeba Spin columns (7K, 0.5 mL) and chymotrypsin were from Thermo Scientific (Breda, the Netherlands). All other chemicals were from Merck (Darmstadt, Germany).

Images of crystal structures were processed in PyMol v2.4 supplied by Schrödinger (Mannheim, Germany). Peaks 7.0 software employed for peptide identification was from Bioinformatics Solution Inc. (Waterloo, Canada). Deuteration level percentages were calculated using HDeXaminer 2.2.0 software (Sierra Analytics, Modesto, CA, USA).

## Proteins used in this study

FIX variants with amino acid substitutions E387A{$217_{CT}$}, E388A{$219_{CT}$} or K394A{$224_{CT}$} were constructed by site directed mutagenesis in a pcDNA3.1(-) vector encoding wild-type FIX[24]. Mutagenesis was performed using the QuikChange kit (Agilent Technologies, Amstelveen, the Netherlands) using appropriate primers. Mutagenesis was verified by sequencing of the FIX encoding parts on the mutant plasmids. Transfection of HEK293 cells and production of recombinant FIX variants was performed essentially as described elsewhere[24]. Immunopurification using a monoclonal antibody directed against the Gla domain (CLB-FIX 11)[25], subsequent activation and quantification of recombinant FIX variants have been described elsewhere[24,26]. Human plasma-derived FIX was obtained as immunopurified concentrate (Nonafact®, Sanquin Plasma Products, Amsterdam, The Netherlands), which was further processed by hydrophobic interaction chromatography (Toyopearl-Phenyl 650M, Tosoh Bioscience, Amsterdam, The Netherlands) and concentrated by anion exchange chromatography (Q-Sepharose, GE Healthcare, Eindhoven, the Netherlands). Plasma-derived FIX was activated using FXIa. FIXa was purified from the activation mixture, and quantified by active-site titration as described[26]. Active site-inhibited FIXa (FIXaEGR) was prepared by incubation of plasma-derived FIXa (66.5 µM) with EGRck (4 mM) for 45 minutes at 37°C. Excess of EGRck was removed by anion exchange chromatography employing Q-Sepharose as outlined previously[24]. FIXaEGR was quantified by the Bradford method[27]. Purified FIX and recombinant FIX variants were stored in 20 mM HEPES (pH 7.4) 150 mM NaCl at -30°C. FIXa, FIXaEGR and FIXa variants were stored at -20°C in a buffer containing 20 mM HEPES (pH 7.4), 150 mM NaCl and 50% (v/v) glycerol.

B-domain-deleted recombinant FVIII was purified with VK34 monoclonal antibody[28] and stored at -20°C in 20 mM HEPES (pH 7.4) 800 mM NaCl, 10 mM $CaCl_2$ and 50% (v/v) glycerol. a-thrombin and FX were obtained as described[29–31]. FXIa was from Enzyme Research Laboratories (South Bend, IN, USA), and Human Serum Albumin (HSA) from Sanquin Plasma Products (Amsterdam, The Netherlands).





## Enzymatic activity of recombinant FIX variants

Activity of wild-type recombinant FIXa, FIXaE387A{$217_{CT}$}, FIXaE388A{$219_{CT}$} and FIXaK394A{$224_{CT}$} (150 nM) towards the substrate $CH_3SO_2$-(D)-CHG-Gly-Arg-*p*Na (0-5 mM) was assessed in 50 mM Tris (pH 7.4), 100 mM NaCl, 5 mM $CaCl_2$ and 0.2% HSA at 37°C as described[24]. Activity towards FX was determined in presence of phospholipids (50%PS/50%PC vesicles prepared as described[28]) and varying concentrations of FX in a buffer containing 50 mM Tris (pH 7.4), 150 mM NaCl, 10 mM $CaCl_2$ and 0.2% HSA at 37°C. FXa formation was quantified using S-2765/I-2581 as described[24]. Kinetic constants for amidolytic activity and FX activation were calculated using the Michaelis-Menten equation to obtain $K_m$ and $k_{cat}$ values.

## Hydrogen/deuterium exchange studies

Plasma-derived FIX, or FIXa, or FIXa-EGR (0.03 mM) were pre-incubated in a buffer containing 200 mM Hepes, 1500 mM NaCl and 50 mM $CaCl_2$ (pH 7.1). Proteins were then diluted 10-fold in $D_2O$ at 24°C and incubated for 10, 50, 100, 500, 10000 and 50000 seconds using an automated sampling handling robot (LEAP technologies, Morrisville, NC, USA)[32]. HDX was quenched adding an equal volume of 1.25 M TCEP-HCl, 2 M Urea (pH 2.5) at 4°C. Further processing of in-line digestion into peptides and liquid chromatography was done at 4°C. Pepsin digestion was performed by passage of the samples over a Poroszyme Immobilized Pepsin Cartridge (Thermo Scientific, Breda, The Netherlands) using isocratic flow of 0.1% formic acid with 5% acetonitrile at 100 µL/min for 5 minutes. Generated peptides were collected on an ethyl-bridged hybrid (BEH) C18 1.7 µm VanGuard pre-column (Waters, Etten-Leur, The Netherlands). Following 30 seconds of washing, the pre-column was switched in line with a Hypersil GOLD C18 analytic column (3 µm, 1 × 30 mm, Thermo Scientific, Breda, The Netherlands). Mass spectrometry analysis was performed as described[16] with the exception that peptides were separated using a 12 minutes gradient going from 8 to 40% of a mobile phase of 0.1% (v/v) formic acid in 80% (v/v) acetonitrile under a flow of 50 µL/min. Data were analyzed as described previously[16].Since relative deuterium uptake of individual peptides was compared, no back-exchange correction was performed.

## Tandem Mass Tag labelling studies

Primary amine labelling of wild-type FIXa was performed using the TMT-126 reagent, while FIXaEGR or recombinant FIXa variants were labelled by the TMT-127 reagent. Protein (0.5 µM) and TMT reagent (2.5 mM) were incubated for 7.5

minutes at 25°C in a buffer containing 20 mM HEPES (pH 7.4), 150 mM NaCl and 5 mM $CaCl_2$ in a volume of 80 µL. The reaction was quenched by incubation with 1 ml of 50% hydroxylamine for 15 min. For pairwise quantification, FIXa species labelled by TMT-126 and TMT-127 were mixed in a 1:1 molar ratio. Reduction, alkylation and proteolytic processing into peptides were performed as described elsewhere[33]. In order to quantify labelling of the N-terminus, peptides were analyzed using $MS^3$ fragmentation in an Orbitrap Fusion mass spectrometer (Thermo Scientific, Breda, The Netherlands). Peptides were separated by reversed phase liquid chromatography on a C18-column packed in-house with ReproSil-Pur C18-AQ, 1.9 µm resin (Dr. Maisch, Ammerbuch-Entringen, Germany) in a 20 cm fused silica emitter (75-360 µm inner-outer diameter, New Objective, Woburn, MA). Elution was performed by increasing solution B (0.1% Formic Acid, 80% acetonitrile) from 5% to 30% (22-132 minutes) and 30% to 60% (132-147 minutes). Peptides were sprayed into an Orbitrap Fusion mass spectrometer. Data-dependent acquisition was initiated by a full scan in the Orbitrap with 120.000 resolution power, a scan range between 400-1500 m/z, $4.0 \times 10^5$ ion count target and maximum injection time of 50 ms. The 10 most intense precursors with a charge state of 2 to 8 were sampled for $MS^2$. $MS^2$ scans were attained following collision induced dissociation (CID) at 35% collision energy and detection in the ion-trap comprising a fragment isolation window of 1.6 m/z and 60 ms maximum injection time. The 5 most intense ions were selected for subsequent $MS^3$ fragmentation to quantify the TMT labels. $MS^3$ fragmentation was performed by higher energy collision induced dissociation (HCD) at 65% collision energy and a $MS^2$ isolation width of 2 m/z. The TMT reporter groups were detected in the Orbitrap with 60000 resolution power.

## RESULTS

### HDX-MS analysis of FIX, FIXa and FIXaEGR

Initial inspection of our present HDX-MS data set revealed 93% coverage of the FIX protease domain and 16% of the light chain (Supplementary Figure 1). As observed previously, peptides from the Gla and EGF-1 domains were not recovered due to the post-translational modifications therein (i.e. γ-carboxylation and glycosylation), and thus remained beyond the scope of the study[16]. Heat maps suggested limited difference between FIX and FIXa, and an overall protection against deuterium incorporation in FIXaEGR (Supplementary Figure 1). The amendments in the HDX protocol, compared with our previous study[16], resulted in higher levels of deuterium uptake. This facilitated the comparison between FIX and its activated counterparts in the present study.

Deuterium uptake plots for all individual peptides are given in Supplementary





Figure 2 and a selection thereof is shown in Figure 1.

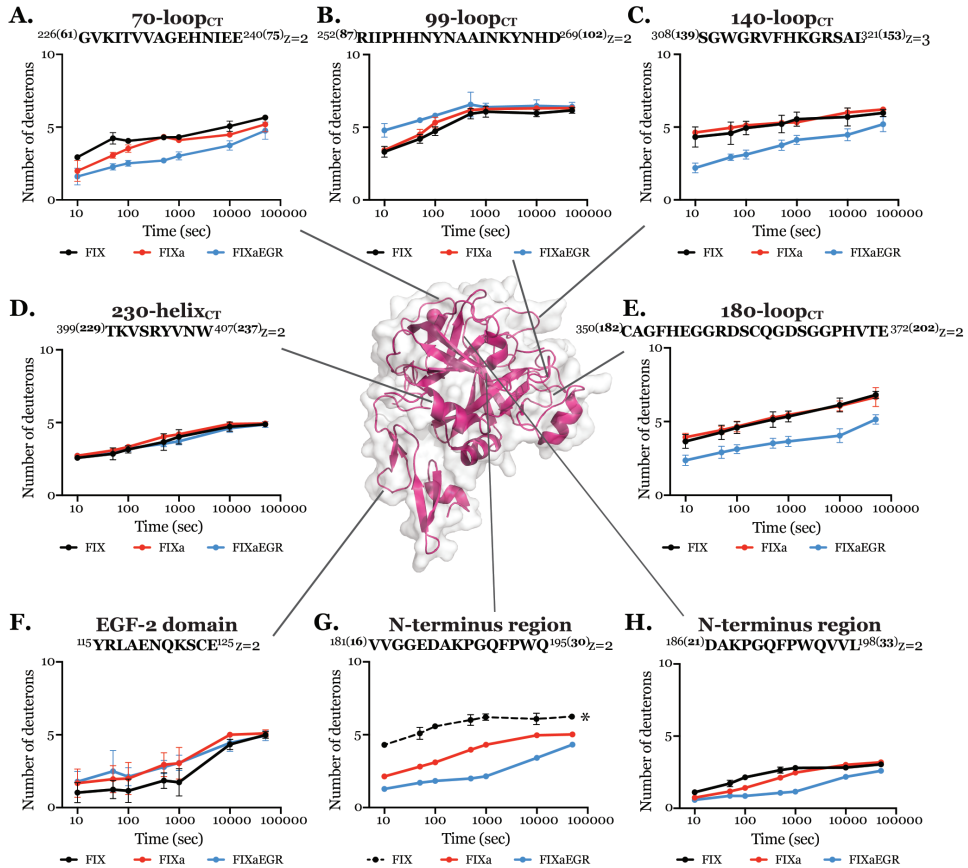


**Figure 1 – HDX-MS of FIX, FIXa and FIXaEGR**

Panels A.-H.: Examples of Hydrogen-Deuterium eXchange (HDX) plots. The peptide sequence is indicated on top of each graph with FIX numbering of the first and last residue. Chymotrypsin numbering is indicated between brackets. Each region is indicated on the crystal structure (PDB code 2wpm[48]). HDX was performed for 7 time points (from 10 to 50000 seconds) as described in Materials & Methods. FIX uptake curves are indicated in black, FIXa is indicated in red while FIXaEGR is shown in blue. Error bars represent the S.D. of 2 to 6 independent measurements. The dashed black curve marked with the asterisk in panel G represents the FIX-unique peptide TRVVGGEDAKPGQFPWQ for comparison with the N-terminal peptide VVGGEDAKPGQFPWQ, which is present in FIXa and FIXaEGR, but in FIX. See Supplementary Figure 2 for the full set of peptides and Supplementary Figure 3 for FIX unique uptake plots.

In comparison with FIXa, FIXaEGR displayed reduced deuterium incorporation in the same peptides as in our previous study[16], including the 70-$loop_{CT}$, 140-$loop_{CT}$, and 180-$loop_{CT}$ (Figure 1A,C,E). Also, the typical increase in deuterium incorporation in the 99-$loop_{CT}$ was apparent, in particular in the initial time points (Figure 1B). In contrast to FIXaEGR, FIXa and the FIX zymogen displayed similar deuterium

uptake. For the vast majority of peptides, there was no appreciable difference between peptides derived from FIX (black) and those from FIXa (red), as virtually all uptake plots were overlapping (Figure 1B,C,D,E and Supplementary Figure 2). Exceptions included the EGF-2 domain (Figure 1F), the 70-loop$_{CT}$ (Figure 1A), and the N-terminus region (Figure 1H).

Apart from the FIX-derived peptides that were shared with FIXa and FIXaEGR, some peptides were zymogen-specific, and comprised the cleavage sites Arg145-Glu146 and Arg180-Val181{16$_{CT}$} (Supplementary Figure 3). These peptides displayed a deuterium uptake of 5 Da and more, which was higher than for most of the other peptides (Figure 1). The enhanced deuterium uptake seems compatible with these cleavage sites being flexible and accessible for proteolysis. Peptides containing Val181{16$_{CT}$} were of particular interest, because they were overlapping with the N-terminal peptide Val181{16$_{CT}$}-Gln195{30$_{CT}$} that was derived from FIXa and FIXaEGR (Figure 1G). Although it remains difficult to compare peptides that are not fully identical, the deuterium uptake for the closest matching peptide Thr179-Gln195{30$_{CT}$} proved strikingly higher than its counterpart that was truncated by two amino acids due to proteolytic activation (dashed black line in Figure 1G). This suggests that the Val181{16$_{CT}$}-containing region loses flexibility upon activation, and is further rigidified by EGR incorporation into the active site (Figure 1G). Similar differences, although much less prominent, were observed in the peptide Asp186{21$_{CT}$}-Leu198{33$_{CT}$} (Figure 1H). This suggests that the changes observed in the N-terminal region are mainly due to the few amino acids surrounding the Arg180-Val181{16$_{CT}$} scissile bond.

## Tandem Mass Tag labelling of the N-terminal region

The changes at the N-terminus of the protease domain (Figure 1G) could reflect the insertion of the newly generated N-terminus into the protease domain, in particular in FIXaEGR. Since HDX accounts for backbone amide changes but not for exposure of primary amines such Lys side chains and the N-terminus, we employed TMT labelling to address this issue. Control experiments (data not shown) demonstrated that the labelling protocol resulted in > 90% labelling of surface-exposed Lys side chains such as Lys265{98$_{CT}$}, Lys316{148$_{CT}$} and Lys400{230$_{CT}$}. As for the N-terminal peptide VVGGEDAKPGQFPW, derivatives with and without TMT labels on Val181{16$_{CT}$} and/or Lys188{23$_{CT}$} were identified and m/z values of these peptide derivatives were used to reconstruct ion chromatograms. As shown in Figure 2A, these resolved four distinct derivatives, which were unlabeled (red peak), labelled on Lys188{23$_{CT}$} only (orange), on Val181{16$_{CT}$} only (black), and labelled in both positions (green). The intensity of these peaks suggested that approximately 80% of the recovered N-terminal peptides did not bear a modified N-terminus, while





approximately 20% did carry a TMT modification at Val181{16$_{CT}$}. This suggests that a predominant fraction of the N-terminus in FIXa is protected from labelling by the TMT reagent.

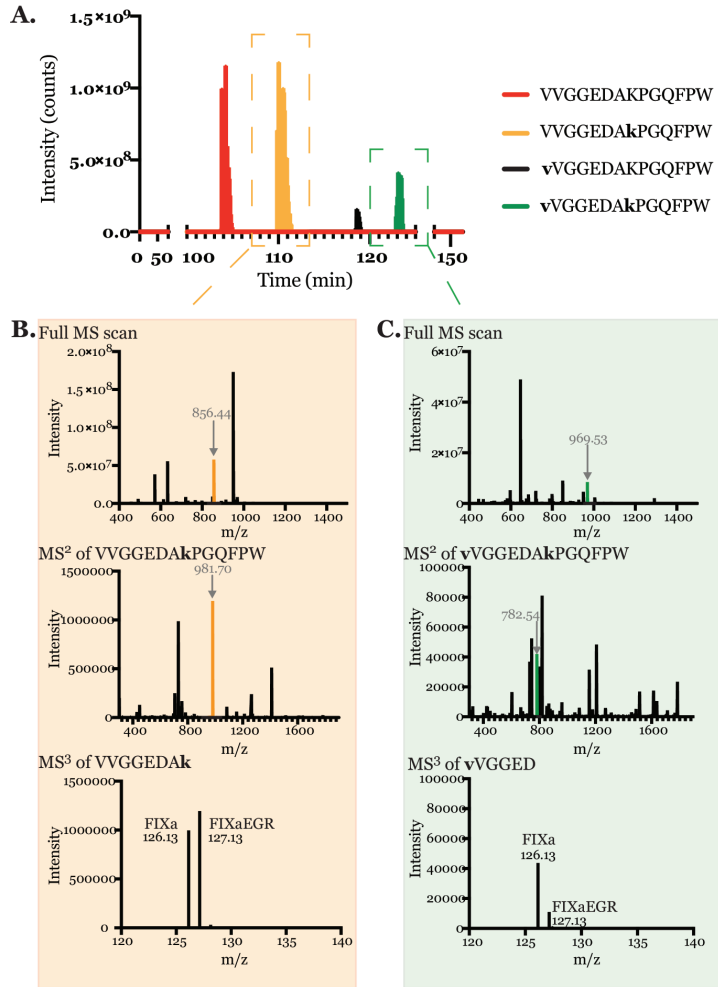


**Figure 2 – Inspection of the N-terminal fragment of the Protease domain of FIX**

A. TMT-labelling of the N-terminus of FIXa and FIXaEGR. N-terminal peptide VVGGEDAKPGQFPW derivatives with and without TMT labels on Val16$_{CT}$ and/or Lys23$_{CT}$ were identified using Peaks software and m/z values of these peptides were used to extract reconstructed ion chromatograms (RICs). RICs were extracted for N-terminal ions VVGGEDAKPGQFPW, VVGGEDA**k**PGQFPW, **v**VGGEDAKPGQFPW and **v**VGGEDA**k**PGQFPW. Small and bold **v** and **k** represent modified V and K residues carrying a Tandem Mass Tag. Peptides were identified from MS² and abundance percentages were estimated by the highest intensity values. B. VVGGEDA**k**PGQFPW peptide (m/z 856.44) was fragmented by CID; subsequently the b8 ion containing the TMT-labelled Lys23 (m/z 981.70) was subjected to MS³ by HCD to obtain the TMT intensities 126.13 and 127.13. C. The double labelled **v**VGGEDA**k**PGQFPW peptide (m/z 969.53) was fragmented by CID; subsequently the b6 ion (m/z 782.54) containing only the TMT-labelled N-terminus (Val16) was subjected to MS3 by HCD to obtain the TMT intensities 126.13 and 127.13.

The ion chromatogram shown in Figure 2A is derived from an equimolar mixture of FIXa and FIXaEGR, where each was separately labelled by a different TMT label (see methods section). This allowed for the quantitative comparison between FIXa and FIXaEGR by MS² and MS³ fragmentation (Figure 2B,C). In the fraction labelled on Lys188{23$_{CT}$} only (orange), the intensity for FIXa and FIXaEGR was similar

(Figure 2B). In contrast, the fraction labelled in both positions (green) labelling of Val181{16$_{CT}$} proved approximately four-fold less intense in FIXaEGR (Figure 2C). These data suggest that the N-terminus of the FIXa protease domain is largely protected in FIXaEGR, but also, although to a lesser extent, in non-inhibited FIXa.

## HDX-MS analysis of the 220-loop$_{CT}$

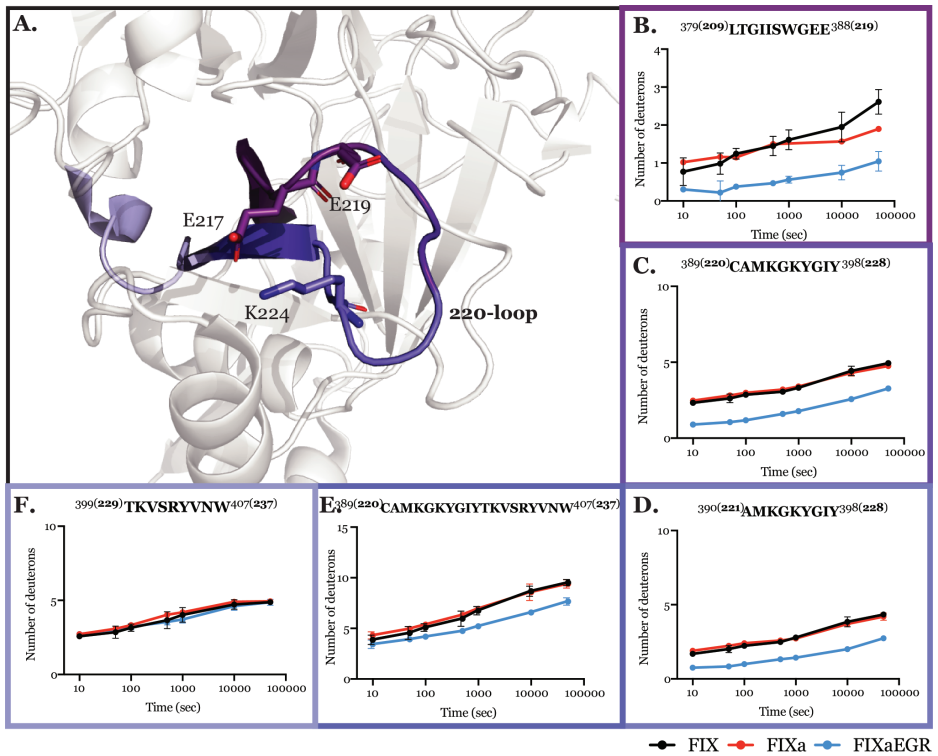


**Figure 3 – HDX-MS plots of FIX, FIXa and FIXaEGR 220-loop$_{CT}$**
A. The 220-loop$_{CT}$ region is highlighted in color gradient on the FIXa crystal structure (PDB code 2wpm[48]). Charged residues E217$_{CT}$, E219$_{CT}$ and K224$_{CT}$ are displayed in sticks representation. B.-F. HDX-MS plots of the 220-loop$_{CT}$ region are shown with FIX uptake curves indicated in black, FIXa in red and FIXaEGR in blue. Peptides are mapped in color gradient in panel A.

We previously identified the 220-loop$_{CT}$ as a section that displays protection against deuterium exchange upon active site occupation by EGR, but not by assembly with FVIIIa[16]. We therefore addressed the question whether this loop, being located at the edge of the activation pocket in FIXa[7,8] displays any changes upon zymogen activation. Interestingly however, no appreciable difference between FIX and FIXa occurred in this region (Figure 3C-F). One peptide (Figure 3B), showed slightly different time courses, but due to experimental variability these were considered as





overlapping. As anticipated, FIXaEGR displayed reduced deuterium uptake in this region. This was particularly prominent in peptides spanning residues 209-219$_{CT}$ and 220-228$_{CT}$ (Figure 3B,C), and decreased upon extension towards the C-terminus (Figure 3E,F). This pinpoints the protection against deuterium uptake in FIXaEGR to the 220-loop$_{CT}$ and its immediately preceding β-sheet (Figure 3A). Apparently, filling the substrate binding pocket with EGR strongly reduces the flexibility of this part of the protein backbone, while non-inhibited FIXa remains indistinguishable from the FIX zymogen in this section.

## Characterization of 220-loop$_{CT}$ variants

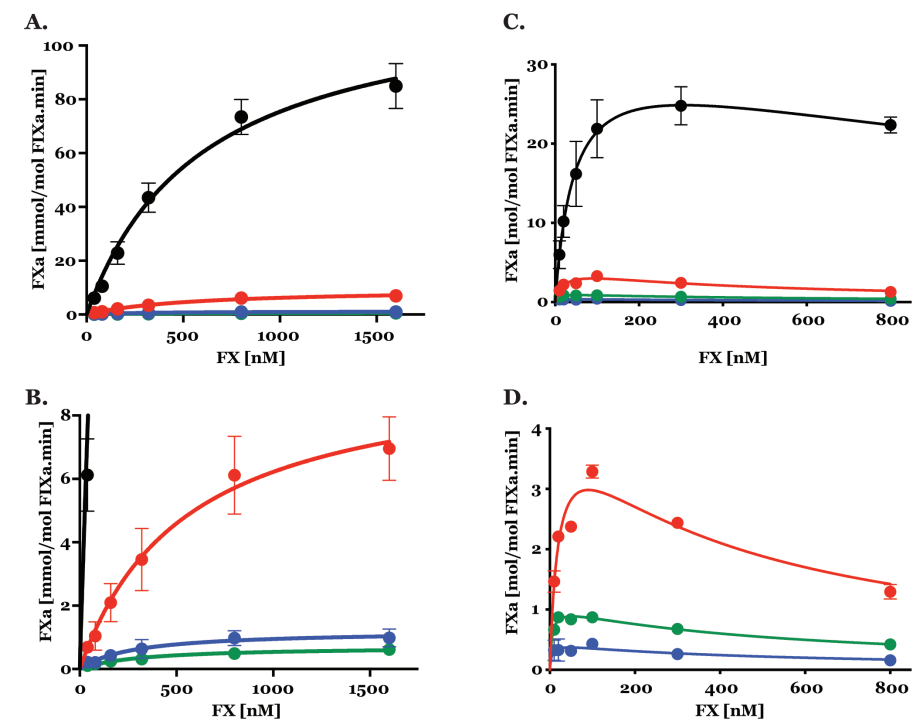


**Figure 4 – Kinetics of FIXa 220-loop variants FIXaE217A$_{CT}$, FIXaE219A$_{CT}$ and FIXaK224A$_{CT}$**
A. FX was converted to FXa in the absence of FVIIIa by 30 nM of wild-type FIXa (black) or FIXa variants FIXaE219A$_{CT}$ (red), FIXaE217A$_{CT}$ (blue), FIXaK224A$_{CT}$ (green). B. Zoom of FIXaE219A$_{CT}$ (red), FIXaE217A$_{CT}$ (blue), FIXaK224A$_{CT}$ (green) kinetics in the absence of FVIIIa. C. FX activation by 0.3 nM of wild-type FIXa (black), FIXaE219A$_{CT}$ (red), FIXaE217A$_{CT}$ (blue), FIXaK224A$_{CT}$ (green) in presence of FVIIIa (0.35 nM). D. Close-up of FIXaE219A$_{CT}$ (red), FIXaE217A$_{CT}$ (blue), FIXaK224A$_{CT}$ (green) kinetics in the presence of FVIIIa. Experimental conditions are described in Materials and Methods.

With regard to the 209-228$_{CT}$ segment, it is interesting to note that this region has previously been observed to be affected by FIX zymogen to enzyme conversion[15].

It further comprises a H-bond network wherein the side chain of Lys394{$224_{CT}$} contacts the carboxylate groups of E387{$217_{CT}$} and E388{$219_{CT}$}[15] (see Figure 3A). To assess the role of this putative stabilizing network, we produced the recombinant FIXa variants FIXaE387A{$217_{CT}$}, FIXaE388A{$219_{CT}$} and FIXaK394A{$224_{CT}$}. All three substitutions had a major detrimental effect on FIXa activity (Figure 4). Residual amidolytic activity towards the synthetic substrate $CH_3SO_2$-(D)-CHG-Gly-Arg-*p*Na (Table 1) was similar for FIXaE387A{$217_{CT}$} and FIXaK394A{$224_{CT}$}, and was mainly due a reduction of $k_{cat}$ (Table 1). For FIXaE388A{$219_{CT}$} $k_{cat}$ was slightly less affected, but still 5-fold lower compared to that of wild-type FIXa. In the absence of FVIIIa, FX activation by FIXaE387A{$217_{CT}$} and FIXaK394A{$224_{CT}$} again proved equally affected (Figure 4A,B and Table 1). The same was observed in the presence of FVIIIa (Figure 4C,D, Table 1). The FIXaE388A{$219_{CT}$} variant differed from the other two in that its defect was less severe. These data suggest that disruption of the putative H-bond network does reduce enzymatic activity. The observation that FIXaE387A{$217_{CT}$} and FIXaK394A{$224_{CT}$} are virtually indistinguishable seems compatible with disruption of a direct interaction between these residues that greatly contributes to FIXa enzymatic activity.

**Table 1 – Kinetic properties of 220-loop$_{CT}$ mutants**

| | Amidolytic activity | | FX activation (in absence of FVIIIa) | | FX activation (in presence of FVIIIa) | |
|---|---|---|---|---|---|---|
| | $K_m$ (mM) | $k_{cat}$ ($min^{-1}$) | $K_{m,app}$ (mM) | $k_{cat,app} \times 10^{-3}$ ($min^{-1}$) | $K_{m,app}$ (nM) | $k_{cat,app}$ ($min^{-1}$) |
| **FIXa wild-type** | 2.0 ± 0.3 | 66.7 ± 4 | 0.6 ± 0.1 | 121 ± 8 | 35 ± 7 | 28 ± 2 |
| **FIXaE217A$_{CT}$** | 1.6 ± 0.4 | 5.3 ± 0.6 | 0.3 ± 0.1 | 1.2 ± 0.2 | nd[a] | 0.4 ± 0.1 |
| **FIXaE219A$_{CT}$** | 3.1 ± 0.5 | 13.3 ± 1 | 0.6 ± 0.1 | 10 ± 1 | nd[a] | 4.2 ± 1.2 |
| **FIXaK224A$_{CT}$** | 2.0 ± 0.7 | 5.3 ± 0.7 | 0.3 ± 0.1 | 0.7 ± 0.1 | nd[a] | 0.9 ± 0.1 |

[a] The $K_{m,app}$ could not be determined (nd) due to substrate inhibition.

**Table 1**
Kinetic constants of the FIXa variants for hydrolysis of $CH_3SO_2$-(D)-CHG-Gly-Arg-*p*Na (indicated as amidolytic activity) and of the natural substrate FX in absence and presence of FVIIIa. Experimental conditions are given in Materials and Methods. Curves for FX activation studies are shown in Figure 4.

The prominent reduction of FIXa activity in these molecular variants raises the possibility that destabilization of the 220-loop$_{CT}$ drives the catalytic domain into a more zymogen-like form. This possibility was addressed by the same TMT labelling method as used for comparing FIXa and FIXaEGR (Figure 2). Pairwise comparison





of mutant and wild-type FIXa is shown in Figure 5.

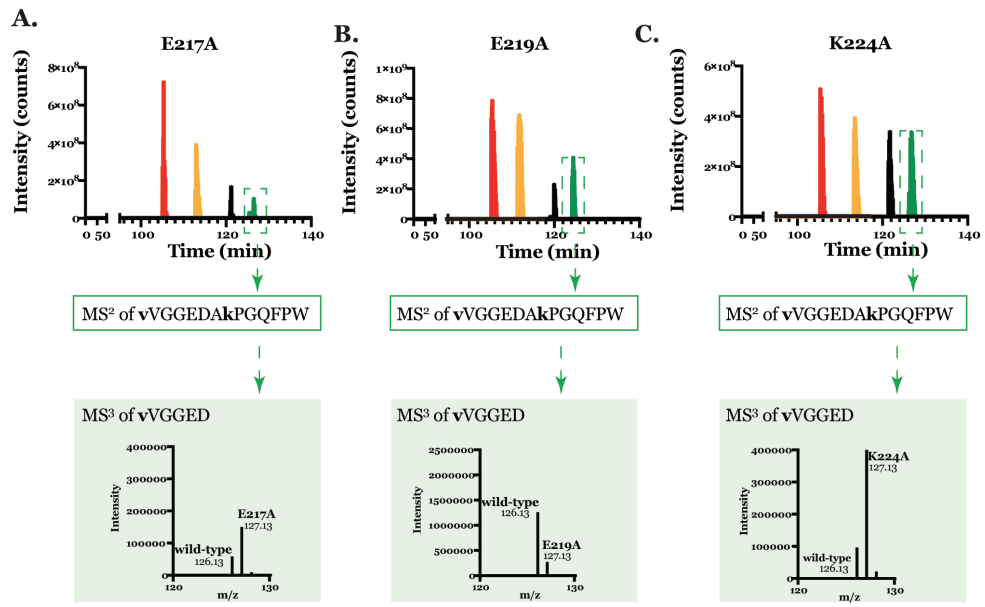


**Figure 5 – Labelling of the N-terminal segment of the Protease domain of FIXa variants**
TMT-labelling of the N-terminus of A) FIXaE217A$_{CT}$, B) FIXaE219A$_{CT}$, C) FIXaK224A$_{CT}$. After TMT-labelling and proteolytic digestion, reconstructed ion chromatograms (RICs) were extracted for N-terminal ions VVGGEDAKPGQFPW (red), VVGGEDA**k**PGQFPW (yellow), **v**VGGEDAKPGQFPW (black) and **v**VGGEDA**k**PGQFPW (green). These peptides were identified from MS² spectra (CID) employing Peaks Studio software. Abundance percentages of the fractions with unlabeled Val16$_{CT}$ were estimated and compared to the labelled Val16$_{CT}$ fractions. A representative TMT quantification spectrum is shown for the b6 ion **v**VGGED for each FIXa variant.

The reconstructed ion chromatograms (Figure 5A,B,C) show that the N-terminal peptide VVGGEDAKPGQFPW was mainly recovered as non-labelled (red) or labelled on Lys188{$23_{CT}$} only (orange). The fractions carrying the label on the N-terminus Val181{$16_{CT}$} only (black) or on both Val181{$16_{CT}$} and Lys188{$23_{CT}$} (green in Figure 5A) appeared more abundant than observed for wild-type FIXa (Figure 2), in particular for the variant FIXaK394A{$224_{CT}$}. Because these data represent equimolar mixtures of wild-type and mutant FIXa, it remains difficult to derive quantitative information directly from these chromatograms, however. Therefore, MS² and MS³ fragmentation was used for further quantification based on the TMT labels. Analysis of the fraction that was labelled on both Val181{$16_{CT}$} and Lys188{$23_{CT}$} (green peaks in Figure 5A) showed that N-terminus labelling in FIXaE387A{$217_{CT}$} and FIXaK394A{$224_{CT}$} was 4-8 fold more prominent than in wild-type FIXa, while labelling was slightly reduced in FIXaE388A{$219_{CT}$} (Figure 5B). These data suggest that the 220-loop$_{CT}$ variants are similar to wild-type FIXa in that their N-terminus is

largely protected against TMT-labelling. However, the extent of protection is lower in FIXaE387A{$217_{CT}$} and FIXaK394A{$224_{CT}$}, which seems compatible with these variants being more zymogen-like. This was not apparent for FIXaE388A{$219_{CT}$}, which displayed a less severe enzymatic defect than the other two variants (Table 1).

## DISCUSSION

During the past five decades, numerous studies have advanced our understanding of the zymogen to enzyme transition within the class of chymotrypsin-like serine proteases. In the 1970s, crystallographic studies have established that chymotrypsinogen and trypsinogen are very similar to their enzyme counterparts, except for a few sections that are disordered in the zymogens. These include some specific surface loops that comprise the 'activation domain' and the position of the N-terminal section which, once cleaved at the Arg15-Ile16 bond, inserts into the catalytic region and stabilizes the catalytic pocket[34–36]. At the same time, however, it has been recognized that zymogens may display low enzymatic activity towards small substrates and active site-directed inhibitors[37,38]. Since then numerous studies have provided evidence that the classical distinction between inactive zymogens and active zymogens is no longer tenable. For instance, tissue-type plasminogen activator displays substantial proteolytic activity in its single-chain form, while lacking the novel N-terminus that has been regarded as a hallmark of serine protease activation[39]. Similarly, prothrombin can be activated by binding to the bacterial protein staphylocoagulase, thus providing an example of ligand-induced zymogen activation, independent of limited proteolysis[31,40]. On the other hand, enzymes such as FVIIa and FIXa, despite being processed at the appropriate cleavage sites, display low enzymatic activity in the absence of their cofactors and thus may seem predominantly zymogen-like. More recently, numerous studies addressing the prothrombin/thrombin pair have established that the classical zymogen/enzyme distinction is blurred by the existence of zymogen-like proteases and protease-like zymogens[23], or, by an equilibrium between closed ('collapsed') and open zymogen (Z* or Z) and enzyme (E* and E) forms[41].

For the FIX zymogen, no crystal structure is available to facilitate comparison with FIXa. By computational techniques, a model for the zymogen has been derived that predicts a substantial orientational change in the catalytic domain, and the exposure of a largely hydrophobic surface upon release of the activation peptide[42]. In this regard, it seems remarkable that our HDX-MS data indicate that on the backbone level the solution structures of FIX and FIXa are nearly indistinguishable, even in peptides that represent the typical 'activation loops'[23], such as the 140-, 180- and 220-loops$_{CT}$ (Figures 1, 3 and Supplementary Figure 2). The few differences that did





occur relate to zymogen-specific peptides spanning the scissile bonds at Arg145 and Arg180, and therefore were anticipated (Supplemental Figure 3). One difference was observed in a peptide from the EGF-2 domain (Figure 1F), wherein the zymogen displayed lower deuterium incorporation. We cannot exclude that FIXa differs from FIX in additional sites in the FIXa light chain, because peptides from the Gla-EGF-1 section were not recovered in our protocol. In this regard it seems of interest that the activation intermediate FIXα, in which only cleavage at Arg145 has occurred, binds to FVIII and displays amidolytic activity, despite the 180-181 scissile bond being intact and the activation peptide still being attached[26]. As such, this FIX derivative may represent an enzyme-like zymogen with the light chain of the FIXa enzyme and the heavy chain of the FIX zymogen. Proteolytic activity, however, remains fully dependent on the cleavage at Arg180, and the generation of the new terminus Val181{$16_{CT}$}[26]. Our present study shows that this cleavage event is accompanied by a reduction in deuterium uptake (Figure 1G) and substantial protection of the N-terminus from labelling (Figure 2).

We previously observed that the 220-loop$_{CT}$ displays reduced deuterium uptake that is not driven by FVIIIa, but by occupancy of the active site[16]. This loop is of particular interest because it is immediately following the region 215-217, which is collapsed in the closed Z* and E* conformations and open in enzyme-like Z and E structures[41]. A putative H-bond network herein has been identified that could stabilize the 220-loop$_{CT}$, involving the side chains of E387{$217_{CT}$}, E388{$219_{CT}$}, and Lys394{$224_{CT}$} (see Figure 3A)[15]. Inspection of 23 available FIXa crystal structures (data not shown) reveals that in all structures the side chains of E387{$217_{CT}$} and Lys394{$224_{CT}$} are sufficiently close (3-4 Å) to support a salt bridge between these two residues. This is supported by our mutagenesis study, which indicates that replacement of either of the two by Ala results in dysfunctional FIXa molecules with an identical phenotype (Figure 4, Table 1). These mutants further displayed an increase in N-terminus labelling (Figure 5), which could be compatible with a more zymogen-like state of these FIXa variants compared to wild-type FIXa. Interestingly, the hemophilia B database contains multiple substitutions in these positions, underlining that disruption of this salt bridge is indeed disease-associated[43].

While substitution of E388{$219_{CT}$} resulted in a less severe phenotype, its defect still is compatible with a major role within the 220-loop$_{CT}$ of FIXa (Figure 4, Table 1). Figure 6 shows two examples from available FIXa structures that indicate that E388{$219_{CT}$} may not participate in the putative H-bond network that has been identified in the structure of FIXa with *p*-aminobenzamidine in the active site[15]. Instead, in structures containing EGR-derived inhibitors, the backbone carbonyl group of E388{$219_{CT}$} interacts with the substrate P1Arg, while its side chain seems to be pulled away from E387{$217_{CT}$} (Figure 6A). A similar position of E388{$219_{CT}$} is

seen in the structure of FIXa stabilized by a synthetic inhibitor that binds beyond the active site (Figure 6B). The dysfunction of the E388A{$219_{CT}$} variant suggests that Ala in this position disturbs the stabilization of the P1Arg-binding pocket, possibly due to a backbone rearrangement within this part of the 220-$loop_{CT}$. It is of interest that, except for FIXa, other serine proteases have Gly in position $219_{CT}$, suggesting that this particular S1-site geometry may be unique for FIXa[44]. It seems conceivable that conformational plasticity of the 220-$loop_{CT}$ allows for multiple conformations of E388{$219_{CT}$} that switch FIXa between free and substrate-bound states during substrate cleavage and subsequent product release, and as such maintains the catalytic cycle.

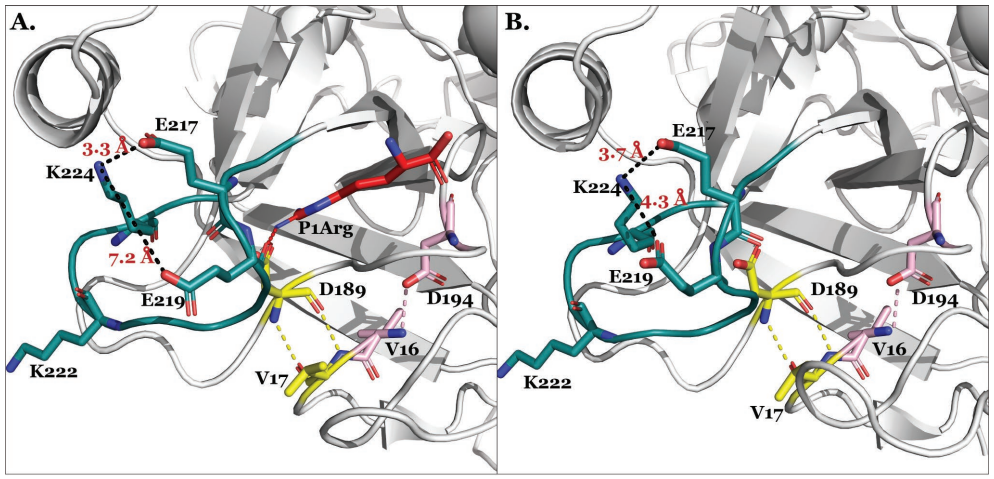


**Figure 6 – Putative network between the 220-loop residues and the N-terminus**
A. Upon occupation of the active site, the interaction of the $E219_{CT}$ carbonyl group with the substrate P1Arg occurs and the distance with $K224_{CT}$ appears to increase (≈7.2 Å, PDB code 2wpm[48]) while $V17_{CT}$ in the N-terminal segment pairs with $D189_{CT}$ that takes further contact with the P1Arg. This suggests that the occupation of the S1 pocket drives the substantial interactions that stabilize the active configuration of FIXa. B. These interactions, however, seem to be missing in absence of a substrate in the S1 pocket and $E219_{CT}$ appears to take a closer contact (distance ≈ 4.3 Å; PDB code 4yzu[49]) with $K224_{CT}$.

One might question whether related coagulation enzymes display a zymogen-like structure similar to FIXa. In this regard the FVII(a) zymogen/enzyme pair is the best documented example. HDX-MS studies have provided ample evidence that FVIIa retains zymogen-like properties following limited proteolysis, and does not spontaneously rearrange onto the active configuration[17,45]. This requires assembly of FVIIa with its cofactor TF, which drives the insertion of the N-terminus into the bottom of the S1-pocket and the rigidification of several surface loops, including the 220-$loop_{CT}$, referred to as activation loop 3[17]. While our HDX-MS data suggest that FVIIa and FIXa both display an overall zymogen-like structure, there are also





differences suggesting that the transition into enzyme in FIXa may be more complex. First, the apparent rigidification at the N-terminus and the 220-$loop_{CT}$, which are driven by TF in FVIIa[17], are largely EGR-driven in FIXa (Figures 1 and 2) with limited contribution by FVIII[16]. Apparently, full activation of FIXa is driven by both cofactor and substrate. This may also be reflected by the effect of cofactor binding on amidolytic activity: while TF increases FVIIa activity substantially[46], assembly with FVIIIa has little or no effect on cleavage of peptide substrates by FIXa[47]. Another difference is that in FVIIa the 220-$loop_{CT}$ contains no acidic and basic residues as in FIXa[17,44]. Thus, FVIIa may lack the putative H-bond network, with its concomitant effect on N-terminus insertion in FIXa (Figure 6). A difference in structural plasticity between FVIIa and FIXa in this region may explain why its rigidification is not cofactor-driven in FIXa, but apparently requires occupation of the ArgP1-site by the pseudo-substrate EGR.

From a regulatory perspective, it might be beneficial that enzymes in the initial phase of coagulation are zymogen-like, and remain strictly cofactor-dependent for their transition into fully competent enzymes. As for FIXa, the dependence on both FVIIIa and active site occupation may represent a dual brake on FIXa function. This would limit the risk of premature FX activation, and subsequent amplification thereof downstream in the cascade, thereby reducing the risk of excessive thrombin formation and disruption of the intricate balance between bleeding and thrombosis.

## AUTHOR CONTRIBUTION

NF, ABM, MvdB, KM and EHTME, designed the study; NF, MBS and EHTME performed the experimental work; FPJvA helped with the development of Mass Spectrometry experiments; NF, ABM, MvdB, KM and EHTME analysed and interpreted data; NF and EHTME made the figures; NF, ABM, MvdB, KM and EHTME wrote the manuscript.

## DECLARATIONS OF INTERESTS

The authors declare no conflict of interest.

## ACKNOWLEDGEMENTS

This study has been funded by the Utrecht Institute for Pharmaceutical Sciences (UIPS) and by the Landsteiner Stichting voor Bloedtransfusie Research (LSBR 1417).

## REFERENCES


1. Davidson CJ, Hirt RP, Lal K, Snell P, Elgar G, Tuddenham EGD, et al. Molecular evolution of the vertebrate blood coagulation network. Thromb. Haemost. 2003;89:420–8.

2. Davie EW, Fujikawa K, Kisiel W. The coagulation cascade: initiation, maintenance, and regulation. Biochemistry 1991;30:10363–70.

3. Page MJ, Di Cera E. Serine peptidases: classification, structure and function. Cell. Mol. Life Sci. CMLS 2008;65:1220–36.

4. Rawlings ND, Barrett AJ. Families of serine peptidases. Methods Enzymol. 1994;244:19–61.

5. Hedstrom L. Serine protease mechanism and specificity. Chem. Rev. 2002;102:4501–24.

6. Schmidt AE, Bajaj SP. Structure-function relationships in factor IX and factor IXa. Trends Cardiovasc Med 2003;13:39–45.

7. Brandstetter H, Bauer M, Huber R, Lollar P, Bode W. X-ray structure of clotting factor IXa: active site and module structure related to Xase activity and hemophilia B. Proc Natl Acad Sci U A 1995;92:9796–9800.

8. Hopfner KP, Lang A, Karcher A, Sichler K, Kopetzki E, Brandstetter H, et al. Coagulation factor IXa: the relaxed conformation of Tyr99 blocks substrate binding. Structure 1999;7:989–996.

9. Goettig P, Brandstetter H, Magdolen V. Surface loops of trypsin-like serine proteases as determinants of function. Biochimie 2019;166:52–76.

10. Bjelke JR, Olsen OH, Fodje M, Svensson LA, Bang S, Bolt G, et al. Mechanism of the $Ca^{2+}$-induced enhancement of the intrinsic factor VIIa activity. J. Biol. Chem. 2008;283:25863–70.

11. Rezaie AR, Esmon CT. Asp-70-->Lys mutant of factor X lacks high affinity Ca2+ binding site yet retains function. J. Biol. Chem. 1994;269:21495–9.

12. Mathur A, Zhong D, Sabharwal AK, Smith KJ, Bajaj SP. Interaction of Factor IXa with Factor VIIIa. Effects of protease domain Ca2+ binding site, proteolysis in the autolysis loop, phospholipid, and Factor X. J Biol Chem 1997;272:23418–23426.

13. Pineda AO, Carrell CJ, Bush LA, Prasad S, Caccia S, Chen Z-W, et al. Molecular dissection of Na+ binding to thrombin. J. Biol. Chem. 2004;279:31842–53.

14. Underwood MC, Zhong D, Mathur A, Heyduk T, Bajaj SP. Thermodynamic linkage between the S1 site, the Na+ site, and the Ca2+ site in the protease domain of human coagulation factor Xa. Studies on catalytic efficiency and inhibitor binding. J. Biol. Chem. 2000;275:36876–84.

15. Schmidt AE, Stewart JE, Mathur A, Krishnaswamy S, Bajaj SP. $Na^{+}$ site in blood coagulation factor IXa: effect on catalysis and factor VIIIa binding. J Mol Biol 2005;350:78–91.

16. Freato N, Ebberink EHTM, van Galen J, Fribourg C, Boon-Spijker M, van Alphen F, et al. Factor VIII-driven changes in activated Factor IX explored by Hydrogen-Deuterium eXchange Mass Spectrometry. Blood 2020;blood.2020005593.

17. Rand KD, Jørgensen TJD, Olsen OH, Persson E, Jensen ON, Stennicke HR, et al. Allosteric Activation of Coagulation Factor VIIa Visualized by Hydrogen Exchange. J. Biol. Chem. 2006;281:23018–24.

18. Mertens K, van Wijngaarden A, Bertina RM. The role of factor VIII in the activation of human blood coagulation factor X by activated factor IX. Thromb. Haemost. 1985;54:654–60.

19. van Dieijen G, Tans G, Rosing J, Hemker HC. The role of phospholipid and factor VIIIa in the activation of bovine factor X. J Biol Chem 1981;256:3433–3442.

20. Lechtenberg BC, Freund SMV, Huntington JA. An ensemble view of thrombin allostery. Biol. Chem. 2012;393:889–98.

21. Krishnaswamy S. The transition of prothrombin to thrombin. J. Thromb. Haemost. 2013;265–76.

22. Vogt AD, Chakraborty P, Di Cera E. Kinetic dissection of the pre-existing conformational equilibrium in the trypsin fold. J. Biol. Chem. 2015;290:22435–45.

23. Huntington JA. Slow thrombin is zymogen-like. J. Thromb. Haemost. 2009;7 Suppl 1(S1STATE):159–64.

24. Fribourg C, Meijer AB, Mertens K. The interface between the EGF2 domain and the protease domain in blood coagulation factor IX contributes to factor VIII binding and factor X activation. Biochemistry 2006;45:10777–10785.

25. Christophe OD, Lenting PJ, Cherel G, Boon-Spijker M, Lavergne JM, Boertjes R, et al. Functional mapping of anti-factor IX inhibitors developed in patients with severe hemophilia B. Blood 2001;98:1416–23.

26. Lenting PJ, Ter Maat H, Clijsters PPFM, Donath MJSH, Van Mourik JA, Mertens K. Cleavage at arginine 145 in human blood coagulation factor IX converts the zymogen into a factor VIII binding enzyme. J. Biol. Chem. 1995;

27. Bradford MM. A rapid and sensitive method for the quantitation of microgram quantities of protein utilizing the principle of protein-dye binding. Anal. Biochem. 1976;72:248–54.

28. Meems H, van den Biggelaar M, Rondaij M, van der Zwaan C, Mertens K, Meijer AB. C1 domain residues Lys 2092 and Phe 2093 are of major importance for the endocytic uptake of coagulation factor VIII. Int. J. Biochem. Cell Biol. 2011;43:1114–21.

29. Mertens K, Bertina RM. Activation of human coagulation factor VIII by activated factor X, the common product of the intrinsic and the extrinsic pathway of blood coagulation. Thromb. Haemost. 1982;47:96–100.

30. Mertens K, Bertina RM. Pathways in the activation of human coagulation factor X. Biochem. J. 1980;185:647–58.

31. Hendrix H, Lindhout T, Mertens K, Engels W, Hemker HC. Activation of human prothrombin by stoichiometric levels of staphylocoagulase. J. Biol. Chem. 1983;258:3637–44.

32. Andersen MD, Faber JH. Structural characterization of both the non-proteolytic and proteolytic activation pathways of coagulation Factor XIII studied by hydrogen–deuterium exchange mass spectrometry. Int. J. Mass Spectrom. 2011;302:139–48.

33. Bloem E, Ebberink EH, van den Biggelaar M, van der Zwaan C, Mertens K, Meijer AB. A novel chemical footprinting approach identifies critical lysine residues involved in the binding of receptor-associated protein to cluster II of LDL receptor-related protein. Biochem J 2015;468:65–72.

34. Freer ST, Kraut J, Robertus JD, Wright HT, Xuong NH. Chymotrypsinogen: 2.5-angstrom crystal structure, comparison with alpha-chymotrypsin, and implications for zymogen activation. Biochemistry 1970;9:1997–2009.

35. Bode W, Huber R. Induction of the bovine trypsinogen-trypsin transition by peptides sequentially similar to the N-terminus of trypsin. FEBS Lett. 1976;68:231–236.

36. Bode W, Schwager P, Huber R. The transition of bovine trypsinogen to a trypsin-like state upon strong ligand binding. J. Mol. Biol. 1978;118:99–112.

37. Morgan PH, Robinson NC, Walsh KA, Neurath H. Inactivation of bovine trypsinogen and chymotrypsinogen by diisopropylphosphorofluoridate. Proc. Natl. Acad. Sci. U. S. A. 1972;69:3312–6.

38. Neurath H, Walsh KA. Role of proteolytic enzymes in biological regulation (a review). Proc. Natl. Acad. Sci. U. S. A. 1976;73:3825–32.

39. Rijken DC, Hoylaerts M, Collen D. Fibrinolytic properties of one-chain and two-chain human extrinsic (tissue-type) plasminogen activator. J. Biol. Chem. 1982;

40. Friedrich R, Panizzi P, Fuentes-Prior P, Richter K, Verhamme I, Anderson PJ, et al. Staphylocoagulase is a prototype for the mechanism of cofactor-induced zymogen activation. Nature 2003;425:535–9.

41. Gohara DW, Di Cera E. Allostery in trypsin-like proteases suggests new therapeutic strategies. Trends Biotechnol 2011;29:577–585.

42. Perera L, Darden TA, Pedersen LG. Modeling human zymogen factor IX. Thromb

Haemost 2001;85:596–603.

43. Rallapalli PM, Kemball-Cook G, Tuddenham EG, Gomez K, Perkins SJ. An interactive mutation database for human coagulation factor IX provides novel insights into the phenotypes and genetics of hemophilia B. J Thromb Haemost 2013;11:1329–1340.

44. Hopfner KP, Brandstetter H, Karcher A, Kopetzki E, Huber R, Engh RA, et al. Converting blood coagulation factor IXa into factor Xa: dramatic increase in amidolytic activity identifies important active site determinants. EMBO J 1997;16:6626–6635.

45. Song H, Olsen OH, Persson E, Rand KD. Sites involved in intra- and interdomain allostery associated with the activation of factor VIIa pinpointed by hydrogen-deuterium exchange and electron transfer dissociation mass spectrometry. J. Biol. Chem. 2014;289:35388–96.

46. Krishnaswamy S. The interaction of human factor VIIa with tissue factor. J. Biol. Chem. 1992;267:23696–706.

47. Hsu YC, Hamaguchi N, Chang YJ, Lin SW. The distinct roles that Gln-192 and Glu-217 of factor IX play in selectivity for macromolecular substrates and inhibitors. Biochemistry 2001;40:11261–9.

48. Zogg T, Brandstetter H. Structural basis of the cofactor- and substrate-assisted activation of human coagulation factor IXa. Structure 2009;17:1669–1678.

49. Parker Jr. DL, Walsh S, Li B, Kim E, Sharipour A, Smith C, et al. Rapid development of two factor IXa inhibitors from hit to lead. Bioorg Med Chem Lett 2015;25:2321–2325.





# SUPPLEMENTARY FIGURES

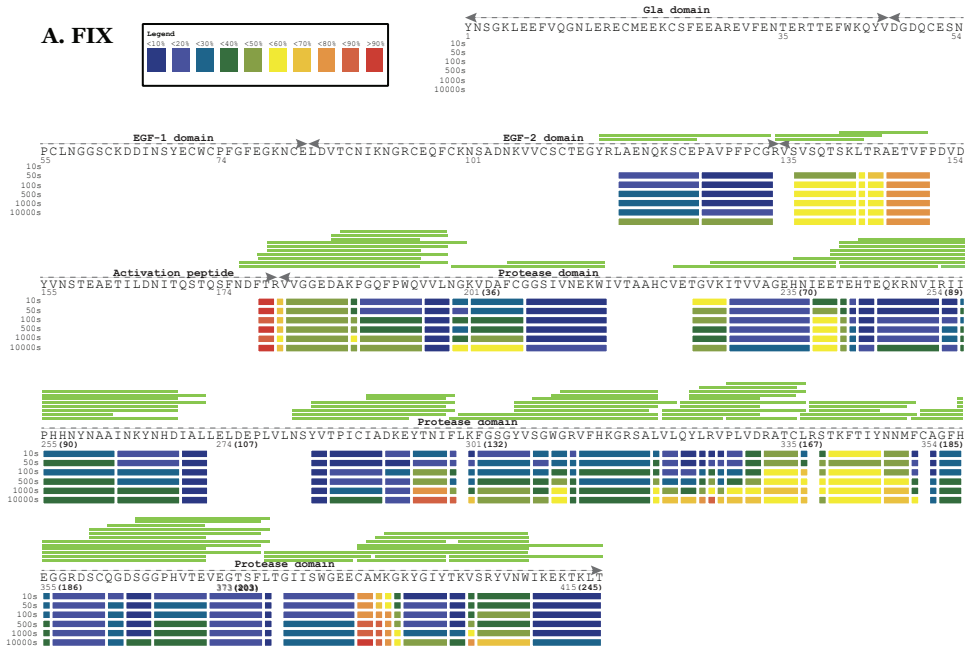


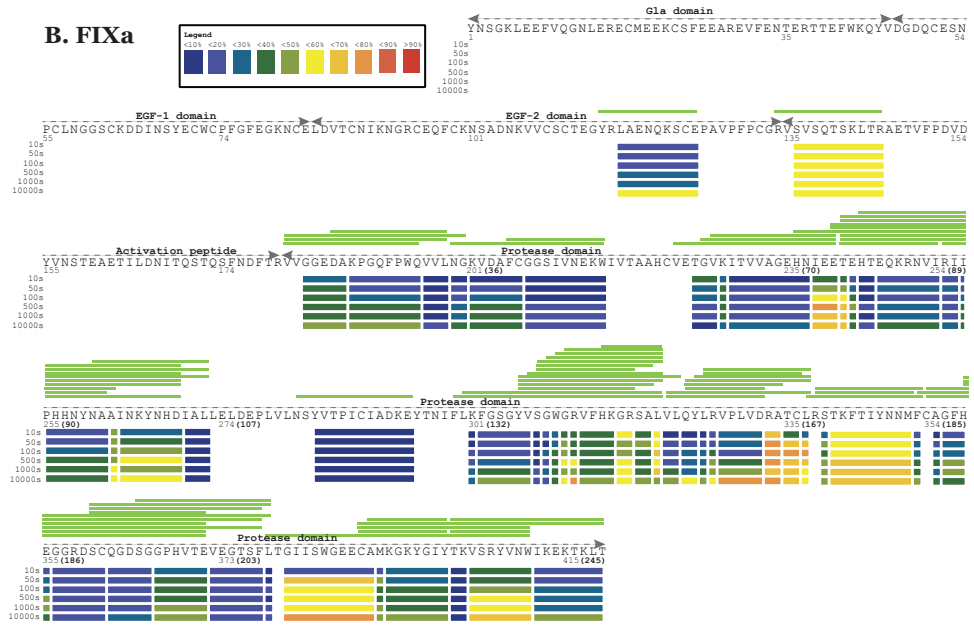

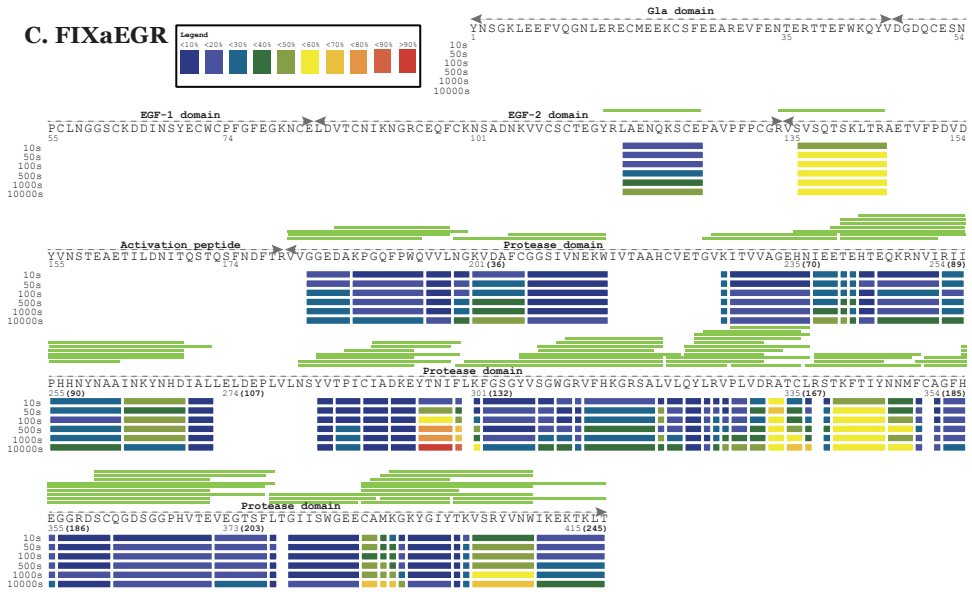


**Supplementary Figure 1 – Heatmaps and coverage of HDX-MS studies of FIX, FIXa and FIXaEGR**

HDX heatmaps for deuterium uptake and protein coverage of A) FIX B) FIXa) and C) FIXaEGR. The deuteration level percentages were calculated with HDExaminer 2.2.0 software. Deuteration levels are indicated for each HDX incubation period.





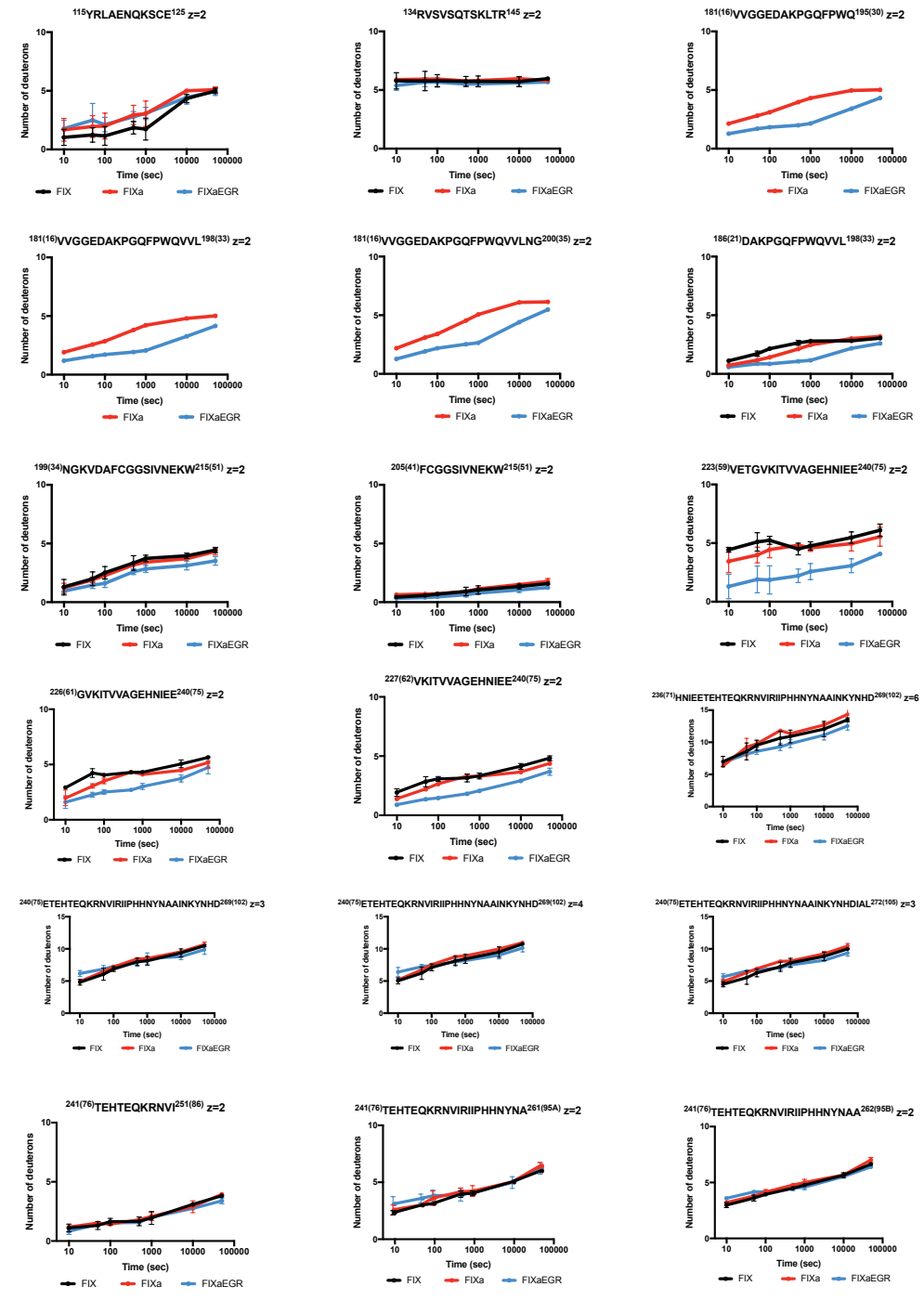

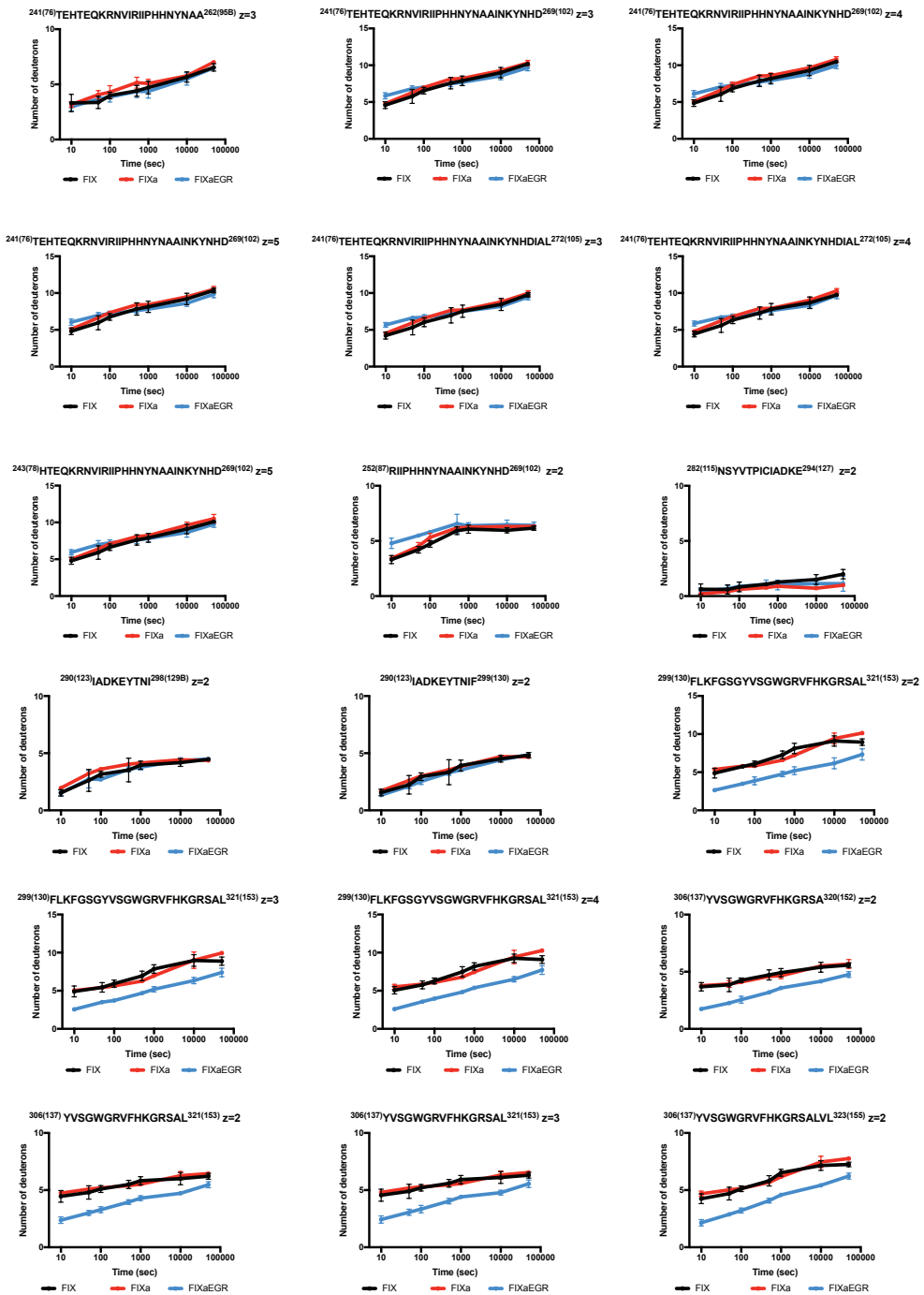
241(76)TEHTEQKRNVIRIIPHHNYNAA262(95B) z=3
241(76)TEHTEQKRNVIRIIPHHNYNAAINKYNHD269(102) z=3
241(76)TEHTEQKRNVIRIIPHHNYNAAINKYNHD269(102) z=4
241(76)TEHTEQKRNVIRIIPHHNYNAAINKYNHD269(102) z=5
241(76)TEHTEQKRNVIRIIPHHNYNAAINKYNHDIAL272(105) z=3
241(76)TEHTEQKRNVIRIIPHHNYNAAINKYNHDIAL272(105) z=4
243(78)HTEQKRNVIRIIPHHNYNAAINKYNHD269(102) z=5
252(87)RIIPHHNYNAAINKYNHD269(102) z=2
282(115)NSYVTPICIADKE294(127) z=2
290(123)IADKEYTNI298(129B) z=2
290(123)IADKEYTNIF299(130) z=2
299(130)FLKFGSGYVSGWGRVFHKGRSAL321(153) z=2
299(130)FLKFGSGYVSGWGRVFHKGRSAL321(153) z=3
299(130)FLKFGSGYVSGWGRVFHKGRSAL321(153) z=4
306(137)YVSGWGRVFHKGRSA320(152) z=2
306(137) YVSGWGRVFHKGRSAL321(153) z=2
306(137)YVSGWGRVFHKGRSAL321(153) z=3
306(137)YVSGWGRVFHKGRSALVL323(155) z=2
Number of deuterons
Time (sec)
FIX
FIXa
FIXaEGR

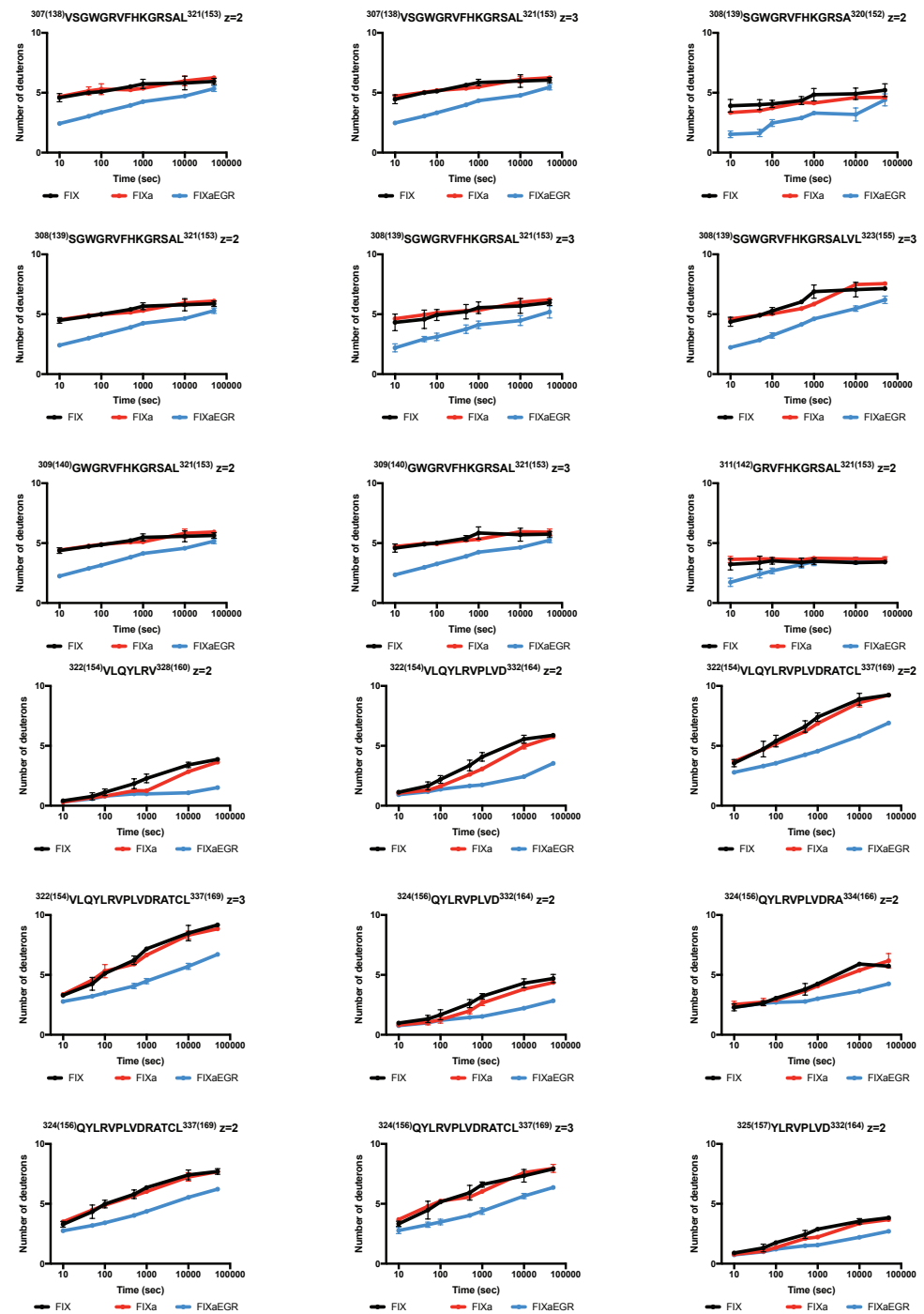
307(138)VSGWGRVFHKGRSAL321(153) z=2
307(138)VSGWGRVFHKGRSAL321(153) z=3
308(139)SGWGRVFHKGRSA320(152) z=2
308(139)SGWGRVFHKGRSAL321(153) z=2
308(139)SGWGRVFHKGRSAL321(153) z=3
308(139)SGWGRVFHKGRSALVL323(155) z=3
309(140)GWGRVFHKGRSAL321(153) z=2
309(140)GWGRVFHKGRSAL321(153) z=3
311(142)GRVFHKGRSAL321(153) z=2
322(154)VLQYLRV328(160) z=2
322(154)VLQYLRVPLVD332(164) z=2
322(154)VLQYLRVPLVDRATCL337(169) z=2
322(154)VLQYLRVPLVDRATCL337(169) z=3
324(156)QYLRVPLVD332(164) z=2
324(156)QYLRVPLVDRA334(166) z=2
324(156)QYLRVPLVDRATCL337(169) z=2
324(156)QYLRVPLVDRATCL337(169) z=3
325(157)YLRVPLVD332(164) z=2
Number of deuterons
Time (sec)
FIX
FIXa
FIXaEGR

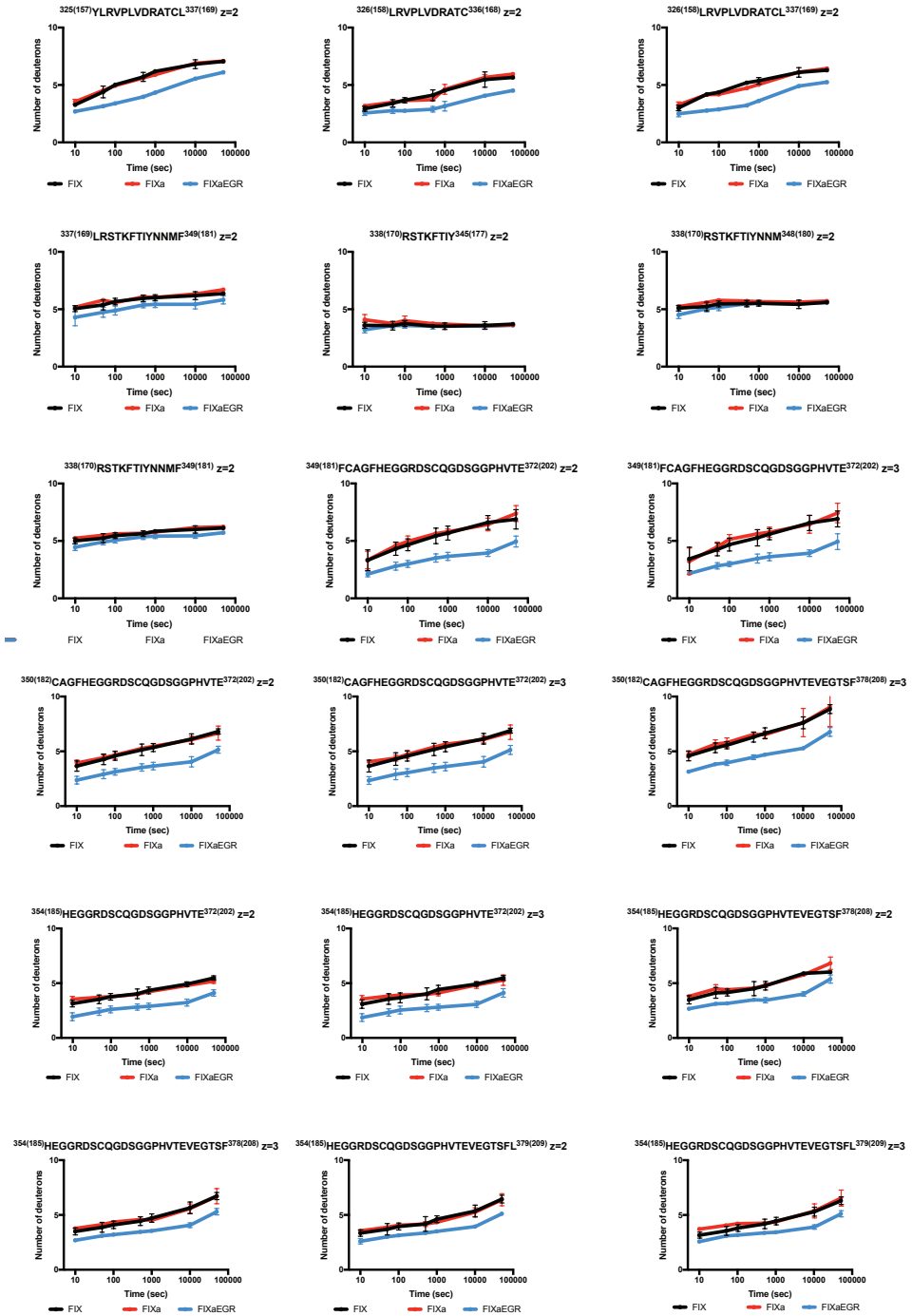


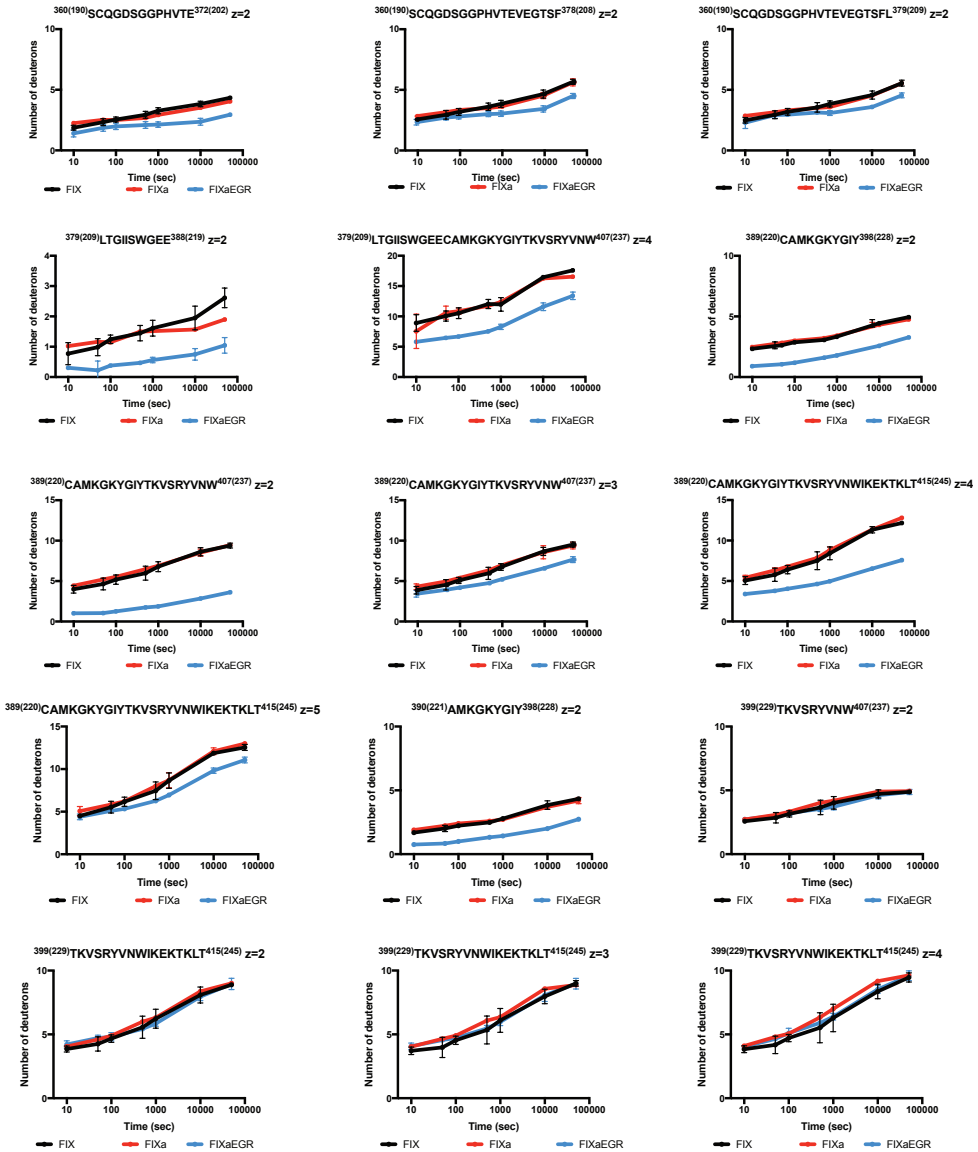


**Supplementary Figure 2 – Complete set of Deuterium uptake plots**

Number of deuterons incorporated is reported as a function of time for individual peptides from FIX (black), FIXa (red) and FIXaEGR (blue). Charge state (z) of the peptides is also shown.

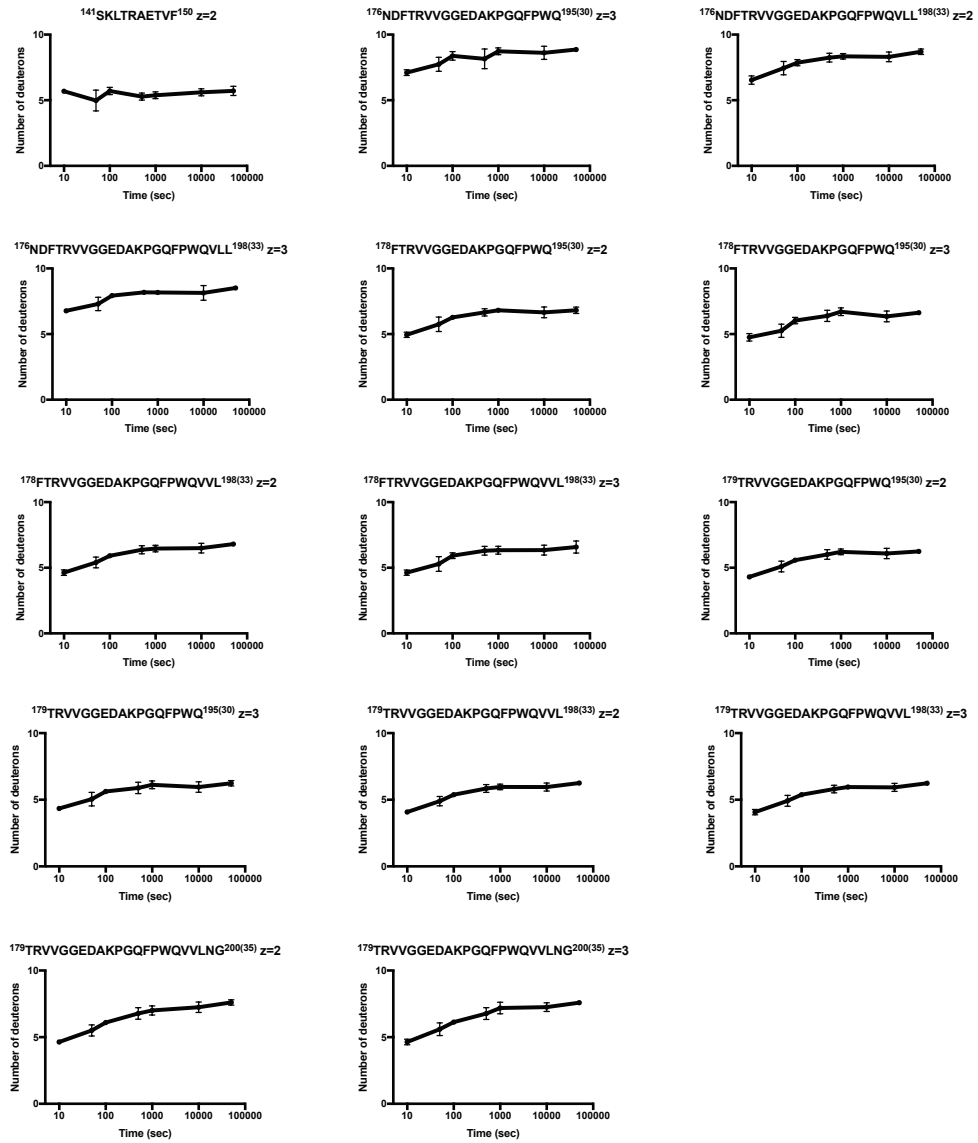


**Supplementary Figure 3 – Deuterium uptake plots of FIX-specific peptides**

Number of deuterons incorporated is reported as a function of time for the individual peptides overlapping the cleavage sites at positions R145 and R180. Charge state (z) of the peptides is also shown.

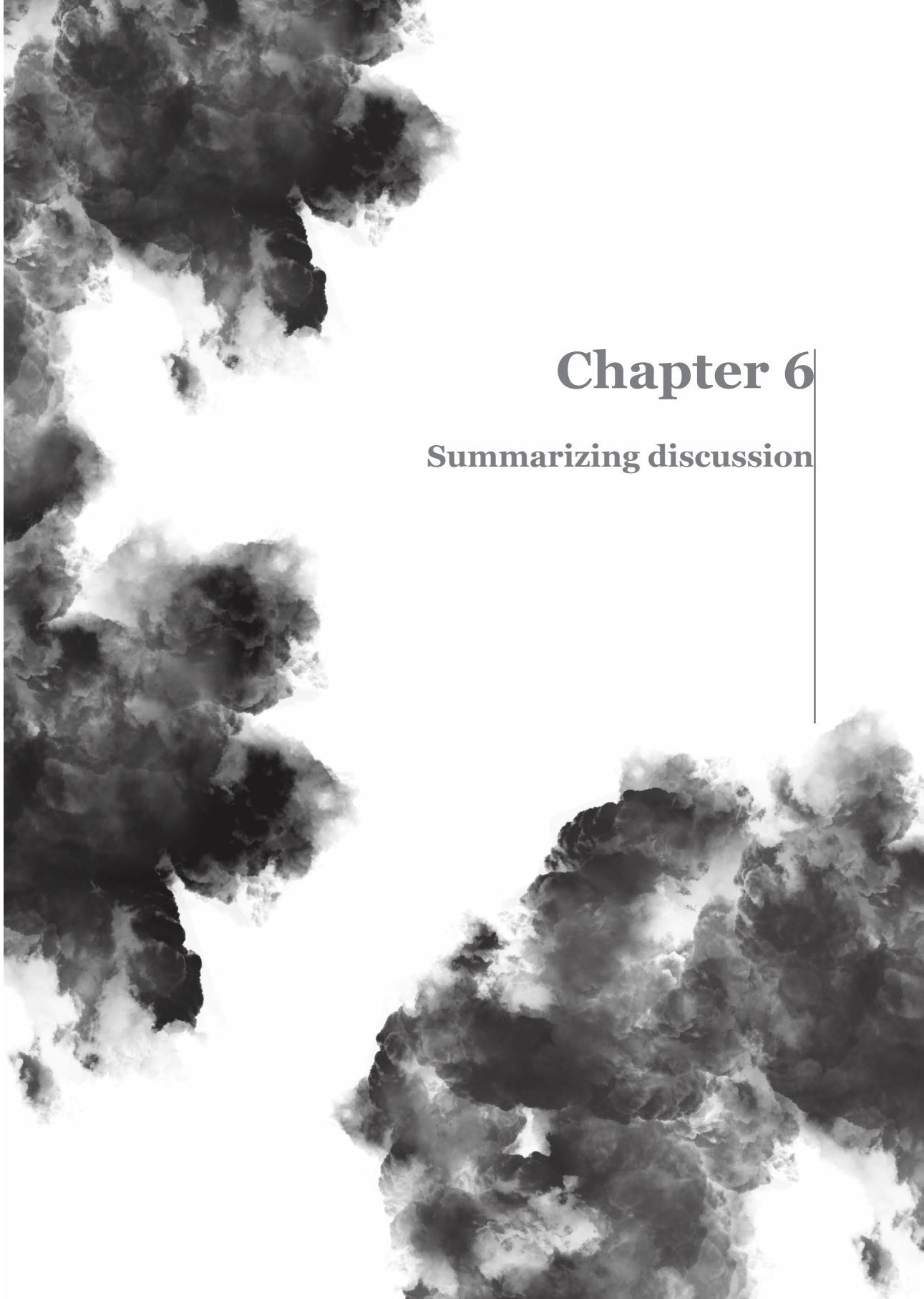

# Chapter 6

## Summarizing discussion

In the past decade, major progress has been made in increasing our understanding of the macromolecular interactions between the coagulation factors of the coagulation cascade. The fine-tuned molecular mechanisms that control the biological action of these factors have remained, however, poorly understood. The cofactors factor VIII (FVIII) and factor V (FV), which share similar structural/functional properties, represent one example. The identity and dynamics of the structural elements that provide the unique biochemical characteristics of these cofactors have remained largely unknown. Another example is the serine protease factor IX (FIX). FIX is a poor enzyme in comparison to other coagulation proteases (*e.g.* thrombin) and requires the interaction with activated FVIII (FVIIIa) to reach its full catalytic potential. As no crystal structure is available of the FIXa-FVIIIa complex, there is only limited information available about the putative changes in FIXa that take place upon binding FVIIIa.

In the present thesis, an integrative biochemical approach has been taken to study the molecular interactions and dynamics of FVIII and FIX upon their activation and subsequent complex assembly on phospholipid membranes. In this chapter, the major conclusions and potential implications of our findings are discussed.

## MULTIFUNCTIONAL ROLES OF FVIII C1 DOMAIN

In chapter 2, we took advantage of the structure and function relationship between FVIII and FV to identify structural elements that mediate their unique role within the coagulation cascade. In particular we focused on the putative ligand binding regions within the FVIII C1 domain. This domain is involved in the binding to procoagulant surfaces, VWF and FIXa[1,2]. In a recent study, we established that substitution of the FVIII C1 domain with that of FV greatly compromises cofactor function. This confirmed the critical role of the C1 domain for the function of FVIII. In addition, it implied that the C1 domain of FV lacks the surface-exposed motifs that are critical for the binding of FVIII to its ligands[3].

Upon structural comparison of the FV and FVIII C1 domains, we identified five unique solvent-exposed hydrophobic residues in the FVIII C1 domain: F2035, F2068, F2127, V2130, and I2139. The corresponding residues of the FV C1 domain are either polar or buried in the protein core (Chapter 2, Figure 1). We found that the corresponding residues in the C2 domain of FVIII were also polar instead of hydrophobic (Chapter 2, Figure 4). Of note, substitution of the FVIII C1 domain with a second FVIII C2 domain also resulted in an impaired cofactor function[4]. From a structural point of view, it is remarkable that the five hydrophobic elements are exposed to the solvent[5]. The combined observations opened the possibility that these residues may contribute to the biological function of FVIIII, for example





by interacting with VWF or FIXa. Replacement of F2127 by alanine affected both the binding to FIXa and VWF, while F2068 and V2125 were found to be mainly important for the binding to VWF. Instead, substitution of a valine at position 2130 was found to impact the FIXa-mediated conversion of FX only. These observations show that FIXa and VWF partially share a binding site on the C1 domain. This is compatible with the notion that VWF can effectively block premature binding of FVIII to FIXa. No direct role could be attributed to the hydrophobic surface-exposed residues F2035 and I2139. The reason why these hydrophobic amino acids are exposed to the solvent on the FVIII C1 domain surface remains therefore a topic for further investigation.

## CHANGES OCCURRING IN FVIII UPON ACTIVATION AND BINDING TO FIXa

In Chapter 3 we focused on the putative structural changes in FVIII upon its activation and binding to FIXa. It has been established that thrombin cleaves FVIII at the border of short acidic regions located at A1-A2 junction, A2-B junction and at the N-terminus of the light chain. As a consequence, the A2 domain remains non-covalently attached to the A1 and A3 domain[6]. Researchers have, so far, been unsuccessful in obtaining a crystal structure of FVIIIa. The structural changes that take place in FVIII upon its activation have therefore remained largely unknown. HDX-MS provides the opportunity to study the structural dynamics of proteins and protein-ligand complexes[7]. For this reason, HDX-MS was employed in chapter 3 to explore the complexity of the molecular changes in FVIII upon its activation and interaction with FIXa.

An increase in deuterium incorporation was observed for A2 domain residues at the interface with the A3 domain in FVIIIa compared to FVIII (Chapter 3, Figure 1B). It has been established that FVIIIa rapidly loses its cofactor function caused by dissociation of the A2 domain from FVIIIa[6]. This may provide an explanation for the observation. However, we cannot exclude that the A2 domain of FVIII changes orientation upon activation of FVIII, thereby exposing cryptic functional sites. If so, this would explain why only a single peptide of the A3 domain at the interface displayed increased deuterium incorporation (Chapter 3, Figure 1B). Other residues of the A3 domain may still interact with the A2 domain in this model. We also observed changes within the A2 domain that are outside the A2-A3 domain interface. Upon activation, region Leu631-Trp637 of the A2 domain showed increased deuterium uptake. In the FVIII crystal structure published by Shen et al, the Leu631-Trp637 region is partially covered by the acidic *a2* region at the N-terminal side of the A2 domain[8] (Chapter 3, Figure 6). Cleavage by thrombin in this region may lead to the

exposure of the Leu631-Trp637 (Chapter 3, Figure 6). This may explain the observed increased deuterium incorporation at this site in FVIIIa.

Upon binding to FIXa, Leu631-Trp637 region showed a marked decrease in deuterium incorporation (Chapter 3, Figure 1C-D). This would indicate either a change in conformation in response to FIXa binding or a direct interaction of FIXa with this region. Substitution of V634 by an alanine residue, known to cause mild Hemophilia A[9], almost completely impaired the ability of FVIII to enhance the activity of FIXa (Chapter 3, Figure 3). Although this effect could be explained by an altered stability of the FVIIIa-V634A compared to the wild-type FVIIIa, we observed that the rate of A2 domain dissociation from the FVIII-V634A variant was indistinguishable from that of wild-type FVIII in absence of FIXa (Chapter 3, Figures 4 and 5). In addition, no differences were found in HDX between FVIII and FVIII-V634A. Therefore, it seems plausible that V634 may directly participate in the interaction with FIXa.

## Novel insight into the FVIIIa binding site on FIXa

In Chapter 4, we made use of HDX-MS to assess the putative changes in FIXa upon complex formation with FVIIIa. Multiple changes in HDX were observed throughout the FIXa molecule (Chapter 4, Figure 2). Because these were dispersed over the entire FIXa molecule, they could not be attributed to a single FVIIIa binding interface only. Allosteric changes, which may occur in the FIXa molecule secondary to FVIIIa binding, are expected to be reflected by altered HDX as well. Multiple changes in HDX were also observed upon comparing FIXa in the presence and absence of a small molecule inhibitor (small pseudo-substrate). We reasoned that these changes in FIXa may predominantly represent allosteric changes (Chapter 4, Figure 4). If true, this would allow to discriminate between allosteric and FVIII-specific changes in FIXa.

Using this argumentation, changes in helices 126-132$_{CT}$, 162-helix$_{CT}$ and helix 236-240$_{CT}$, which are part of exosite II in FIXa[10], could be attributed to FVIIIa-specific changes (Chapter 4, Figure 4). This implies that exosite II may directly interact with FVIIIa. The crystal structure of the homologous snake venom FVa in complex with snake venom FXa show that the helices 126-132$_{CT}$, 162-helix$_{CT}$ and helix 236-240$_{CT}$ of FXa are involved in the interaction with FVa[11]. This reinforces the suggestion that Exosite II may contribute directly to FVIIIa binding. Exosite II is also known as the "basic Exosite" as it comprises a large number of basic amino acid residues[10]. Natural substitution of most of these charged residues are linked to the bleeding disorder Hemophilia B[12], demonstrating their critical role for the function of FIXa. Site-directed mutagenesis of the lysine and arginine residues in the exosite followed by enzyme kinetic studies and SPR studies of the purified proteins revealed that these





residues indeed contribute to FVIIIa binding (Chapter 4, Figure 5A). This again confirmed the model that Exosite II is critical for effective interaction with FVIIIa. The mechanism behind the functional defect in FIXa of the Hemophilia B variants within the basic exosite thus seems to involve impaired binding to FVIIIa.

## Allosteric changes in FIXa

The mechanism of FIXa activation was further addressed in Chapter 5. HDX-MS and chemical footprinting MS with amine-directed tandem-mass-tags (TMTs) was employed to assess the difference between FIX, FIXa and FIXa irreversibly bound to a small pseudo-substrate. Results showed that the precursor FIX was indistinguishable from its activated form (Chapter 5, Figure 1). Although this seems surprising, it does agree with the observation that FIXa is a poor enzyme in the absence of FVIIIa. This implies that FIXa remains in a zymogen-like state in the absence of FVIIIa. Marked changes in HDX were observed between FIXa and FIXa bound to the pseudo-substrate (Chapter 5, Figure 1). As mentioned-above, the changes in HDX in FIXa upon FVIIIa binding and substrate binding largely overlap. We propose therefore that the substrate-bound FIXa represents FIXa in its active state.

The proteolytic activation of serine proteases generates a novel N-terminus, which then refolds and inserts into the catalytic domain[13]. This transition allows for the formation of the oxyanion hole and the S1 substrate binding pocket[13,14]. In our study, the N-terminal segment of the catalytic domain displayed a reduction in HDX, in particular upon binding of the pseudo-substrate to FIXa (Chapter 5, Figure 1). In the FIX zymogen, this segment displayed relatively high HDX, suggesting more flexibility than in FIXa. This implies that the region containing the newly generated N-terminus (V181, or V16 in chymotrypsin numbering) loses flexibility upon proteolytic activation, and is further rigidified by incorporation of a substrate into the active site. This also opens the possibility that the N-terminus may be only fully inserted into the catalytic domain in the substrate-bound form of FIXa. However, chemical footprinting revealed that both in free FIXa and substrate-bound FIXa, only a small fraction of the N-terminus is available for chemical modification. This implies that the N-terminus is largely protected in FIXa. However, the apparent insertion of the N-terminus remains insufficient to drive FIXa into its enzymatic competent form.

Another prominent finding relates to one of the surface loops in the protease domain, the so-called 220-loop in chymotrypsin numbering. FIXa displayed reduced deuterium uptake upon occupation of the S1-pocket in the substrate-binding site (Chapter 5, Figure 3), which was not observed upon complex formation between FVIIIa and FIXa (Chapter 4, Figure 1). This suggests that the flexible 220-loop is stabilized or rearranged only after substrate incorporation. One way of 220-

loop stabilization could involve a putative H-bond network between the charged residues E217, E219 and K224. To address this possibility, we mutated E217, E219 or K224 into alanine residues and assessed the function of these variants. All three substitution variant showed impaired activity in FX activation studies, in particular E217A and K224A (Chapter 5, Figure 4). In these two variants, the disruption of the H-bond network in the 220-loop was associated with an increased accessibility of the N-terminus for modification. This suggests that these FIXa variants are in a more zymogen-like state than wild-type FIXa. Mutations at these amino acid positions in the 220-loop are also known to cause Hemophilia B[12], which underlines the physiological relevance of these putative stabilizing interactions within the 220-loop.

Together, Chapters 4 and 5 suggest the existence of an interplay between N-terminus, 220-loop and substrate-binding site. This stabilizes FIXa in an active conformation that, once assembled with FVIIIa, further rigidifies in order to effectively activate FX. Thus, substrate-specific and cofactor-specific rearrangements activate the allosteric network that is necessary for the transition of FIXa into a fully competent enzyme.

## FUTURE PERSPECTIVES

Although we provide a deeper knowledge on the FIXa-FVIIIa complex assembly and mechanisms of function of the single constituents of this complex, much remains to be learnt to obtain improved therapeutics for patients suffering from Hemophilia A or B. The concept of FVIII-bypassing agents, *e.g.* with the therapeutic antibody emicizumab, has provided great results in terms of patient care[15,16]. This bispecific antibody replaces FVIIIa by binding both FX and FIXa. The full catalytic potential of FIXa is, however, not reached by the binding of the antibody[17]. What if we could also gain control over the allosteric changes in FIXa using an optimized antibody or a small molecule? Exosite II of FIXa may be the target of choice. Small molecules that specifically prevent the changes in the allosteric network may, on the other hand, be employed as novel anti-thrombotic agents.

A challenge in our HDX-MS studies remains linked to the impossibility of visualizing changes occurring in the EGF-1 and Gla domains of FIXa. This is the consequence of the intrinsic characteristics of these domains such as high density of negative charges and post-translational modifications in the light chain of FIXa. Changes in these domains upon complex formation of FIXa with FVIIIa have remained elusive, while they probably are driving the assembly on biomembranes. Cryo-electron microscopy (Cryo-EM) may represent an alternative approach to study the FVIIIa-FIXa complex on phospholipid membranes. The attention for Cryo-EM has reached a peak in popularity in 2017 when the Nobel prize was awarded to Jacques Dubochet, Joachim





Frank and Richard Henderson "for developing a technique to image biomolecules". An advantage of Cryo-EM is that it can visualize proteins and protein complexes in their natural state[18]. In collaboration with the group of Professor Friedrich Förster at Utrecht University, we managed to obtain Cryo-EM images of the ternary complex formed by FIXa-FVIIIa-FX on phospholipid vesicles. Figure 1 shows a micrograph in negative staining of a phospholipid vesicle decorated with these proteins. These initial studies show great promise to gain further insight into the assembly of the FVIIIa-FIXa complex.

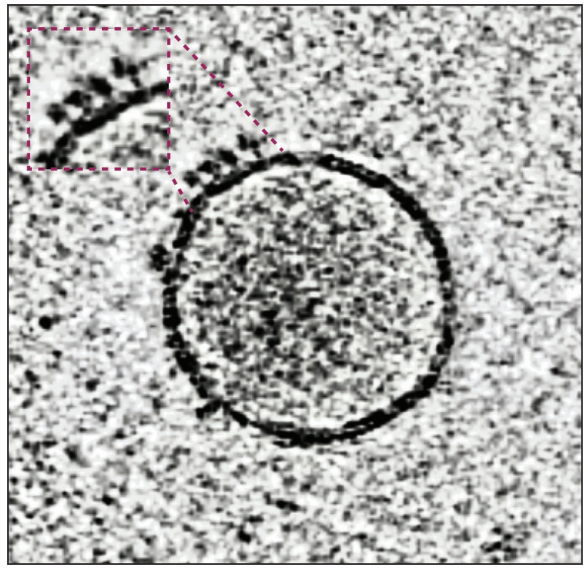

**Figure 1**
Negative staining of an EM micrograph showing a phospholipid vesicle decorated with constituents of the FX-activating complex (picture was taken at a magnification of 79.000x). The zoom-in displays densities compatible with the presence of protein decorating a phospholipid bilayer. The picture was taken by Robert Englemeier, MSc.

In conclusion, we believe that it is only via *viribus unitis* of cofactor, substrate and biomembranes that FIXa can be pushed from its zymogen-to-protease continuum into a fully productive enzyme. Innovations in structural biology show their value in improving our knowledge of proteins or protein complexes and in the identification of their interactive regions in the near future.

## REFERENCES


1. Chiu PL, Bou-Assaf GM, Chhabra ES, et al. Mapping the interaction between factor VIII and von Willebrand factor by electron microscopy and mass spectrometry. *Blood*. 2015;126(8):935–938.

2. Jacquemin M, Lavend'homme R, Benhida A, et al. A novel cause of mild/moderate hemophilia A: mutations scattered in the factor VIII C1 domain reduce factor VIII binding to von Willebrand factor. *Blood*. 2000;96(3):958-965.

3. Ebberink EH, Bouwens EA, Bloem E, et al. Factor VIII/V C-domain swaps reveal discrete C-domain roles in factor VIII function and intracellular trafficking. *Haematologica*. 2017;102:686-694

4. Wakabayashi H, Fay PJ. Replacing the factor VIII C1 domain with a second C2 domain reduces factor VIII stability and affinity for factor IXa. *J Biol Chem*. 2013;288(43):31289-31297.

5. Chandler D. Interfaces and the driving force of hydrophobic assembly. *Nature*. 2005;437(7059):640-647.

6. Fay PJ. Factor VIII structure and function. *Int J Hematol*. 2006;83(2):103–108.

7. Mayne L. Hydrogen Exchange Mass Spectrometry. *Methods Enzym*. 2016;566:335–356.

8. Shen BW, Spiegel PC, Chang CH, et al. The tertiary structure and domain organization of coagulation factor VIII. *Blood*. 2008;111(3):1240–1247.

9. McGinniss MJ, Kazazian HH, Hoyer LW, Bi L, Inaba H, Antonarakis SE. Spectrum of mutations in CRM-positive and CRM-reduced hemophilia A. *Genomics*. 1993;15(2):392-398.

10. Misenheimer TM, Buyue Y, Sheehan JP. The heparin-binding exosite is critical to allosteric activation of factor IXa in the intrinsic tenase complex: the role of arginine 165 and factor X. *Biochemistry*. 2007;46(26):7886–7895.

11. Lechtenberg BC, Murray-Rust TA, Johnson DJ, et al. Crystal structure of the prothrombinase complex from the venom of Pseudonaja textilis. *Blood*. 2013;122(16):2777–2783.

12. Rallapalli PM, Kemball-Cook G, Tuddenham EG, Gomez K, Perkins SJ. An interactive mutation database for human coagulation factor IX provides novel insights into the phenotypes and genetics of hemophilia B. *J Thromb Haemost*. 2013;11(7):1329–1340.

13. Page MJ, Di Cera E. Serine peptidases: classification, structure and function. *Cell Mol Life Sci CMLS*. 2008;65(7-8):1220-1236.

14. Zogg T, Brandstetter H. Activation mechanisms of coagulation factor IX. *Biol Chem*. 2009;390(5-6):391–400.

15. Kitazawa T, Esaki K, Tachibana T, et al. Factor VIIIa-mimetic cofactor activity of a bispecific antibody to factors IX/IXa and X/Xa, emicizumab, depends on its ability to bridge the antigens. *Thromb Haemost*. 2017;117(7):1348-1357.

16. Franchini M, Marano G, Pati I, et al. Emicizumab for the treatment of haemophilia A: a narrative review. *Blood Transfus Trasfus Sangue*. 2019;17(3):223-228.

17. Kitazawa T, Igawa T, Sampei Z, et al. A bispecific antibody to factors IXa and X restores factor VIII hemostatic activity in a hemophilia A model. *Nat Med*. 2012;18(10):1570–1574.

18. Carroni M, Saibil HR. Cryo electron microscopy to determine the structure of macromolecular complexes. *Methods*. 15;95:78-85.

# Appendix

## SUMMARY

The complex formed by the serine protease activated factor IX (FIXa) and its cofactor activated factor VIII (FVIIIa) plays a central role in the coagulation cascade. Major progress has been made to understand the biochemistry of the membrane-bound FIXa-FVIIIa complex that converts factor X (FX) into activated FX (FXa). Yet, detailed insight into the role of structural elements of FVIII and FIX that drive the particularly effective proteolytic mechanism is still lacking. In the present thesis, we employ footprinting approaches coupled to mass spectrometry to gain novel insights into the molecular changes that occur upon activation and complex assembly of FVIII and FIX.

In **Chapter 1** we provide an overview of the state-of-the-art knowledge about the coagulation cascade with focus on the structure and activation mechanism of FIX and FVIII. We further address the key interactive sites between FIXa and FVIIIa and the present knowledge about the FIXa-FVIIIa complex assembly. Finally, we introduce Hydrogen-Deuterium eXchange Mass Spectrometry (HDX-MS), directed to identify structural changes upon complex formation or protein activation.

In **Chapter 2** we explore the identity of FVIII regions contributing to FIXa and von Willebrand factor (VWF) interactions. We built upon the previous observation that replacement of the FVIII C1 domain for the one of factor V (FV) reduced VWF binding and cofactor function. Through structure and primary sequence comparison of FVIII and FV, we identified five surface-exposed hydrophobic residues unique to the FVIII C1 domain. Site-directed mutagenesis followed by enzyme kinetic studies and protein binding studies showed that residues F2068, V2130, and especially F2127 contribute to VWF and/or FIXa interaction. Novel information is therefore provided about the role of specific hydrophobic residues of the C1 domain in the FVIII life cycle.

In **Chapter 3**, we employ HDX-MS to investigate the changes in FVIII upon its activation and assembly with FIXa. HDX-MS of thrombin-activated FVIII revealed changes at the A2 – A3 domain interface that are compatible with a rapid dissociation of the A2 domain from FVIIIa. However, in presence of FIXa, the uptake at the A2 – A3 domain interface was similar to that of non-activated FVIII. This indicated that the A2 domain is retained in FVIIIa upon binding to FIXa. Our results also showed that the A2 domain surface loop L631-Y636 displayed a marked decrease in deuterium uptake in FVIIIa in presence of FIXa. Guided by this finding, the hemophilia A variant FVIII-V634A was constructed. This showed a major reduction in its ability to enhance the activity of FIXa. Additional enzyme kinetics studies and HDX-MS studies demonstrated that the A2 domain of FVIII-V634A was not retained by FIXa. Together, these results suggest that we have identified a region in FVIII that

contributes to the interaction with FIXa.

In **Chapter 4** we focus on the molecular rearrangement in FIXa upon complex assembly with FVIIIa using HDX-MS analysis. The amount of changes and their dispersion throughout the FIXa molecule was unlikely to be attributed simply to a single FVIIIa binding interface. These changes in HDX were partially overlapping with those observed upon interaction of FIXa with a small substrate. The effect on FIXa that was specific for FVIIIa was clustered on the so-called basic Exosite (or Exosite II) comprising three helices of the protease domain. Hemophilia B FIXa variants involving amino acid substitutions of lysine and arginine residues in Exosite II revealed reduced binding to FVIIIa in enzyme kinetics studies. These data imply that Exosite II contributes directly to the interaction with FVIIIa.

In **Chapter 5** we employ footprinting mass spectrometry by HDX and Tandem-Mass Tags (TMT) labelling to address the conformational changes occurring upon the conversion from FIX into FIXa. HDX-MS displayed only minor differences between FIX and FIXa. This implies that FIXa is largely zymogen-like. A decreased deuterium uptake in FIXa compared to FIX was localized at the N-terminus region and was more prominent when the FIXa active site was occupied by a small substrate. These data link the occupation of the active site to a loss of flexibility at the N-terminus. TMT-labelling of the N-terminus showed that the N-terminus is predominantly protected from labeling, and that occupation of the active site increases protection only to a minor extent. In addition, occupation of the active site also reduced deuterium uptake within the 220-loop backbone. Mutagenesis within the 220-loop revealed that a putative H-bond network may contribute to FIXa activity. TMT-labeling of the N-terminus of these variants suggested that these 220-loop variants are more zymogen-like than wild-type FIXa.

Finally, in **Chapter 6** we discuss the most important findings of this thesis and suggest directions for future research.





## SAMENVATTING

Het serine protease geactiveerd factor IXa (FIXa) en de geactiveerde vorm van de cofactor VIII (FVIIIa) vormen samen een complex dat een centrale rol speelt binnen de stollingscascade. Aan het oppervlak van geactiveerde bloedplaatjes of andere circulerende cellen zet dit enzym-cofactor complex stollingsfactor X (FX) om in geactiveerd FX (FXa). De laatste decennia is grote vooruitgang geboekt in ons inzicht in de biochemie van de activering van FX. Niettemin zijn de structurele interacties tussen FVIIIa en FIXa die de proteolytische activiteit van dit complex aansturen nog grotendeels onbegrepen. In dit proefschrift gebruiken we biochemische labelingstechnieken, ook wel '*footprinting*' genoemd (*i.e.* een chemische afdruk) die in combinatie met massaspectrometrie nieuwe inzichten kunnen geven in de moleculaire veranderingen die optreden bij activatie en complexvorming van FVIII en FIX.

In **hoofdstuk 1** wordt een overzicht gepresenteerd van de meest recente kennis op het gebied van bloedstelping (hemostase), met specifieke aandacht voor de structuur en activeringsmechanisme van FIX en FVIII. De huidige kennis over de vorming van het FVIIIa-FIXa complex en de daarin essentiële interacties worden hier besproken. Eén van de methoden die we hier beschrijven om deze interacties in kaart te brengen is gebaseerd op de mate van uitwisseling tussen waterstof met deuterium zoals die met behulp van massaspectrometrie ('*Hydrogen-Deuterium eXchange Mass Spectrometry*', HDX-MS) gedetecteerd kan worden. Deze uitwisseling weerspiegelt de toegankelijkheid van eiwitsegmenten voor hun directe omgeving, en daarmee structurele veranderingen die optreden als gevolg van activering of complexvormving.

In **hoofdstuk 2** ligt de nadruk op de identificatie van gebieden in FVIII die interacties aangaan met FIXa en von Willebrand factor (VWF). In een eerdere studie is gebleken dat uitwisseling van één van de cel-bindende eiwitdomeinen (het C1-domein) van FVIII met dat van de homologe stollingsfactor V de binding met VWF sterk verminderde. Door vergelijking van de twee structuren en de aminozuursequenties ervan konden vijf hydrofobe, naar buiten gekeerde aminozuren geïdentificeerd worden die uniek zijn voor het C1-domein van FVIII. Mutagenese van deze specifieke aminozuren gevolgd door studies naar enzym kinetiek en eiwitbinding lieten zien dat residuen F2068, V2130, en in het bijzonder F2127, bijdragen aan de binding met VWF en/of FIXa. Deze studies hebben ons nieuwe inzichten opgeleverd over het belang van de afzonderlijke hydrofobe residuen in het C1-domein voor de functie van FVIII en voor de stabilisatie ervan in de bloedsomloop.

In **hoofdstuk 3** gebruiken we HDX-MS om veranderingen in FVIII te detecteren die optreden tijdens activering en binding met FIXa. Door trombine geactiveerd FVIII laat gedurende HDX-MS veranderingen zien in het raakvlak tussen de A2-

en A3-domeinen. Dit is waarschijnlijk vooral toe te schrijven aan dissociatie van het A2-domein na FVIII activering. In aanwezigheid van FIXa daarentegen, komt de waterstof-deuterium uitwisseling in datzelfde gebied overeen met die van niet-geactiveerd FVIII. Dit suggereert dat het A2-domein geassocieerd blijft in FVIIIa na binding met FIXa. Daarnaast was er in aanwezigheid van FIXa een sterke terugname van waterstof-deuterium uitwisseling te zien in een ongestructureerde lus van het A2-domein, tussen aminozuren Leu631 en Tyr636. Op basis van deze waarneming is de hemofilie A variant FVIII-V634A geconstrueerd. De gezuiverde vorm van deze variant liet een grote reductie zien in de FVIII-gemedieerde versterking van enzymatische activiteit van FIXa. Tijdens verdere karakterizering van FVIII-V634A bleek dat het A2-domein niet geassocieerd bleef in aanwezigheid van FIXa zoals gezien werd voor normaal FVIII. Deze resultaten suggereren een tot nu toe onbekende bijdrage van dit deel van FVIII aan complexvorming met FIXa.

In **hoofdstuk 4** wordt HDX-MS ingezet om precieze moleculaire heroriëntatie in FIXa te detecteren als gevolg van binding met FVIIIa. De verandering in uitwisseling van waterstof en deuterium was dermate sterk, en ook verspreid over het hele FIXa molecuul, dat het onwaarschijnlijk leek dat dit alleen door binding aan FVIIIa veroorzaakt werd. Een deel van de veranderingen in HDX-MS was ook zichtbaar wanneer de actieve conformatie van FIXa werd gestabiliseerd met behulp van een klein tripeptidesubstraat. Naast deze veranderingen was er ook een aantal specifiek door FVIIIa veroorzaakte veranderingen. Deze spitsten zich toe op een basisch oppervlak in FIX ('*exosite II*') dat bestaat uit drie helices van het protease domein. Aminozuursubstituties in deze helices, die tevens bekende met hemofilie B geassocieerde mutaties omvatten, lieten een verminderde binding aan FVIIIa zien. Hieruit kon geconcludeerd worden dat de '*exosite II*' belangrijk is voor de directe interactie tussen FIXa en FVIIIa.

In **hoofdstuk 5** zijn twee '*footprinting*' technieken gecombineerd, zowel HDX-MS als labeling van primaire amines door Tandem-Mass Tags (TMT), om veranderingen in eiwitstructuur te detecteren die optreden tijdens de omzetting van FIX in FIXa. In eerste instantie was er nagenoeg geen verschil meetbaar in HDX-MS tussen FIX en FIXa. Er werd echter wel een reductie in deuterium uitwisseling waargenomen in het N-terminale gedeelte van het protease domein. Deze reductie was nog prominenter in substraat-gebonden FIXa. Daarmee kon een verband worden gelegd tussen enzymatische activiteit, *i.e.* de conformatie van het actief centrum ('*active site*'), en bescherming van de N-terminus tegen waterstof-deuterium uitwisseling. Daarnaast was er een verminderde uitwisseling in één van de eiwitlussen, het zogenaamde 220-segment, wanneer FIXa in een substraat-gebonden conformatie was. Aminozuurmutaties in datzelfde segment verstoorden de enzymatische activiteit. Labeling van primaire amines liet zien dat deze moleculaire varianten meer op het





FIX zymogeen lijken dan normaal FIXa. Dit impliceert een direct verband tussen het 220-segment, de toegankelijkheid van de N-terminus, en de enzymatische activiteit van FIXa.

Tenslotte worden in **hoofdstuk 6** de bevindingen uit dit proefschrift bediscussieerd. Tevens worden suggesties gedaan voor verder onderzoek.

## CURRICULUM VITAE

Nadia Freato was born on July 6th 1989 in Cittadella, Padua, Italy. She grew up in the province of Vicenza where she attended high school with scientific orientation at the "Liceo scientifico G.B. Quadri". In September 2008 she moved to Trieste to pursue her scientific passion and attend her Bachelor in Biology at the University of Trieste (Italy). She soon became passionate of the lab life and during her studies she worked for two years in the research group of Prof. dr. Sergio Crovella under the supervision of Dr. Ludovica Segat at the children hospital Burlo Garofolo of Trieste. She graduated with a thesis entitled "Mannose-Binding Lectin (MBL2) and MBL-Associated Serine Protease-2 (MASP2) gene polymorphisms in a Brazilian population from Rio de Janeiro". In September 2012 Nadia started her Master in Functional Genomics at the University of Trieste while continuing her work at the children hospital Burlo Garofolo. She performed her final Master internship at the children hospital Burlo Garofolo of Trieste. She graduated in October 2014 with full marks under the supervision of Dr. Eulalia Catamo with a thesis entitled "HLA-G promoter polymorphisms and their influence in Hepatitis C virus infection". In July 2015 she moved to The Netherlands to start her PhD project under the supervision of Prof. dr. Koen Mertens, Prof. dr. Sander Meijer and Dr. Maartje van den Biggelaar at the department of Molecular and Cellular Hemostasis of Sanquin Research in Amsterdam. The results of her studies are described in this thesis. Currently she works on the profiling of antibodies subclasses in plasma at the department of Molecular and Cellular Hemostasis of Sanquin Research in Amsterdam.

# PUBLICATION LIST

*van Galen J, ***Freato N**, Przeradzka MA, Ebberink EHTM, Boon-Spijker M, van der Zwaan C, van den Biggelaar M, Meijer AB. Hydrogen-deuterium exchange mass spectrometry identifies activated factor IX-induced molecular changes in activated factor VIII *Thromb Haemost*. 2020 Dec 10. doi: 10.1055/s-0040-1721422.

**Freato N**, Ebberink EHTM, van Galen J, Fribourg C, Boon-Spijker M, van Alphen FPJ, Meijer AB, van den Biggelaar M, Mertens K. Factor VIII-driven changes in activated factor IX explored by hydrogen-deuterium exchange mass spectrometry *Blood*. 2020 Dec;136(23):2703-2714.

*Przeradzka MA, ***Freato N**, Boon-Spijker M, van Galen J, van der Zwaan C, Mertens K, van den Biggelaar M, Meijer AB. Unique surface-exposed hydrophobic residues in the C1 domain of factor VIII contribute to cofactor function and von Willebrand factor binding *J Thromb Haemost*. 2020 Feb;18(2):364-372.

Catamo E, Zupin L, **Freato N**, Polesello V, Celsi F, Crocè SL, Masutti F, Pozzato G, Segat L, Crovella S. HLA-G regulatory polymorphisms are associated with susceptibility to HCV infection *HLA*. 2017 Mar;89(3):135-142.

Zupin L, Polesello V, Casalicchio G, **Freato N**, Maestri I, Comar M, Crovella S, Segat L. MBL2 polymorphisms in women with atypical squamous cells of undetermined significance *J Med Virol*. 2015 May;87(5):851-9.

Casalicchio G, **Freato N**, Maestri I, Comar M, Crovella S, Segat L. Beta defensin-1 gene polymorphisms and susceptibility to atypical squamous cells of undetermined significance lesions in Italian gynecological patients *J Med Virol*. 2014 Dec;86(12):1999-2004

*both authors contributed equally

## In revision:

**Freato N**, van Alphen FPJ, Boon-Spijker M, van den Biggelaar M, Meijer AB, Mertens K, Ebberink EHTM. Probing activation-driven changes in coagulation factor IX by mass spectrometry *J Thromb Haemost*. minor revision requested

## AKNOWLEDGEMENTS

As all good things come to an end, also my PhD ride is now concluded.

Through these years, Sanquin had soon become my second home. What I learnt is that to make of a house a home you need the right people and good food. Although on the latter point I kept on complaining, I met plenty of amazing people here and I couldn't have wished for a better environment for this journey.

As I am getting sentimental, I am tempted now to write a poem but I promised, not only to myself, to keep it short, so here we go.

Koen, thank you for believing in me. Your patient guidance and support in these years made me sharpen my thinking and shaped the researcher I am today.

Sander, your positive energy is something really precious to all the PhD students that come across your path. Thank you for that and thank you for your trust, it helped me immensely and it meant a lot.

Maartje I admire your strength and your attitude, I feel lucky to have learnt so much from you. Thank you for the multiple chances you gave me and for always encouraging me. You were (are) an example for me.

To my coauthors, I am extremely grateful for your contribution in uplifting the chapters of this thesis.

My dear paranymphs, without you these years would have been for sure more boring. Małgosia and Ellie, thanks for being there for me once more.

To the proteomics and bioinformatics groups, thank you for the inspiring interactions about science, music or whatever was on the table. Thanks for always switching to English whenever I was entering a room, I profoundly appreciated it. I'm also grateful for the constant support, I was lucky to be part of this group.

To the old (ok, not that old) guard of PhD students and post-docs, thank you all for lightening up the looong days in the lab, for the fun nights out and for making my time in The Netherlands extra special.

The nasty thing about Academia and leaving abroad is that sooner or later you get to say a lot of goodbyes, I would like to thank from the bottom of my heart all the people I met in these years. Thank you for accepting me and for making me feel





always welcome.

Ai miei amici di "casa", grazie perché ogni volta che tornavo era come non fossi mai andata via.

Alla mia famiglia, vi ringrazio, specialmente per l'ultimo periodo del mio PhD, mi avete supportato in modi che nemmeno immaginate.

Robi, questa tesi la dedico a te e alla tua pazienza di questi anni. Grazie per essere il mio compagno in tutto e credere in me prima ancora che ci creda io. Ti amo.

And now, *Ad maiora!*

Nadia